

University of Southampton Research Repository ePrints Soton

Copyright © and Moral Rights for this thesis are retained by the author and/or other copyright owners. A copy can be downloaded for personal non-commercial research or study, without prior permission or charge. This thesis cannot be reproduced or quoted extensively from without first obtaining permission in writing from the copyright holder/s. The content must not be changed in any way or sold commercially in any format or medium without the formal permission of the copyright holders.

When referring to this work, full bibliographic details including the author, title, awarding institution and date of the thesis must be given e.g.

AUTHOR (year of submission) "Full thesis title", University of Southampton, name of the University School or Department, PhD Thesis, pagination

UNIVERSITY OF SOUTHAMPTON

FACULTY OF NATURAL AND ENVIRONMENTAL SCIENCES
SCHOOL OF CHEMISTRY

**The Synthesis of 2,2,3,3-Tetrafluorinated
Galactose and Glucose Derivatives**

by

Samuel Ben Golten

Thesis for the degree of Doctor of Philosophy

November 2012

UNIVERSITY OF SOUTHAMPTON

ABSTRACT

FACULTY OF NATURAL AND ENVIRONMENTAL SCIENCES

SCHOOL OF CHEMISTRY

The Synthesis of 2,2,3,3-Tetrafluorinated Galactose and Glucose

Derivatives

by Samuel Golten

The incorporation of polyfluorinated regions into carbohydrates has been proposed as a strategy to improve the typically low protein–carbohydrate affinity. The creation of a hydrophobic region, while maintaining a potential for attractive dipolar interactions (mediated by the polarised C–F bond) may increase binding affinity.

This thesis describes the synthesis of previously reported 2,3-dideoxy-2,2,3,3-tetrafluorogalactopyranose and 2,3-dideoxytetrafluoroglucopyranose. Further optimisations have been carried out to provide highly efficient and enantioselective routes to both compounds. The synthesis of the novel 2,3-dideoxy-2,2,3,3-tetrafluorogalactofuranose via a modification to the pyranose route has been successfully achieved and optimised.

The large scale synthesis of these compounds has enabled their further derivatisation. This has included the development of phosphorylation methodology for 2,2,3,3-tetrafluorogalactose in both pyranose and furanose isomers. The synthesis of the first disaccharides to contain a tetrafluoroethylene moiety has been accomplished, providing tetrafluorinated analogues of known bioactive disaccharides. Studies have also been carried out towards different glycosylation methodologies of 2,2,3,3-tetrafluorinated sugars, enabling access to glycosylation by both electrophilic and nucleophilic reagents.

Detailed conformational analysis has been implemented, with the results displaying high similarities between 2,2,3,3-tetrafluorogalactopyranosides and natural non-fluorinated carbohydrates.

Table of Contents

Chapter 1. Introduction	1
1.1 Fluorine.....	1
1.1.1 Fluorine as an H-Bond Acceptor	2
1.1.2 Fluorine Mediated Multipolar Interactions.....	3
1.1.3 Fluorination to Investigate Biological Processes	5
1.2 Fluorinated Carbohydrates	6
1.3 Carbohydrates	8
1.4 Fluorinated Carbohydrates for the Investigation of <i>Polar Hydrophobicity</i>	10
1.4.1 Polar Hydrophobicity	10
1.4.2 Tetrafluorinated Carbohydrates	10
1.4.3 Nomenclature of Tetrafluorinated Carbohydrates	11
1.5 Synthesis of Polyfluorinated Carbohydrates	11
1.6 2,3-Dideoxy-2,2,3,3-Tetrafluoro Sugars	13
1.6.1 Halogen-Metal Exchange Mediated Cyclisation	13
1.6.2 Synthesis of 2,2,3,3,-Tetrafluoro- Glucose and Galactose.....	13
1.7 Glycosylation of 2,3-Difluoro Sugars	15
1.8 Conformation of Carbohydrates	16
1.9 Aims	17
1.9.1 Fluorinated Monosaccharide Targets.....	17
1.9.2 Structural Studies	18
1.9.3 Glycosylation	18
1.9.4 Synthesis of Tetrafluoro Analogues of Known Inhibitors of Mycobacterial Biosynthesis	18
Chapter 2. The Synthesis of Tetrafluorinated Galactose Derivatives...	21
2.1 2,3-Dideoxy-2,2,3,3-Tetrafluorogalactopyranose.....	21
2.1.1 Commercial Starting Materials to Tetrafluoro Alkene 1.45.....	21
2.1.2 Asymmetric Dihydroxylation	22

2.1.3	Benzylation, Formylation and Cyclisation	23
2.2	Synthesis of 2,3-Dideoxy-2,2,3,3-Tetrafluorogalactofuranose	25
2.2.1	Selective Silylation	25
2.2.2	Furanose Synthesis	26
2.2.3	Silyl Migration Induced Isomerisation	27
2.2.4	Towards the Synthesis of an Alkyl Galactofuranoside	29
2.2.5	Non-Migratory Protecting Group Strategy	30
2.2.6	Alkyl Tetrafluorogalactofuranoside	32
2.3	Conclusions	34
Chapter 3. Structural Studies		35
3.1	Methyl Galactosides	35
3.1.1	Methyl Galactoside Anomers 600 MHz NMR	35
3.1.2	X-Ray Crystal Structures: Methyl Galactoside Anomers	36
3.2	Crystal Structure of 4,6-Di- <i>O</i> -Benzyl-2,2,3,3-Tetrafluorogalactose	38
3.3	Crystal Structures of Monobenzyl-2,2,3,3-Tetrafluorogalactoses	39
3.4	Anomeric Equilibration via Mutarotation	40
3.5	Conclusions	42
Chapter 4. Synthesis of Tetrafluoroglucose Derivatives		43
4.1	Mitsunobu and Isourea Mediated S _N 2	43
4.2	Inversion by Displacement of a Triflate	45
4.2.1	Inversion of Hydroxyl β- to Tetrafluoroethylene	46
4.2.2	Inversion of Hydroxyl α- to the Tetrafluoroethylene	47
4.3	Sharpless Asymmetric Epoxidation	50
4.4	Return to Cyclic Sulfate	51
4.4.1	Oxidation of Sulfite to Sulfate	51
4.4.2	Nucleophilic cyclic sulfate opening and acid hydrolysis	52
4.5	Completion of the Glucose Synthesis	54
4.6	Methyl Glucoside Anomers	56

4.7	Towards the Synthesis of 4-Amino-Tetrafluoroglucose	57
4.7.1	Background.....	57
4.7.2	Planned Synthesis of 4-Amino-Tetrafluoroglucose (4.37).....	57
4.7.3	Towards the Displacement of Triflate with Azide	58
4.8	Conclusions.....	59

Chapter 5. Towards the Glycosylation of 2,2,3,3-Tetrafluorogalactose 61

5.1	Strong Acid Activators	61
5.1.1	Hemiacetal and Acetate as Donors	61
5.1.2	Trichloroacetimidate as Donor	63
5.1.3	Decarboxylative Glycosylation.....	66
5.2	Glycosyl Triflate as Donor	67
5.2.1	Formation of the Glycosyl Triflate	68
5.2.2	Glycosylations	68
5.3	Conclusions.....	70

Chapter 6. Synthesis of Tetrafluorinated Ligands for the Investigation of Enzymatic Processes Relating to Mycobacteria 71

6.1	Introduction.....	71
6.1.1	Background.....	71
6.1.2	Uridine Diphosphate Galactose Mutase (UGM)	72
6.1.3	Galactofuranosyl Transferase 2	76
6.2	Tetrafluorogalactosyl Phosphates for UGM.....	78
6.2.1	Pyranose	78
6.2.2	Furanose	80
6.3	Tetrafluorofuranosyl Furanose Disaccharides for GlfT2	84
6.3.1	Donors and Acceptors	84
6.3.2	Glycosylation	85
6.3.3	Deprotections	86
6.4	Conclusions.....	87

Chapter 7. Conclusions and Future Work.....	89
7.1 Tetrafluorogalactopyranose	89
7.2 Tetrafluorogalactofuranose	89
7.3 Tetrafluoroglucose	89
7.3.1 Synthesis	89
7.3.2 Screening	90
7.3.3 4-Aminotetrafluoroglucose	90
7.4 Glycosylation.....	91
7.4.1 Activation of Anomeric Position by Derivatisation	91
7.4.2 Anomeric Alkylation	91
7.5 Phosphorylation	92
7.6 Tetrafluorinated Disaccharides.....	92
7.7 Analysis.....	93
Chapter 8. Experimental.....	95
Chapter 9. References	163
Chapter 10. Appendices.....	169
10.1 Appendix A: X-Ray Crystal Structure Data	169
10.2 Appendix B: Analytical Chiral HPLC Data	202

DECLARATION OF AUTHORSHIP

I, Samuel Golten

declare that the thesis entitled

‘The Synthesis of 2,2,3,3-Tetrafluorinated Galactose and Glucose Derivatives’

and the work presented in the thesis are both my own, and have been generated by me as the result of my own original research. I confirm that:

- § this work was done wholly or mainly while in candidature for a research degree at this university;
- § where any part of this thesis has previously been submitted for a degree or any other qualification at this university or any other institution, this has been clearly stated;
- § where I have consulted the published work of others, this is always clearly attributed;
- § where I have quoted from the work of others, the source is always give. With the exception of such quotations, this thesis is entirely my own work;
- § I have acknowledged all main sources of help;
- § where the thesis is based on work done by myself jointly with others, I have made clear exactly what was done by others and what I have contributed myself;
- § parts of this work has been published as papers:
Linclau, B.; Golten, S.; Light, M.; Sebban, M.; Oulyadi, H. *Carbohydr. Res.* **2011**, *346*, 1129-1139.
Linclau, B.; Golten, S.; Light, M. *J. Carbohydr. Chem.* **2011**, *30*, 618-625.

Signed:

Date:

Preface

The research described in this thesis was carried out under the supervision of Dr. Bruno Linclau at the University of Southampton between September 2009 and November 2012. No part of this thesis has previously been submitted for a degree. All work is my own unless otherwise stated.

Acknowledgements

My first thanks must go to Bruno. I would like to acknowledge all the help he has given me over the past three years. He was a constant source of guidance, support and encouragement.

Additionally, I thank my advisor Martin Grossel for the feedback he provided.

I would also like to thank all those people I worked with in the Linclau group. In no particular order, Jean, Konrad, Kylie, Cath, Nathan, Carole, Clément, Lewis, Cindy, Zhong, Craig, Leona, Julien, Nha and also the many others who I shared the lab with at any point.

The reasons I would like to thank them are many, firstly for all the help given to me when I first started. Secondly, for answering my incessant questions relating to my work and letting me bounce ideas off them, even when they were busy. Thirdly, for providing an enjoyable and friendly environment to work in, with many non-chemistry conversations that kept me sane. Lastly for ignoring me when I occasionally became a bit stressed and probably not that pleasant.

I must also mention those people in the Harrowven, Brown and Whitby groups, who I shared the office with. They were only too happy to provide chemicals, equipment, advice and conversation. The same goes to those working on other floors.

My thanks to the service staff include Neil for keeping the NMR running and always performing my special requests, John, Julie and Chrissie for running all the MS samples that I could not, Karl and the others for being friendly in stores, (even if Karl insists on taking the piss), Mark Light for providing the X-ray structures and also all the guys in the glassblowing workshop.

Thanks go to INTERREG for providing the funding that allowed me to do this project, as well as the guys in LeHavre who looked after me during my short placement. Thanks to Carole and Nathan for proofreading this thesis at various stages.

I would also like to thank all those who provided me with human interaction outside of chemistry (many of whom are the same). I am grateful to the many friends I made for helping me relax when not at work and being always happy to listen to me. I want to thank my family for the same reasons and for letting me talk about chemistry.

Finally, I must give enormous thanks to my girlfriend, who has constantly given me the confidence to keep going.

Thanks to Charles Grey, 2nd Earl Grey, for providing the fuel that made possible the writing of this thesis.

Abbreviations

AD	Asymmetric Dihydroxylation	HOE	Heteronuclear Overhauser Effect
ADP	Adenosine diphosphate	HOESY	Heteronuclear Overhauser Effect correlation spectroscopy
AE	Asymmetric Epoxidation	HMBC	Heteronuclear multiple bond correlation
aq	Aqueous	HMQC	Heteronuclear multiple quantum coherence
AQN	Anthroquinone	HPLC	High-Performance Liquid Chromatography
ax	Axial	HRMS	High resolution mass spectrometry
BOM	Benzyloxymethyl	IC ₅₀	Half maximal inhibitory concentration
CI	Chemical Ionisation	Imid	Imidazole
COSY	Correlation spectroscopy	IR	Infra Red
CSD	Cambridge Structural Database	IPA	propan-2-ol
DBU	1,8-Diazabicyclo[5.4.0]undec-5-ene	IUPAC	International Union of Pure and Applied Chemistry
DCE	1,2-Dichloroethane.	<i>J</i>	Coupling Constant
DCM	Dichloromethane	M	mol dm ⁻³
DET	Diethyl tartrate	<i>M.</i>	<i>Mycobacterium</i>
DHQ	Dihydroquinine	min	Minutes
DHQD	Dihydroquinidine	MOM	Methoxymethyl
DIAD	Diisopropylazodicarboxylate	mp	Melting Point
DIC	Diisopropylcarbodiimide	Ms	Methanesulfonyl
DIPEA	Diisopropylethylamine	MS	Mass Spectrometry
DMAP	4-(Dimethylamino)pyridine	NIS	<i>N</i> -Iodosuccinimide
DMP	Dess-Martin periodinane	NMR	Nuclear Magnetic Resonance
DMF	<i>N,N</i> -Dimethylformamide	NOE	Nuclear Overhauser Effect
DMSO	Dimethylsulfoxide	NOESY	Nuclear Overhauser Effect correlation spectroscopy
<i>e.e.</i>	Enantiomeric excess	Nu	Nucleophile
eq	Equatorial	<i>-p</i>	Pyranose
equiv	Equivalents	PHAL	Phthalazine
EI	Electron impact	PNB	<i>para</i> -Nitrobenzoyl
ES	Electrospray	PG	Protecting group
<i>-f</i>	Furanose	ppm	Parts Per Million
FAD	Flavin adenine dinucleotide	PTSA	<i>para</i> -Toluene sulfonic acid
FAD _{red}	Reduced FAD	Py	Pyridine
gal	Galactose	quant.	Quantitative
GDP	Guanosine diphosphate	r.t.	Room Temperature
glc	Glucose	Recryst.	Recrystallisation
GlT	Galactofuranosyl transferase	R _f	Retention Factor
h	Hour(s)	STD	Saturation Transfer Difference

SET	Single electron transfer	TFA	Trifluoroacetic acid
Temp	Temperature	TFSI	Trifluoromethanesulfonamide
TB	Tuberculosis	THF	Tetrahydrofuran
TBAF	Tetra- <i>n</i> -butylammonium fluoride	TLC	Thin-Layer Chromatography
TBDMS	<i>tert</i> -Butyldimethylsilyl	TMS	Trimethylsilyl
TBDPS	<i>tert</i> -Butyldiphenylsilyl	Ts	<i>p</i> -Toluene sulfonyl
TES	Triethylsilyl	UDP	uridine diphosphate
Tf	Trifluoromethanesulfonyl	UGM	UDP-Galactose mutase

Chapter 1. Introduction

1.1 Fluorine

Fluorine is the most electronegative element, described by Pauling¹ as a *superhalogen*. This lends a high level of polarisation to the C–F bond and means that the six non-bonding electrons are held very tightly, giving a small van der Waals radius of 1.47 Å.²

The presence of a carbon-fluorine bond can affect the strength of adjacent bonds; C–C bonds are strengthened, while allylic C=C bonds are weakened. Conformational changes can result from substitution of hydrogen with fluorine. This includes steric effects such as the repulsion between 1,3-fluorines and electronic effects such as the fluorine-*gauche* effect. The *gauche* effect describes the weak preference for a *gauche* conformation in 1,2-difluorinated alkanes, due to hyperconjugation from the σ C–H orbital to the σ^* C–F orbital.³

Fluorine has a strong influence on the acidity and basicity of nearby functional groups.⁴ For example, the pK_a of ethanol is 15.9 and this value is reduced to 12.5 for 2,2,2-trifluoroethanol,⁵ further examples are shown in **Figure 1.1**.⁶ This is of great importance because modification of pK_a can affect the binding affinity and bioavailability of a biologically active compound.⁷

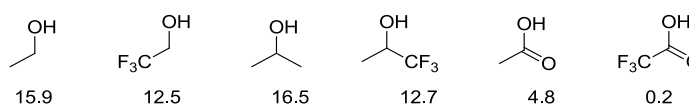


Figure 1.1 The effect of fluorination on pK_a s

Although fluorination is thought to increase the hydrogen bond donating capacity of a proximal alcohol, it has been found that this is complicated by the potential for intramolecular F...HO interactions. The significance of this has been detailed recently by research between our group and collaborators.⁸ It was shown that the presence of a 1,2-*gauche* (or 1,3-*cis*) relationship between a fluorine and hydroxyl can significantly decrease the H-bond acidity of the hydroxyl (as in **1.1**, **1.3** and **1.4**, **Figure 1.2**). This was ascribed to intermolecular F...HO interactions, which was consistent with the observed increase in acidities for those alcohols *anti*- to a fluorine atom (as in **1.2** and **1.5**).

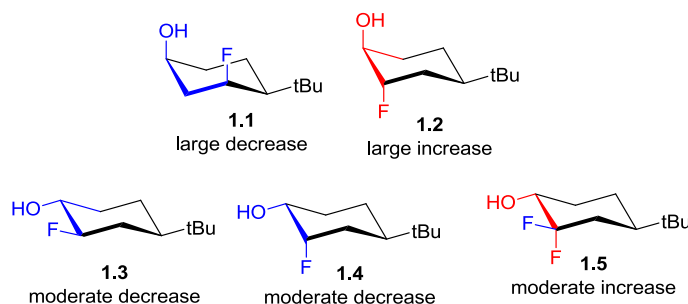


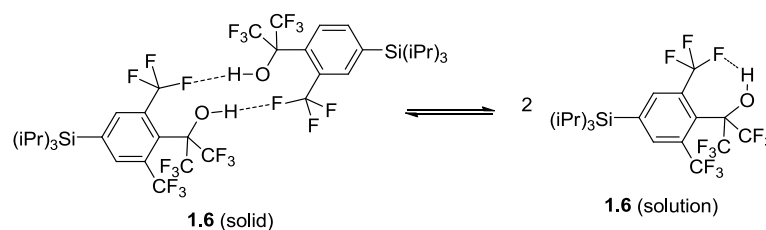
Figure 1.2 Selected effects on H-bond acidities compared to non-fluorinated cyclohexanol⁸

1.1.1 Fluorine as an H-Bond Acceptor

Fluoride (F^-) is a strong hydrogen bond acceptor. Hydrogen difluoride contains the strongest known hydrogen bond, with an enthalpy of around 37 kcal (155 kJ) mol^{-1} .^{9,10} The capability of organofluorine to accept a hydrogen bond has been discussed for some time¹¹ but this phenomenon is, however, still disputed.¹²

A survey of the Cambridge Structural Database (CSD) and Protein Data Bank found only a very small number of potential hydrogen bonds involving C–F.¹³ Some of these were accounted for by highly favourable conditions (such as high ionic character of the fluorine). Others were disputed as actually being bonds at all, either due to errors in original measurements or failure to meet the stated criteria for a hydrogen bond. One of the most convincing examples was a 10-membered ring comprising two N–H \cdots F contacts. The reluctance of fluorine as an H-bond acceptor was attributed to its low polarisability and the low accessibility of its electrons. Aromatic or other sp^2 hybridised fluorine atoms are even worse hydrogen bond acceptors than aliphatic fluorines. The strength of a $H_3CF\cdots HOH$ bond has been calculated as 2.38 kcal mol^{-1} with a distance of 1.95 Å.¹⁴

A clear observation of both inter and intramolecular O–H \cdots F bonding was made with respect to fluorinated alcohol **1.6** (Scheme 1.1).¹⁵ Two intermolecular hydrogen bonds, with lengths of 2.01 Å were observed in the crystal structure. On dissolution in hexane, an intramolecular hydrogen bond was deduced from IR and NMR experiments.

Scheme 1.1 Example of fluorine involvement in hydrogen bonding¹⁵

Further support for the existence and importance of fluorine's hydrogen bond accepting capability comes from the fact that incorporation of $F\cdots H$ bonding terms (based on analysis of crystal structures) into a computational force-field was shown to have greater accuracy.¹⁶ Extensive analysis of the Protein Data Bank revealed $C-F\cdots H$ interactions, including the observation that bifurcated interactions were common for CF_2 .

Close intermolecular interactions between fluorine and hydrogen atoms in 2-fluoro-2-phenylcyclopropane derivatives have also been attributed to weak $X-H\cdots F-C$ bridges¹⁷ ($X = O$ or N). The crystal structures of several related compounds revealed hydrogen bonded dimers with $C-H\cdots F-C$ contacts mostly shorter than the sum of van der Waals radii. Non-fluorinated counterparts showed distinctly different crystal structures, indicating that the close interactions are not solely due to packing effects.

In $DMSO-d_6$, the signal of a hydroxyl proton involved in an H-bond is shifted compared to the chemical shift in an apolar solvent.¹⁸ In addition, the values of scalar coupling between F and $O-H$ can give information about the presence of H-bonds in fluoroorganic compounds. The measurement of these and other parameters, such as the temperature dependence of the OH chemical shift and changes in the frequency of OH bands in the IR spectra has allowed the examination of intramolecular $F\cdots HO$ interactions of fluorinated saccharides in solution.¹⁹ Observations made were consistent with the presence of a weak hydrogen bond (~ 3 Å) in 4-deoxy-4-fluorolevoglucosans, between a fluorine and hydroxyl group in a 1,3-diaxial relationship.

There is significant evidence that organofluorine can behave as a weak H-bond acceptor, especially when there are no other potential acceptors nearby and also when the fluorine atom is directed towards the donor.¹⁹

1.1.2 Fluorine Mediated Multipolar Interactions

The hydrophobic effect causes an entropically unfavourable aggregation of water molecules and is thus a driving force for hydrophobic particles to group together in aqueous medium.²⁰ Polyfluorinated carbon chains induce greater hydrophobic desolvation than hydrocarbons. This is not due to an intrinsically greater hydrophobicity, but is a result

of fluorocarbons' greater surface area.²¹ Therefore, hydrophobic desolvation can be increased by incorporation of fluorinated regions, which is of relevance to binding hydrophobic pockets in protein binding sites.²²

Diederich *et al.* identified a significant difference in activity between inhibitors of thrombin (a serine protease) containing fluorines at varying positions on an aromatic ring.²³ **Figure 1.3** shows the sudden reduction in inhibition constant as the fluorine atom is moved from the 2- position in **1.8** to the 4- position in **1.10**. The presence of a fluorine atom leads to a decrease in polarisability of the aromatic ring, which results in higher hydrophobicity, hence enhancing desolvation. The binding of the 2-fluoro and 3-fluoro substrates (**1.8** & **1.9**) was comparable to the non-fluorinated substrate (**1.7**). However, the significant enhancement of binding in **1.10** demonstrates an attractive interaction between the fluorine and the binding site. Subsequent examination of the binding mode revealed a close contact between the fluorine atom and an H–C–C=O moiety.

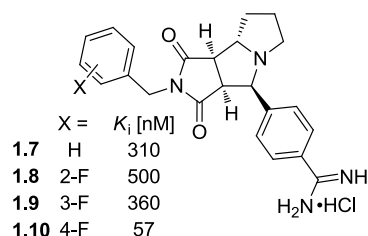


Figure 1.3 Activities of fluorinated thrombin inhibitors²³

Figure 1.4 shows a crystal structure of inhibitor **1.10** (specifically its Ar-F moiety) in complex with thrombin.²⁴ Close contacts include not just F...H, but also F...C $_{\alpha}$ and F...C=O, which were also found in many other complexes in the CSD. Investigation of further inhibitors supported the conclusion that this moiety gives a strongly fluorophilic environment.

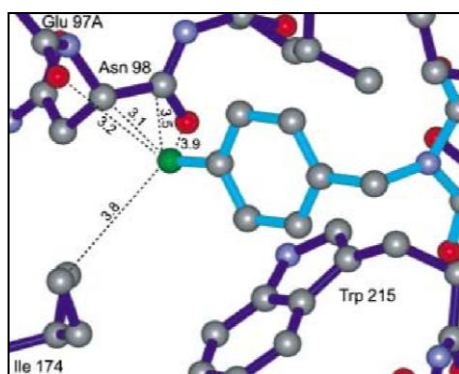


Figure 1.4 Crystal structure of the binding mode of a 4-fluorobenzyl moiety (of **1.10**, **Figure 1.3**) with thrombin. F-protein contacts < 4 Å are highlighted with dotted lines

Vulpetti *et al.* have described a method of fragment screening based on identification of fragment-protein binding interactions.²⁵ Mixtures of fluorinated fragments (12 or 36) were analysed by ^{19}F NMR in the presence and absence of a protein. Specific NMR protocols enabled the identification of any binding fragments. This technique can give data towards fragment-based drug discovery, but also indicate potential fluorophilic regions in proteins.²⁶

Following on from this, comparison of ^{19}F NMR and fluorine-protein interactions in crystal structures lead to the observation of an empirical relationship between chemical shift and said intermolecular interactions.^{27,28} Greater shielding (indicated by a more negative ppm value) is symptomatic of increased electron density. While deshielded fluorines (e.g. $\text{O}-\text{CF}_3$) were more commonly involved in hydrophobic interactions and $\text{F}\cdots\text{C}=\text{O}$ contacts, shielded fluorines (e.g. CH_2F) were more frequently observed in hydrogen bond type interactions. A greater number of close contacts were observed for more highly shielded fluorine atoms.

1.1.3 Fluorination to Investigate Biological Processes

In a biological context, fluorine is often used to beget certain desired properties to a substrate. The introduction of fluorine can impart changes in physical and pharmacokinetic properties, conformation and stereoelectronics, lipophilicity, acidity/basicity and certain ligand-protein interactions.²⁹ Carbon-fluorine is the strongest single bond in organic chemistry³⁰ and this can make it less susceptible to metabolism than $\text{C}-\text{O}$.³¹

The carbon-fluorine bond has a length of 1.35 Å, between that of $\text{C}-\text{H}$ (1.09 Å) and $\text{C}-\text{O}$ (1.43 Å). Therefore on purely steric grounds, fluorine is a reasonable replacement for hydrogen (van der Waals radius 1.2 Å), while in search of biological information.^{32,33}

An example of enhanced biological activity after replacement of a hydrogen with a fluorine atom is shown in **Figure 1.5**, which shows the generic structure of a number of halomethyl androstane-17 β -carbothioates. The activity (in mice) of **1.11** was increased more than two-fold by fluorination (**1.12**).³⁴ Further modifications lead to **1.13**, which is now in use as an inhaled corticosteroid for the treatment of asthma, marketed as fluticasone propionate.³⁵

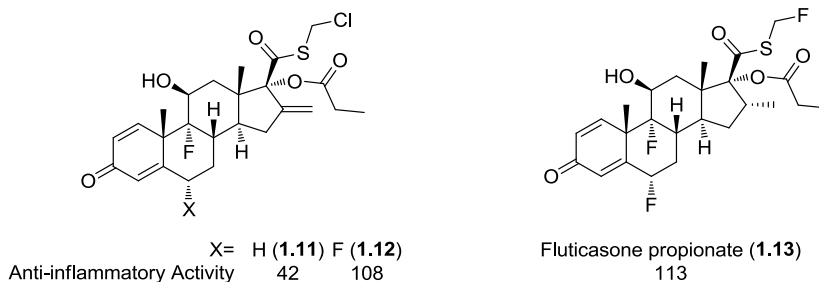


Figure 1.5 Structures and anti-inflammatory activities of some halomethyl androstane-17 β -carbothioates.³⁴ Activity in mouse relative to fluocinolone acetonide (100)

In addition to imparting a complex influence on ligand-protein interactions, the presence of fluorine enables further techniques to analyse binding affinity/specificity via the use of ^{19}F NMR.^{25,36} Fluorine-19 has 100% abundance and a high magnetogyric ratio ($25.2 \times 10^{-7} \text{ rad s}^{-1} \text{ T}^{-1}$ compared to $26.8 \times 10^{-7} \text{ rad s}^{-1} \text{ T}^{-1}$ for ^1H), which gives this technique high sensitivity. Also the general dearth of fluorine in natural compounds⁷ simplifies analysis, through the absence of background noise.

1.2 Fluorinated Carbohydrates

Fluorine is also used as a replacement for hydroxyl groups, especially in carbohydrates.³⁷⁻⁴⁰ The removal of hydroxyl groups is a well-established method of investigating protein-carbohydrate interactions, with the aim of identifying which hydroxyl groups in a substrate are important for the interaction with the protein binding site. While the use of hydrogen as a replacement for OH can give information about the total hydrogen bonding contribution,¹² fluorine is used due to its potential as a weak hydrogen bond acceptor. The aim is to therefore distinguish between acceptor and donor interactions in a complex. By this means, a number of fluorinated carbohydrates have provided information about the presence (or absence) of a hydrogen-bond to a protein, in which the sugar supplies the donor.

While undertaking the strategy of *deoxyfluorination* for the purpose of investigating interactions, a number of examples have been found in which the fluorinated sugars showed increased binding affinity compared to their non-fluorinated counterparts. It was observed that introduction of fluorine atoms lead to an increased affinity to the glucose binding site in glycogen phosphorylase.⁴⁰ Glucose (1.14) binds glycogen phosphorylase with an inhibition constant (K_i) of 2.0 mM. The substitution of the anomeric hydroxyl with a fluorine (1.15, **Figure 1.6**) decreased this value, as did fluorination at the 2-position, (1.16) though not significantly. Vicinal difluorination gave a stronger binding affinity than

either monofluorinated compound for the α -anomer (**1.17**), while even the β -anomer (**1.18**) still had greater binding affinity than glucose itself.

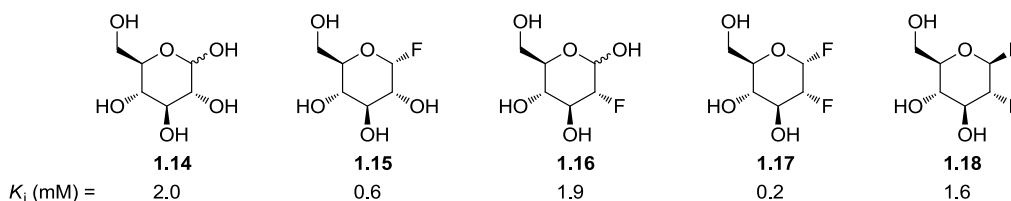


Figure 1.6 Inhibitors of glycogen phosphorylase showing enhanced binding of fluorinated compounds⁴⁰

The 2-fluoro- β -glucosyl fluoride **1.18** was also shown to be a potent inhibitor of β -glucosidase in brain, liver, spleen and kidney tissues.⁴¹ This indicates distribution of the compound and in particular, transport across the blood/brain barrier. Inhibition was attributed to the accumulation of relatively stable 2-fluoroglucosyl-enzyme intermediates.

Guanosine diphosphate(GDP)-mannosyl hydrolase catalyses the hydrolysis of GDP-mannose. The 2-deoxy-2-fluoro-(GDP)-mannose has a 16-fold reduced k_{cat} and 2.5-fold higher K_M compared to GDP-mannose, for this hydrolase enzyme.⁴² This was used as evidence to support a dissociative mechanism, given the destabilisation of a cation that would occur in the presence of a fluorine atom.

Recent examples of increased binding of fluorinated carbohydrates include a fluorinated oligosaccharide, found to have enhanced binding to the pathogenic protein TgMIC1 (protozoan parasite) compared to the natural substrate.³⁷ A hydroxyl group was replaced by a fluorine atom to probe adhesion, with the fluorinated ligand enabling ^{19}F NMR studies. Substitution of a ribosomal hydroxyl group by a fluorine atom was found to be much more effective at stabilising the complex than inserting a hydrogen atom.⁴³ Results were consistent with a C–F \cdots H–N weak hydrogen bonding type interaction.

Enhanced binding from fluorination is also seen with the human erythrocyte glucose transporter protein. The interaction of 3-deoxy-3-fluoroglucose (**1.20**, **Figure 1.7**) with the transporter protein was investigated by an optical method based on the observation of sugar exit from preloaded erythrocytes.^{44,45} It was found that 3-fluoro-glucose (**1.20**) has equivalent binding to the glucose carrier to glucose (**1.14**).⁴⁵ This indicates the ability of F to substitute for OH, especially given the observed loss of affinity for 3-deoxyglucose.

More recently, the transport of 3-F-glucose (**1.20**) was compared to hexafluorinated pyranose **1.21**⁴⁶ by ^{19}F NMR studies, which were able to distinguish intracellular and extracellular resonances.³⁶ The permeability of hex-F-pyranose **1.21** was determined to be $9.5 \mu\text{m s}^{-1}$ (α) and $3.2 \mu\text{m s}^{-1}$ (β), compared to 3-F-glucose (**1.20**), $0.58 \mu\text{m s}^{-1}$ (α) and $0.44 \mu\text{m s}^{-1}$.⁴⁶ This indicated a transport rate in the region of tenfold higher than 3-F-

glucose, and by inference therefore glucose. This is despite the loss of stereochemical information, the significance of which is apparent from the low transport speed of galactose (**1.19**).⁴⁵

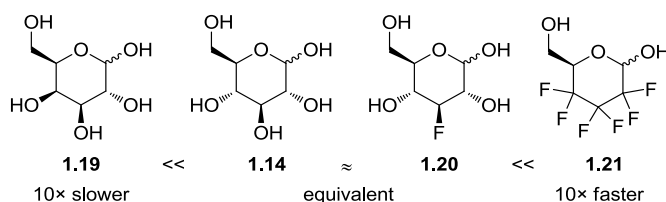


Figure 1.7 Relative transport rates through the red blood cell membrane⁴⁶

Several control experiments were used as evidence that greater transport was due to enhanced binding affinity and not simply increased lipophilicity.⁴⁶ These included reducing the temperature from 37 °C to 25 °C, which resulted in no observed transport of **1.21**. Exchange based on diffusion should be only reduced by 4%. Also, exchange of **1.21** was reduced by a factor of 3 after introduction of a known inhibitor of glucose efflux.

Further investigation of fluorinated hexose analogues with respect to the above glucose transporter comes with the synthesis of 2,3,4-trifluorinated glucose (**1.22**) and altrose (**1.23**) (**Figure 1.8**).⁴⁷ Both compounds were found to transport less well than glucose. However, the glucose analogue (**1.22**) was transported ~70% better than the altrose (**1.23**), indicating that the protein was able to recognise the stereogenicity associated with the C–F bonds.

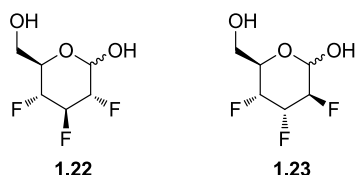


Figure 1.8 2,3,4-Trifluoro analogues of glucose and altrose⁴⁷

1.3 Carbohydrates

Carbohydrates have been identified as essential in a large variety of processes required by living cells and organisms.^{48,49} They are found in several forms, including monosaccharides, oligosaccharides, polysaccharides, glycosides and glycoconjugates, the latter two of which contain sugars covalently bonded to an aglycon. Key events in which carbohydrates are required include development, growth, function and survival of organisms or cells.^{48,50} It is due to this involvement that they have been utilised frequently and effectively to investigate and influence biological processes.⁵¹ Glycosylated medicinal compounds include antitumor agents, antibiotics, antiparasitics, antivirals, antifungal agents

and cardiac glycosides.⁵² A key target for therapeutic agents also involves the synthesis of carbohydrate mimics to imitate protein-carbohydrate interactions.^{53,54}

Carbohydrates are also frequently used as probes to investigate protein-carbohydrate interactions.^{12,40,55,56} Indeed, the use of synthetic sugar derivatives is one of the main modes of investigating protein-carbohydrate interactions, other than site-directed mutagenesis.

The predominant interactions by which saccharides bind to proteins are hydrogen bonding, metal association, hydrophobic packing and ionic interactions.⁵⁴ Carbohydrates possess numerous hydroxyl groups, most of which are stereochemically defined. Each hydroxyl is capable of participating in up to three hydrogen bonds (1 donor, 2 acceptors). As hydrogen bonds are highly directional, this generally confers a very high degree of selectivity to carbohydrate based molecular interactions.⁵⁷

Typically, hydrophobic interactions (which are vital in many drug/receptor interactions) provide a much greater binding affinity enhancement than hydrogen bonding interactions. Hydrophobic interactions have been described as providing a minimum of 3.2-fold increase in affinity per methyl group, while neutral hydrogen bonds contribute in the region of zero and 15-fold. Indeed, specificity is also not only due to hydrogen bonding, but often due to the spatial requirements of hydrophobic binding.⁵⁸

In carbohydrates, binding affinity is often low, due to the scarcity of hydrophobic groups. Also, any hydrogen bonds in sugar-protein interactions receive competition from the aqueous solvent.^{54,59} The replacement of hydrogen bonds to many water molecules by similar interactions with a binding site does not have a significant energetic benefit. This is complicated further by the fact that many interactions rely on water-mediated hydrogen bonds.^{12,54}

Although hydrogen bonding provides high specificity, desolvation of the limited hydrophobic surface areas is the main driving force for binding affinity.^{60,61} This can explain the regularly observed increase in binding when a ligand is made more lipophilic.^{61,62} Davis *et al.* describe the hydrophobic areas above and below the ring of glucose (**1.14**, **Figure 1.9**) as being fundamental to binding.^{63,64} They have demonstrated this by the design and synthesis of carbohydrate receptors. These compounds were able to bind monosaccharides via CH- π interactions, even in aqueous medium.

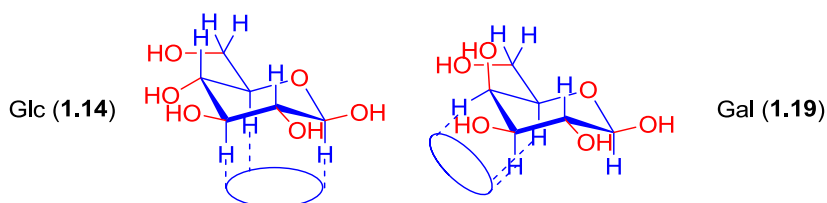


Figure 1.9 Representation of hydrophobic surface areas of glucose and galactose

1.4 Fluorinated Carbohydrates for the Investigation of *Polar Hydrophobicity*

1.4.1 Polar Hydrophobicity

A proposed explanation for the increased binding affinity of polyfluorinated carbohydrates (such as **1.21**) is known as polar hydrophobicity. As mentioned previously, fluorocarbons have a large hydrophobic surface area, which enhances the entropic term on binding proteins in aqueous medium. In addition, fluorine has the potential to form attractive dipolar interactions with a binding site, as already discussed. The combination of these effects has been termed *polar hydrophobicity* by DiMagno⁶⁵ and represents a strategy towards the enhancement of carbohydrate–protein binding.

1.4.2 Tetrafluorinated Carbohydrates

To further investigate polar hydrophobicity and the potential of polyfluorinated carbohydrates as ligands of improved binding, the synthesis of tetrafluorinated sugars (including **1.24** and **1.25**, **Figure 1.10**) was carried out.⁶⁶

Sugars containing the CF_2CF_2 moiety are well placed to study polar hydrophobicity and carbohydrate-protein interactions. They contain a heavily enough fluorinated region to give rise to a large hydrophobic surface area. However, unlike hexafluoro compound **1.21**, they maintain a stereochemically defined hydroxyl group in the ring. This may be important for binding selectivity, via involvement in highly directional hydrogen bonding interactions.

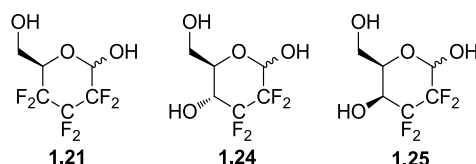


Figure 1.10 Comparison of hexafluoro and tetrafluoro monosaccharides

The steric consequences of replacement of CHOH with CF_2 are not too large. The comparative bond lengths, van der Waal's radii² and overall size are shown in **Figure 1.11**.

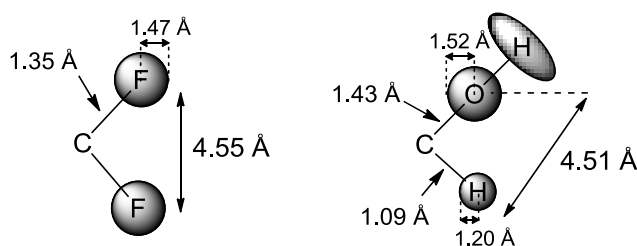


Figure 1.11 Comparison of sizes of CF_2 and CHOH moieties

1.4.3 Nomenclature of Tetrafluorinated Carbohydrates

The nomenclature for describing carbohydrates in which a CHOH has been replaced by a CHF is relatively straightforward. These have been described as x-deoxy-x-fluoroglycopyranose, using a parent sugar name (e.g. glucose) to describe the stereocenters present (see **1.16** and **1.22**, **Figure 1.12**). However, the nomenclature for carbohydrate analogues employing the CF₂ moiety does not follow the same pattern. IUPAC states that “if ‘deoxy’ removes a centre of chirality, the resulting names contain stereochemical redundancy”.⁶⁷ In these cases, the stem name must be chosen so as to describe the configurations at the asymmetric centres. Achiral centres are ignored for the purpose of assigning the parent name.

The stem is used from the aldose containing the reduced number of stereocenters and the achiral carbon atoms are described by using the deoxy prefix in combination with a descriptor of the total number of carbon atoms (e.g. hexo).

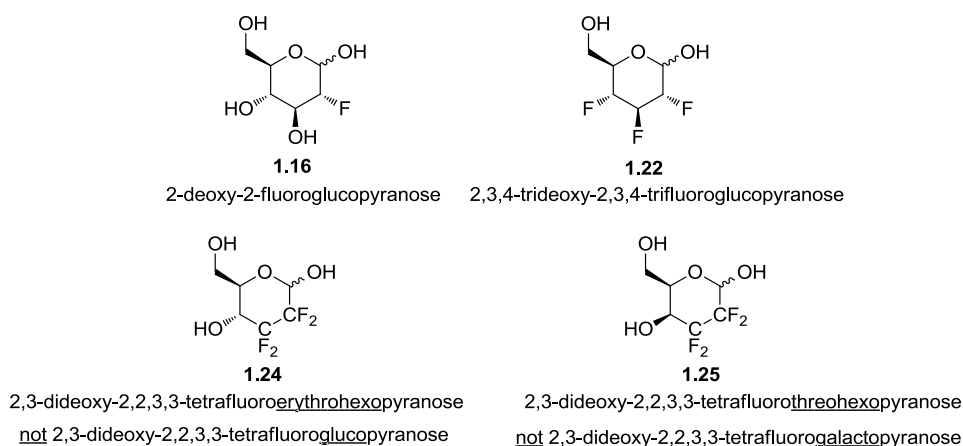


Figure 1.12 Nomenclature of fluorinated carbohydrates

Therefore, tetrafluoroglucose **1.24** should actually be described as an erythrohexose, while tetrafluorogalactose **1.25** should be described as a threohexose (**Figure 1.12**). These terms indicate the stereocenters that are present without describing those that have been removed.

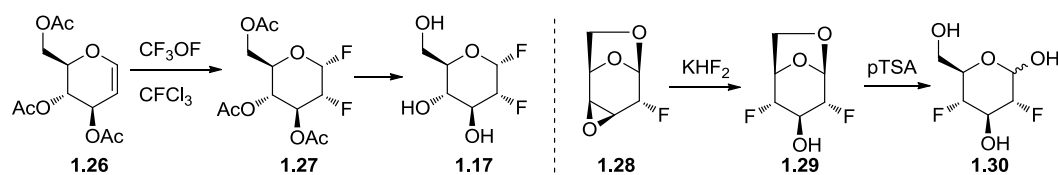
However, the system used to name compounds in this thesis will continue to follow the trivial names of the parent sugars for which the compounds are designed as analogues. This decision has been made so as to increase the ease of comprehension for the reader.

1.5 Synthesis of Polyfluorinated Carbohydrates

1,2-Difluoroglucose analogue **1.17** has been prepared from galactal **1.26** using trifluoromethyl hypofluorite, as shown in **Scheme 1.2**.⁶⁸ 2,4-Difluoroglucose (**1.30**) was synthesised from anhydro sugar **1.28** using potassium bifluoride.⁶⁹ The synthesis of 2,3- or

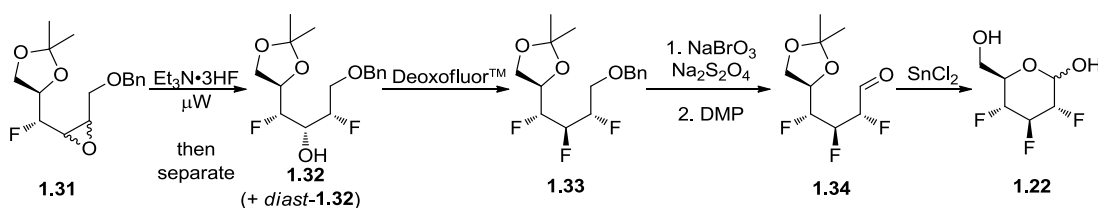
3,4-difluoro hexopyranoses is not reported in the literature, though late stage anhydro intermediates have been reported.⁷⁰

Scheme 1.2 Syntheses of difluoro glucose analogues^{68,69}



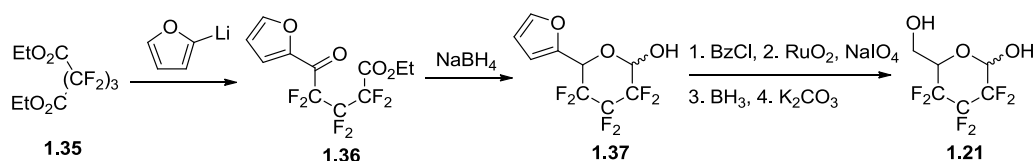
The synthesis of 2,3,4-trifluoroglucose **1.22** is shown in **Scheme 1.3**.⁴⁷ Epoxide **1.31** (synthesised in 4 steps from basic starting materials)⁷¹ is opened using $\text{Et}_3\text{N}\cdot 3\text{HF}$ as a fluoride source. This gives two diastereomers (**1.32**), which can be separated and fluorinated with DeoxofluorTM giving fluoride **1.33** with inversion of configuration. Debenzylation and oxidation provides aldehyde **1.34**, which cyclises on deprotection of the acetonide.

Scheme 1.3 Synthesis of 2,3,4-trifluoroglucose from epoxide **1.31**⁴⁷



Whereas the synthesis of trifluoroglucose **1.22** is complicated by the requirement for three fluorinations, each at a position with defined stereochemistry, hexafluoropyranose **1.21** does not have these constraints. Hexose **1.21** was synthesised from commercially available hexafluoro diester **1.35**,⁴⁶ as shown in **Scheme 1.4**. Reaction with furanyl lithium gives intermediate **1.36**, which is reduced with NaBH_4 . This allows cyclisation to give **1.37**. Protection of the hydroxyl is followed by oxidative cleavage to give the carboxylic acid, which is reduced to give the alcohol at C-6. Subsequent deprotection provides pyranose **1.21**.

Scheme 1.4 Racemic synthesis of 2,2,3,3,4,4-hexafluoropyranose⁴⁶

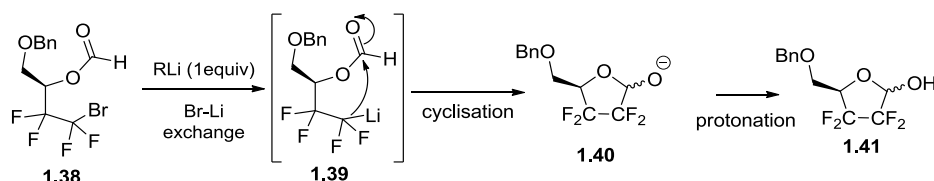


1.6 2,3-Dideoxy-2,2,3,3-Tetrafluoro Sugars

1.6.1 Halogen-Metal Exchange Mediated Cyclisation

The synthesis of monosaccharides containing the tetrafluoroethylene moiety has been made possible by the utilisation of aldehydes' potential for trapping perfluoroalkyl lithiums.⁷² The intramolecular version of this reaction was developed in the Linclau group for the synthesis of carbohydrates containing the $-\text{CF}_2\text{CF}_2-$ moiety.⁷³ As shown in **Scheme 1.5**, bromine-lithium exchange of perfluoroalkyl bromide **1.38** provides the perfluoroalkyl lithium **1.39**, which can then cyclise onto the formic ester, to give **1.40**. Protonation during workup gives the desired sugar (**1.41**). Undesired side-reactions were minimised by optimisation of the reaction conditions, to ultimately use a single equivalent of methyllithium at -78°C .

Scheme 1.5 Mechanism and some possible products of the anionic cyclisation⁷³



This reaction permits the synthesis of several 2,2,3,3-tetrafluoro saccharides, including the ribofuranose analogue **1.41** (**Scheme 1.5**) and also the examples shown in **Figure 1.13**. Ribopyranose **1.42** and fructofuranose (**1.43**) and fructopyranose (**1.44**) were synthesised via similar routes,⁷⁴ while the synthesis of glucose **1.24** and galactose **1.25** required the incorporation of an additional stereocenter.⁶⁶

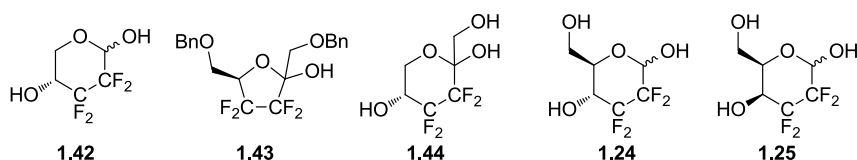
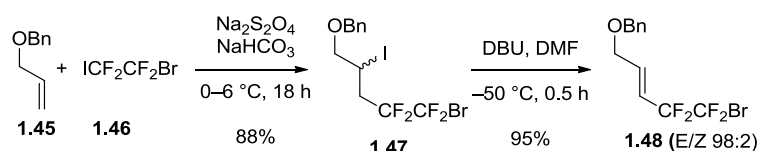


Figure 1.13 2,2,3,3-Tetrafluoro sugar analogues

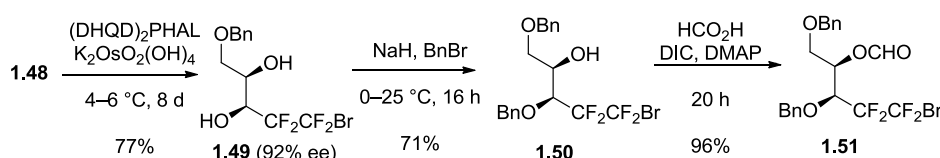
1.6.2 Synthesis of 2,2,3,3,-Tetrafluoro- Glucose and Galactose

The syntheses of tetrafluoro- glucose (**1.24**) and galactose (**1.25**) analogues diverge from the same key intermediate. The tetrafluoroethylene unit is incorporated in the first step, via the radical mediated addition of 1-bromo-2-iodotetrafluoroethane (**1.46**) across the double bond of allyl benzyl ether (**1.45**) (**Scheme 1.6**). The radical reaction is initiated by sodium dithionite, which forms $\text{SO}_2^{\cdot-}$. The resultant iodide (**1.47**) is eliminated with high *E/Z* selectivity to give *E*-alkene **1.48**.

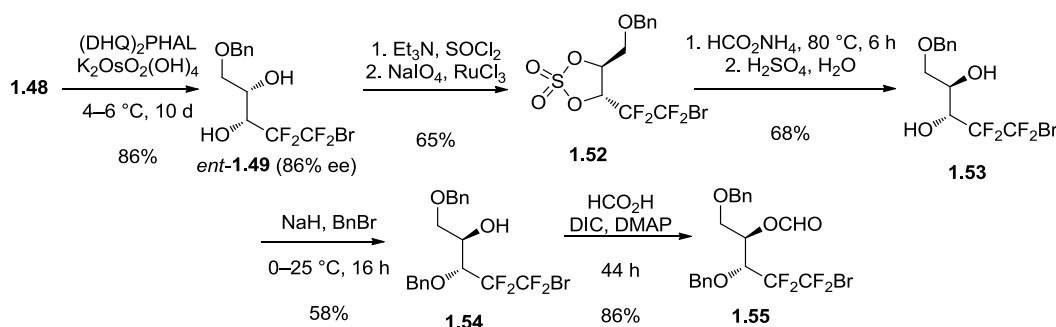
Scheme 1.6 First steps towards tetrafluoro galactose and glucose

The galactose synthesis proceeds by a modified β -Sharpless Asymmetric Dihydroxylation (AD) to obtain diol **1.49** in high enantiomeric excess (*e.e.*) (**Scheme 1.7**). Utilisation of the (DHQD)₂PHAL (dihydroquinidine₂phthalazine) ligand provides an *e.e.* of 92%. This can be increased by using (DHQD)₂AQN (anthraquinone), which gives 96% *e.e.*, though the yield for this ligand was only 67%.

The increased acidity of the hydroxyl group proximal to the perfluoroalkyl group is exploited in a selective monobenylation to give **1.50**. The remaining hydroxyl group is then formylated using standard conditions to give cyclisation precursor **1.51**.

Scheme 1.7 Steps towards the tetrafluoro galactose (**1.25**)

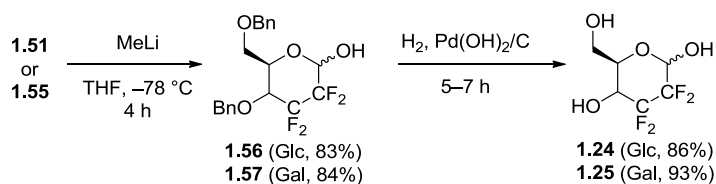
As glucose is the C4-epimer of galactose, some extra steps are required to install the desired stereochemistry of the tetrafluoro analogue. In this case, the α -Sharpless AD provides the enantiomeric form of diol **1.49** (**Scheme 1.8**). The cyclic sulfate (**1.52**) is then formed in two steps, allowing S_N2 ring opening by ammonium formate, which is hydrolysed (along with the sulfate) to give diol **1.53**, which has the stereochemistry required for the final product. Monobenylation and formylation (as with the galactose) then provide formate **1.55** as a suitable substrate for the anionic cyclisation.

Scheme 1.8 Steps towards the tetrafluoro glucose (**1.24**)

The subsequent cyclisations proceed for both formates (**1.51** & **1.55**) with high yields and by-products minimised (**Scheme 1.9**). Deprotection of the benzyl groups was achieved

using hydrogenolysis with Pearlman's catalyst ($\text{Pd}(\text{OH})_2/\text{C}$), which gives the desired glucose (**1.24**) and galactose (**1.25**).

Scheme 1.9 Anionic cyclisations to form tetrafluoro- glucose (**1.24**) and galactose (**1.25**).⁶⁶

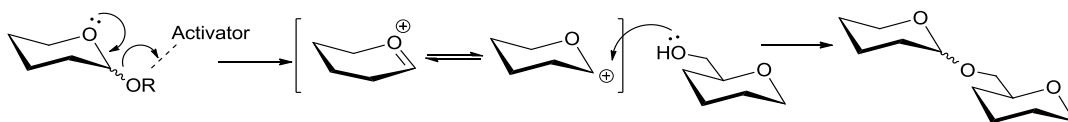


1.7 Glycosylation of 2,3-Difluoro Sugars

Glycosylation is possibly the most important reaction in sugar chemistry. The standard means of glycosylation involve the combination of a glycosyl donor, a glycosyl acceptor and an acid activator. The glycosyl donor is a sugar, often activated at the anomeric position by a leaving group, which is used in conjunction with a promoter. The requirement for the acceptor is simply the possession of a hydroxyl group that will act as the nucleophile in the reaction.

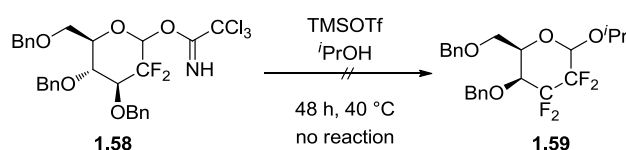
Mechanistically, several factors can influence the route of glycosylation, such as the leaving group, neighbouring group participation (anchimeric effect) and the anomeric effect.⁷⁵ It is commonly proposed that glycosylation proceeds via an S_N1 mechanism, as shown in **Scheme 1.10**, though the oxonium ion has never been observed spectroscopically. There are also occasions where an S_N2 explanation is more likely.⁷⁶

Scheme 1.10 A mechanistic explanation of chemical glycosylation via S_N1



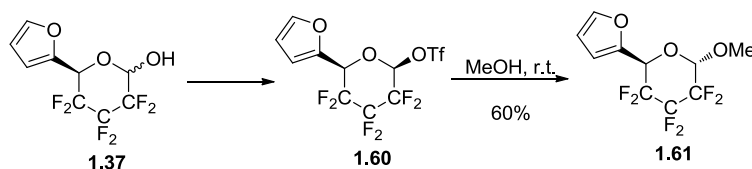
The electron withdrawing effect of fluorine atoms has a negative impact on nucleophilic substitution reactions. This has been identified as the cause of difficulties associated with glycosylation of 2,3-difluorinated carbohydrates. This is borne out by examples such as trichloroacetimidate **1.58**, as shown in **Scheme 1.11**.

Scheme 1.11 Example of unreactivity of 2,3-difluoro sugars to glycosylation⁷⁷



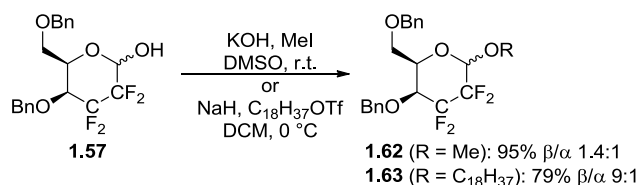
An example of a successful glycosylation of a 2,3-difluoro sugar brings us back to hexafluorohexose **1.21**, mentioned earlier. DiMagno *et al.* used a key intermediate (**1.37**) to develop a method for glycosylation. The glycosylation was achieved via solvolysis of the triflate, using methanol, ethanol and 222-trifluoroethanol.⁶⁵

Scheme 1.12 Glycosylation by solvolysis of a hexafluorohexose⁶⁵



The glycosylation of the aforementioned 2,2,3,3-tetrafluoro sugars has been achieved via anionic methods (i.e. the deprotonated anomeric hydroxyl is the nucleophile).⁶⁶ The reaction was carried out by using a base and an alkyl iodide or triflate (**Scheme 1.13**).

Scheme 1.13 Anionic Alkylation (Glycosylation)⁶⁶

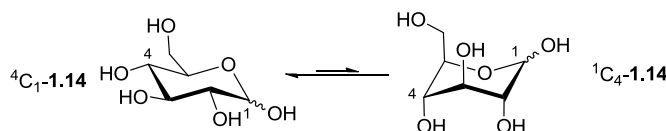


While the anionic method is a viable means to gaining access to alkyl glycosides of 2,2,3,3-tetrafluoro sugars, it requires an activated electrophile. Also, control of anomeric selectivity can be very important in glycosylation.

1.8 Conformation of Carbohydrates

It is generally accepted that the conformation of carbohydrates plays an important role in molecular recognition.⁷⁸ For most hexoses, the equilibrium lies towards the ⁴C₁ chair conformation (**Scheme 1.12**, left), though it is possible for unfavourable 1,3-diaxial interactions to lead to an inversion to the ¹C₄ conformation (**Scheme 1.12**, right).

Scheme 1.14 Common chair conformations



Conformational analysis by means of X-ray diffraction has been carried out on hexafluoropyranose **1.64**⁴⁶ and trifluoro glucose (**1.22**) and altrose (**1.23**)⁴⁷ (**Figure 1.14**).

These analyses showed that these three polyfluorinated sugars do adopt the 4C_1 chair conformation with minimal distortion (**Figure 1.15**).

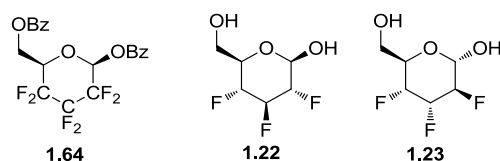


Figure 1.14 Polyfluorinated carbohydrates for which crystal structures have been determined^{46,47}

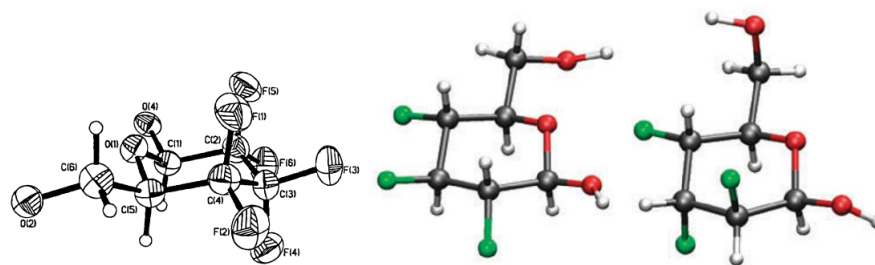


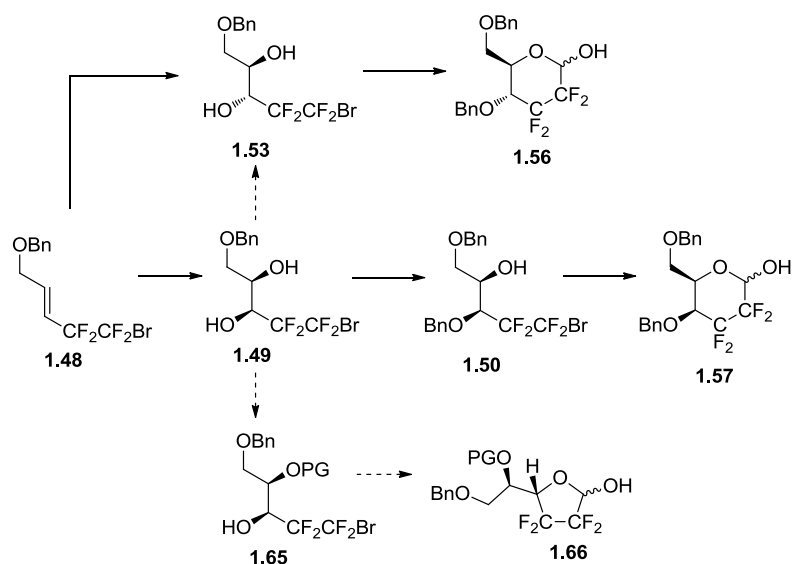
Figure 1.15 Crystal structures of the compounds shown in **Figure 1.14**. Left to right: **1.64** (benzoates omitted for clarity); **1.22** (β -glucose); **1.23** (α -altrose).

1.9 Aims

1.9.1 Fluorinated Monosaccharide Targets

The main objective of this project is the synthesis of tetrafluorinated carbohydrates so as to contribute towards investigation of the effect of polyfluorination on protein-carbohydrate recognition. This project will focus on 2,2,3,3-tetrafluorinated analogues of D-galactose and D-glucose. Extensive work has already been carried out on the 2,2,3,3-tetrafluoro analogues of these sugars in their pyranose forms (**1.56** & **1.57**, **Scheme 1.15**). The large scale synthesis of these compounds will be attempted, so as to enable further work on derivatisations, structural analyses and biological screening. Efforts will be made to further optimise the syntheses with particular focus on the inversion methodology required for the glucose analogue.

A new synthetic target is the furanose analogue of the galactose (**1.66**). The significance of galactofuranose in nature is detailed in **Section 6.1**. The synthesis of tetrafluorogalactofuranose **1.66** is envisaged via selective protection of diol **1.49**.

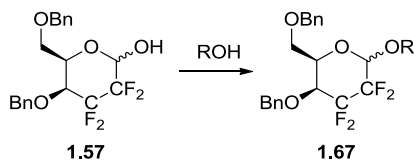
Scheme 1.15 Target Sugars

1.9.2 Structural Studies

As described above, conformation plays an important role in protein-carbohydrate recognition events. In this vein, it is very important to investigate whether our tetrafluoro analogues adopt conformations akin to the non-fluorinated substrates.

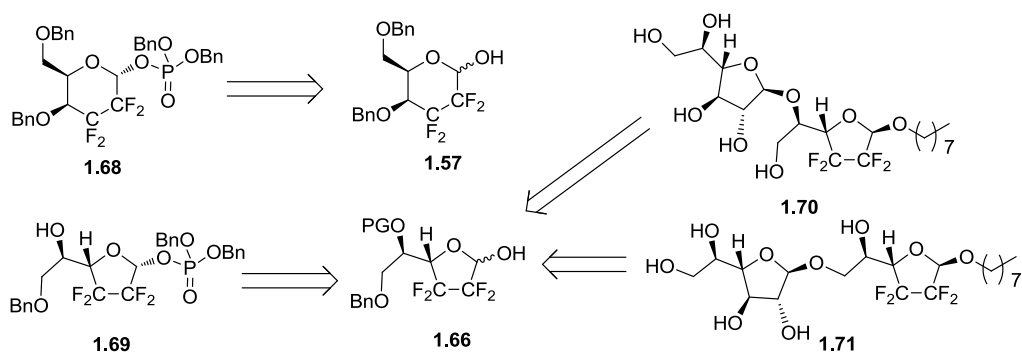
1.9.3 Glycosylation

So as to enable easier incorporation of our fluorosugars into more complex structures that may represent analogues of biological processes, the aim is to investigate alternative methods of glycosylation. This will focus on the development of a method that uses the fluorosugar as the electrophile in combination with an alcohol (**Scheme 1.16**).

Scheme 1.16 Proposed glycosylation of 2,2,3,3-tetrafluorogalactose

1.9.4 Synthesis of Tetrafluoro Analogues of Known Inhibitors of Mycobacterial Biosynthesis

The final aim of this project is to utilise the tetrafluoro sugars for the synthesis of analogues of bioactive compounds. Synthetic targets include phosphate intermediates **1.68** and **1.69** (**Scheme 1.17**) and disaccharides (**1.70** and **1.71**).

Scheme 1.17 Selective tetrafluoro galactose derivative targets

Chapter 2. The Synthesis of Tetrafluorinated Galactose Derivatives

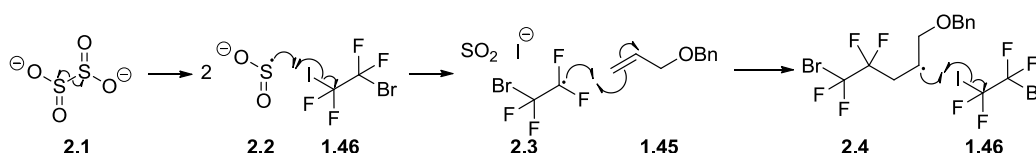
2.1 2,3-Dideoxy-2,2,3,3-Tetrafluorogalactopyranose

As described in **Section 1.6**, we already have access to an acceptable synthesis of the tetrafluorogalactose (**1.57**). However, further desired optimisations would include increasing the *e.e.* (currently 92–96%) and optimisation of moderately yielding steps such as the dihydroxylation (currently 67–77% yield) and benzylation (71%). In addition, access to larger quantities of the tetrafluorogalactose required upscaling of the synthesis. Hence, optimisation of the large-scale synthesis is reported herein.

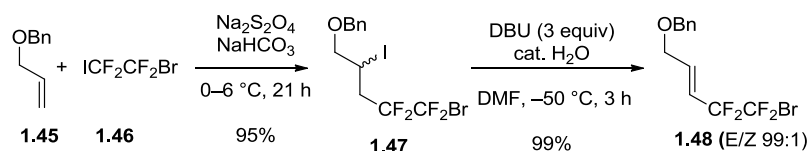
2.1.1 Commercial Starting Materials to Tetrafluoro Alkene 1.45

The first step is the dithionite mediated addition between 1-bromo-2-iodotetrafluoroethane (**1.46**) and allyl benzyl ether (**1.45**) (**Scheme 2.2**). These are typical reaction conditions used to generate perfluoro alkyl radicals which can then react with alkenes. The reaction proceeds by a radical mechanism, initiated by $\text{SO}_2^{\bullet-}$ (**2.2**), which is formed by homolysis of $\text{Na}_2\text{S}_2\text{O}_4$ (**2.1**) in acetonitrile,⁷⁹ as depicted in **Scheme 2.1**. Initiation by the thionite radical anion **2.2** generates the RCF_2^{\bullet} (**2.3**) by single electron transfer (SET) to the electropositive iodine atom. The resultant radical (**2.4**) abstracts an iodine atom from the perfluoroalkyl starting material (**1.46**) to regenerate the RCF_2^{\bullet} radical. This reaction was achieved to a 95% yield on an 86 g (200 mmol) scale (**Scheme 2.2**).

Scheme 2.1 Radical mechanism towards the formation of iodide **1.47**



The subsequent elimination step to form alkene **1.48** initially brought much lower yield than was achieved by the previous researcher within the group (88%).⁶⁶ High conversion is desirable as the separation of the product (**1.48**) and starting material (**1.47**) is very difficult. Several attempts were made to increase the degree of conversion; however this was not achieved until a reaction was carried out starting from a batch of iodide **1.47** that had been recovered from a dihydroxylation reaction that used impure alkene.

Scheme 2.2 First steps of 4FGal p synthesis optimised on large scale

It was realised that this iodide was contaminated with ~5 mol % of diol **1.49**. Whereas up to now great care had been taken to use anhydrous DMF, this observation suggested that added water could be advantageous. Indeed, repeating the reaction with the addition of a similar amount of water gave comparable results. Ultimately, it was found that the best conversion was achieved when no water was added, but when the reaction solvent was exchanged from extra dry DMF (<0.005% H₂O) to laboratory grade DMF (<0.2% H₂O). These conditions gave 99% yield of **1.48** on a 23 g (50 mmol) scale, with 99:1 *E/Z* selectivity (**Scheme 2.2**). It is possible that the combination of a trace amount of water and excess DBU (3 equivalents) generates HO[−], which can act as a catalytic base.

2.1.2 Asymmetric Dihydroxylation

The Sharpless AD was optimised by the previous researcher to accommodate for its lower reactivity due to the electron-poor nature of alkene **1.48**. Standard conditions generally employ 1 mol% of ligand with 0.2 mol% of osmium catalyst and a reaction time of around 24 h.⁸⁰ Optimisations for this alkene (**1.48**) had included using a higher ligand and catalyst loading (2 mol% and 0.8 mol% respectively) and a longer reaction time (8 days). A number of asymmetric ligands employing different spacer units were also tried and found to give different levels of enantiopurity. Herein is described additional work carried out to increase the enantiomeric excess further.

Determination of *e.e.* was carried out by chiral analytical HPLC. Although the method was already optimised by the previous researcher in the group,⁶⁶ a higher resolution was required to enable accurate measurement of very high enantiopurities. The optimum conditions that were found employed hexane/IPA (95:5) as eluent, 3 mg mL^{−1} of sample and a flow rate of 1 mL min^{−1}, the combination of which gave good baseline separation. **Figure 2.1a** shows the HPLC trace of the racemate (*rac*-**1.49**), with retention times of 18 and 20 min for **1.49** and *ent*-**1.49**, respectively.

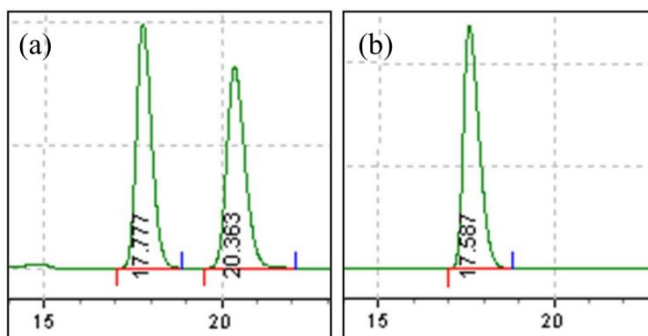


Figure 2.1 Analytical chiral HPLC of diol **1.49**: (a) Racemate; (b) **1.49**

The use of (DHQD)₂AQN as the ligand gave the highest *e.e.* (97%), while (DHQD)₂PHAL gave only 92%. We have now shown that it is possible to access >99% *e.e.* (**Figure 2.1b**) by recrystallisation of the diol. The white solid obtained after chromatographic purification was suspended in hexane then heated to 40 °C. Diethyl ether was added until dissolution. After several days, crystals were filtered off and washed with hexane. The reaction has now been optimised to give a 93% yield on a 25 g (75 mmol) scale (**Scheme 2.3**). The recrystallisation was realised with a yield of 80%, which denotes an overall yield of 75%. In addition, recovery of the mother liqueur provides more diol of inferior *e.e.*, which can then be recrystallised again to increase the enantiopurity.

The workup has also been modified to facilitate recovery of the expensive ligand.⁷⁴ This was achieved by initial extraction of the reaction mixture with EtOAc, followed by washing the organics with aqueous HCl. These extracts were neutralised, allowing for extraction of the ligand into EtOAc, which was ready for re-use after chromatographic purification. Up to 92% of the ligand used could be recycled in this way. For optimal results, EtOAc must be used for the initial extraction rather than Et₂O as was used previously.

Scheme 2.3 Optimised asymmetric dihydroxylation

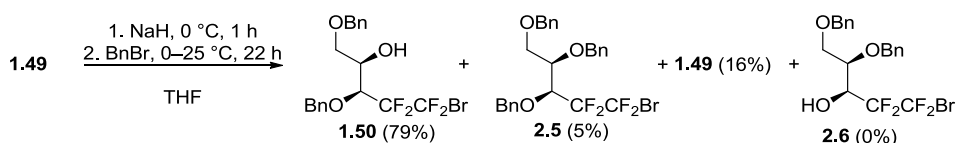


2.1.3 Benzylation, Formylation and Cyclisation

The selective benzylation is possible due to the increased acidity of the hydroxyl group proximal to the perfluoroalkyl moiety.^{66,81} Thus, deprotonation is carried out using 1 equivalent of a strong base (NaH) followed by treatment with an electrophile (BnBr). The reaction has now been performed on a large scale (12 g, 30 mmol), giving a 79%

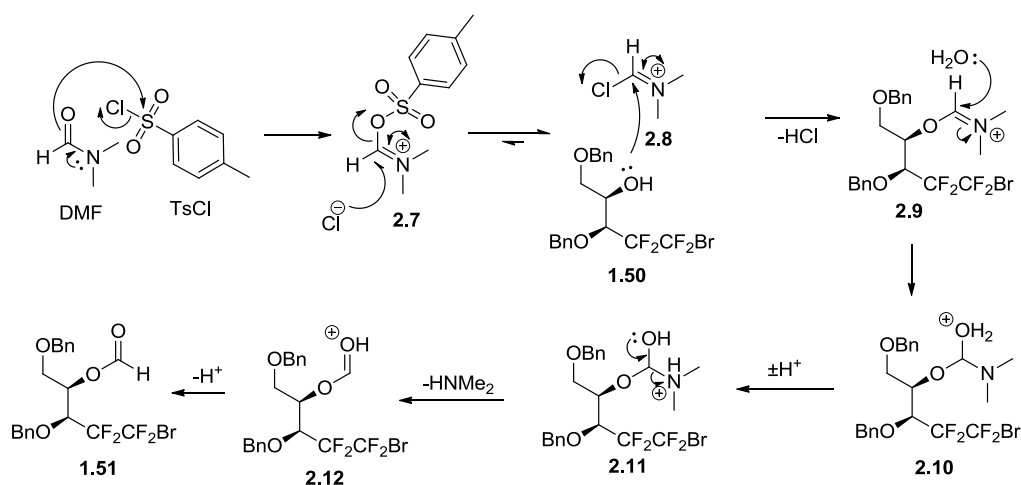
yield. The product of dibenzylation (**2.5**, **Scheme 2.4**) was also isolated in 5% yield, and 16% yield of starting diol was recovered. None of the undesired “reverse” monobenzylation product (**2.6**) has ever been observed.

Scheme 2.4 Selectivity of monobenzylation

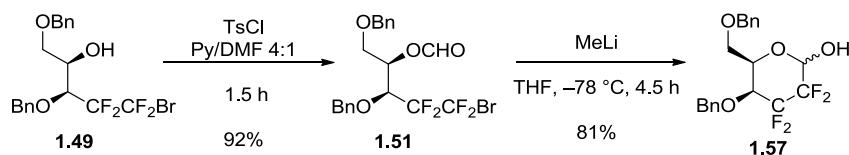


The next step is formylation of the remaining hydroxyl group in **1.50**. Although this was previously achieved using diisopropyl carbodiimide (DIC) and formic acid in the presence of dimethylaminopyridine (DMAP),⁶⁶ an alternative method has since been explored, based on the use of a Vilsmeier-Haack type⁸² intermediate (**Scheme 2.5**). DMF and tosyl chloride are stirred together in pyridine, allowing the formation of iminium salt **2.7**. Tosylate is then displaced by chloride and the resultant species (**2.8**) is activated sufficiently to be attacked by alcohol **1.50**. Aqueous workup allows hydrolysis and loss of dimethylamine, to give the formate **1.51**.

Scheme 2.5 Mechanism of TsCl/DMF enabled formylation



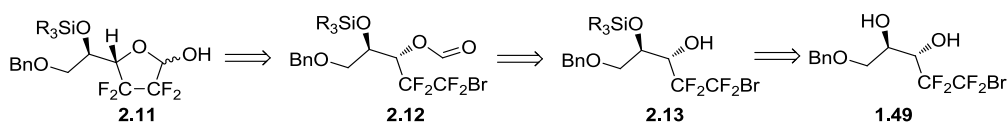
This reaction has been employed in favour of the DIC/HCO₂H method, as it is more reliable, efficient and uses cheaper reagents. In addition, the workup proved very simple, with a quick extraction into hexane providing clean product suitable for the next step. This reaction has been achieved to a 92% yield on a 12 g (25 mmol) scale (**Scheme 2.6**). The synthesis of formate **1.51** allowed the cyclisation to give pyranose **1.57**, which was achieved to a yield of 81% on an 11 g (20 mmol) scale and a 91% yield on a 1 g (2.5 mmol) racemic sample.

Scheme 2.6 New method of formylation, followed by the cyclisation

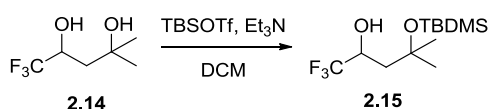
2.2 Synthesis of 2,3-Dideoxy-2,2,3,3-Tetrafluorogalactofuranose

Given the importance of galactosyl furanose containing glycosides and oligosaccharides (detailed in **Section 6.1**), we chose to investigate the synthesis of the furanose analogue of our tetrafluoro galactose.

The synthesis of 2,2,3,3-tetrafluorogalactofuranose (**2.11**) was envisaged via a selective protection of the hydroxyl group β to the perfluoroalkyl group (**Scheme 2.7**). Whereas the strong electron withdrawing character of the tetrafluoroalkyl group renders the hydroxyl group in the α- position more acidic, the nucleophilicity of this alcohol is reduced for the same reason. Thus, the hydroxyl more distant from the fluorination was expected to display greater nucleophilicity.

Scheme 2.7 Retrosynthesis of tetrafluorogalactofuranose (**2.11**)

Indeed, selective silylation of hydroxyl groups further from a fluorinated position has been achieved previously.^{83,84} An example is shown in **Scheme 2.8**, in which it can be seen that selectivity was observed for the hydroxyl further from the CF₃. This is a remarkable result, given tertiary alcohols are not easy to protect as TBDMS-ethers.

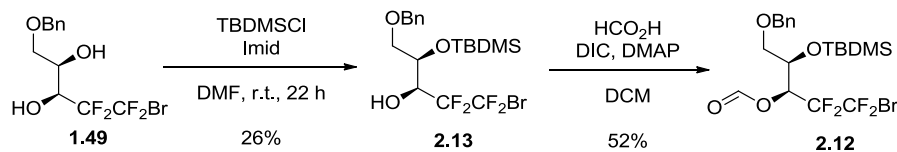
Scheme 2.8 Selective silylation of a fluorinated diol⁸⁴

2.2.1 Selective Silylation

The diol was initially subjected to standard silylation conditions (**Scheme 2.9**), which gave a relatively low yield (26%), though the reaction was fully selective. The identity of product **2.13** was confirmed by COSY NMR and analysis of the product of subsequent formylation (**2.12**). The quantity of base, time and temperature of the reaction were all

varied and imidazole also replaced by Et₃N and DMAP. However, the highest yield achieved was still only 34%.

Scheme 2.9 Initial silylation using TBDMS group



Following the low conversion, the slightly less bulky chlorotriethylsilane (TESCl) was used. Selected trials using this reagent are shown in **Table 2.1**. A trial using excess TESCl in DMF with imidazole (entry 1) resulted in over silylation to give bis-silyl product **2.18** in 50% yield. The reaction was repeated with only 1 equivalent of TESCl (entry 2), and the desired product (**2.16**) was formed, albeit in a low 26% yield. Imidazole was replaced with Et₃N/DMAP (entry 3), giving an acceptable 64% yield. However, the increased reactivity resulted in the formation of undesired side-products, regioisomer **2.17** and the product of bis-silylation (**2.18**). These products were minimised by performing the reaction at reduced temperature (entry 4), though the reaction time had to be increased. A reaction performed on 2 g (entry 5) gave a good yield of 81%. The reaction was also carried out on a much larger scale (20 g, 60 mmol), with the time extended to 3 days (entry 6), giving an 80% yield.

Table 2.1 Silylation using TESCl

Entry	TESCl (equiv)	Solvent	Base (equiv)	DMAP (equiv)	Temp (°C)	Time (h)	Yields (%)		
							2.16	2.17	2.18
1	1.2	DMF	Imid (2.5)	0	25	17	-	-	50
2	1.0	DMF	Imid (2.5)	0	25	25	26	-	-
3	1.0	DCM	Et ₃ N (1.2)	0.1	25	38	64	4	3
4	1.1	DCM	Et ₃ N (1.2)	0.1	5	47	56 ^[a]	2	3
5 ^[b]	1.1	DCM	Et ₃ N (1.2)	0.1	5	45	81	6	3
6 ^[c]	1.1	DCM	Et ₃ N (1.2)	0.1	5	70	80	6	10

[a] Part of compound lost prior to weighing; [b] 2 g scale; [c] 20 g scale

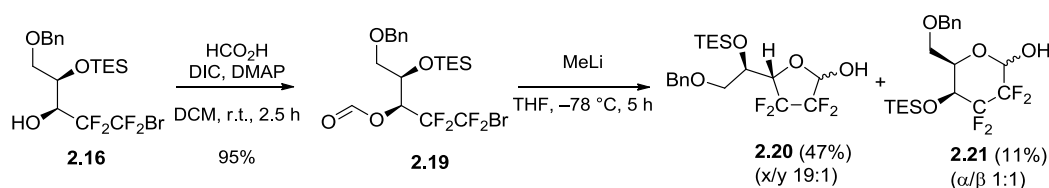
2.2.2 Furanose Synthesis

With access to the protected alcohol **2.16**, subsequent formylation was carried out with a yield of 95% on a 10 g (20 mmol) scale. Formic acid/DIC conditions were used, as

complete conversion with the tosyl chloride method could not be achieved. This is likely to be because of the reduced nucleophilicity due to closer proximity to the perfluoroalkyl group.

Anionic cyclisation (1 g, 3 mmol scale) gave desired furanose **2.20** in 47% yield (**Scheme 2.10**). Unusually, the proton NMR appeared to contain only one anomer, and a ratio of approximately 19:1 was visible in the fluorine NMR. Identification of which anomer is the major has not been possible due to overlapping peaks in the proton spectrum, which prevented a reliable NOE experiment.

Scheme 2.10 Synthesis of protected galactofuranose

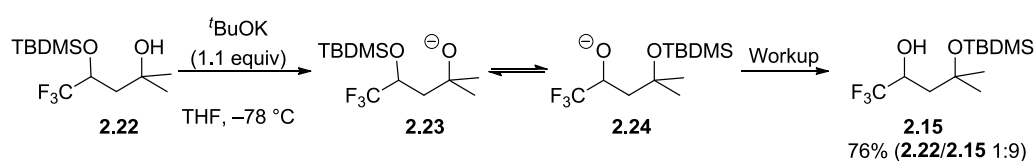


The yield of cyclisation was significantly lower than that achieved during the pyranose synthesis. This is partly due to the formation of by-product **2.21** in 11% yield. This compound is the pyranose isomer, whose formation can be explained by silyl migration during the reaction.

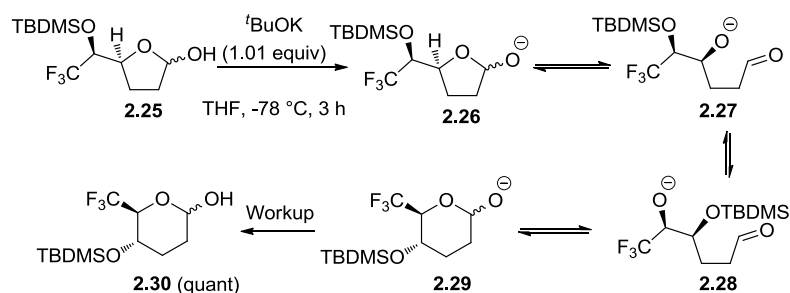
2.2.3 Silyl Migration Induced Isomerisation

The migration of silyl groups with respect to their vicinity to fluorinated carbons has been observed previously by Yamazaki *et al.* They described the conversion of **2.22** to **2.15** with $t\text{BuOK}$ (1.1 equiv), as shown in **Scheme 2.11**.⁸⁴

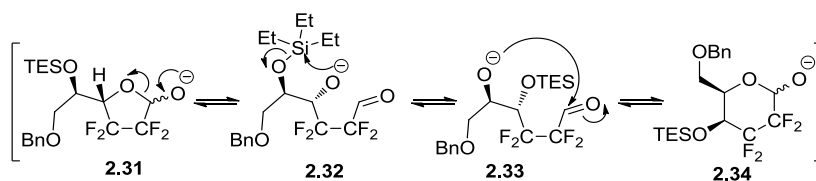
Scheme 2.11 Migration of silyl group from oxygen α to CF_3 to oxygen γ to CF_3



This can be rationalised by the greater stability of oxyanion **2.24** compared to **2.23**, as borne out by difference in pK_a between propan-2-ol (16.5) and 2,2,2-trifluoroethanol (12.5). Fast isomerisation of furanose **2.25** to pyranose **2.30** was also observed (**Scheme 2.12**). Again, the silyl group favours the position further from the fluorination, leading to the formation of the most stable conjugate base (**2.28**) under thermodynamic equilibration conditions.

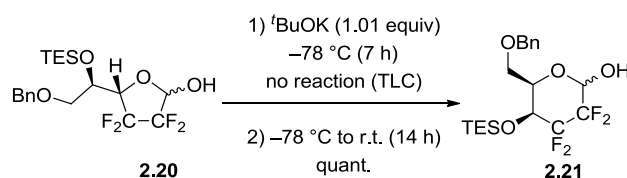
Scheme 2.12 Silyl migration induced furanose-pyranose isomerisation⁸⁵

A similar reasoning can be used to explain the formation of pyranose **2.21**. As described earlier, protonation only occurs during workup, so the species present in the reaction is oxanion **2.31** (Scheme 2.13). The silyl migration occurs when the furanose is in its acyclic form (**2.32**). In this case, the migration is towards the compound with the silyl group nearest the fluorination (**2.33**), which is contrary to the preferences seen above. Although the α -oxanion (**2.32**) is still the more stable of the two, under thermodynamic conditions the pyranose (**2.34**) is a lower energy configuration than the furanose (**2.31**).

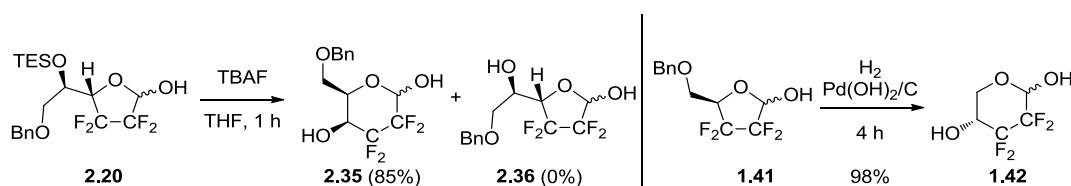
Scheme 2.13 Mechanism to explain the formation of pyranose **3.8**

The furanose/pyranose equilibrium is generally found to be towards the pyranose,⁸⁶ but in this case this effect is increased even further by destabilisation of the furanose form from the fluorine atoms. This is supported by additional isomerisation experiments that were carried out.

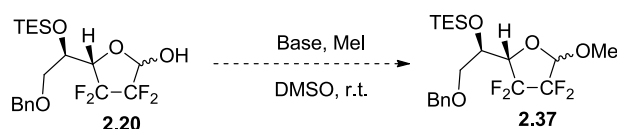
The literature isomerisation conditions (1 equiv $t\text{BuOK}$, THF, $-78\text{ }^{\circ}\text{C}$)⁸⁴ were applied to furanose **2.20** (Scheme 2.14). The reaction proceeded with little observable (TLC) conversion even after 7 h at $-78\text{ }^{\circ}\text{C}$. However, complete conversion took place after stirring overnight at room temperature. At reduced temperatures the energy barrier for the formation of **2.33** from **2.32** is not reached, however once the reaction was allowed to warm up, the greater stability of **2.34** compared to **2.31** governs the position of the equilibrium.

Scheme 2.14 Isomerisation of furanose **3.7** to pyranose **3.8**

Similar results can be seen upon removal of the silyl group. Deprotection gave rapid conversion to **2.35** (Scheme 2.15), with this being the sole compound isolated from the reaction. This fast isomerisation has also previously been demonstrated for tetrafluororibose **1.41**, to give pyranose **1.42** (Scheme 2.15).^{73,74}

Scheme 2.15 Furanose to pyranose isomerisations upon deprotection**2.2.4 Towards the Synthesis of an Alkyl Galactofuranoside**

The methylation of furanose **2.20** using anionic alkylation conditions⁶⁶ was attempted as described in Scheme 2.16 and Table 2.2.

Scheme 2.16 Methylation of tetrafluorogalactofuranose

Initially, the methylation was attempted using conditions employed for the methylation of galactopyranose **1.57** (entry 1). This resulted in removal of the silyl group and methylation of both remaining hydroxyls to give pyranose **2.38**. Interestingly, this was isolated as a single (β) anomer. In the next attempt (entry 2), the quantity of MeI and base were reduced, which did prevent dimethylation. Monomethylation was observed in 66% yield, but the silyl group had also been removed prior to methylation, resulting in the inevitable isomerisation to methyl pyranoside **2.39** (Figure 2.2) and 21% of the hemiacetal (**2.35**). The order of reagents was changed (entry 3), so that deprotonation would only be possible after the MeI was already present. This reduced the loss of the silyl group, but isomerisation to the pyranose was still prevalent under the basic conditions and so methyl pyranoside **2.40** and hemiacetal **2.21** were formed. For the final attempt, a milder base

(K₂CO₃) was used (entry 4). From this reaction, no desilylation was observed, but all compounds had again isomerised to their pyranose forms, before methylation.

Table 2.2 Methylation trials

Entry	MeI equiv	Base (equiv)	First Reagent	Time (h)	Isolated Yield (%)				
					β -2.38	2.39 (α/β)	2.35	2.40 (α/β)	2.21
1	8.0	KOH (4.0)	KOH	15	40				
2	1.1	KOH (1.1)	KOH	15		66 (0.7:1)	21		
3	1.1	KOH (1.1)	MeI	8		28 (0.9:1)	18	17 (1:0.9)	9
4	1.1	K ₂ CO ₃ (1.1)	MeI	4				20 (0.9:1)	25

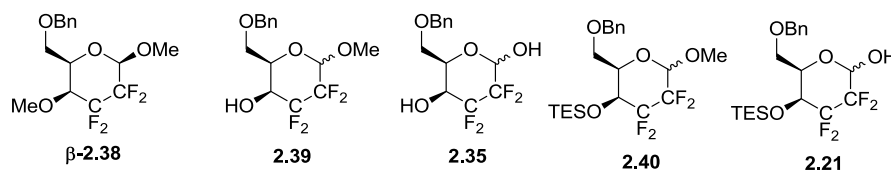
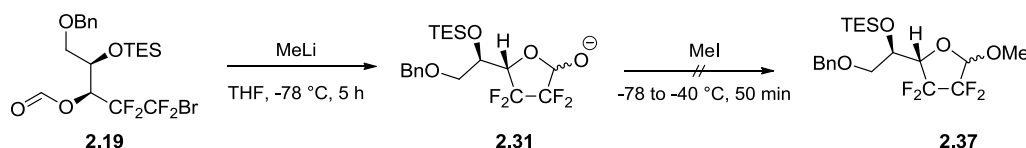


Figure 2.2 Undesired pyranose products isolated from the attempted methylation

In order to form the methyl galactofuranoside by an alternative strategy, the anionic cyclisation was carried out as normal, with MeI being added before the usual NH₄Cl quench. As the cyclisation should give the deprotonated furanose (**2.31**), addition of MeI could give rise to the methyl galactoside (**2.37**), as shown in **Scheme 2.17**. This reaction was attempted, but no methylation products were isolated, rather the usual yields of the hemiacetal furanose **2.20** (51%) and pyranose **2.21** (12%).

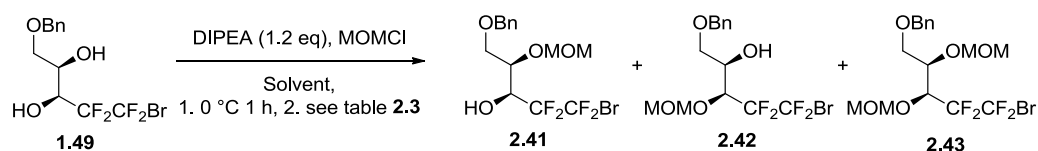
Scheme 2.17 Attempted one-pot cyclisation and methylation



2.2.5 Non-Migratory Protecting Group Strategy

The utilisation of the migratory silyl protecting group can be seen to have two major disadvantages: reduction of the cyclisation yield and prevention of the alkylation. It is for these reasons that the synthesis of 2,2,3,3-tetrafluorogalactofuranose was reinvestigated with a non-migratory protecting group.

Methoxymethyl (MOM) was chosen as this was foreseen to also be selective under nucleophilic conditions, to give **2.41**. Other possible products formed from this reaction include the undesired regioisomer **2.42** (**Scheme 2.18**) and the bis-MOM product **2.43**.

Scheme 2.18 Monomethoxymethylation of diol **1.49**

Utilisation of generic literature conditions⁸⁷ (entry 1, **Table 2.3**) gave the desired product in 14% yield after 25 h. The temperature was then increased to 40 °C (entry 2), which significantly improved the yield to 42%, though the two undesired by-products **2.42** and **2.43** were also isolated in low yields. In an attempt to increase conversion further, the temperature was raised to 80 °C (entry 3) but an inferior yield (21%) resulted, possibly due to the change of solvent. Entry 4 was carried out on a 5 g scale and included the addition of DMAP. This gave a better conversion to the product, but approximately one quarter of it could not be separated from the bis-product (**2.43**), which was formed in 16% yield. For entry 5 (performed on 6 g) the temperature was returned to r.t. with the aim of increasing selectivity. The reaction was allowed to continue for 5 days. This gave similar results to entry 2, but further progress was made with respect to the separation of **2.41** and **3.35**.

Table 2.3 Selected reactions towards optimisation of MOM protection

Entry	MOMCl equiv	DMAP equiv	Solvent	Temp (°C)	Time (h)	Crude Ratio (1.49/2.41/2.42/2.35) ^[a]	Isolated Yield (%)			
							1.49	2.41	2.42	2.43
1	1.1	0	DCM	25	25	66 : 26 : 8 : 1	34	14	-	-
2	1.2	0	DCM	40	17	31 : 51 : 7 : 11	30	42	3	8
3	2	0	DMF	80	32	67 : 28 : 0 : 2	43	21	-	2
4^[b]	1.5	0.1	DCM	40	20	11 : 67 : 5 : 17	15	65^[c]	3	16 ^[c]
5^[b]	1.2	0.1	DCM	25	124	34 : 52 : 8 : 6	31 ^[d]	50^[e]	9 ^[d]	7 ^[c]
6^[b]	1.2	0.1	DCE	83	5	11 : 73 : 11 : 5	11 ^[d]	70^[e]	11 ^[d]	5 ^[c]
7^[b]	1.2	0.1	DCE	83	15	8 : 75 : 11 : 6	9 ^[d]	68^[e]	11 ^[d]	7 ^[c]

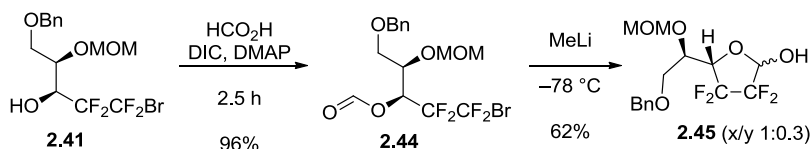
[a] Crude ¹⁹F NMR; [b] Gram or multigram scale; [c] **3.35** not separated from part of **3.33**; [d] **3.34** not separated from **1.46**

Optimisation of the reaction was attempted again using elevated temperatures (entries 6 & 7). On these occasions, a solvent more similar to DCM, 1,2-dichloroethane (DCE) was chosen. This gave moderately improved yields, with decreased formation of **2.43** and it was found that longer reaction time (i.e. overnight, entry 7) had little effect on the yields.

An attempt was made to synthesise the benzyloxymethyl (BOM) analogue, as this would allow global deprotection of the final sugar in a single step. However, this was much lower yielding and therefore not pursued.

The completion of the synthesis was thus commenced with the formylation of the remaining hydroxyl group (**Scheme 2.19**). After a few trials, 96% yield was attained on 3 g (8 mmol) and the observation was made that shorter reaction times provide better results. The anionic cyclisation to give **2.45** was realised on a 3 g (7 mmol) scale with a more acceptable 62% yield, (compared to 47% when the TES group was present).

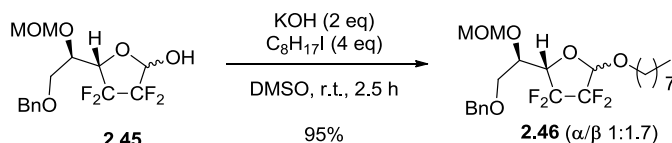
Scheme 2.19 Formylation and cyclisation



2.2.6 Alkyl Tetrafluorogalactofuranoside

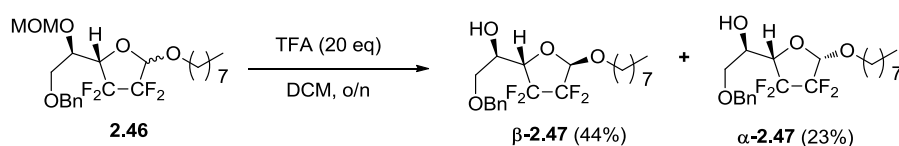
With the new, non-migratory protecting group in place, alkylation using basic conditions was achieved without difficulty to a 95% yield on a 1.5 g (4 mmol) scale (**Scheme 2.20**). This demonstrates another advantage of using the new protecting group strategy. Separation of the anomers was not possible at this stage.

Scheme 2.20 Alkylation of the MOM-protected furanose



For the removal of the MOM group, the use of AcOH/H₂O⁸⁸ resulted in no reaction overnight. However, trifluoroacetic acid (20 equiv)⁸⁹ was much more effective, with the resultant anomers (**Scheme 2.21**) being separable by HPLC (hexane/acetone 90:10). As predicted, the MOM group was selectively removed without reaction occurring at the anomeric centre and the benzyl group also remained in place. The identification of the anomers required Nuclear Overhauser effect (NOE) NMR spectroscopy (see below).

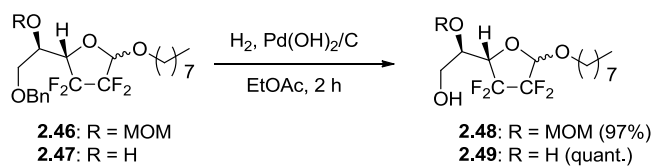
Scheme 2.21 Removal of MOM protecting group



The benzyl group was removed by hydrogenolysis to give **2.47** (**Scheme 2.22**), though the two anomers were not separable while the MOM group was still present. The benzyl

group can also be removed from compound **2.47**, to give fully deprotected octyl glycoside **2.50**.

Scheme 2.22 Debenzylations



The identity of the two isolated anomers was determined by 1D NOE NMR. This was used to observe the presence or absence of a through-space interaction between H-1 and H-4 (**Figure 2.3**).

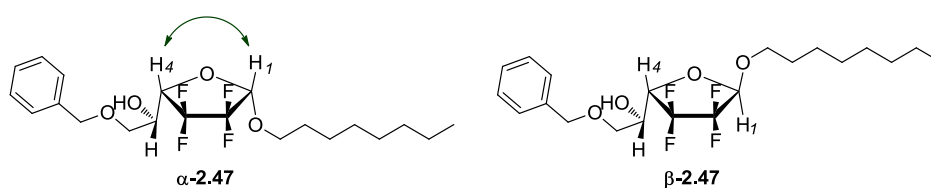


Figure 2.3 Alpha and beta octyl glycosides, showing key potential NOE interaction

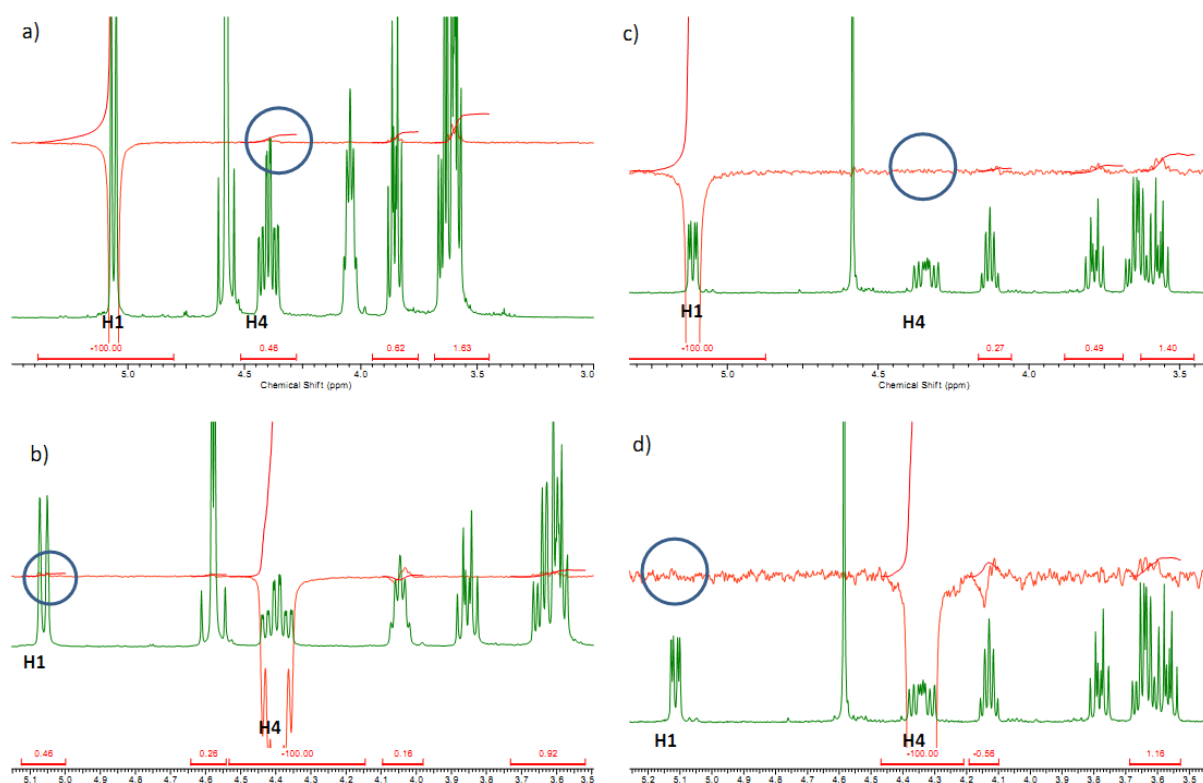


Figure 2.4 NOE NMR of $\alpha\text{-2.47}$ (a and b) and $\beta\text{-2.47}$ (c and d). Irradiation of H-1: a and c. Irradiation of H-4: b and d

The relevant protons were irradiated independently for both anomers, with the results shown in **Figure 2.4**. An interaction between the two protons is visible in the spectra on

the left (*a* and *b*), indicating that this is the alpha anomer, while no interaction is visible on spectra *c* and *d*, which confirms that this is the beta anomer.

2.3 Conclusions

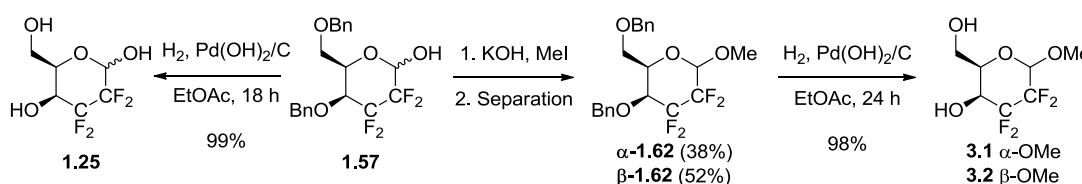
The synthesis of 2,2,3,3-tetrafluorogalactopyranose (**1.25**) has been optimised further. The desired compound is now available with an overall yield of 53%, or 43% for *enantiopure* material, which is accessed by recrystallisation of a key intermediate. The synthetic methodology for the synthesis of the novel compound, 2,2,3,3-tetrafluorogalactofuranose (**2.20** or **2.45**) has been developed and optimised. This synthesis can be achieved via the use of two differing protecting group strategies. Insights have also been gained into the migration of silyl groups with respect to proximity to fluorination (acidity) and furanose/pyranose isomerisation (configurational stability).

Chapter 3. Structural Studies

3.1 Methyl Galactosides

The importance of conformational analysis of novel carbohydrates is described in **Section 1.8** and hence, tetrafluorinated galactose and derivatives were studied by NMR spectroscopy and X-ray crystallography in order to find out about their conformation. The deprotection of benzyl protected **1.57** was achieved by hydrogenolysis to give fully deprotected tetrafluorinated galactose **1.25** in 99% yield on a 1 g (3 mmol) scale. In order to avoid complications arising from the analysis of a mixture of anomers, alkylation⁶⁶ was carried out to provide methyl galactosides **3.1** and **3.2** (**Scheme 3.1**). The two anomers can be separated by preparative HPLC (hexane/acetone 90:10), when carried out prior to removal of the benzyl groups.

Scheme 3.1 Synthesis of methyl galactoside anomers



3.1.1 Methyl Galactoside Anomers 600 MHz NMR

The solution phase conformation was investigated by NMR spectroscopy, which was performed externally by Prof. Hassan Oulyadi (Université de Rouen, France). Extensive ^1H , ^{13}C and ^{19}F studies in CDCl_3 and D_2O , including $^{19}\text{F}(^1\text{H}_x)$ double irradiation experiments facilitated the assignment of each coupling constant. These values were found to be consistent with both anomers (**3.1** and **3.2**) existing in a $^4\text{C}_1$ chair conformation in these solvents.⁹⁰ For both anomers, H-1 gave rise to a dd, due to vicinal coupling from F2ax and and long range w coupling to either F3eq or F3ax, depending on the orientation of H-1. No coupling was observed between H-1 and F2eq. Coupling between H-4 and H-5 was not present, or very small (1.1 Hz), which is consistent with those values observed for the non-fluorinated counterparts.

The conformation was further confirmed by 2D ^1H - ^{19}F Heteronuclear Overhauser Effect correlation spectroscopy (HOESY). Evidence includes the strong HOE observed between F-3ax and H-5 (for both anomers), as well as HOEs for several 1,3-diequatorial interactions and 1,3-equatorial/axial interactions (**Figure 3.1**).

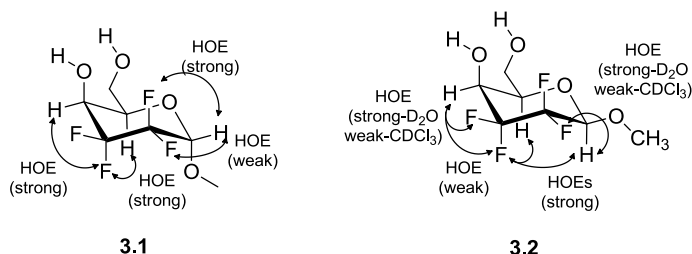


Figure 3.1 HOE interactions observed for both methyl galactoside anomers

The coupling constants between axial fluorine-2 and carbon-1 ($^2J_{\text{F2ax-C1}}$) are known to vary significantly depending on the orientation of an electronegative group at carbon-1.⁹¹ For the α -anomer (**3.1**), $^2J_{\text{F2ax-C1}} = 37.9$ Hz, while for the β - (**3.2**), $^2J_{\text{F2ax-C1}} = 26.6$ Hz. This is consistent with the general observation that a *trans* relationship between F2ax and O-1 results in a larger coupling constant than a *gauche* relationship. In addition, an equatorially oriented proton is expected to resonate at a lower field than a similar but axially oriented hydrogen.⁹² This was observed for **3.1**, in which the peak from H-1 is found 0.7 ppm downfield of the peak from H-1 of **3.2**. Full NMR analysis can be found in the experimental section.

3.1.2 X-Ray Crystal Structures: Methyl Galactoside Anomers

In addition to analysis using NMR spectroscopy, recrystallisation using Et₂O enabled the collection of X-ray diffraction structures. The crystal structures displayed no disorder and both anomers were found to exist in the $^4\text{C}_1$ chair conformation. The unit cell of α -methyl galactoside **3.1** possessed three rotameric forms (**Figure 3.2**). The rotation about the C5-C6 bond can be described as *trans-gauche* (*tg*), *gt* and *gg*, with respect to the position of O6 compared to O5 and C4.

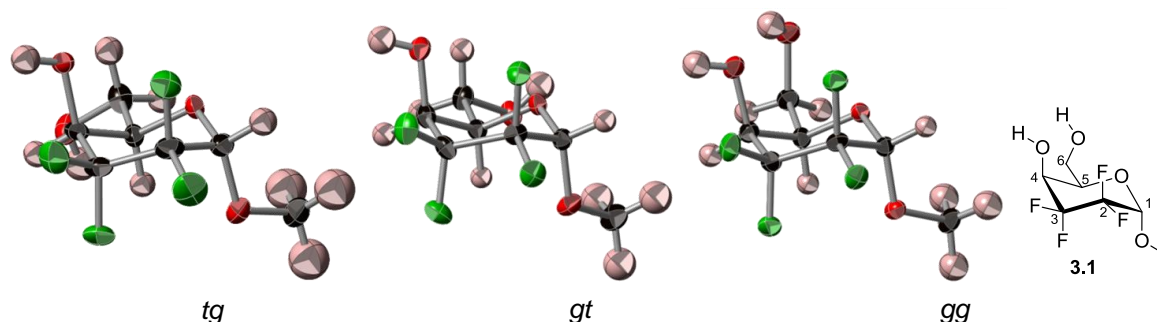


Figure 3.2 Three rotameric forms found in the crystal structure of α -MeGal **3.1**

The β -methyl galactoside (**3.2**) was similarly found to contain two rotamers in the unit cell, this time the *tg* and *gt* (**Figure 3.3**). The presence of several rotamers can be explained by a driving force to increase the number of strong intermolecular OH \cdots O hydrogen bonds.

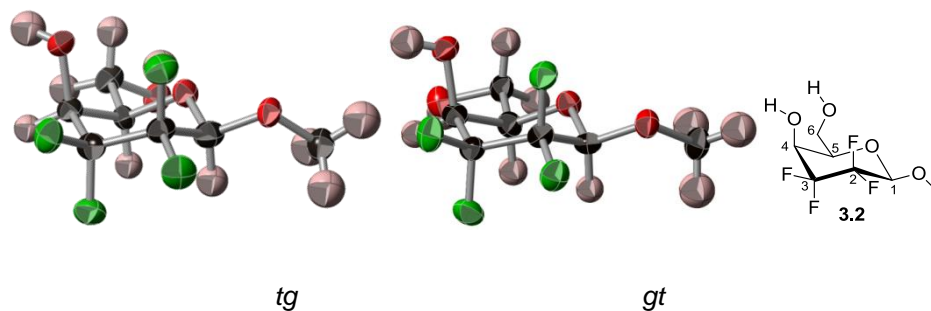


Figure 3.3 Two rotameric forms found in the crystal structure of β -MeGal **3.2**

For both anomers, some distortion of the chair is visible due to 1,3-diaxial repulsive interactions between fluorine and oxygen atoms. Other than the overall 4C_1 conformation, further analysis of specific bond lengths reveals evidence of the lack of deviation from the conformation of natural (non-fluorinated) sugars. The donation of electron density from a non-bonding orbital of C5 results in the shortening of C1–O5 and a lengthening of C1–O1 (Endo-anomeric effect, **Figure 3.4**). Similarly, donation from the non-bonding orbital of O1 in the opposite direction results in the lengthening of C1–O5 and C1–O1 (Exo-anomeric effect, **Figure 3.4**).

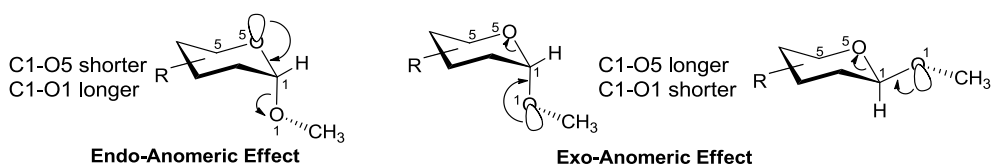


Figure 3.4 Some bond length changes resulting from anomeric effects

With respect to tetrafluorinated sugars **3.1** and **3.2**, trends analogous to those seen for methyl galactosides **3.3** and **3.4** are observed, as shown in **Figure 3.5**. Another important observation is the positioning of the methyl group in the correct orientation to allow the O1 lone pair to be antiperiplanar to the antibonding orbital of the C1–O5 bond.

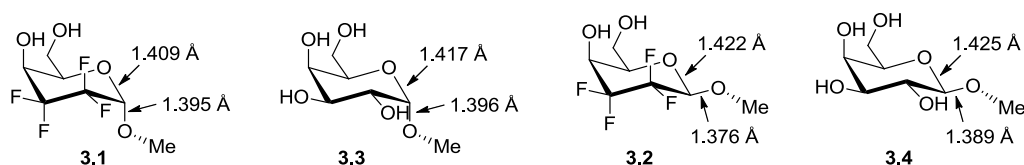


Figure 3.5 Comparison of some bond lengths between 4F and non-fluoro methyl galactosides⁹³

The torsion angles between the endocyclic oxygen (O1) and the methoxy group are shown in **Table 3.1**. From this table it can be seen that the angles fall within the expected values of 60–80°, with the exception of the *gt* rotamer of methyl galactoside **3.2** (entry 6).

Table 3.1 O5-C1-O1-C7 Torsion Angles

Entry	Compound	Angle (°)
1	3.1 (<i>tg</i>)	70.8
2	3.1 (<i>gt</i>)	61.6
3	3.1 (<i>gg</i>)	73.4
4	3.3	64.0
5	3.2 (<i>tg</i>)	76.8
6	3.2 (<i>gt</i>)	92.5
7	3.4	77.1

An interesting phenomenon observed for β -galactoside **3.2** was a significantly ordered packing effect (**Figure 3.6**). The packing results in corrugated sheets consisting of alternating fluororous and hydrophilic regions. This result is consistent with observations made previously for 1,2,3-trifluoro monosaccharides, which also contained these two separated domains.⁴⁷ This effect was not seen for the α -anomer (**3.1**).

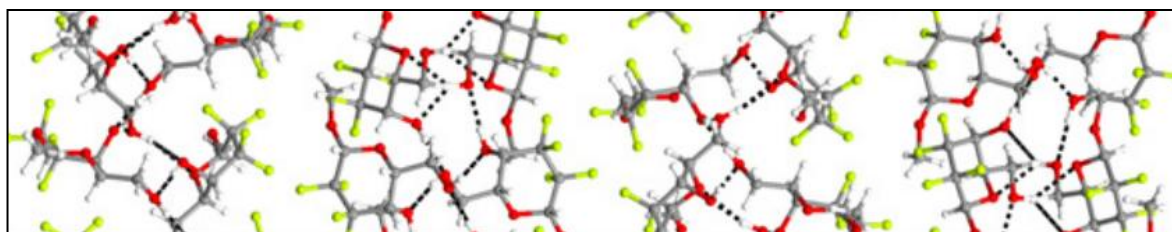


Figure 3.6 Ordered packing of β -methyl galactoside **3.2**. Yellow = fluorine, red = oxygen, white = hydrogen, grey = carbon, dotted lines indicate selected hydrogen bonds.

3.2 Crystal Structure of 4,6-Di-*O*-Benzyl-2,2,3,3-Tetrafluorogalactose

The recrystallisation of di-benzyl protected hexose **1.53** (**Figure 3.7**) was achieved using a combination of hexane and Et₂O. In this case, a single (*tg*) structure was observed (**Figure 3.7**), again showing the ⁴C₁ chair conformation, with some slight distortion similar to the structures above.⁹⁴

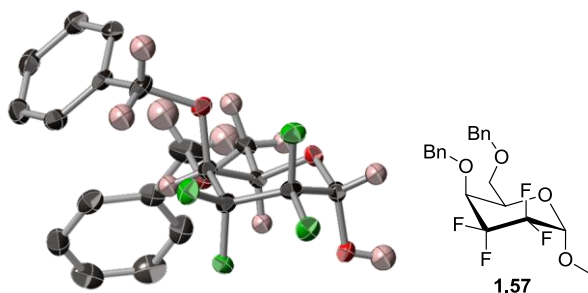


Figure 3.7 Crystal structure of compound **1.57** (aromatic hydrogens omitted for clarity)

Evidence of repulsion between O-1 and F-3ax can again be seen from the visible deviation from the parallel that would be expected between the two axial bonds. This distortion is evidence of the repulsive interaction between the O & F atoms. Despite this repulsion, the compound did crystallise in the single α -anomer. The existence of the α -anomer permits the formation of an intermolecular hydrogen bond between the anomeric hydroxyl and O-6 from a neighbouring molecule. This gives rise to a helical packing structure, involving two molecules per turn.⁹⁴

3.3 Crystal Structures of Monobenzyl-2,2,3,3-Tetrafluorogalactoses

The synthesis of 6-monobenzyl galactopyranose **2.35** is discussed in **Section 2.2**. This compound was also found to be crystalline and the crystal structure is shown in **Figure 3.8**. The structure obeys the 4C_1 chair conformation and, as with pyranose **1.57**, crystallises as the α -anomer, again due to stabilisation from intermolecular hydrogen bonding. Again, a single *tg* rotamer was observed.

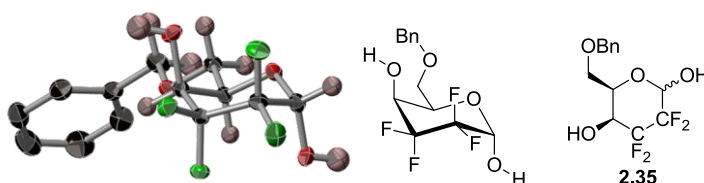
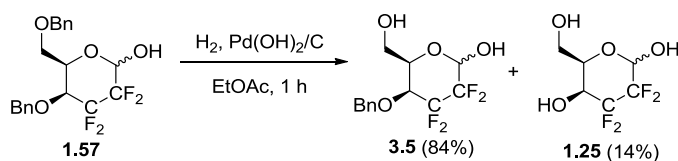


Figure 3.8 Crystal structure of compound **2.35** (aromatic hydrogens omitted for clarity)

The hydrogenolysis of **1.57** to give the deprotected **1.25** is described earlier. On one occasion, inadequate reaction time resulted in incomplete debenzylation to give a high yield of 4-monobenzyl pyranose **3.5** (**Scheme 3.2**).

Scheme 3.2 Incomplete debenzylation



Although **3.5** was not the required compound, the solid was recrystallised (acetone), enabling the collection of an X-ray structure (**Figure 3.9**). This also shows the 4C_1 chair conformation with similar moderate distortions as observed for the previous structures. In this case, the crystal structure shows a single *gt* rotamer. Interestingly, this compound crystallised as the β -anomer. This may in part be due to repulsive interactions between O-1 and F-3ax. It is also possible that this is simply due to intermolecular hydrogen bonding interactions via the anomeric hydroxyl.

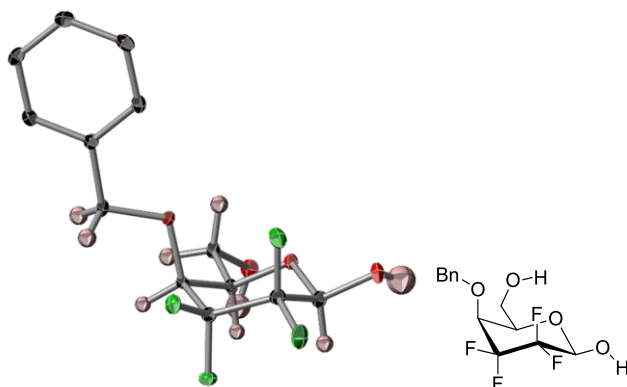


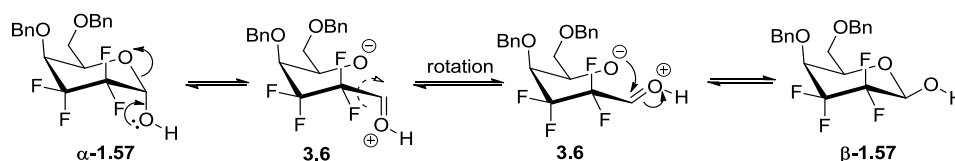
Figure 3.9 Crystal structure of compound **3.5** (aromatic hydrogens omitted for clarity)

The recrystallisation of the fully deprotected reducing sugar (**1.25**) has not been possible so far.

3.4 Anomeric Equilibration via Mutarotation

The crystallisation of galactose **1.57** as the single α -anomer permits investigation of the equilibria between both anomers. Once dissolved in solution, the sugar would be expected to undergo mutarotation to give the β -anomer (**Scheme 2.15**).

Scheme 3.3 Mutarotation between anomers



To investigate the rates of equilibration and positions of equilibria, the crystals (10 mg) were dissolved in deuterated solvents and changes monitored by ^{19}F NMR. The results of this can be seen in the graphs in **Figure 3.10** and a summary of the data is found in **Table 3.2**. Equilibration occurred fastest in chloroform (entry 3), methanol (entry 4) and acetone (entry 5) while it was much slower for benzene (entry 1), diethyl ether (entry 2), DMSO (entry 6) and acetonitrile (entry 7). The addition of base (KOH, ~ 0.3 equiv) drastically increased the rate of isomerisation (entry 8). This is consistent with the expected increased acidity of the anomeric hydroxyl due to the electron withdrawing fluorine atoms and is an effect that has been observed previously for a 2,2,3,3-tetrafluoro pyranose (**1.41**).⁹⁵ In terms of the equilibrium ratio, chloroform was the only solvent in which the β - anomer was slightly favoured. Benzene, diethyl ether, acetone and acetonitrile all gave more α - than β -, while methanol DMSO resulted in an approximately equal ratio.

Table 3.2 Selected data obtained from equilibration experiments

Entry	Compound	Solvent	Equilibration Time (h)	Final Ratio (α/β)
1	1.57	C ₆ D ₆	700	56:44
2	1.57	Et ₂ O- <i>d</i> ₁₀	800	60:40
3	1.57	CDCl ₃	25	46:54
4	1.57	CD ₃ OD	70	52:48
5	1.57	(CD ₃) ₂ CO	30	55:45
6	1.57	DMSO- <i>d</i> ₆	600	51:49
7	1.57	CD ₃ CN	650	55:45
8	1.57	DMSO+KOH	0.2	50:50
9	2.35	CDCl ₃	35	55:45
10	2.35	(CD ₃) ₂ CO	200	53:47
11	2.35	DMSO- <i>d</i> ₆	2000	49:51
12	1.56	CDCl ₃	<40 ^[a]	52:48
13	1.56	DMSO- <i>d</i> ₆	<40 ^[a]	59:41

[a] Estimated, as starting point was non-crystalline mixture of anomers

6-*O*-Benzyl galactose **2.35** was also submitted to similar experiments (entries 9–11). For this compound, equilibration favoured the α -anomer in chloroform (entry 9). Acetone and DMSO (entries 10 & 11) showed similar anomeric ratios to dibenzyl compound **1.57**, though the equilibrations were remarkably slower. The curves for equilibration of **2.35** are shown in **Figure 3.11**.

For comparison, the dibenzyl tetrafluoroglucose (**1.56**) was also investigated for its anomeric ratios. It was not possible to recrystallise this compound, but nevertheless samples were dissolved and measurements taken until no further changes were observed. This gave notable differences compared to the galactose, in that the ratio was not towards the β - in chloroform (entry 12), and was significantly towards the α - in DMSO (entry 13).

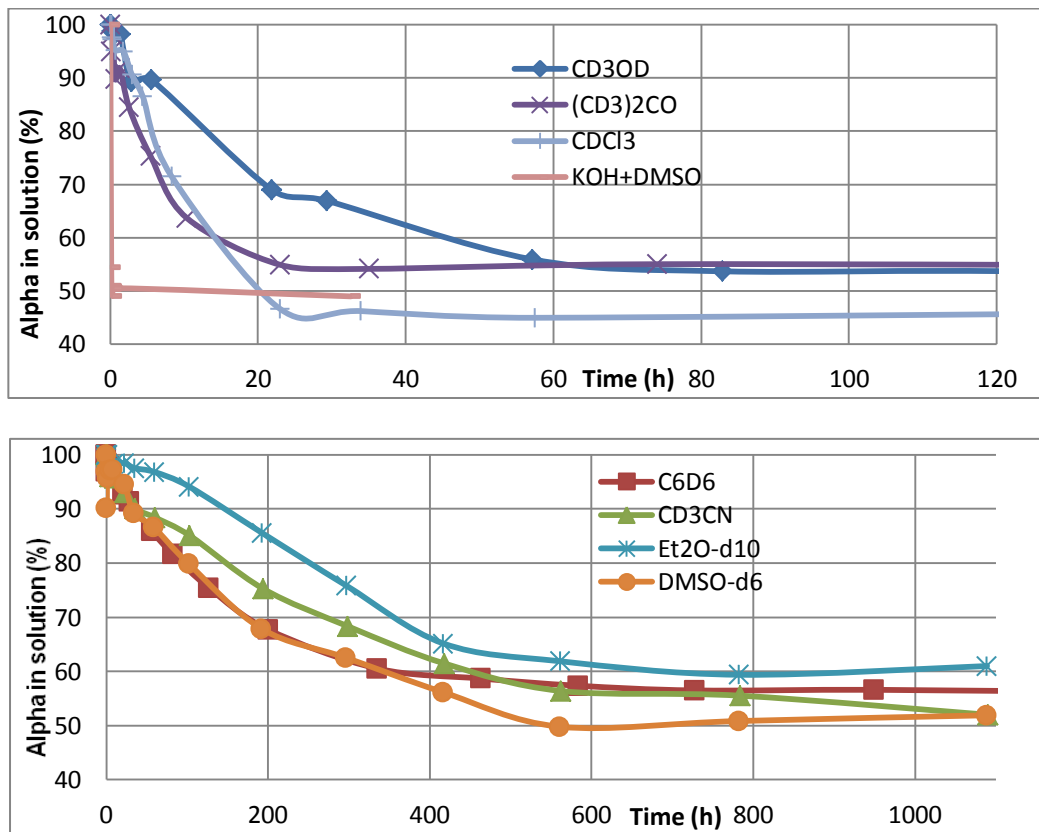


Figure 3.10 Equilibration of α -1.57 to β -1.57 in various deuterated solvents. Graphs separated due to large difference in timescales

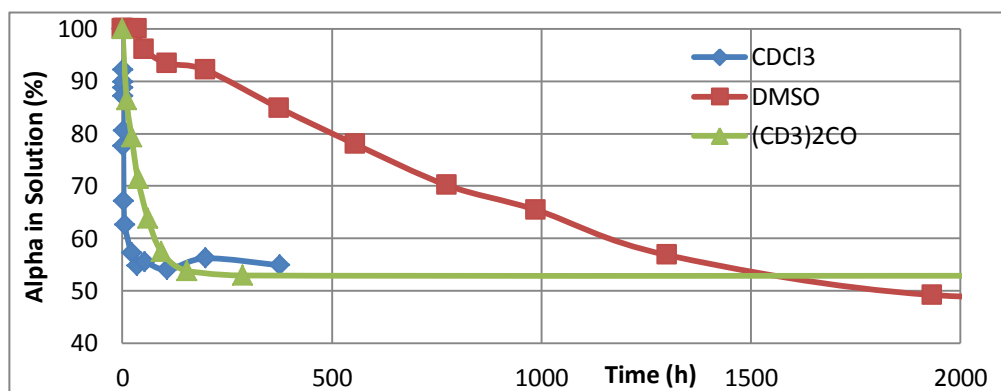


Figure 3.11 Equilibration of α -2.35 to β -2.35

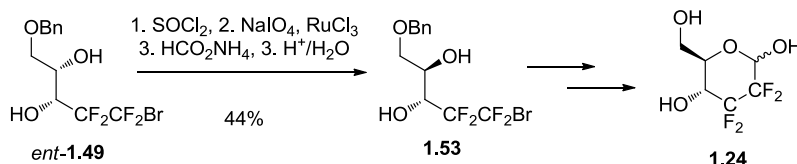
3.5 Conclusions

The synthesis of methyl galactosides **3.1** and **3.2** has facilitated thorough conformational analyses, which shows the compliance of our polyfluorinated substrates to the conformational features associated with carbohydrates. Crystal structures of three benzyl protected tetrafluoro galactoses have also shown similar results. Experiments have also been carried out to investigate the anomeric equilibrium of some benzyl protected tetrafluorinated pyranoses.

Chapter 4. Synthesis of Tetrafluoroglucose Derivatives

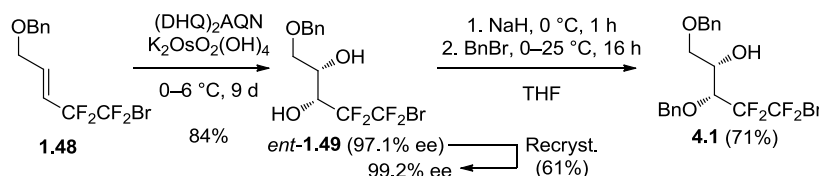
As discussed in the introduction, the synthesis of the tetrafluoro glucose analogue (**1.24**) is less efficient than the galactose synthesis. This is due to the necessity for an inversion of stereochemistry of a hydroxyl group required to access *anti*-diol **1.53**. This conversion of *syn*-diol **1.49** to **1.53** requires several steps and gives a yield of 44% (**Scheme 4.1**).⁶⁶

Scheme 4.1 Published monoinversion of diol **1.49**



To enable work on the optimisation of this route, diol *ent*-**1.49** was re-synthesised on scale. As with the galactose synthesis, further optimisations to the Sharpless AD have given improved results. Utilisation of the AQN ligand spacer unit gives 97% *e.e.*, which has since been increased by recrystallisation (**Scheme 4.2**). The reaction was achieved to give an 84% yield on a 14 g (40 mmol) scale, with a 61% yield for the recrystallisation.

Scheme 4.2 α -Sharpless AD and monobenzylation

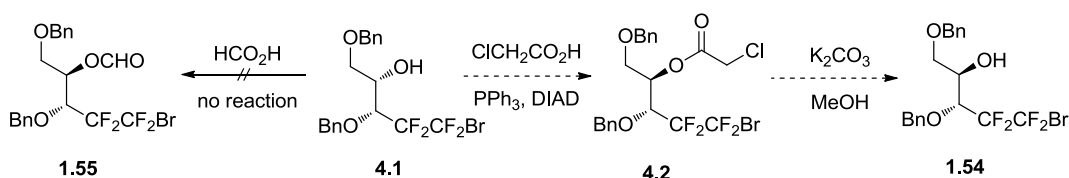


The first method towards inversion discussed here focus on the inversion of the hydroxyl at C-4. Therefore, the hydroxyl at C-3 was selectively protected using the benzylation conditions to give alcohol **4.1**, as shown in **Scheme 4.2**.

4.1 Mitsunobu and Isourea Mediated S_N2

Prior to settling on the cyclic sulfate method of inversion, several other routes were attempted by a previous researcher working on this project.⁹⁶ The first of these was the commonly used alcohol inversion method, the Mitsunobu reaction (**Scheme 4.3**). This proved unsuccessful,⁹⁶ however it was only attempted using formic acid, with the aim of accessing formate **1.55** directly. An alternative strategy, described herein, is to use chloroacetic acid, which is known to be effective with relatively hindered alcohols.^{97,98} The resultant ester would then be hydrolysed to give inverted alcohol **1.54**, as shown in **Scheme 4.3**.

Scheme 4.3 Inversion via Mitsunobu chemistry



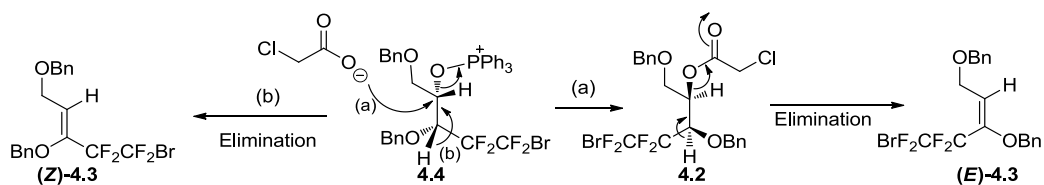
The trials are detailed in **Table 4.1**. Initial reaction gave none of the desired product (entry 1). Changing the solvent to THF⁹⁹ (entry 2) resulted in elimination to alkene (**Z**)-**4.3** (**Scheme 4.4**). Therefore, two further solvents were also screened, based on their known effectiveness in this reaction,^{100,101} (entries 3 & 4). Only toluene (entry 4) resulted in the formation of desired product, though in very low yield. The stereochemistry of the isolated product was confirmed by hydrolysis to alcohol **1.54**.

Table 4.1 Solvent screen for Mitsunobu reaction

Entry	Solvent	Isolated Yield (%)		
		4.1	(Z)-4.3	4.2
1	MeCN	65	0	0
2	THF	22	78	0
3	DMF	52	0	0
4	Toluene	0	50	3.3

Elimination often resulted from this reaction and the regiochemistry of the resultant alkene gives insight at which stage the elimination interferes. The required antiperiplanar elimination of the desired product (**4.2**) would lead to the (*E*)-alkene (**E**-**4.3**), as shown in **Scheme 4.4** (pathway *a*). However, the alkene isolated was (*Z*)-**4.3**, as confirmed by comparison with reported data.⁹⁶

Scheme 4.4 Alternative pathways leading to different isomers of 4.3

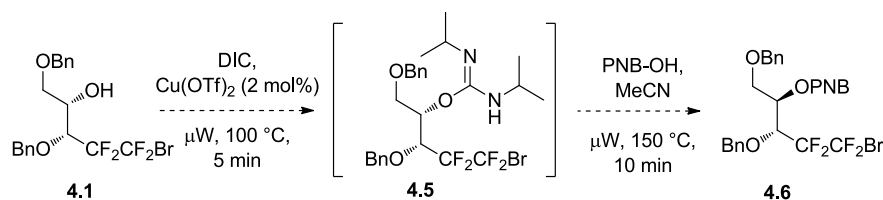


This indicates that elimination occurred prior to inversion and therefore before the formation of ester **4.2**. This side-reaction has been observed previously in alcohols flanked by vicinal alkyl substituents.¹⁰²

Another method for the inversion of alcohols relies on the formation of an isourea, followed by displacement with a carboxylic acid, as shown in **Scheme 4.5**. This reaction is performed in a microwave with a copper (II) triflate catalyst.^{103,104} As with the Mitsunobu

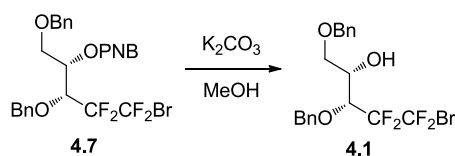
reaction, work had previously been carried out with the aim of direct formation of the formate **1.55**, using formic acid. The strategy here was to instead use *p*-nitrobenzoic acid (PNB-OH), as this was known to be more an effective reagent in the reaction.¹⁰⁴

Scheme 4.5 Inversion of the alcohol via isourea formation



The first attempt gave 90% yield of recovered alcohol **4.1**. A *p*-nitrobenzoate ester was isolated in 9% yield. However, this turned out to be the product of straight esterification (**4.7**), as identified by subsequent hydrolysis (**Scheme 4.6**). Due to the low solubility of PNB-OH in MeCN, the reaction solvent was switched to THF. This resulted in isolation of ester **4.7** in 5% yield, along with 9% yield of alkene (**Z**)-**4.3** and 45% recovered starting alcohol **4.1**.

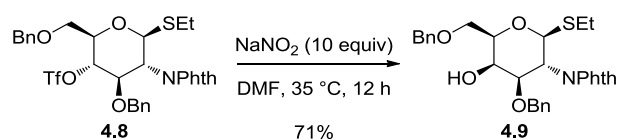
Scheme 4.6 Methanolysis of *p*-nitrobenzoate ester for diagnosis of stereochemistry



In order to investigate the first step of the reaction separately, the isourea was isolated by filtration of the crude through neutral alumina. IR spectroscopy showed the characteristic isourea peak at 1665 cm^{-1} after the standard 5 minutes. A strong carbodiimide peak at 2112 cm^{-1} was still visible, so the reaction was resubmitted to the microwave for further 5 minutes, though only slightly more conversion was observed. The isourea was isolated in 41% yield (with 35% starting material). This was then submitted to the second step (**Scheme 4.5**), but only the elimination product (**Z**)-**4.3** was recovered (67% yield).

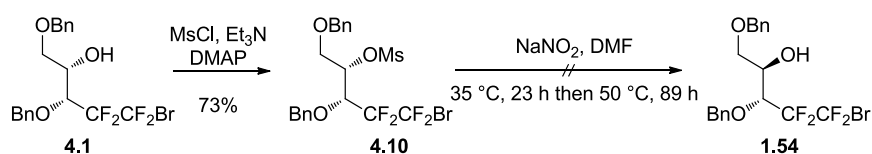
4.2 Inversion by Displacement of a Triflate

After the lack of success at inversions using the methods discussed above, an alternative was investigated. The inversion of a triflate by attack of a nitrite nucleophile is reported primarily for the inversion of hydroxyl groups in carbohydrates, as in **Scheme 4.7**.¹⁰⁵⁻¹⁰⁷ The triflate is displaced by NO_2^- to give the nitrite ester, which breaks down to give the inverted alcohol, as in **4.9**.

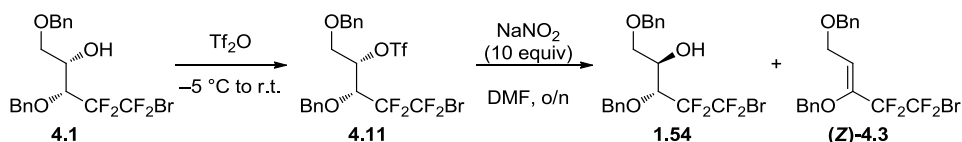
Scheme 4.7 S_N2 displacement of a triflate by NO₂⁻

4.2.1 Inversion of Hydroxyl β- to Tetrafluoroethylene

As the triflation reaction initially proved problematic, the mesylate (**4.10**) was synthesised instead. The mesylation was known to give high conversion,⁹⁶ however, the product (**4.10**) was completely unreactive towards NaNO₂, even after 4 days at 50 °C (Scheme 4.8).

Scheme 4.8 Attempted displacement of mesylate by nitrite

Therefore, the decision was made to return to the triflate (**4.11**). It was postulated that the low yield of isolated triflate was not due to lack of conversion but instability of triflate **4.11**. For this reason, a number of displacement reactions were attempted directly on the crude triflate, after work-up (Scheme 4.9).

Scheme 4.9 Displacement of triflate by nitrite

A small proportion of the trials carried out are summarised in Table 4.2. The initial attempt (entry 1) resulted in low yields of desired product (**1.54**) and elimination product (**(Z)-4.3**) (Scheme 4.9). The temperature was decreased (entry 2) in order to limit elimination, but the conversion was still low. For entry 3, both steps were carried out in the same flask with the aim of preventing moisture from causing decomposition of the triflate. The solvent from the first step was evaporated by connection of a vacuum line directly to the flask. This also gave several unidentified by-products and a low isolated yield of desired product. Use of the pure triflate (entry 4) gave several inseparable by-products with a low yield of desired product. Significant amounts of elimination product **4.3** were also formed, as was observed before.

Table 4.2 Attempted displacement of triflate by NaNO₂

Entry	Starting Material (4.1/4.11)	Temp (°C)	Isolated Yields (%)		
			4.1	(Z)-4.3	1.54
1	17:83	35	15	13	29
2	33:67	0	35	6	19
3	^[a]	35	0	9	15
4	0:100	r.t.	n/a	22	33

^[a] Concentrated triflation reaction mixture used directly without exposing to air

An added complication to this reaction was the lack of complete conversion for the triflation. Therefore, efforts were made to optimise the triflation (**Table 4.3**). Entry 1 shows 62% conversion, however the presence of starting material causes difficulties in the following step as the separation of the two alcohols (**4.1** and **1.54**) is very challenging. Increasing the amounts of Tf₂O and pyridine (entry 2) gave no improvement. However, utilisation of slightly different conditions (2 h at 0 °C then overnight at r.t.)¹⁰⁸ successfully gave an isolated yield of 83% with no starting material recovered (entry 3).

Table 4.3 Optimisation of triflation

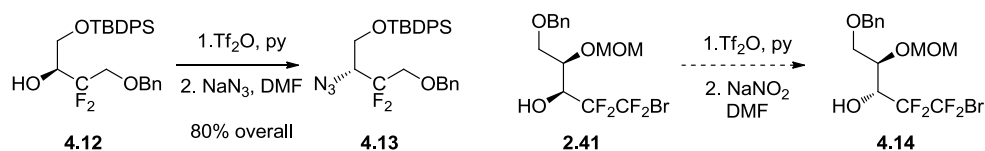
Entry	Time (h)	Temp (°C)	Tf ₂ O (equiv)	Py (equiv)	Conversion (%) ^[a]	
					4.1	4.11
1	2	−5 to 25	1.3	2.0	16	62
2	2	−5 to 25	2.6	4.0	34	54
3	16.5	0 to 25	2.0	2.0	0	83 ^[b]

^[a] Based on ¹⁹F NMR, as crude used directly in next step ^[b] Isolated yield after chromatography.

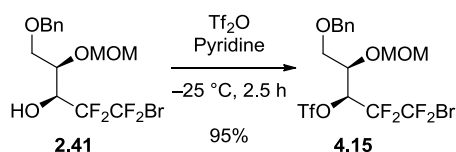
4.2.2 Inversion of Hydroxyl α - to the Tetrafluoroethylene

One of the main obstacles to using the nitrite method was facile elimination due to the presence of a relatively acidic proton α - to the tetrafluoroethylene group. Consequently an alternative route was envisaged using the intermediate synthesised for the galactofuranose synthesis (**2.41**). The resultant triflate (**4.15**) was predicted to be less susceptible to elimination.

S_N2 reactions are not normally expected to be successful at positions with an adjacent difluoromethyl group. The electron withdrawing effect gives rise to a shorter C–O bond, while electrostatic repulsion from the many fluorine lone pairs hinders the approach of a negatively charged nucleophile.¹⁰⁹ Despite this, there is precedent for a similar reaction using azide as the nucleophile.^{110,111} **Scheme 4.10** illustrates the similarity between a known example¹¹⁰ of the displacement of a triflate α - to a difluorinated carbon and a potential strategy for the synthesis of our desired tetrafluoro glucose.

Scheme 4.10 S_N2 α- to CF₂

Triflation overnight initially resulted in good yield of the desired product, but with 70% loss of the MOM protecting group. This was in all probability due to the presence of small amounts of triflic acid and was prevented by reducing the reaction time from 17.5 to 2.5 h. This provided desired triflate **4.15** in 95% yield (**Scheme 4.11**).

Scheme 4.11 Triflation of alcohol **3.33**

With the triflate in hand, trials began on the displacement reactions (**Table 4.4**), which were performed overnight with 10 equivalents of the nucleophile. Carrying out the reaction at room temperature gave a low yield of desired product, with over half the starting triflate recovered. This confirms the greater stability of this triflate (**4.15**), compared to **4.11**, which was never isolated from reaction with nitrite.

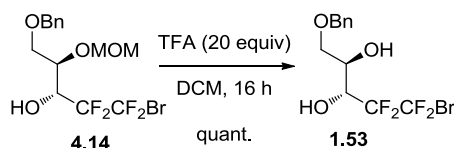
Table 4.4 Attempted nucleophilic displacements to give inverted alcohol **4.14**

Entry	Reagent(s)	Temp (°C)	Yields/Conversions ^[a] (%)		
			4.14	4.15	(Z)-4.16
1	NaNO ₂	25	13	53	0
2	NaNO ₂	60	38	0	24
3	NaNO ₂ , 15-crown-5	60	39	0	29
4	CF ₃ CO ₂ Cs ^[b]	60	0	72	28 ^[a]
5	NaOBz	60	15 ^[c]	0	85 ^[a]
6	NaNO ₂ , ⁿ Bu ₄ NBr	60	27	0	26
7	CCl ₃ CO ₂ Na	60	0	62	38 ^[a]
8	CF ₃ CO ₂ Na	60	6	60	35 ^[a]
9	NaNO ₂	40	52	15	33 ^[a]

^[a] Triflate **4.15** and alkene **4.16** were not separable, so in these cases crude ratios are reported;
^[b] 3.2 equiv, solvent: butanone; ^[c] benzoate product

In order to confirm the identity of the product (**4.14**), the MOM group was removed with TFA (**Scheme 4.12**), to give diol **1.53**, which is a known compound.

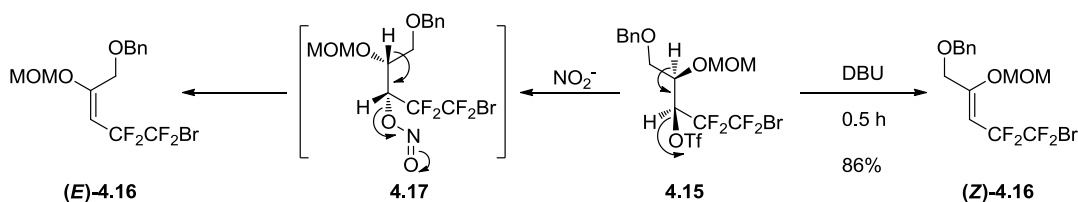
Scheme 4.12 Removal of MOM to confirm identity of compound



Increasing the temperature from 25 to 60 °C (entry 2) boosted conversion to provide 38% yield of desired product. However, elimination had also occurred, giving alkene (**Z**)-**4.16** in 24% yield. The addition of a crown ether to sequester the sodium¹¹² provided little difference (entry 3), while changing the nucleophile for cesium trifluoroacetate¹¹³ resulted in no reaction (entry 4). The crude ratio of products is reported for reactions in which both the alkene (**4.16**) and triflate (**4.15**) were isolated, as these compounds were not separable.

Formation of the benzoate¹¹⁴ did occur, though with low conversion (entry 5). An alternative source of nitrite that has been used effectively¹⁰⁶ is tetra-*n*-butylammonium nitrite, so an attempt was made to generate this in situ, using sodium nitrite and tetra-*n*-butylammonium bromide (entry 6). This gave a slightly lower yield, with significant elimination. Other nucleophiles, such as trichloroacetate and trifluoroacetate (entries 7 & 8) resulted largely in elimination. It was suspected that elimination may have been occurring after the formation of the ester (or pseudoester), so a control experiment was carried out, in which the elimination of the triflate was induced directly, using DBU (**Scheme 4.13**). The product from this was identical to that isolated from the trials in **Table 4.4** indicating that elimination was occurring prior to S_N2 inversion.

Scheme 4.13 Mechanistic explanation of different elimination products

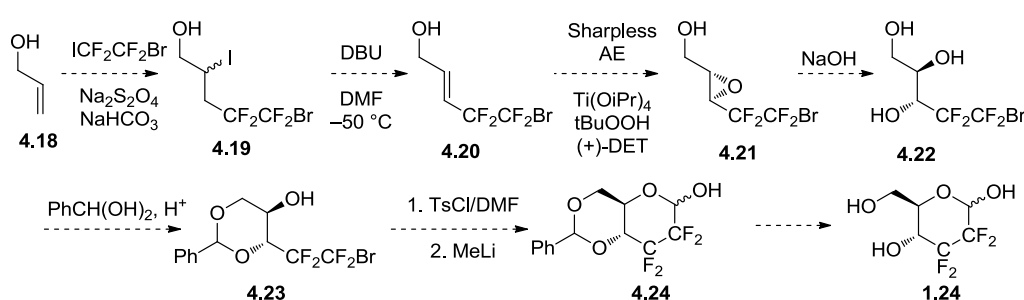


Reducing the temperature to an intermediate level (entry 9) did improve the reaction, but significant amounts of elimination still occurred. With this in mind, and in light of the fact that even a high yielding reaction would require an extra MOM deprotection step, the decision was made to not pursue this further.

4.3 Sharpless Asymmetric Epoxidation

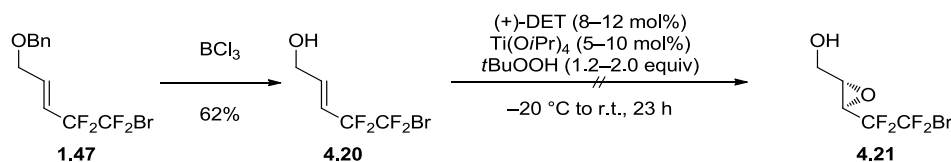
An altogether different strategy for the synthesis of 2,2,3,3-tetrafluoroglucose **1.24** is shown in **Scheme 4.14** and is based on a Sharpless asymmetric epoxidation (AE)¹¹⁵ rather than the dihydroxylation. The nucleophilic opening of epoxide **4.21** should lead to triol **4.22**, which could then be protected with a benzylidene acetal, which would be expected to form the 6-membered ring as in **4.23**. The usual formylation and cyclisation would lead to protected tetrafluoro glucose **4.24**. As the Sharpless AE requires an allylic alcohol, the first two steps (radical coupling and elimination) would have to be optimised for use with the allyl alcohol starting material (**4.18**).

Scheme 4.14 Synthesis of tetrafluoro via Sharpless Asymmetric Epoxidation



In order to investigate the epoxidation step immediately, allylic alcohol **4.20** was accessed by the debenzylation of intermediate **1.47** (**Scheme 4.15**). Boron trichloride was used, as opposed to hydrogenation, so as to avoid reduction of the alkene. The resultant allylic alcohol was subjected to the Sharpless AE conditions.¹¹⁶ However, no reaction was observed, even after letting the reaction warm to r.t. overnight. A repeated attempt with increased quantities of all reagents was also unsuccessful and again only starting material was isolated. The unreactivity is due to the electron-poor character of the double bond.

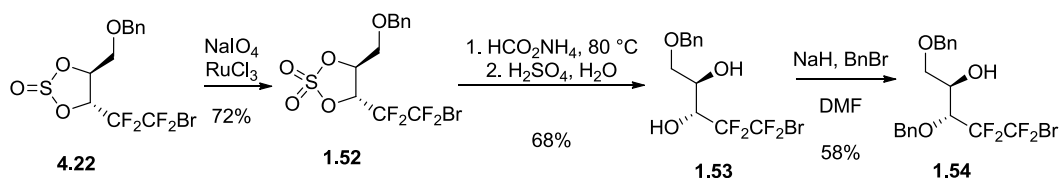
Scheme 4.15 Debenzylation to obtain reagent **4.20** and subsequent attempted Sharpless AE



4.4 Return to Cyclic Sulfate

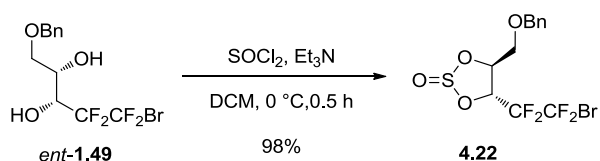
Due to the lack of success with other routes, the decision was made to return to the published route and optimise the lower yielding steps, which have been identified in **Scheme 4.16**.

Scheme 4.16 Less efficient steps of published tetrafluoroglucose synthesis⁶⁶



The large scale formation of cyclic sulfite **4.22** was accomplished on a 5 g (13 mmol) scale to a 98% yield (**Scheme 4.17**). The subsequent step is the oxidation to form cyclic sulfate **1.52**.

Scheme 4.17 Cyclic sulfite ester formation



4.4.1 Oxidation of Sulfite to Sulfate

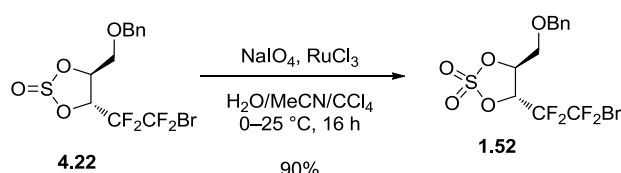
The oxidation optimisation is shown in **Table 4.5**. Replication of the published procedure⁶⁶ (entry 1) resulted in only 53% yield. Following a slightly different method,¹¹⁷ which used a different workup and much more periodate (entry 2) resulted in an improved yield of 63%. Several literature procedures did not use CCl_4 , so an alternative preparation¹¹⁸ was implemented, which also employed a different workup (entry 3), though this did not improve the yield. It was postulated that the presence of water was causing decomposition of the sulfate product (**1.52**), so a trial was carried out in the absence of water (entry 4). For solubility reasons, NaIO_4 had to be substituted for $t\text{BuN}_4\text{IO}_4$ in this trial and the resulting yield was very low. Finally, reducing the temperature at the beginning of the reaction¹¹⁹ proved very beneficial (entries 5 & 6). The modified workup also provided a much purer crude material.

Table 4.5 Optimisation of the oxidation of sulfite **4.22** to sulfate **1.52**

Entry	Solvent (H ₂ O/MeCN/CCl ₄)	Concentration (mL mmol ⁻¹)	NaIO ₄ equiv	Temp (°C)	Time (h)	Workup ^[a]	Yield (%)
1	3 : 2 : 2	6	1.2	25	15	A	53
2	3 : 2 : 2	7	4.1	25	17	B	63
3	1 : 25 : 0	9	1.6	25	25	C	58
4	0 : 1 : 1	3	1.2 ^[b]	25	75	D	2
5	3 : 2 : 2	6	1.2	0–25	18	C	85
6^[c]	3 : 2 : 2	6	1.2	0–25	16	C	90

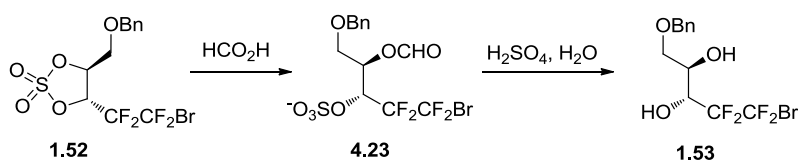
[a] A) Filter through Celite then aqueous wash, B) Extract into DCM then filter through Celite,
C) Extract into Et₂O then aqueous wash, D) Filter through Celite; [b] *t*Bu₄NIO₄; [c] 4 g scale

Therefore, oxidation of 4 g (10 mmol) was achieved to a 90% yield (**Scheme 4.18**), which allowed work on the optimisation of the nucleophilic opening and subsequent hydrolysis.

Scheme 4.18 Optimised sulfite oxidation

4.4.2 Nucleophilic cyclic sulfate opening and acid hydrolysis

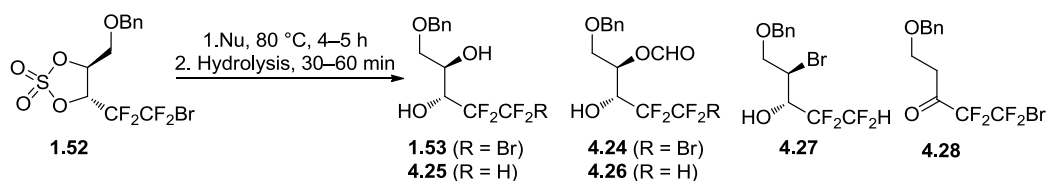
As with the Mitsunobu and isourea strategies, the original plan by the previous researcher in the group was to access the formate (**4.24**) directly, using formate as the nucleophile. However, hydrolysis of the sulfate group in **4.23** (**Scheme 4.19**) is required and this tended to also result in hydrolysis of the formate, giving diol **1.53**. Consequently, the acid and water were increased to 10 and 1 equiv respectively, so as to isolate solely the diol, which was thus obtained in 68% yield.⁶⁶

Scheme 4.19 Sulfate opening and hydrolysis of the sulfate and formate

Herein is reported further work on the optimisation of this step (**Table 4.6**). In an attempt to increase the hydrolysis even further, much harsher conditions were used (entry 1). This resulted in reasonable, though lower yield of the product. Reduction of the acid/water to an intermediate level (entry 2) gave an unexpected result. The perfluoroalkyl

bromide group was reduced to the corresponding tetrafluoroethyl group. This phenomenon was observed for both the diol (**4.24**, **Scheme 4.20**) and the formate (**4.25**). As a control, the reaction was repeated with ammonium benzoate (entry 3). The formation of the benzoate would simplify analysis as there was no chance it would be removed so easily under the hydrolysis conditions. Surprisingly, in this case no loss of bromide was observed. A modified workup was also under investigation for the trial in entry 2, so the procedure in entry 3 was repeated exactly using ammonium formate (entry 4). Again, the debrominated diol and formate (**4.24** & **4.25**) were both isolated.

Scheme 4.20 Products formed during cyclic sulfate opening and hydrolysis



Utilisation of sodium nitrite as a nucleophile (as per the attempted triflate displacements described earlier), with 0.5 equivalents of acid and water¹²⁰ and extended hydrolysis time resulted in no debromination (entry 5), though the yield of diol **1.53** was only 41%. In an effort to avoid hydrolysis of the formate, the acid and water were decreased drastically (entry 6). This gave 48% diol and 21% formate, which is a combined yield of 69%, comparable to that which was published for the diol formation.

Table 4.6 Optimisation of nucleophilic cyclic sulfate opening and hydrolysis

Entry	Nucleophile	Hydrolysis Substances (equiv)	Isolated Yields (%)					
			1.53	4.24	4.25	4.26	4.27	4.28
1	HCO ₂ NH ₄	H ₂ O (1000), H ₂ SO ₄ (100)	57	-	-	-	-	-
2	HCO ₂ NH ₄	H ₂ O (100), H ₂ SO ₄ (10)	-	-	38	3	-	-
3	PhCO ₂ NH ₄	H ₂ O (100), H ₂ SO ₄ (10)	-	52 ^[a]	-	-	-	-
4	HCO ₂ NH ₄	H ₂ O (100), H ₂ SO ₄ (10)	-	-	21	9	-	-
5	NaNO ₂	H ₂ O (0.5), H ₂ SO ₄ (0.5) ^[b]	41	-	-	-	-	-
6	HCO ₂ NH ₄	H ₂ O (0.001), H ₂ SO ₄ (0.001)	48	21	-	-	-	-
7	HCO ₂ NH ₄	H ₂ O (1), H ₂ SO ₄ (1)	-	4	10	25	30	-
8 ^[c]	HCO ₂ NH ₄	H ₂ O (1), H ₂ SO ₄ (1)	-	2	12	32	21	-
9	CF ₃ CO ₂ Cs	H ₂ O (1), H ₂ SO ₄ (1)	5	-	-	-	-	54
10	HCO ₂ NH ₄	H ₂ O (10), H ₂ SO ₄ (1) ^[d]	33	20	-	-	-	-
11	HCO ₂ NH ₄	AcCl 2M in MeOH (1)	53	18	-	-	-	-
12	HCO ₂ NH ₄	AcCl 2M in MeOH (3)	64	-	-	-	-	-
13 ^[e]	HCO ₂ NH ₄	AcCl 2M in MeOH (3)	76	1	-	-	-	15

[a] benzoate product; [b] hydrolysis for 17 h [c] workup different from this point on;

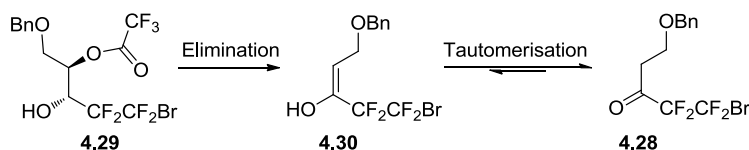
[d] storage as a solution in THF for a week may have decreased the concentration; [e] 3.5 g scale

In order to decrease the reductive debromination, the acid/water was kept at a low level of 1 equivalent (entry 7). However, this again resulted in the isolation of several debrominated products. This included alcohol **4.26** (Scheme 4.20), which has been formed from attack of the cyclic sulfate by the bromide now present in the reaction mixture. Modification of the workup conditions (changing the quench from NaHSO_3 ¹²⁰ to NaHCO_3) gave similar results (entry 8).

The use of a potentially more reactive nucleophile (cesium trifluoroacetate) resulted largely in the formation of ketone **4.28** (entry 9). This is due to elimination to give enol **4.30** (Scheme 4.21), which had tautomerised to the ketone.

The use of 10 equivalents of water while maintaining the acid at 1 equivalent appeared to prevent the loss of bromine (entry 10). However, this may have been partly due to degradation of the acid as it had been stored in THF for some time, to enable easier addition of small quantities. This would be consistent with the low yields observed for this trial.

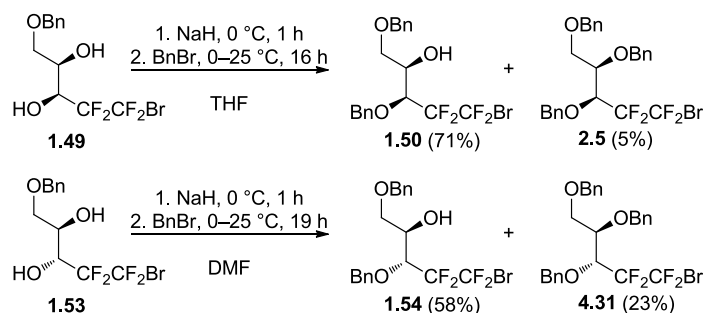
Scheme 4.21 Explanation of the formation of ketone **4.27**



A more reliable method for storage of acid in solution is to use acetyl chloride in methanol, which forms HCl. This was used as an alternative and in this case the addition of water was not needed. The yield is significantly higher (entry 11), being 71% combined for the formate and diol. Increasing the acetyl chloride from 1 to 3 equivalents (entries 12 & 13) was enough to completely hydrolyse the formate. To this end, the reaction was achieved to a 76% yield on 3.5 g (8 mmol) scale. Surprisingly, 15% yield of elimination product **4.28** was also isolated in scale-up, though this was not investigated further.

4.5 Completion of the Glucose Synthesis

The benzylation of *syn*-diol **1.49** in the synthesis of the galactose was reported to a 71% yield in THF by the previous researcher within the group.⁶⁶ However, the benzylation of *anti*-diol **1.53** was performed in DMF and reported to a 58% yield, with 23% yield of the product of double benzylation **4.31** (Scheme 4.22).

Scheme 4.22 Published monobenzylations⁶⁶

Consequently, attempts were made to improve this reaction (Table 4.7). The use of DMF was clearly justified, as although reaction in THF significantly curbed the formation of tris-benzyl product **4.31**, conversion to desired product was very slow (entry 1). Performing the reaction overnight gave no more than 24% yield, while an extra 3 days (entry 2) increased this, but only to 44%. The use of DMF (entry 3) gave an improved yield of 66%, though the formation of by-product **4.31** had increased. An attempt was made to control this by reducing the temperature (entry 4), but even after 2 days only 48% yield was observed and the formation of double benzylated product **4.31** was not reduced. Thus, 65% yield was achieved on a 2 g (5 mmol) scale using the original conditions.

Table 4.7 Attempted optimisations towards the monobenzylation of diol **1.53**

Entry	Time (h)	Temp (°C)	Solvent	Isolated Yields (%)		
				1.53	4.31	1.54
1	20	0–25	THF	57	2	24
2	95	0–25	THF	38	4	44
3	18	0–25	DMF	20	10	66
4	41	0–5	DMF	23	9	48
5 ^[a]	20	0–25	DMF	21	10	65

^[a] Reaction performed on a 2 g Scale

The difference in reactivity between **1.49** and **1.53** can be rationalised by invoking the 5-membered ring intermediate formed on chelation with sodium (Figure 4.1). The stereochemistry of the different starting materials means that this intermediate will be destabilised for **4.33**, due to both alkyl groups appearing on the same side.

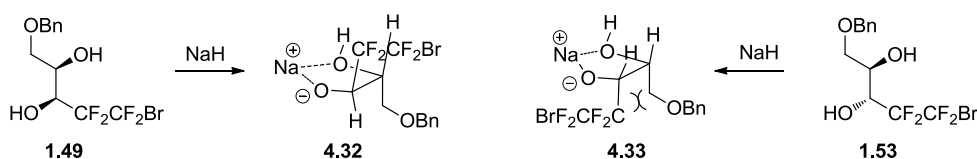
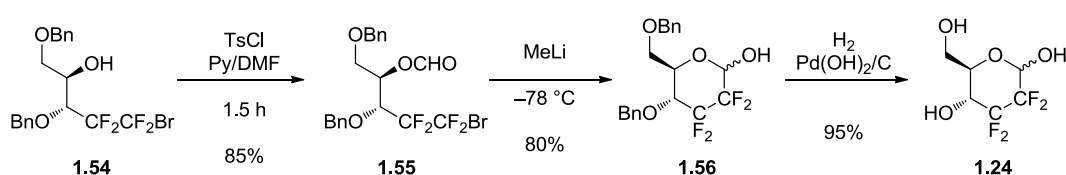


Figure 4.1 5-Membered ring formed between sodium and oxyanion

The chelation by sodium to form **4.32** increases the solubility, which is beneficial to the benzylation. However, in the reaction employing diol **1.53**, the destabilisation of the chelate causes the formation of a precipitate, when carried out in THF. This reduced solubility would be detrimental to the reaction progress.

With alcohol **1.51** in hand, formylation using TsCl/DMF was performed on a 2 g (4 mmol) scale to an 85% yield (**Scheme 4.23**). Although this is similar to the published yield, (which used DIC and HCO₂H), the new method required only 1.5 h instead of 44 h. Cyclisation proceeded at 83% yield and a portion of the product was debenzylated with 95% yield to give pyranose **1.24**.

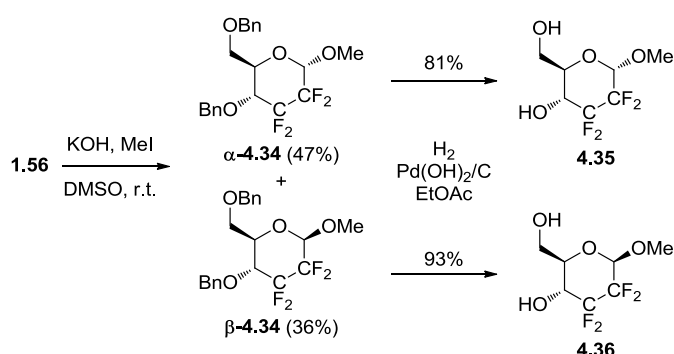
Scheme 4.23 Conclusion of the tetrafluoro glucose synthesis



4.6 Methyl Glucoside Anomers

The synthesis of methyl glucosides **4.35** and **4.36** would facilitate conformational analyses, as described for the methyl galactosides in **Section 3.1**. Benzyl-protected tetrafluoro glucose **1.56** was methylated using iodomethane (**Scheme 4.24**). Separation of the anomers was possible only after preparative HPLC with toluene/hexane (75:25) as the eluent. Debenzylation was then carried out using hydrogenolysis to give **4.35** and **4.36**.

Scheme 4.24 Methylation and deprotection of tetrafluoro glucose



Solution phase conformational analyses will be performed using NMR techniques, as discussed for methyl galactosides (**3.1** and **3.2**). Although X-ray diffraction studies would provide further information, recrystallisation has not been possible for these glucosides.

4.7 Towards the Synthesis of 4-Amino-Tetrafluoroglucose

4.7.1 Background

The capacity for the 4-hydroxyl group in our tetrafluoro sugars to be involved in hydrogen-bonding was discussed in the introduction (**Section 1.1**). However, this hydroxyl group is not necessarily an equivalent for those present in glucose.

The introduction of fluorine atoms can affect the hydrogen bond acidity of a neighbouring hydroxyl group. This is a complex effect, especially in cyclic systems, due to the potential for intramolecular F...HO interactions⁸ (see **Section 1.1**). If the H-bond acidity of the 4-hydroxyl group in tetrafluoroglucose **1.24** was increased, compared to glucose **1.14**, this would result in a reduced H-bond accepting capacity. Studies on the effect of fluorination on amine H-bond basicity have not been carried out, but it is our reasoning that an amine, such as in **4.37** (**Figure 4.2**) would have better H-bond accepting capacity than the alcohol. Therefore, it is of interest to develop a synthesis of the 4-amino derivative of tetrafluorinated glucose (**4.37**). If a binding interaction required a good hydrogen bond acceptor at the 4-position, aminoglucose **4.37** may be a more suitable replacement for **1.14** than **1.24**.

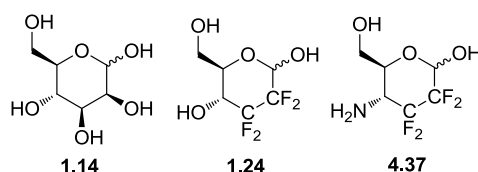
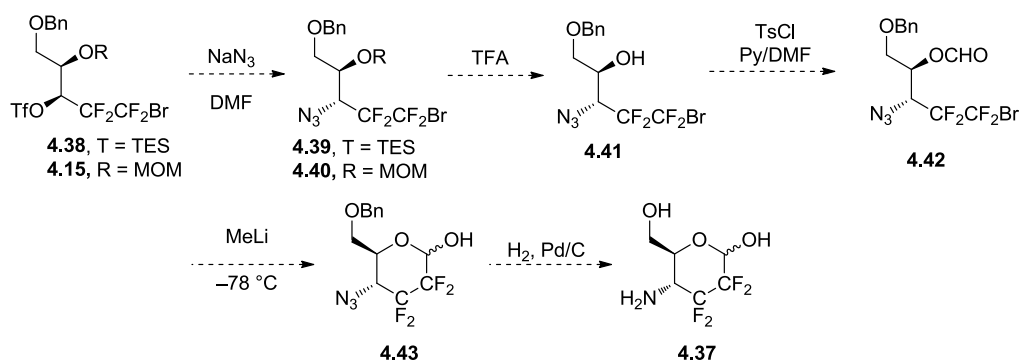


Figure 4.2 Glucose and tetrafluorinated potential bioisosteres

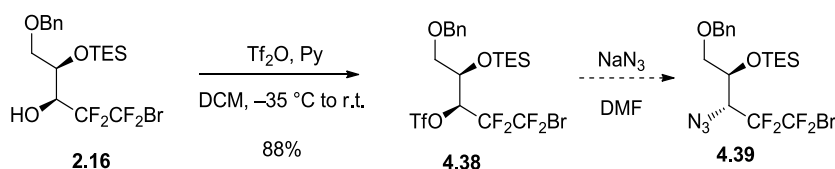
4.7.2 Planned Synthesis of 4-Amino-Tetrafluoroglucose (**4.37**)

The synthesis of 4-amino 2,2,3,3-tetrafluoro glucose (**4.37**) was envisaged via the nucleophilic displacement of triflate **4.15** (or **4.38**, **Scheme 4.25**). This would provide azide **4.40** (or **4.39**), which has the appropriate glucose stereochemistry. Removal of the protecting group would then be followed by the usual formylation and cyclisation to give **4.43**. Finally, the azide could be reduced to an amine in the same step as the debenzoylation to give 4-aminoglucose **4.37**.¹²¹

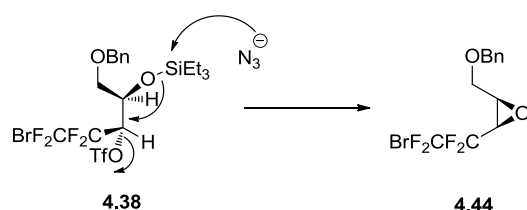
Scheme 4.25 Proposed synthesis of 4-amino tetrafluoroglucose **4.37**

4.7.3 Towards the Displacement of Triflate with Azide

Initially, the reaction was investigated using triflate **4.38**, which bears the silyl protecting group. This was synthesised from alcohol **2.16** with an 88% yield (**Scheme 4.26**).

Scheme 4.26 Triflation and subsequent displacement by azide

The first attempt to form azide **4.39** from the triflate resulted in isolation of epoxide **4.44** in 43% yield. The formation of this epoxide is most likely due to the azide anion attacking the silyl group, as shown in **Scheme 4.27**. This side-reaction was not prevented by modification of the conditions to those which have been observed to displace a triflate in the presence of a silyl group (tetra-*n*-butyl ammonium azide in toluene).¹²²

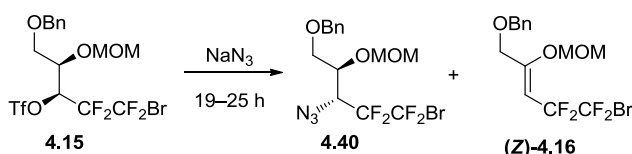
Scheme 4.27 Explanation for the formation of epoxide **4.44**

Therefore, further trials were performed using the MOM-protected triflate (**4.15**) (**Scheme 4.28**), the synthesis of which is discussed in **Section 4.2**. Formation of azide **4.40** was initially attempted using sodium azide and DMF overnight at 25 °C. This resulted in an inseparable mixture of three compounds. Fluorine NMR revealed the starting triflate (**4.15**) and alkene **4.16**, in addition to an unknown substance that may have been the desired azide

(4.40). Separation was not possible, as only a single spot was observed by TLC, however crude NMR showed a ratio of 28:55:17 triflate/alkene/suspected azide.

It was possible that amines present in the DMF were the cause of elimination. Prior to the next trial the DMF was frozen under argon then allowed to thaw under vacuum. This was repeated several times in order to remove trace amines from the solvent. However, the same outcome was observed for this trial as the previous one. Finally, the reaction was also performed in DMSO, which again gave similar ratios of substances, though the proportion of alkene was slightly reduced in favour of the triflate starting material.

Scheme 4.28 Reaction of triflate **4.16** with azide



Bearing in mind the above results, and the results of numerous similar experiments using nitrite, it is predicted that any efforts to increase conversion will lead to further elimination. However, attempting to reduce elimination is likely to decrease the yield of product. Therefore, this was not pursued further.

4.8 Conclusions

A comprehensive investigation of alternative routes to 2,2,3,3-tetrafluoroglucopyranose **1.24** has been carried out. This has included the exploration of inversion of a hydroxyl group via S_N2 reaction at the highly unfavourable position *alpha*- to a perfluoroalkyl moiety, which was developed to a moderate yield. The original route from diol **1.49** has been optimised from 16% to 29%, mostly by optimisations to the sulfate formation and hydrolysis. Enantiopure material can now also be accessed by recrystallisation of a key intermediate, as was discovered for the galactose synthesis. Medium scale synthesis has allowed the alkylation and synthesis of methyl glucosides **4.34** and **4.35**.

Chapter 5. Towards the Glycosylation of 2,2,3,3-Tetrafluorogalactose

As discussed in the introduction, glycosylation of sugars containing many fluorine atoms nearby the anomeric carbon is very challenging. Both S_N1 and S_N2 type reactions at the anomeric centre are significantly impeded by the presence of the electronegative fluorine atoms. However, the development of a method in which the fluorosugar is the electrophile is highly desirable. This would allow for easier incorporation into glycosides and glycoconjugates, synthesis of oligosaccharides and also possibly greater control of anomeric selectivity.

5.1 Strong Acid Activators

The use of strong Lewis and Brønsted acids¹²³ as activators was conceived as a strategy for overcoming the lack of reactivity of the fluorosugars. Trials were conducted on 2,2,3,3-tetrafluorogalactopyranose (**1.57**), using low enantiopurity material.

5.1.1 Hemiacetal and Acetate as Donors

The glycosylation was initially tested using ethanol as an acceptor, with trifluoromethanesulfonimide (TF_2NH , TFSI) (entry 1, **Table 5.1**). These mild conditions gave no reaction, so the temperature was increased to 111 °C, which required replacing the acceptor with benzyl alcohol and using toluene as solvent (entry 2). This resulted in complete decomposition of the material. A control reaction in the absence of TFSI (entry 3) showed the stability of **1.57** to the high temperature. Addition of the catalyst caused decomposition within 30 min (entry 4). Further controls in the absence of BnOH, including entries 5 & 6, indicated the pyranose should be stable at 65 °C in the presence of TFSI. No reaction occurred under these conditions after 7 h (entry 7).

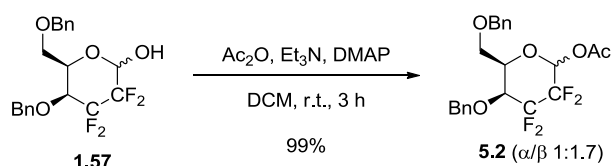
Table 5.1 Stability of tetrafluorogalactose **1.57**

Entry	Temp (°C)	Time (h)	Result
1 ^{[a][b]}	25	4	no reaction
2	111	15	decomposition
3 ^[c]	111	16	no reaction
4 ^[d]	111	0.5	decomposition
5 ^[d]	50	2.5	no reaction
6 ^[d]	70	14	decomposition
7	65	7	no reaction

[a] Solvent was DCM; [b] Ethanol used as acceptor; [c] no catalyst; [d] no acceptor

Further investigation used both the hemiacetal (**1.57**) and the acetate (**5.2**), which was synthesised in 99% yield, as shown in **Scheme 5.1**. This was expected to increase the reactivity by the provision of a better leaving group.

Scheme 5.1 Acetylation of tetrafluoro galactose **1.53**



A more polar solvent (MeCN) was also used to better stabilise the ionic intermediate. The tetrafluoro sugar (**1.57**) was found to be stable at reflux in MeCN, even in the presence of TFSI (entry 1, **Table 5.2**). Acetate **5.2** suffered partial deacetylation to form hemiacetal **1.57**, though no glycosylation was observed (entry 2). The much stronger Lewis acid, tin triflimide ($\text{Sn}(\text{NTf}_2)_4$) gave similar results (entry 3). As BnOH was found to have formed Bn_2O due to a condensation reaction, it was replaced by heptan-1-ol. Also, the large amount of alcohol was suspected of negatively affecting the catalyst, so the number of equivalents was reduced (entry 4), though this resulted in no reaction.

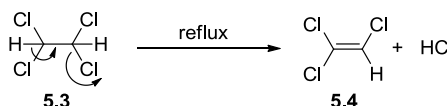
Table 5.2 Glycosylation attempts on hemiacetal **1.57** and acetate **5.2**

Entry	R	Nucleophile (equiv)	Catalyst	Solvent	Temp (°C)	Time (h)	Result
1	H	none	TFSI	MeCN	82	65	no reaction
2	Ac	BnOH (5)	TFSI	MeCN	82	4.5	Bn_2O , partial Ac loss
3	Ac	BnOH (5)	$\text{Sn}(\text{NTf}_2)_4$	MeCN	82	7	Bn_2O , partial Ac loss
4	Ac	EtOH (2)	$\text{Sn}(\text{NTf}_2)_4$	MeCN	82	5	no reaction
5	Ac	$\text{C}_7\text{H}_{15}\text{OH}$ (2)	none	$\text{TCE}^{[a]}$	147	3	no reaction
6	H	$\text{C}_7\text{H}_{15}\text{OH}$ (2)	$\text{Sn}(\text{NTf}_2)_4$	$\text{TCE}^{[a]}$	147	1	decomposition
7	H	none	TFSI	$\text{TCE}^{[a]}$	100	0.5	no reaction
8	H	none	TFSI	$\text{TCE}^{[a]}$	120	0.5	partial decomposition
9	Ac	$\text{C}_7\text{H}_{15}\text{OH}$ (2)	TFSI	$\text{TCE}^{[a]}$	100	4	partial Ac loss
10	Ac	$\text{C}_7\text{H}_{15}\text{OH}$ (2)	TFSI	MeNO_2	103	21	decomposition, Ac loss
11	Ac	$\text{C}_7\text{H}_{15}\text{OH}$ (3)	$\text{Sn}(\text{NTf}_2)_4$	MeNO_2	103	6.5	partial Ac loss
12	Ac	Indole (5)	$\text{Sn}(\text{NTf}_2)_4$	MeCN	82	7	no reaction

[a] Activated by preheating overnight at reflux

The use of “activated” 1,1,2,2-tetrachloroethane (TCE, **5.3**) is a strategy for the generation of catalytic amounts of acid. Heating TCE overnight at reflux (147 °C) causes the formation of small amounts of hydrochloric acid (and trichloroethene, **5.4**), as in **Scheme 5.2**. Using this method, no reaction was observed in the absence of a Lewis acid (entry 5), while inclusion of one caused decomposition (entry 6). Control experiments determined the sugar to be stable at 100 °C with a Lewis acid (entries 7 & 8), though no glycosylation was observed, even with the acetate (entry 9).

Scheme 5.2 Generation of acid by heating TCE

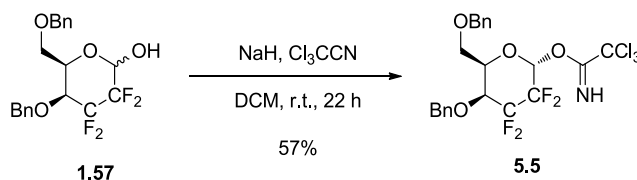


The use of a higher boiling polar solvent (nitromethane) also resulted in either partial decomposition or loss of the acetate to form hemiacetal **1.57** (entries 10 & 11). Finally, as a control, the highly reactive nucleophile indole was observed to give no reaction (entry 12).

5.1.2 Trichloroacetimidate as Donor

Trichloroacetimidates are widely recognised as effective donors in the glycosylation reaction. They are employed for their ease of formation, reactivity, anomeric control and versatility as glycosyl donors.¹²⁴ Imidate **5.5** was therefore synthesised (**Scheme 5.3**), as it was predicted to be more reactive than the acetate (**5.2**). As expected,¹²⁵ the trichloroacetimidate formation was selective for the α -anomer, as confirmed by ^{13}C NMR ($^2J_{\text{C1-F2ax}} = 41 \text{ Hz}$, $^2J_{\text{C1-F2eq}} = 28 \text{ Hz}$).

Scheme 5.3 Synthesis of the trichloroacetimidate



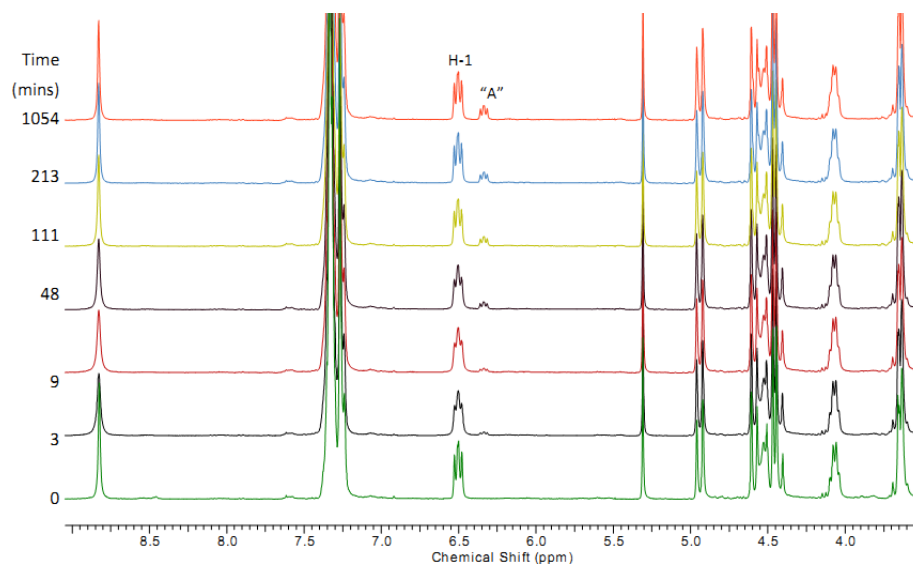
Attempted glycosylation of trichloroacetimidate **5.5** resulted in the loss of the imidate to form the hemiacetal (**1.57**) (entry 1, **Table 5.3**). When the Lewis acid was changed to TFSI (entry 2), some of the starting material remained, while another peak observed in the ^1H NMR indicated a third compound (labelled **A** in **Figure 5.1** & **Table 5.3**).

Table 5.3 Attempted glycosylations of trichloroacetimidate (**5.5**)

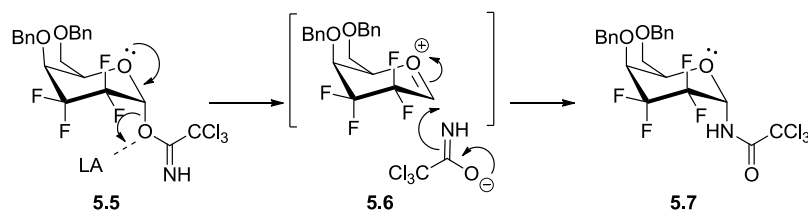
Entry	Nucleophile (equiv)	Catalyst (mol %)	Solvent	Temp (°C)	Time (h)	Product(s) ^[a] 1.57/5.5/A ^[b]
1	EtOH (2)	Sn(NTf ₂) ₄ (5)	MeCN	82	2	1:0:0
2	EtOH (2)	TFSI (5)	MeCN	82	2	1:0.5:0.3
3	none	Sn(NTf ₂) ₄ (50)	CDCl ₃	25	15	0:1:0.3
4	none	Sn(NTf ₂) ₄ (10) ^[c]	MeCN	50	22	1:0:0.2
6	C ₇ H ₁₅ OH (2)	TFSI (5)	TCE ^[d]	100	0.5	1:0:0
7	C ₇ H ₁₅ OH (2)	TFSI (5)	MeNO ₂	103	4	1:0:0
8	C ₇ H ₁₅ OTBS (2)	TFSI (5)	MeCN	82	21	1:0:0
9	C ₇ H ₁₅ OTBS (2)	TFSI (5)	MeNO ₂	103	20	1:0:0
10	C ₇ H ₁₅ OH (5)	TfOH (5)	MeNO ₂	103	3	1:0.05:0
12	indole (5)	Sn(NTf ₂) ₄ (10)	MeNO ₂	103	2	1:0:0

^[a] crude ¹H NMR; ^[b] suspected to be **5.7** or **5.8**; ^[c] new batch of Sn catalyst from this point; ^[d] preheated overnight at reflux

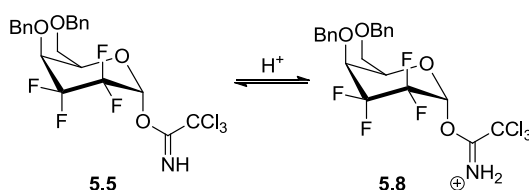
In order to monitor the formation of this unknown compound, an experiment was carried out in CDCl₃ with 0.5 equiv of Lewis acid (entry 3). **Figure 5.1** shows the resultant NMRs, from which the new peak can be seen at 6.3 ppm. This increased to ~0.3 equivalents then increased no further. Isolation by chromatography was not successful. Efforts to characterise the unknown product included using an increased number of equivalents of a fresh batch of Sn(NTf₂)₄ in the absence of alcohol (entry 4), though high conversion did not occur and the isolation of the unknown was not achieved.

**Figure 5.1** ¹H NMR of compound **5.5** and 0.5 equiv of Sn(NTf₂)₄ over time

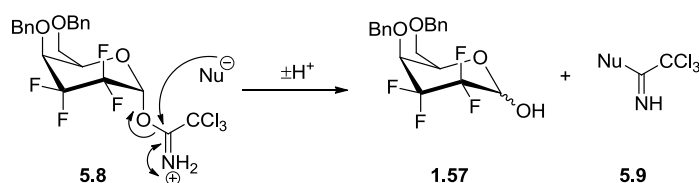
A possible explanation for this observation is the Ferrier rearrangement, which is known to occur with trichloroacetimidates.¹²⁶ This describes the rearrangement of the imidate to form an acetamide (**5.7**), as shown in **Scheme 5.4**. If this were the case, it would indicate formation of the oxonium ion intermediate, the key species required for S_N1 glycosylation.

Scheme 5.4 Ferrier rearrangement of trichloroacetimidate **5.5**

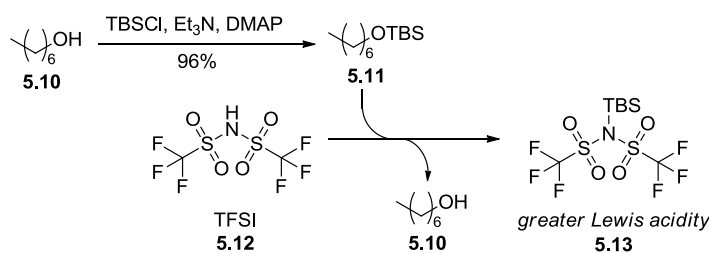
Another possible explanation would be the formation of imminium **5.8** (**Scheme 5.5**). This would have a very similar NMR to the starting material and would explain the absence of the new compound after chromatography. As this compound was not isolable, further analysis (such as ^{13}C NMR) has not been possible.

Scheme 5.5 Protonation of **5.5** to form imminium ion **5.8**

Attempted glycosylations of **5.5** in activated TCE and nitromethane at elevated temperatures both resulted in complete conversion to hemiacetal **1.57** (entries 6 & 7). The frequent formation of the hemiacetal is likely due to attack at the imidate carbon by the nucleophile, allowing the fluorosugar to act as a leaving group, as shown in **Scheme 5.6**.

Scheme 5.6 Formation of hemiacetal from trichloroacetimidate

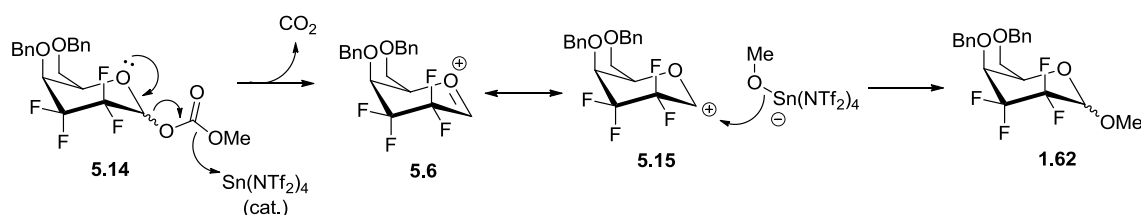
A different approach to the glycosylation was to use a silyl ether in conjunction with a protic Lewis acid (TFSI). As in **Scheme 5.7**, the silyl group would be expected to transfer to the Lewis acid (**5.12**), giving **5.12**, which has greater Lewis acidity, and alcohol **5.10**. To this end, silyl ether **5.11** was synthesised from heptanol (**5.10**). Attempted reaction with trichloroacetimidate **5.5** resulted in recovery of hemiacetal **1.57**, in two different polar solvents (entries 8–9), as did the use of triflic acid (entry 10).

Scheme 5.7 Intended outcome of using a silyl ether with a protic Lewis acid

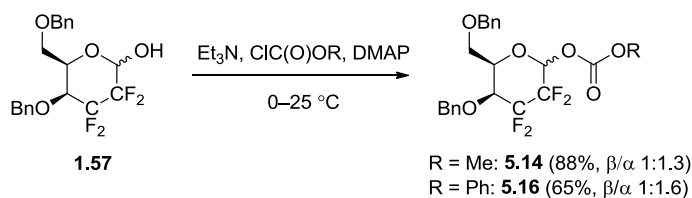
As a final control, the alcohol was replaced with the highly nucleophilic carbon-nucleophile, indole, though this resulted in 83% yield of recovered pyranose **1.57** (entry 12).

5.1.3 Decarboxylative Glycosylation

A method that has been shown to work for glycosylation involves the use of a carbonate starting material.¹²⁷⁻¹²⁹ The desired product is obtained through loss of CO₂, as shown in **Scheme 5.8**.

Scheme 5.8 Proposed glycosylation via decarboxylation of carbonate

Methyl and phenyl carbonates (**5.14** and **5.16**, respectively) were synthesised as shown in **Scheme 5.9**. Selected results from the attempted decarboxylative glycosylations are shown in **Table 5.4**. The carbonates were treated with Sn(OTf₂)₄ and subjected to reflux.

Scheme 5.9 Synthesis of pyranosyl methyl carbonate

The methyl carbonate (**5.14**) was found to be surprisingly stable, after it was recovered from refluxing with the Lewis acid in acetonitrile overnight (entry 1). Changing the solvent to nitromethane resulted in the formation of another compound, though this was not the desired methyl galactoside.⁶⁶ Use of the phenyl carbonate gave very slow conversion to a similar unknown in refluxing nitromethane (entries 3 & 4). Only traces of these unknowns were isolated and characterisation has not been possible, though they do appear to be very

similar to the carbonate starting material, with only slight changes in ^1H NMR chemical shifts.

Table 5.4 Attempted decarboxylative glycosylations

Entry	R	Solvent	Time (h)	Result
1	Me	MeCN	18	no reaction
2	Me	MeNO ₂	20	traces of unknown formed ^[a]
3	Ph	MeNO ₂	5	no reaction
4	Ph	MeNO ₂	19	traces of unknown formed ^[a]

^[a]Observed with recovered starting material, not desired product, similar to starting material

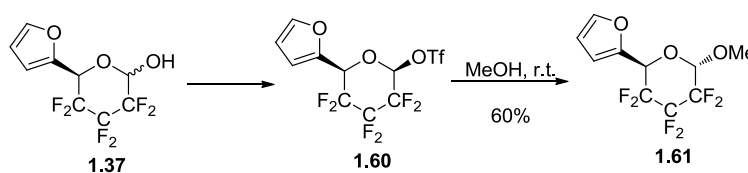
In conclusion, efforts towards the *cationic* glycosylation of a 2,2,3,3-tetrafluoro galactose have not been successful. However, significant insights have been gained into the vastly superior stability of these compounds compared to non-fluorinated sugars.

5.2 Glycosyl Triflate as Donor

Although not one of the most common donors, glycosyl triflates have been used for many years, due to their very high reactivity. Their instability means their use is limited to either *in situ* formation or use immediately after preparation.¹³⁰ Crich *et al.* formed glycosyl triflates by reaction of mannosyl sulfoxides with Tf₂O and a base. These were used to form the highly unfavoured 1,2-cis glycosides and gain important insights into the possible mechanistic pathways.^{131,132} β -Glycosylation of α -mannosyl triflates was achieved not via S_N2 pathway but by using substituents that destabilised the oxocarbenium ion thereby reducing the solvent separation of the ion pairs, (which favours α -glycosylation). The reaction therefore proceeded via highly associated contact ion-pairs, giving β -selectivity from α -mannosyl triflates.¹³²

As mentioned in the introduction, DiMagno *et al.* were able to glycosylate their hexafluoro pyranose (**1.37**) via solvolysis of the triflate (**1.60**) as in **Scheme 5.10**. After the failure of previous methods of glycosylation of our tetrafluoro substrate, the formation of glycosyl triflate **5.17** was envisaged as an alternative.

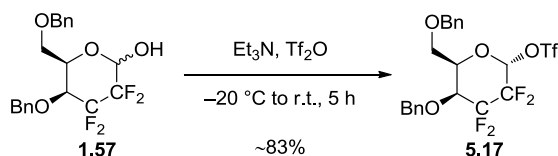
Scheme 5.10 Glycosylation of hexafluoropyranose via glycosyl triflate⁶⁵



5.2.1 Formation of the Glycosyl Triflate

Prior to work on the glycosylation step, optimisations had to be made to the triflation. A number of attempted triflations revealed that pyridine is best avoided as a base due to its propensity to react with the product. Lutidine was unsuccessful, while triethylamine gave the product (**5.17**) in a good yield (**Scheme 5.11**).

Scheme 5.11 Optimised formation of glycosyl triflate



Full purification and characterisation of the triflate was not possible due to its rapid decomposition at room temperature. However, assignment of the anomeric configuration was provided by ^{13}C NMR of the crude product (**Figure 5.2**). The coupling constants ($^2J_{\text{C1-F2}}$) observed for C-1 (44 Hz and 28 Hz) are indicative of an axial electronegative substituent⁹¹ (i.e. the α -anomer).

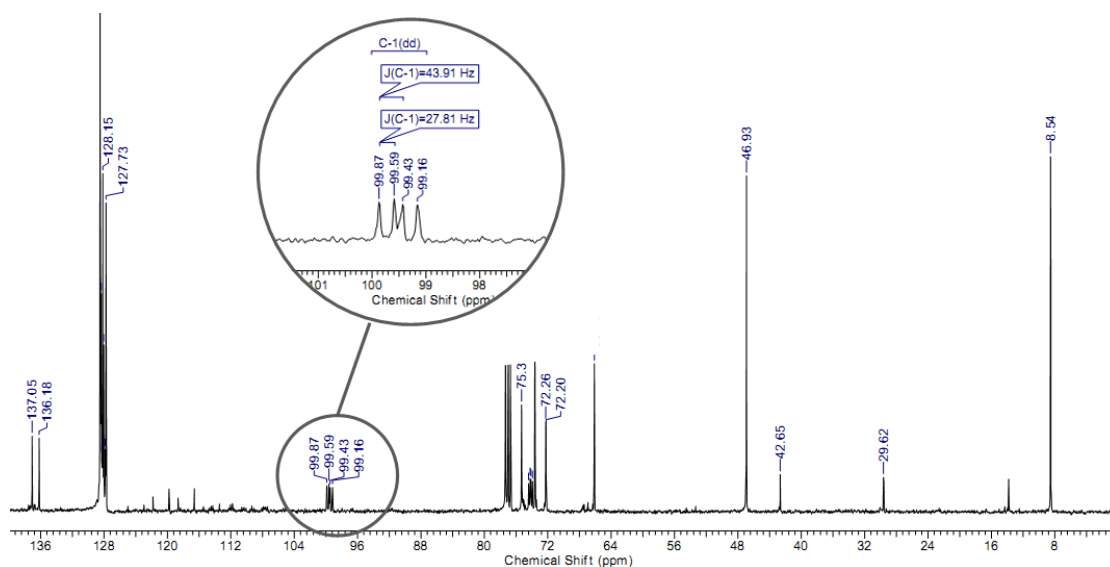
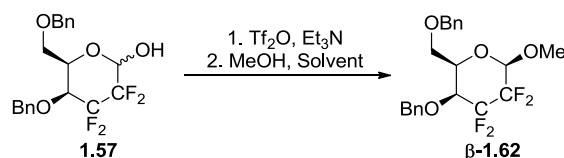


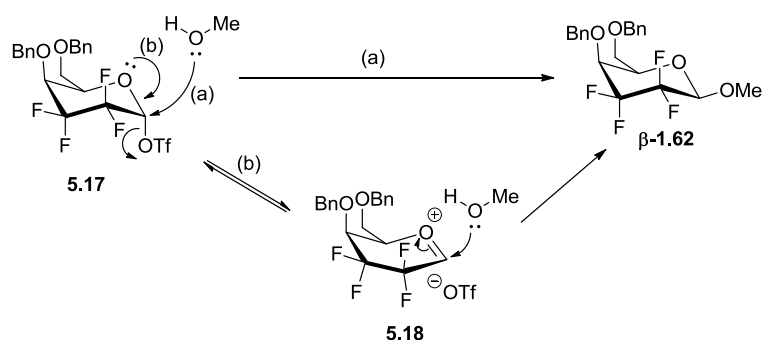
Figure 5.2 Crude ^{13}C NMR of triflate **5.17**, showing expansion of dd from carbon-1

5.2.2 Glycosylations

The instability of the triflate (**5.17**) necessitated immediate use of the crude material without further purification. For this reason, yields for the glycosylations are reported over two steps from the hemiacetal (**1.57**) (**Scheme 5.12**).

Scheme 5.12 Glycosylation via triflate

Selected details of glycosylations are shown in **Table 5.5**. Initially, a replication of the conditions used by DiMagno (i.e. solvolysis) was attempted (**Table 5.5**, entry 1). This gave a good yield of 68%. Surprisingly, only the β -anomer was formed, which provides a strong indication that the reaction was proceeding via an $\text{S}_{\text{N}}2$ mechanism. However it may be that, as discussed by Crich¹³², the high selectivity actually derives from highly associated contact ion pairs (**5.18**, **Scheme 5.13**). The presence of the triflate ion on the *bottom* face of the sugar would prevent attack of methanol, leading to the β -glycoside.

Scheme 5.13 Explanations for the observed β -selectivity, either (a) $\text{S}_{\text{N}}1$ or (b) contact ion pairs

As the desired product was formed using solvolysis, the next step was to investigate the reaction using a reduced number of acceptor equivalents (entries 2 & 3). Two solvents were screened (MeCN and DCM). Acetonitrile provided a low yield of 18%; other products were formed but separation and characterisation was not possible. It may be that these derive from reaction of the glycosyl triflate with acetonitrile. The use of DCM (entry 3) provided a better yield of 41%. This is a significant result, as it shows the potential of this reaction to be a viable means towards the glycosylation of 2,2,3,3-tetrafluoro sugars. Additional optimisation is discussed further in the future work section.

Table 5.5 Glycosylations of tetrafluoro galactosyl triflate **5.17**

Entry	MeOH equiv	Solvent	Time (days)	Yield of β -1.62 (%) ^[a]
1	366	MeOH	3	68
2	3	MeCN	3	18
3	3	DCM	3	41

^[a] Yield includes triflation step

5.3 Conclusions

The glycosylation of 2,2,3,3-tetrafluoro galactose by acid catalysis has been thoroughly investigated. Although the desired reaction was not achieved, the suspected high stability of the tetrafluoro sugar has been demonstrated. It has been shown, however, that glycosylation can be achieved via a glycosyl triflate donor and this provides an alternative to the use of a base and electrophile (anionic alkylation).

Chapter 6. Synthesis of Tetrafluorinated Ligands for the Investigation of Enzymatic Processes Relating to Mycobacteria

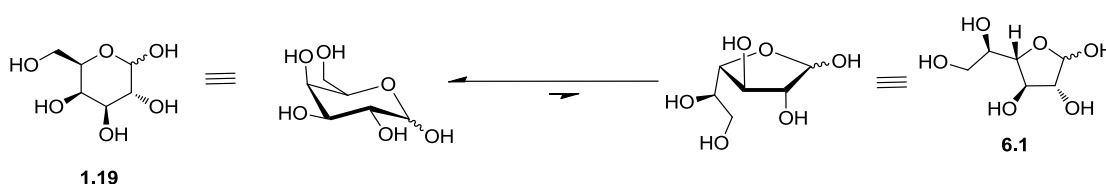
6.1 Introduction

6.1.1 Background

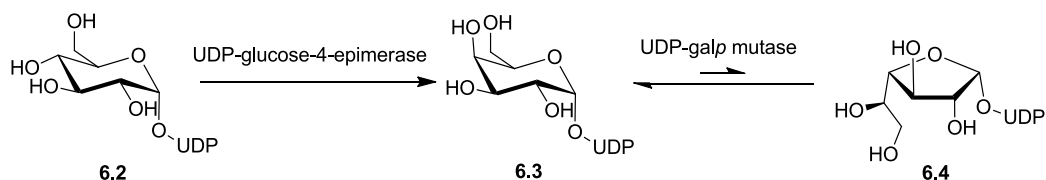
Tuberculosis (TB) is second only to HIV/AIDS as greatest killer worldwide. In 2010, 8.8 million people fell ill and 1.4 million died from TB. It mostly affects young adults in their most productive years and in recent years multi-drug resistant strains have become more prevalent. It is caused by a species of bacteria called *Mycobacterium tuberculosis*. The cell wall of *M. tuberculosis* consists of a peptidoglycan-arabinogalactan-mycolic acid complex.¹³³ One of the major components of this is the arabinogalactan, which consists of arabino- and galactofuranose residues.

Galactofuranose (the five-membered ring form of galactose, **6.1**) is shown in **Scheme 6.1**. The equilibrium between the two isomers lies far towards the pyranose (**1.13**).⁸⁶ Mammals contain galactose residues exclusively in the pyranose form, however myriad microorganisms rely on galactofuranose (Gal_f) residues. The same observation has been made with respect to arabinose. This is relevant for many microorganisms, including bacteria (e.g. *M. tuberculosis*), protozoa (e.g. *Leshmania*, which is responsible for leishmaniasis) and fungi responsible for paracoccidioidomycosis. As the bacterial cell wall is constructed partly from galactofuranose residues, they are required for its survival and infectivity. The absence in mammals but prevalence in pathogenic microorganisms makes them an attractive therapeutic target.^{134,135}

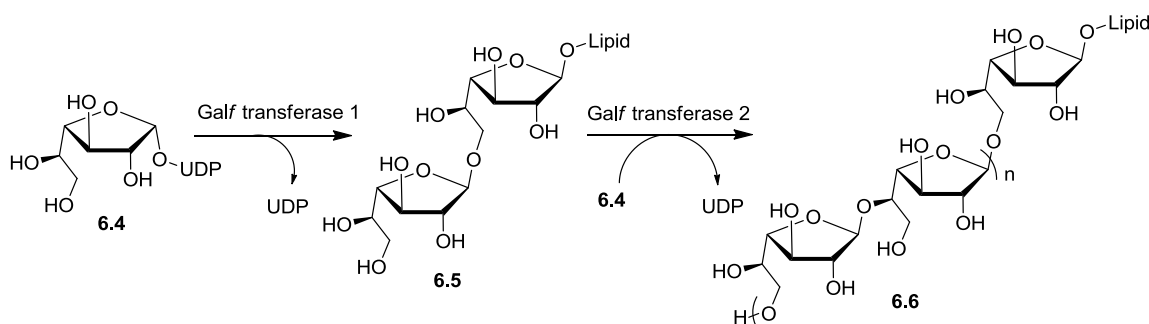
Scheme 6.1 Galactose isomers and different representations



Two key enzymatic reactions in the biosynthesis of gal_f are shown in **Scheme 6.2**. Uridine diphosphoryl (UDP)-glucose (**6.2**) is converted by UDP-glucose-4-epimerase to the galactose form (**6.3**). The enzyme UDP-Galactopyranose mutase (UGM) then performs the ring-contraction to provide the UDP-galactofuranose.^{136,137}

Scheme 6.2 Enzymatic synthesis of Galf from Glcp

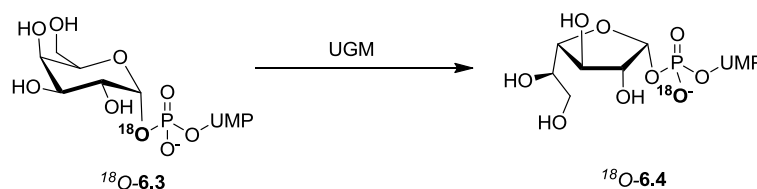
The UDP-Galf is then incorporated into the *galactan* by the processes shown in **Scheme 6.3**. UDP-Galf (6.4) is a substrate for the bifunctional enzyme galactofuranosyl transferase 1 (GlfT1). GlfT1 links the first Galf unit to the lipid, while also incorporating the second, with either a 1→5 or a 1→6 linkage to give 6.5.¹³⁸ A second bifunctional transferase (GlfT2) then takes several more UDP-Galf residues to synthesise a longer chain of approximately 35 Galf residues containing exclusively alternating 1→5 and 1→6 linkages (6.6).¹³⁹ From this point, other enzymes take over and the chains ultimately are incorporated into the cell-wall.

Scheme 6.3 Synthesis of the Galf chain by Galf transferases

6.1.2 Uridine Diphosphate Galactose Mutase (UGM)

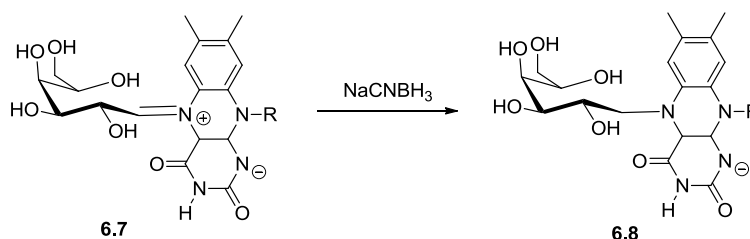
The isomerisation step (ring contraction) is catalysed by UGM. Fundamentally, this enzyme mediates the equilibrium in such a way to facilitate a pyranose/furanose ratio of 93:7, respectively.¹³⁷ UGM is a flavoprotein, in that it utilises flavin adenine dinucleotide (FAD), a cofactor commonly associated with roles in oxidation or reduction.

Due to its importance in the synthesis of the mycobacterial cell-wall, extensive studies have been carried out with the aim of elucidating the mechanism of this enzymatic process. A significant insight into the mechanism comes from an ¹⁸O labelling experiment (**Scheme 6.4**), which showed unequivocally that the C1–O1 bond is cleaved during the isomerisation.¹⁴⁰ 2-Fluoro and 3-fluoro analogues of UDP-Galp^{141,142} and UDP-Galf¹⁴³ were found to be substrates (of varying activities, see later) for the process. These results rule out any mechanism involving the oxidation or dehydration of these positions, or the transfer of the UDP moiety to O-2.

Scheme 6.4 Oxygen-labelling of UDP-Galp¹⁴⁰

Zhang *et al.* demonstrated the importance of FAD, by the observation that the rate of conversion was considerably increased in the presence of FAD_{red} (reduced FAD).¹⁴⁴ Indeed, it has been put forward more recently that UGM is actually inactive under non-reducing conditions.¹⁴⁵

The indirect proof of FAD's unusual role (i.e. not oxidation or reduction) in the mechanism was provided by the characterisation of covalently-linked acyclic compound **6.8** (Scheme 6.5).¹⁴⁶ The isolation of **6.8** reveals the presence of flavin-iminium ion **6.7**, from which it was formed by reduction.

Scheme 6.5 Flavin-iminium ion trapped with NaCNBH₃

Further confirmation of the role of FAD_{red} comes from the crystal structures,¹⁴⁷ which show C-1 of the galactose in close proximity to N-5 of the FAD, under reduced conditions (**Figure 6.1**). Under non-reducing conditions, the hexose is directed away from the FAD, which may help to explain the lack of activity under these conditions. Also, OH-4 of the pyranose is observed in close proximity to the C-4 carbonyl of FAD, with a potential hydrogen bond providing an explanation of the enzyme's discrimination against UDP-glucose.

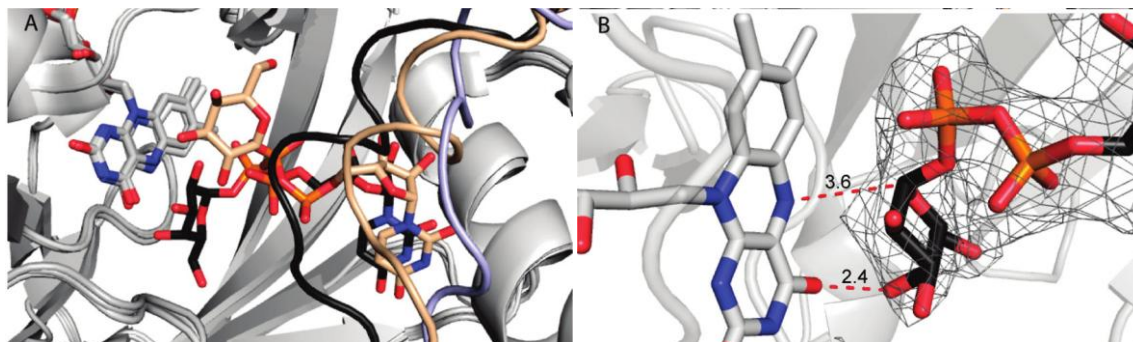
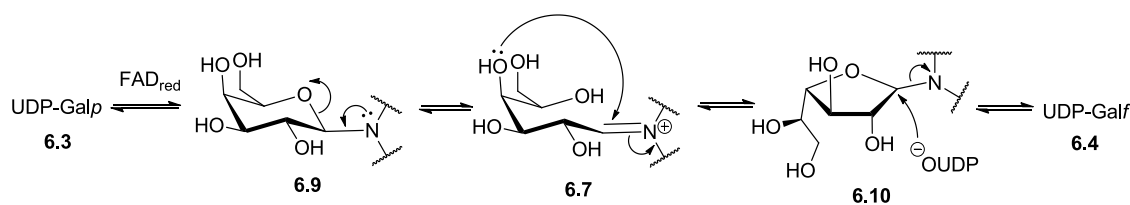


Figure 6.1 Crystal structure of enzyme-substrate complex. Light brown indicates substrate in complex with oxidised UGM, black indicates substrate with reduced UGM¹⁴⁷

Similar conclusions were drawn from STD (Saturation transfer difference) NMR, with regards to the conformation of the enzyme-substrate complex.¹⁴⁵ The proposed mechanism is shown in **Scheme 6.6**. There is still debate as to whether the attack of FAD_{red} proceeds via an S_N2,¹⁴⁸ SET or S_N1 mechanism.^{143,149}

Scheme 6.6 Proposed mechanism of UDP-Gal ring-contraction¹⁴⁶

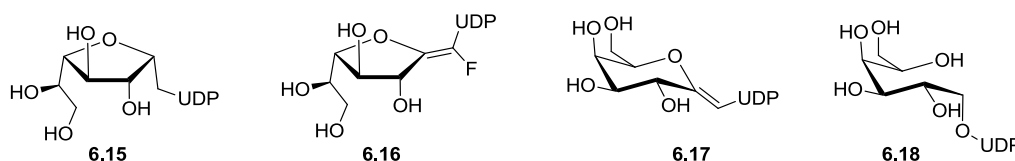


A large part of the investigation into this process has focussed on the synthesis of UDP-glycoside based analogues, a selection of which is shown in **Table 6.1**. Compounds **6.3** and **6.4** are the natural pyranose and furanose substrates, respectively. The K_M value is the Michaelis constant, and defines the substrate concentration at which the rate is half the maximum. The k_{cat} value is the turnover number, indicating the maximum number of substrate molecules converted per minute (per enzyme). 2- & 3-Fluorinated pyranosides (**6.11**¹⁴² and **6.12**¹⁴¹) and furanosides (**6.13** and **6.14**¹⁴³) showed reasonable binding affinities, but conversion of the 2-fluoro- substrates (**6.11** and **6.13**) was markedly slower. This is likely due to a destabilisation of **6.7**. As such, these compounds were found to be good inhibitors (see below, **Table 6.2**).

Table 6.1 Activities of selected UDP-Gal analogues (as UGM substrates)

Entry	Descriptor	Structure	Generic Structure	K_M (μM)	k_{cat} (min^{-1})
6.3	Galp	$R_1 = R_2 = \text{OH}$		805 ¹⁰⁷	2120 ¹⁰⁷
6.11	2FGalp ¹⁴²	$R_1 = \text{F}, R_2 = \text{OH}$		203 ¹⁰⁷	0.04 ¹⁰⁷
6.12	3FGalp ¹⁴¹	$R_1 = \text{OH}, R_2 = \text{F}$		280 ¹⁰⁷	5.5 ¹⁰⁷
6.4	Galf ^f	$R_1 = R_2 = \text{OH}$		16 ¹⁰⁷	2210 ¹⁰⁷
6.13	2FGalf ¹⁴³	$R_1 = \text{F}, R_2 = \text{OH}$		65 ¹⁴³	2 ¹⁴³
6.14	3FGalf ¹⁴³	$R_1 = \text{OH}, R_2 = \text{F}$		861 ¹⁴³	342 ¹⁴³

In addition to the insights provided by relative activities, investigation of inhibition can also be useful in giving mechanistic information (furthermore, the inhibition of this process would be desirable, as described earlier, for therapeutic purposes). As well as some of the compounds mentioned already, a number of other UDP-Gal analogues (including those shown in **Figure 6.2**) have been investigated for their capacities to inhibit UGM. Conformationally/configurally locked analogues including C-glycoside **6.15** and exo-glycals **6.16** and **6.17** are important probes for the mechanism,^{150,151} as is the acyclic galactitol **6.18**.¹⁴⁹

**Figure 6.2** Selection of compounds tested as inhibitors of UGM

From **Table 6.2**, it can be seen that 2- and 3- fluoro UDP-Gal analogues (**6.11–6.14**) were effective inhibitors of the native enzyme, with the 3FGalf being the best, at 98.6% inhibition.¹⁵² C-glycoside **6.15** is locked in the α -furanose configuration of the mutase substrate and was also found to be a good inhibitor at over 90%. However, as with the 3-fluoro analogues, there is a large drop off in inhibition under reducing conditions, indicating a significant change in enzyme-substrate complex conformation. Exo-glycal furanoside **6.16** was a poor inhibitor, though time-dependent inactivation was observed,¹⁵³ suggesting the build-up of a covalent adduct. In contrast, exo-glycal pyranoside **6.17** did not show time-dependent inactivation, though it was a reasonable inhibitor, suggesting a specific binding mode that prevents reaction with the enzyme.¹⁵¹

Galactitol **6.18**, designed as a mechanistic probe, was not turned over, but was a significant inhibitor under reducing conditions. This is consistent with an S_N1 or SET mechanism, while an S_N2 mechanism would be expected to turnover this substrate.¹⁴⁹ Regarding the inhibition data in **Table 6.2**, it must be noted that UDP itself shows 50.6%

inhibition under reducing conditions, indicating that the uridine plays a significant role in binding compared to the sugar moiety.¹⁴⁹

Table 6.2 Inhibition studies of UDP-Gal analogues

Entry	Descriptor	Inhibition (%)	
		Non-reducing conditions	Reducing conditions ^[a]
6.11	2FGalp ¹⁴²	54 ¹⁴³	<i>nd</i> ^[b]
6.12	3FGalp ¹⁴¹	71 (19) ¹⁴³	(6) ¹⁴³
6.13	2FGalp ¹⁴³	61 ^[c]	<i>nd</i>
6.14	3FGalp ¹⁴³	98.6 (87) ^[c]	(10) ^[d]
6.15	C-Galp ¹⁵⁰	91 (81)	2 (14)
6.16	Exo-Galp ¹⁵³	<i>nd</i> ^[c]	<10
6.17	Exo-Galp ¹⁵¹	42	<10
6.18	GalOH ¹⁴⁹	<i>nd</i>	54.1
[a] Addition of sodium dithionite; [b] not determined; [c] Time-dependent inactivation observed; [d] Brackets indicate value when no preincubation with enzyme was performed;			

6.1.3 Galactofuranosyl Transferase 2

Once converted from the pyranose, the UDP-galactofuranose takes its role as a substrate for two galactosyl transferase enzymes. The first (Glft1) links a chain of about two Galf units to the lipid, while the second connects the third and subsequent residues to give the longer chain.¹³⁸ This chain of 30–35 Galf sugars is assembled with alternating 1→5 and 1→6 linkages. Glft2 uses the same active site to catalyse both types of transfer reaction.¹⁵⁴ The enzyme has been found to be highly specific with regards to the formation of this Galf chain.

This sequence specificity was investigated by the use of fluorosugar chain termination agents.¹⁵⁵ The UDP-Galf analogues (**6.19** and **6.20**, **Figure 6.3**) possess a fluorine atom in one of the positions where polymerisation would otherwise occur. Once these blocked substrates were incorporated into the chain, it was found that rather than link to the other position (e.g. 5 instead of 6), termination occurred. This demonstrates the high level of fidelity of this enzyme.

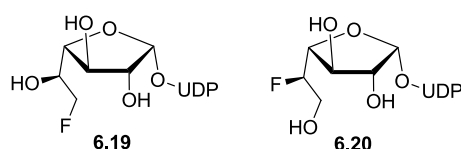


Figure 6.3 5- and 6-Fluoro UDP-Galf analogues¹⁵⁵

The same effect was observed for 6-deoxy galf and 5-deoxy galf analogues (**6.21** and **6.22**) and 5-fluoro-araf analogue **6.23**.¹⁵⁶ Once incorporated, no extension was observed if the specific hydroxyl required for the next linkage was not available.

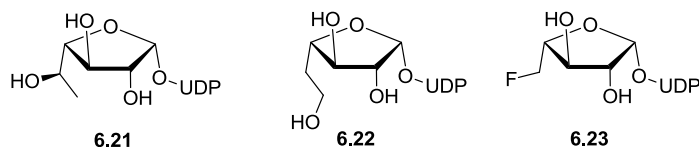


Figure 6.4 Deoxy UDP-glycofuranoside analogues

Several octyl $\beta(1\rightarrow6)$ and $\beta(1\rightarrow5)$ linked galactofuranosyl disaccharides, including those shown in **Figure 6.5** were investigated as acceptors for GlfT2. The disaccharides deprotected at the reducing sugar (**6.24** and **6.27**) were recognised by the enzyme and converted to their corresponding trisaccharide products.¹⁵⁷ Those possessing benzyl groups on one Galf unit (as depicted in **Figure 6.5**, **6.25** and **6.28**) were not substrates, suggesting a lack of space in the binding pocket. However, the methylated equivalents (**6.26** and **6.29**) showed better activity compared to the fully deprotected **6.24** and **6.27**. Indeed, methoxy analogues **6.26** and **6.29** were found to inhibit native-type acceptors **6.24** and **6.27** with IC_{50} values of 3.32 and 3.36 mM, respectively. This finding is significant because it suggests the existence of a hydrophobic pocket in the acceptor binding site.

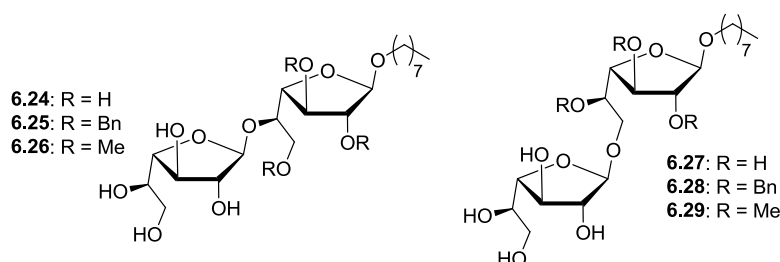


Figure 6.5 $\beta(1\rightarrow6)$ and $\beta(1\rightarrow5)$ linked galactofuranosyl dissaccharides¹⁵⁷

Methoxy UDP-Galf analogues including those shown in **Figure 6.6** were investigated as donors for the transferase (in conjunction with two synthetic trisaccharide acceptors).¹⁵⁶ Lowary *et al.* found that donors bearing methoxy groups at the 2-, 5- and 6- positions were not substrates and at best poor inhibitors. This suggests a disruption to substrate binding, implying a lack of steric space in the donor binding site.

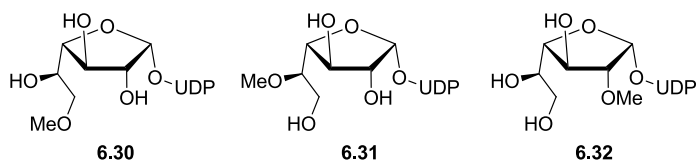


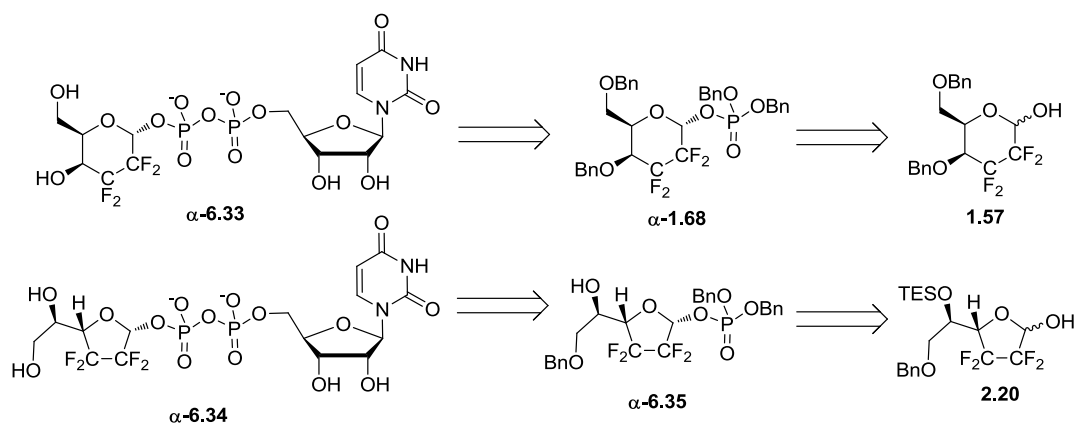
Figure 6.6 Methoxy donor substrate analogues

6.2 Tetrafluorogalactosyl Phosphates for UGM

With access to the tetrafluoro galactose in both pyranose (**1.57**) and furanose (**2.20**) isomers, the investigation of tetrafluorinated analogues of bioactive glycosides is possible. The synthesis of UDP glycosides **6.33** and **6.34** and would allow their investigation as inhibitors of UDP-galactose mutase. The incorporation of our tetrafluoro galactose units into UDP-galactoside analogues is made possible by collaboration with Prof S. Vincent (FUNDP Namur, Belgium), who has the capability to convert glycosyl monophosphates (**1.68** and **6.35**, **Scheme 6.7**) to uridine diphosphates (**6.33** and **6.34**).

Hence, the protected monophosphate precursors (α -**1.68** and α -**6.35**) were synthesised. The α -anomers were targeted, for direct comparison of inhibition with known UDP-gal based UGM inhibitors.^{143,149-151,153}

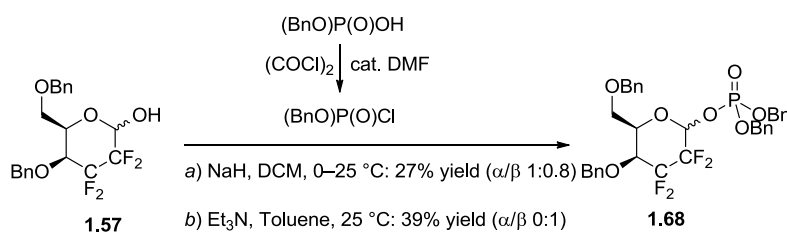
Scheme 6.7 Final and intermediate targets



6.2.1 Pyranose

For handling and availability reasons, the phosphorylation methodology was developed on tetrafluoro pyranose **1.57**. Initially, various methods based on the use of dibenzyl phosphoric acid, with the sugar acting as the electrophile^{158,159} were attempted, but all resulted in no reaction. Although there would possibly be less control of anomeric selectivity, the strategy was modified to involve deprotonation of the anomeric hydroxyl group, prior to addition of the phosphorylating agent.

Dibenzyl phosphoric acid ((BnO)₂P(O)OH) was converted to the more reactive dibenzyl phosphoryl chloride ((BnO)₂P(O)Cl).¹⁶⁰ Deprotonation with NaH followed by treatment with (BnO)₂P(O)Cl resulted in a low 27% yield. Use of conditions reported for the phosphorylation of a 2,2-difluorosugar (Et₃N & toluene)¹⁶¹ increased the yield to a moderate 39% (**Scheme 6.8**).

Scheme 6.8 Phosphorylation with dibenzyl phosphoryl chloride and a base

In addition to the moderate yields, obstacles to success included the difficulty of separating phosphate **1.68** from remaining hemiacetal **1.57** and inconsistencies in the dibenzyl phosphoryl chloride synthesis. With respect to these factors, the commercially available diphenyl phosphoryl chloride $((\text{PhO})_2\text{P}(\text{O})\text{Cl})$ was found to be a superior reagent (**Table 6.3**). This gave 67% yield of a single anomer with no recovery of starting material (entry 1). This was determined to be the undesired β -anomer by ^{13}C NMR.⁹¹

The base was changed to sodium hydride (entry 2), which gave a 1:1 mixture of both anomers. Reduction of the starting temperature from 0 °C to −40 °C successfully increased the ratio to 3:1 in favour of the desired (α) anomer (entry 3). At this point the reactions were continued using a different crop of starting material, which was (until dissolution) only the α -anomer. This should not have made a substantial difference to the ratio of products, as the starting material was stirred with base for 30 min prior to addition of diphenyl phosphoryl chloride. The rapid anomeric equilibration of pyranose **1.57** in the presence of base is detailed in section 3.4.

Table 6.3 Phosphorylations with $(\text{PhO})_2\text{P}(\text{O})\text{Cl}$

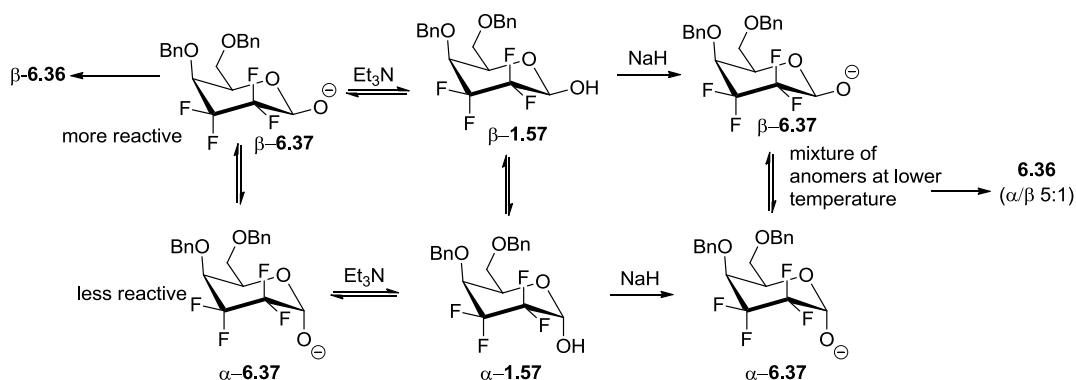
Entry	1.53 (α/β)	Solvent	Base (equiv)	Temp (°C)	Yield (%) ^[a]	6.36 (α/β) ^[b]
1	1:1	Toluene	Et_3N (1.2)	25	67	0:1
2	1:1	THF	NaH (2.0)	0 to 25	78	1:1
3	1:1	THF	NaH (2.0)	−40 to 25	94	3:1
4	1:0	THF	NaH (2.0)	−78 to 25	85	5:1
5	1:0	THF	NaH (2.0)	−30 to 25	79	5:1
6	1:0	THF	NaH (2.0) ^[c]	−40 to 25	86	4:1
7 ^[e]	1:0	THF	NaH (2.0) ^[d]	−40 to 25	95	5:1

^[a] Isolated ^[b] ^{19}F NMR ^[c] $(\text{PhO})_2\text{P}(\text{O})\text{Cl}$ added immediately after NaH;
^[d] $(\text{PhO})_2\text{P}(\text{O})\text{Cl}$ added after 10 min ^[e] 1.5 g scale

Modulation of the temperature (entries 4 & 5) did not make a significant difference to the anomeric ratio of the products, nor did reducing the amount of time between addition of base and diphenyl phosphoryl chloride (entries 6 & 7). Hence, the reaction was accomplished to 95% yield on a 1.5 g (4 mmol) scale. Anomeric separation was not possible at this stage.

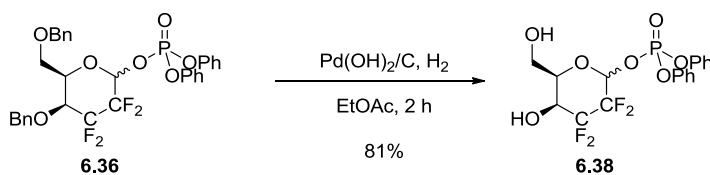
The anomeric selectivity could be explained by different reactivities of the two anomers. At room temperature, anomerisation is quicker and the results would suggest that the β -reacts much faster. At lower temperatures, anomerisation is slower so the isolated products more closely reflect the ratio of anomers at this temperature in solution (**Scheme 6.9**).

Scheme 6.9 Anomeric selectivity: temperature affects the rate of anomerisation



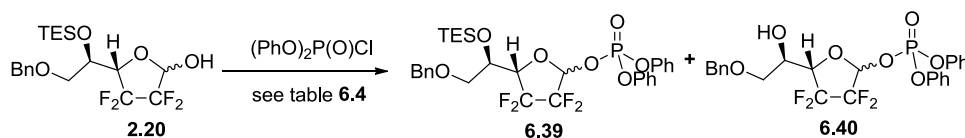
Removal of the benzyl groups by hydrogenolysis (**Scheme 6.10**) gave glycosyl phosphate **6.38** as an inseparable mixture of anomers. Removal of the phenyl groups was carried out by our collaborators, as they have the facilities to handle the resultant free phosphates.

Scheme 6.10 Debenzylation using hydrogenation



6.2.2 Furanose

With the phosphorylation optimised for the pyranose, a number of conditions were attempted on the furanose (**2.20**), as shown in **Scheme 6.11**. The TES-protected substrate was used because these reactions were carried out prior to the development of the MOM-based synthesis.

Scheme 6.11 Phosphorylation of tetrafluoro furanose

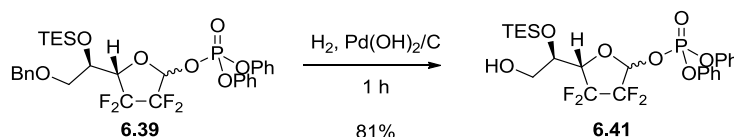
Utilisation of the conditions optimised for the pyranose provided a good yield (entry 1, **Table 6.4**), though some of the desilylation product (**6.40**) was also isolated. Variation of the temperature (entries 2 & 3) did not reduce the desilylation or have a significant effect on the anomeric ratio. Increasing the reaction time to 3 days, so as to achieve complete desilylation was attempted (entry 4), but surprisingly none of **6.40** was isolated from this reaction. Finally, the conditions used for β -phosphorylation of the pyranose (**Table 6.3**, entry 1) gave a high yield with an approximately equal ratio of anomers (entry 5). As the identity of the two anomers was not known at this stage, the conditions giving a ~1:1 ratio were the most appropriate for further reactions. The reaction was achieved to a quantitative yield on a 5 g (7 mmol) scale (entry 6).

Table 6.4 Phosphorylation of furanose **2.20**

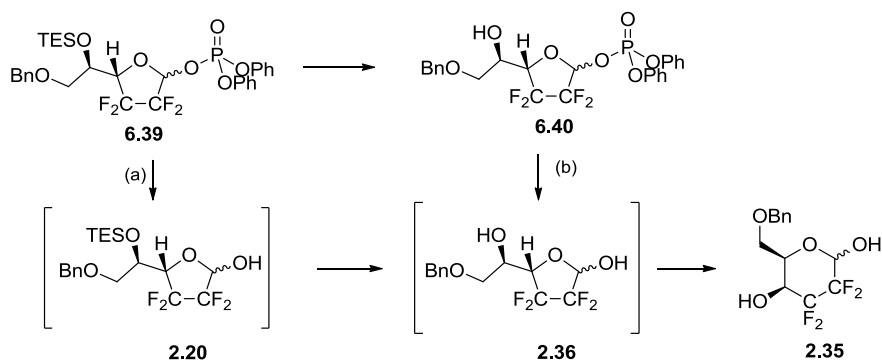
Entry	Base	Solvent	Temp (°C)	Time (h)	Yield (%)		Ratio (β/α)	
					6.39	6.40	6.39	6.40
1	NaH	THF	-40 to 25	16	80	8	1:0.3	1:0.6
2	NaH	THF	0 to 25	17	57	29	1:0.4	1:1
3	NaH	THF	-60 to 25	4	59	35	1:0.4	1:0.7
4	NaH	THF	0 to 25	67	71	0	1:0.3	-
5	Et ₃ N	Toluene	25	2.5	93	0	0.9:1	-
6 ^[a]	Et ₃ N	Toluene	25	2	quant.	0	0.8:1	-

[a] 5 g scale

Removal of the benzyl group was straightforward and accomplished in 1 h by hydrogenolysis (**Scheme 6.12**).

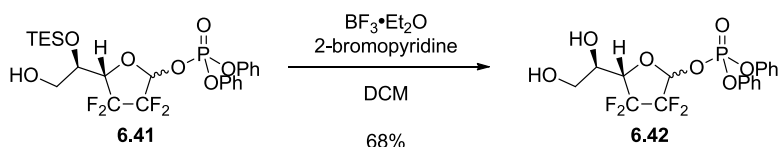
Scheme 6.12 Debenzylation of phosphoryl furanose **7.8**

Removal of the silyl protecting group proved to be less easy than anticipated, with dephosphorylation observed as a side reaction. As the resultant compound of dephosphorylation and desilylation was blocked at neither the 1- nor the 4-position, this allows the rapid isomerisation to pyranose **2.35** (**Scheme 6.13**).

Scheme 6.13 Loss of phosphate either before (a) or after (b) desilylation

A number of alternative desilylation conditions were tried to no avail. These included fluoride sources such as TBAF, pyridine-HF and ammonium fluoride,¹⁶² as well as reducing the temperature to 0 °C.¹⁶³ The observed desilylation during the phosphorylation step suggested that the workup may have been the cause (30 minutes stirring with aqueous ammonium chloride). To this end, a silyl protected furanose (**6.41**) was dissolved in aqueous saturated NH₄Cl, however no desilylation was observed after 3.5 h, which indicates that it was occurring during the phosphorylation reaction itself. It is possible that fluoride was attacking the phosphate.

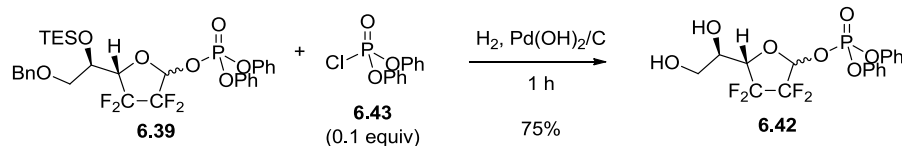
Due to the previous lack of anomeric control in the phosphorylation, an anomerisation reaction was attempted, using boron trifluoride diethyl etherate and 2-bromopyridine.¹⁶⁴ Although no change was observed in anomeric ratio, the silyl group was removed to give furanosyl phosphate **6.42** in 68% yield (**Scheme 6.14**). Desilylation using the Lewis acid BF₃•Et₂O is reported in the literature.¹⁶⁵

Scheme 6.14 Desilylation using boron trifluoride diethyl etherate

Though not possible up to this point, the anomeric separation of fully deprotected glycosyl phosphate **6.42** was completed by HPLC (DCM/MeOH 95:5).

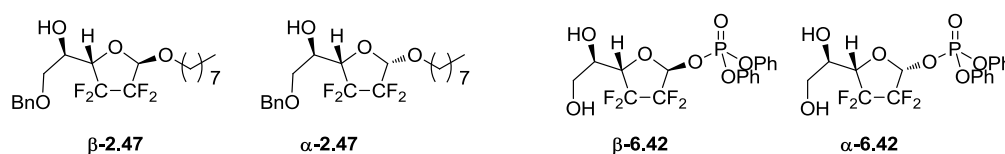
Interestingly, the large scale hydrogenolysis performed on an inseparable mixture of phosphate **6.39** and unreacted diphenyl phosphoryl chloride (**6.43**) resulted in removal of the TES group (**Scheme 6.15**). The unexpected removal of silyl protecting groups under hydrogenation conditions has been observed previously,^{166,167} however in our case it was advantageous. This deprotection was only observed when the starting material was contaminated by the phosphoryl chloride reagent (**6.43**), the identity of which was confirmed by ³¹P NMR.

Scheme 6.15 Unanticipated double deprotection



Anomeric assignment was attempted by extensive NMR experiments carried out on the two anomers of **6.42**, including NOEs, ^{19}F (^1H), ^{19}F - ^{19}F COSY and ^1H - ^{19}F COSY. However, none of these gave conclusive results as to the anomeric identification, which was ultimately achieved by comparison of the ^{19}F NMR spectra with those of the corresponding octyl glycosides **2.47**, Scheme 6.16.

Scheme 6.16 Galactofuranoside anomers



A strong correlation between the pairs of anomers of the compounds in Scheme 6.16 can be observed in their respective fluorine NMR spectra (Figure 6.7). While not absolutely conclusive, this gives a very strong indication of the identities of the two anomers of **6.42**.

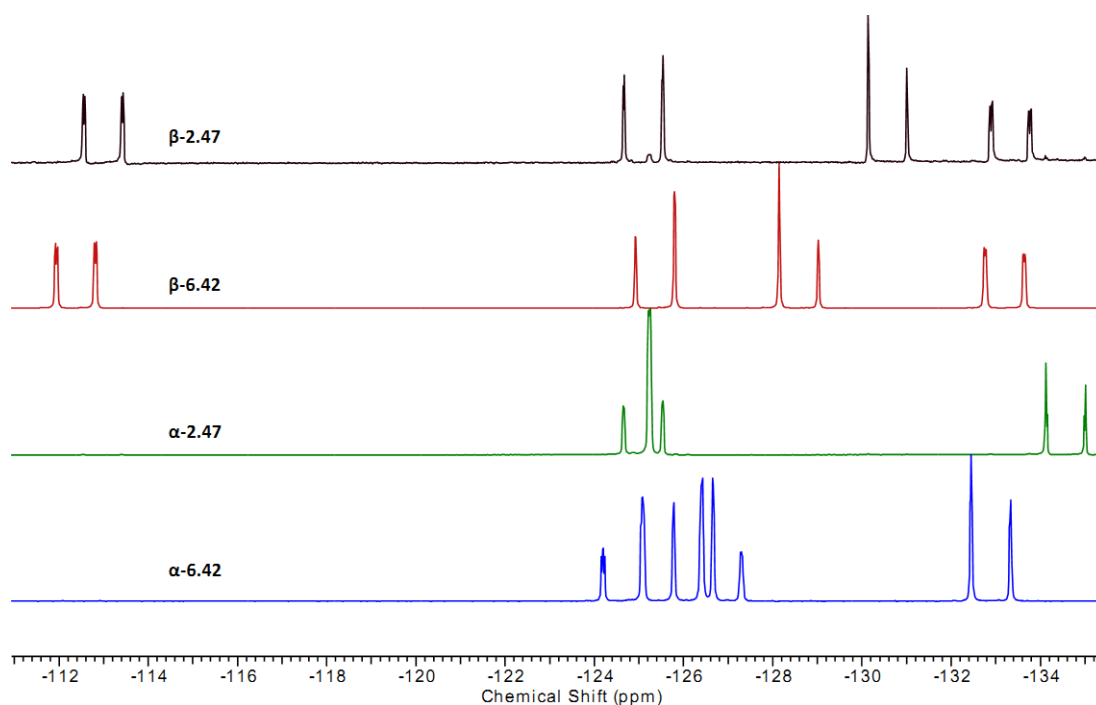


Figure 6.7 ^{19}F NMR spectra of **2.47** and **6.42**

6.3 Tetrafluorofuranosyl Furanose Disaccharides for GlfT2

As discussed in the introduction, disaccharides **6.26** and **6.29** were found to be acceptor substrates for galactofuranosyl transferase 2.¹⁵⁷ The binding of these substrates suggests the presence of a hydrophobic pocket. However, the lack of turnover of the benzyl derivatives implies a lack of space. Therefore, investigation of the activities of tetrafluorofuranosyl disaccharides **1.70** and **1.71** (**Figure 6.8**), (bearing the small yet hydrophobic tetrafluoroethylene moiety) is of interest.

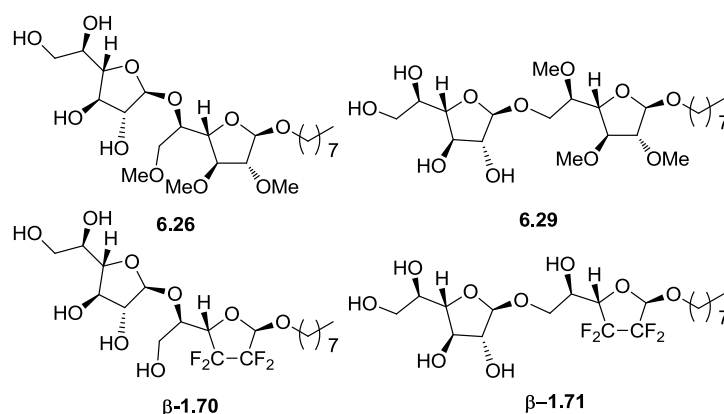


Figure 6.8 Comparison of targets (**1.70** & **1.71**) with known substrates (**6.26** & **6.29**)

6.3.1 Donors and Acceptors

The synthesis of octyl glycoside acceptors **2.47** and **2.48** (**Figure 6.9**) was covered in **Section 2.2**. The anomers of **2.47** are separable by HPLC, while those of **2.48** are not.

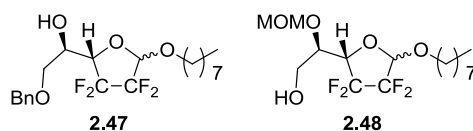
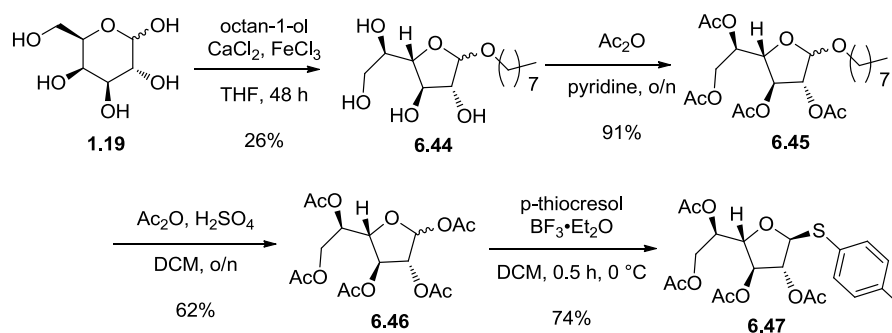


Figure 6.9 Novel tetrafluoro glycosyl acceptors

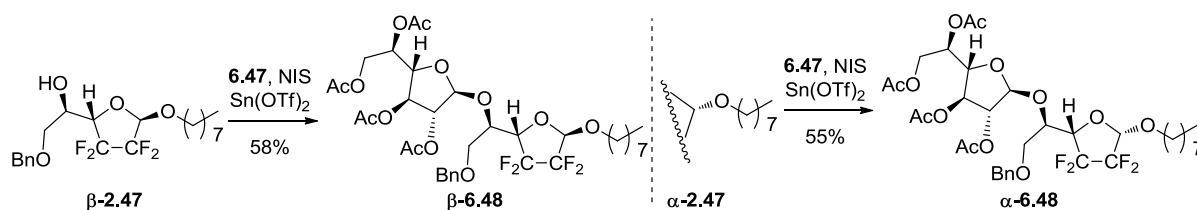
Donor **6.47** was synthesised in 4 steps using known procedures,^{157,168,169} as shown in **Scheme 6.17**.ⁱ D-Galactose (**1.19**) was converted to the octyl furanoside (**6.44**) using iron trichloride.¹⁶⁸ This was then protected using acetylations followed by exchanging the octyl group for an acetate to give **6.46**.¹⁶⁹ This was activated further by incorporation of a thiocresyl group into the anomeric position, giving acceptor **6.47**.¹⁵⁷

ⁱ Reactions performed by 3rd year undergraduate project student Jessica Gusthart, under direct supervision

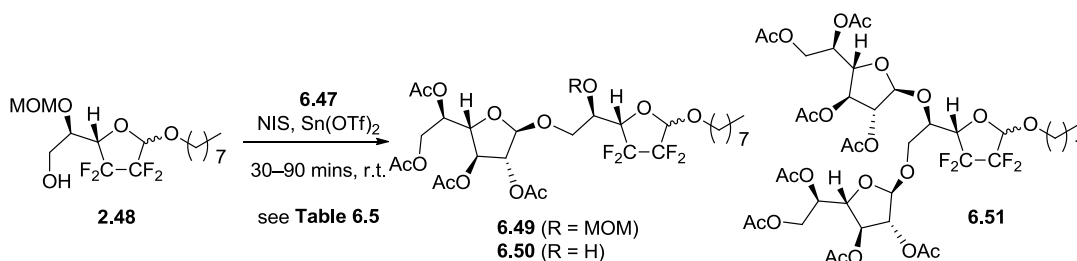
Scheme 6.17 Synthesis of glycosyl donor **6.47**

6.3.2 Glycosylation

The 1→5 linked disaccharides were synthesised from both anomers of **2.47**. These were separately coupled to donor **6.47**, with yields just below 60% for each (**Scheme 6.18**). Over 20% of starting material was also recovered for both reactions.

Scheme 6.18 Glycosylation to form protected 1→5 linked disaccharides

The synthesis of the 1→6 linked disaccharides required the use of acceptor **2.48**, which was used as a mixture of anomers (**Scheme 6.19**). Under the same conditions as for acceptor **2.47** (entry 1, **Table 6.5**) the desired product (**6.49**) was isolated in 19% yield. The product in which the MOM group had been removed (**6.50**) was also isolated in 20% yield. The loss of the MOM group is not a major problem, but the donor (**6.47**) continued to react with disaccharide **6.50** to give trisaccharide **6.51** in 16% yield (**Scheme 6.19**).

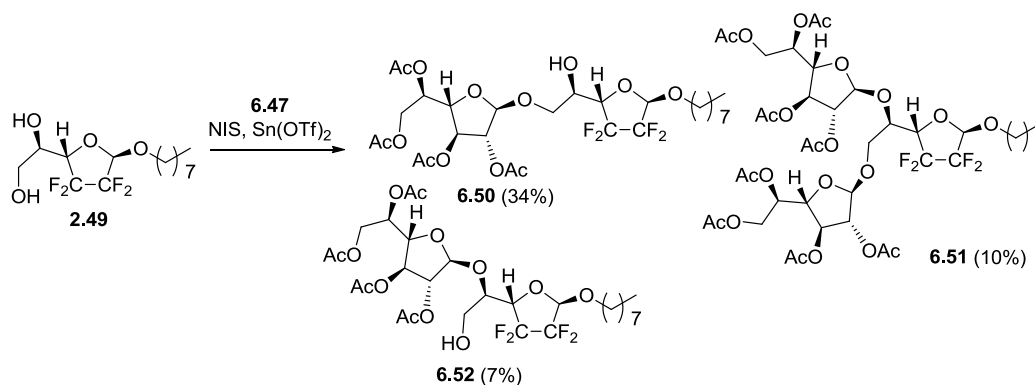
Scheme 6.19 Glycosylation to form 1→6 linked disaccharide

In an attempt to control the formation of this undesired trisaccharide, the reagents were reduced to ~1 equivalent and the time and temperature decreased (entry 2). This resulted in a slightly reduced yield of trisaccharide **6.51**. Further reduction of time and temperature on scale-up (entry 3) gave a total yield of 64% of the two desired disaccharides.

Table 6.5 Glycosylation to form 1→6 linked disaccharide

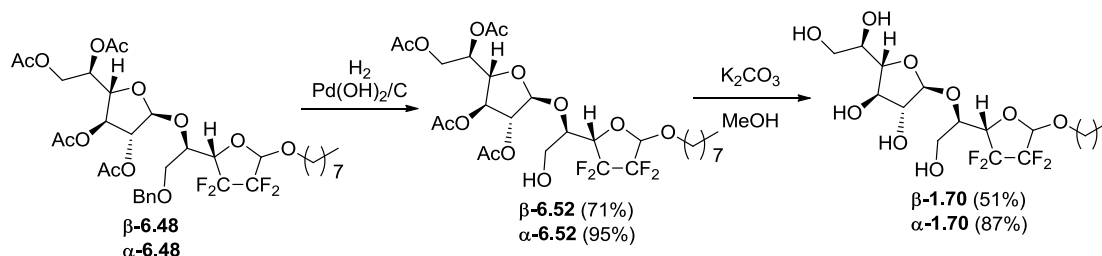
Entry	6.47 (equiv)	NIS (equiv)	Time (min)	Temp (°C)	Isolated Yields (%)		
					6.49	6.50	6.51
1	1.18	1.1	103	25	19	20	16
2	1.05	1	21	10	21	30	11
3	0.95	1	15	5–10	48	16	7

Glycosylation using the fully deprotected octyl glycoside **2.49** was also attempted, with selectivity expected to derive from the preference for reaction at the primary (6-) position. This resulted in reaction of the donor at both positions (**Scheme 6.20**), though selectivity was in favour of the desired product (**6.50**). Although this would possibly be a viable divergent route to both products, they were completely inseparable so this strategy was abandoned. The trisaccharide (**6.51**) was also isolated in 10% yield.

Scheme 6.20 Attempted glycosylation using acceptor **3.41**

6.3.3 Deprotections

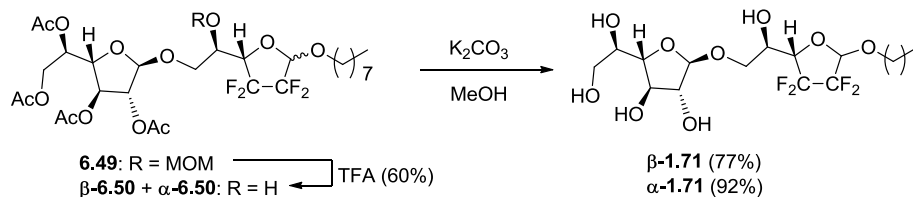
The benzyl group was removed from both anomers of **6.48**, as shown in **Scheme 6.21**. The acetates were then removed by methanolysis¹⁷⁰ to provide final products **β-1.70** and **α-1.70**.

Scheme 6.21 Deprotections of 1→5 linked disaccharides

The MOM group was removed from 1→6 linked disaccharides **6.49** using TFA, which successfully gave **6.50**, without affecting the glycosidic bonds. The resultant products were combined with those obtained from the glycosylation. Removal of the MOM group also

enabled separation of the anomers by HPLC. Subsequent methanolysis reactions removed the protecting groups from the non-reducing sugars to give both anomers of **1.71**.

Scheme 6.22 Deprotections of 1→6 linked disaccharides



6.4 Conclusions

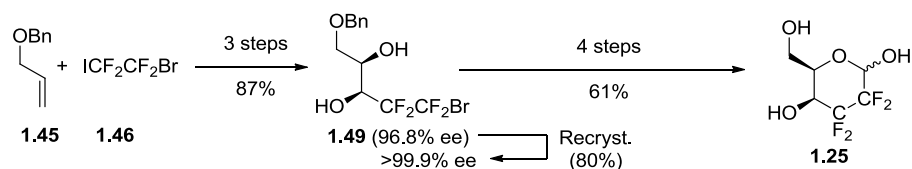
Methodology for the phosphorylation of our tetrafluoro sugars has been developed. Different anomeric selectivities have been observed, with the discovery of a completely selective β - phosphorylation of the pyranose. The synthesis of these compounds to a reasonable scale has enabled their conversion to uridine diphosphates, analogues of known UDP-galactose mutase inhibitors. The orthogonally protected tetrafluoro galactofuranose (**2.45**) has been used to synthesise four novel octyl disaccharides. These are tetrafluorinated analogues of known galactosyl transferase substrates and investigation of their properties as inhibitors or substrates will be carried out.

Chapter 7. Conclusions and Future Work

7.1 Tetrafluorogalactopyranose

Optimisations to the synthesis of 2,2,3,3-tetrafluorogalactopyranose (**1.25**) have been increased the overall yield from 37% to 53%. The enantiopurity of the final product has also been increased from 96.8% to >99.9%, by the recrystallisation of a key intermediate, diol **1.49** (Scheme 7.1).

Scheme 7.1 Synthesis of galactose **1.25** via diol **1.49**

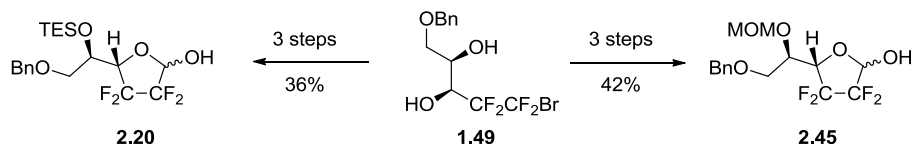


The execution of this synthesis on a large scale has enabled the use of the benzyl protected galactopyranose (**1.57**) as a substrate for further derivatisations (see below).

7.2 Tetrafluorogalactofuranose

The synthesis of the novel 2,2,3,3-tetrafluorogalactofuranose has been carried out, with an overall yield of 36% after 6 steps. This was achieved via the selective protection of diol **1.49**, by formation of either a silyl ether or methoxy methyl ether (Scheme 7.2).

Scheme 7.2 Synthesis of tetrafluorinated galactofuranose from diol **1.49**



Galactofuranose **2.45** (or **2.20**) represents a new addition to our arsenal of tetrafluorinated monosaccharide units. This will provide more options for the investigation of tetrafluorinated sugars as analogues of natural carbohydrates.

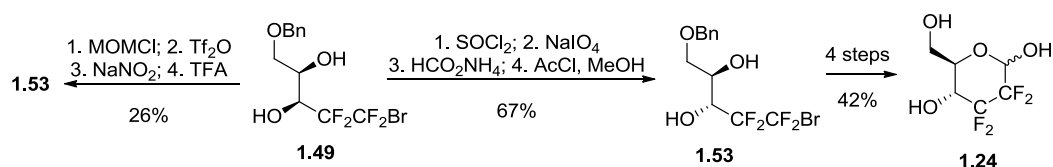
7.3 Tetrafluoroglucose

7.3.1 Synthesis

The synthesis of 2,2,3,3-tetrafluoroglucopyranose (**1.24**) has been optimised from 16% to 29%. The enantiopurity of the final product has also been increased from 97.1% to 99.2% by the inclusion of a recrystallisation.

Primary efforts have focussed on the conversion of *syn*-diol **1.49** to *anti*-diol **1.53**, which is an inversion required to install the correct stereochemistry at the 4-position of the final product (**1.24**), Scheme 7.3.

Scheme 7.3 Inversion of diol **1.49** to enable the synthesis of glucose **1.24**



Several alternative methods of inversion were investigated, including the use of nitrite for the displacement of a triflate vicinal to the tetrafluorinated alkyl group. This strategy was shown to give the desired product, with moderate yields. The previously reported⁶⁶ method of cyclic sulfate formation and hydrolysis has also been further optimised, giving an improved yield of 67% for the four steps (compared to 44%).

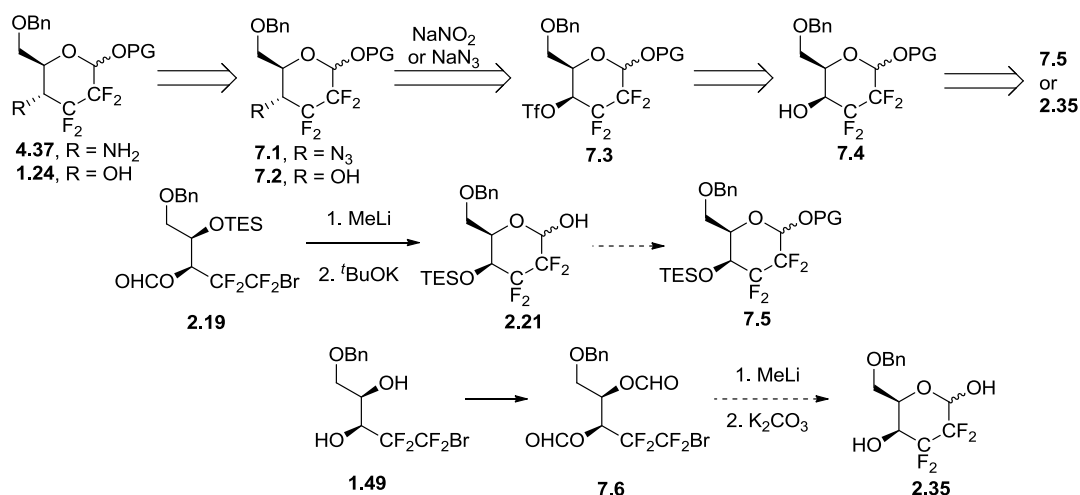
7.3.2 Screening

The resynthesis of the 2,2,3,3-tetrafluorinated glucose **1.24** and galactose **1.25** permits further biological screening. These two compounds will be assessed for their potential to cross the erythrocyte membrane by 2D ¹⁹F Exchange Spectroscopy NMR, as described by DiMagno and O'Hagan.^{46,47}

7.3.3 4-Aminotetrafluoroglucose

The synthesis of 4-amino-tetrafluoroglucopyranose (**4.37**) has been attempted, but was not successful, however an alternative strategy is described in **Scheme 7.4**. This would involve investigation of the S_N2 displacement of a triflate formed at the 4-position of the pyranose, using NaN₃ (or NaNO₂). This triflate (**7.3**) would be made from pyranose **7.4**, which could be synthesised in two ways. Treatment of the products of the cyclisation of formate **2.19** with base would give isomerisation to the TES-protected pyranose **2.21**. An alternative would be to investigate the cyclisation of diformate **7.6**. If the formate was still present after the reaction, hydrolysis would remove it, which would be followed by swift isomerisation to pyranose **2.35**. It is possible that the formate would not survive the cyclisation, in which case **2.35** would be the sole product.

Scheme 7.4 Proposed alternative synthesis of tetrafluoro 4-aminoglucose (**4.37**)

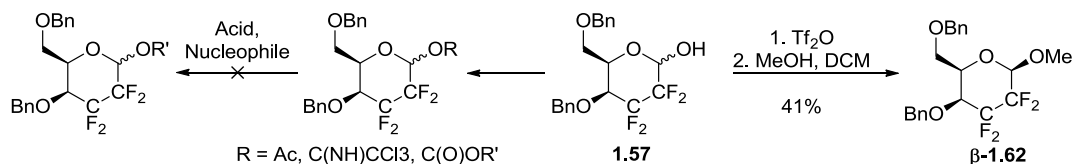


7.4 Glycosylation

7.4.1 Activation of Anomeric Position by Derivatisation

It has been found that the glycosylation of 2,2,3,3-tetrafluorogalactopyranose is not possible by acid catalysis (**Scheme 7.5**, left). However, the glycosylation has been achieved in moderate yield via the formation of a glycosyl triflate.

Scheme 7.5 Strategies for the glycosylation of pyranose **1.57**



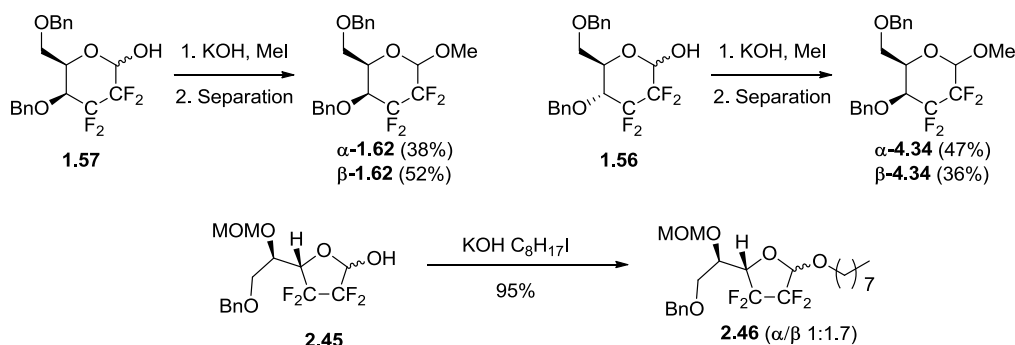
Further optimisation of the glycosylation reaction the glycosyl triflate would be advantageous for the incorporation of 2,2,3,3-tetrafluoroglycosides into more complex substrates. Future work could include attempting to combine the triflation and glycosylation steps, which would make the reaction easier to perform and may improve the overall yield. Optimisation of glycosylation step would require testing of alternative conditions to access a higher yield with less equivalents of nucleophile. Other alcohols would also need to be trialled as acceptors, as well as other fluorinated sugars as donors. Investigation of the anomeric selectivity of both the triflation and glycosylation would also be of great interest.

7.4.2 Anomeric Alkylation

Another means of glycosylation that has been shown to be very effective for these 2,2,3,3-tetrafluorinated sugars is the anomeric alkylation, as shown in **Scheme 7.6**. This

method has been used for the galactopyranose (**1.57**), as reported previously, in addition to the glucose (**1.56**) and galactofuranose (**2.45**). Different anomeric ratios were observed for each substrate.

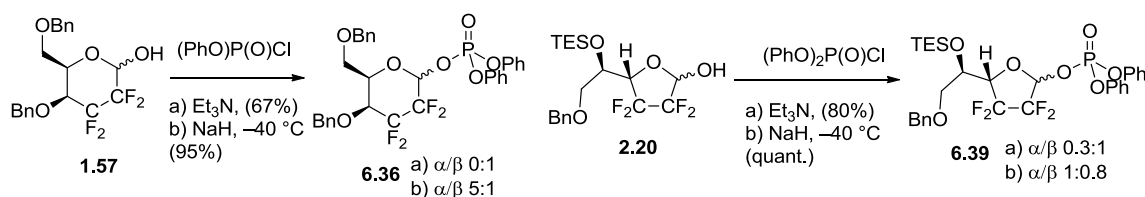
Scheme 7.6 Anomeric alkylation of tetrafluoro sugars, using alkyl iodides



7.5 Phosphorylation

Methodology has also been developed for the phosphorylation of 2,2,3,3-tetrafluorinated galactopyranose and furanose with moderate control of anomeric selectivity (**Scheme 7.7**).

Scheme 7.7 Phosphorylation of tetrafluorinated galactopyranose and furanose

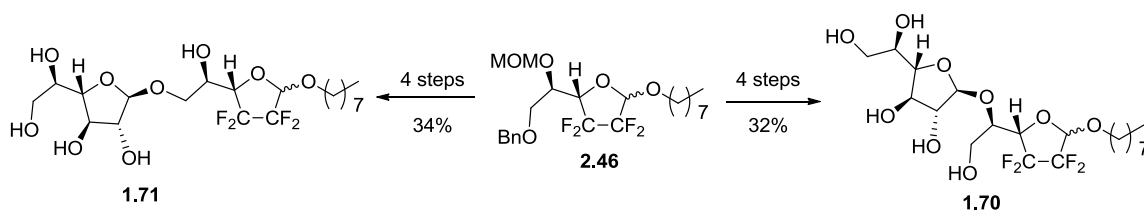


The described phosphorylations have permitted the synthesis of the first tetrafluorinated UDP-galactose analogues, which are of interest due to their resemblance to existing UDP-galactose mutase inhibitors.

7.6 Tetrafluorinated Disaccharides

The synthesis of novel alkyl galactofuranosyl disaccharides employing 2,2,3,3-tetrafluorogalactofuranose as the reducing sugar has been achieved (**1.70** & **1.71**, **Scheme 7.8**). This was made possible by the synthesis of galactofuranose **2.46**, which bears orthogonal protecting groups.

Scheme 7.8 Incorporation of tetrafluorogalactofuranose into two disaccharides



The synthesis of these compounds allows their investigation as substrates or inhibitors of galactofuranosyl transferase, a key enzyme involved in the construction of the mycobacterial cell wall.

7.7 Analysis

Recrystallisations have enabled the acquisition of five novel crystal structures of 2,2,3,3-tetrafluorinated galactopyranoses (**Figure 7.1**). The full data for these structures can be found in the appendix.

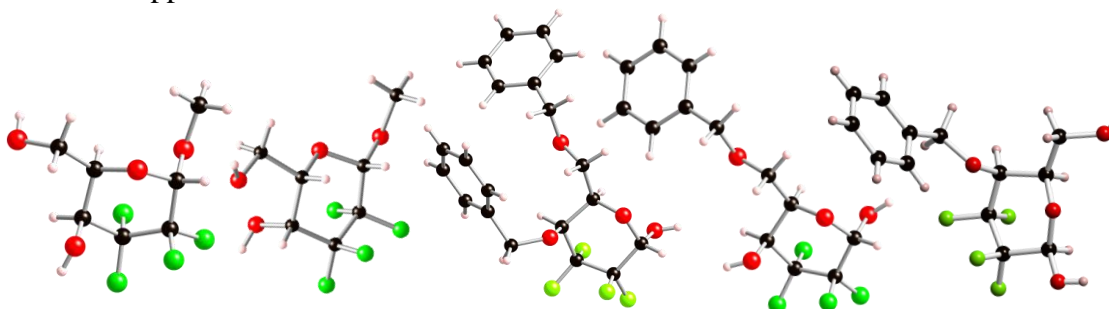


Figure 7.1 X-ray crystal structures obtained (left to right 3.1, 3.2, α -1.57, α -2.35, β -3.5)

These structures, in combination with data obtained from extensive NMR studies of methyl galactosides **3.1** and **3.2** have been used as evidence to support the conclusion that our tetrafluorinated sugars adopt conformations similar to those found for non-fluorinated carbohydrates. The conformation of carbohydrate mimics is very important given the influence of conformation on carbohydrate-protein binding interactions.

Chapter 8. Experimental

8.1 General Methods

Chemical reagents were obtained from commercial sources and used without further purification, unless stated otherwise. Anhydrous solvents were distilled immediately prior to use, with the exception of anhydrous DMF and DMSO which were purchased in sealed containers from commercial sources. THF was distilled from Na/benzophenone immediately prior to use. DCM and Et₃N were dried over CaH₂. All glassware was flame-dried under vacuum and cooled under N₂ prior to use. Water or air sensitive reactions were performed under inert atmosphere, using dry solvents.

Reactions were monitored by TLC (Merck Kieselgel 60 F₂₅₄, aluminium sheet). Detection was carried out using one of the following dyeing reagents: Anisaldehyde-reagent: a solution of 5.1 mL p-anisaldehyde, 2.1 mL AcOH and 6.9 mL H₂SO₄ in 186 mL EtOH gives a reagent that will show varied coloured spots after development with a heat gun. KMnO₄-reagent: a solution of 3 g KMnO₄, 20 g K₂CO₃ and 5 mL NaOH (aq., 5 w%) in 300 mL H₂O gives a reagent that will show yellow spots after development with a heat gun.

Column chromatography was performed on silica gel (60 Å). Particle size 35–70 µm, or 40–63 µm. All reported solvent mixtures are volume measures.

Preparative HPLC was carried out using Biorad Bio-Sil D 90-10 columns (250 × 22 mm at 15–20 mL min⁻¹ and 250 × 10 mm at 5 mL min⁻¹). Analytical chiral HPLC was performed on an Agilent Technologies 1120 Compact LC system using a normal phase Chiralcel OD-H column with 254 nm detection, eluted with IPA/hexane 5:95.

¹H, ¹⁹F and ¹³C NMR spectra were recorded at room temperature on a Bruker AV300 or AV400 spectrometer. ¹H and ¹³C chemical shifts (δ) are quoted in (ppm) relative to residual solvent peaks as appropriate. ¹⁹F spectra were externally referenced to CFCl₃. A narrow scan-width (-100 to -150 ppm) was used for those compounds in which the peaks in the ¹⁹F spectra fell within that range. The coupling constants (*J*) are given in Hertz (Hz). The proton NMR signals were designated as follows: s (singlet), d (doublet), t (triplet), q (quartet), quin (quintet), sxt (sextet), spt (septet), m (multiplet), or a combination of the above. Atom numbering used in NMR spectra tabulation refers to the positions depicted below.

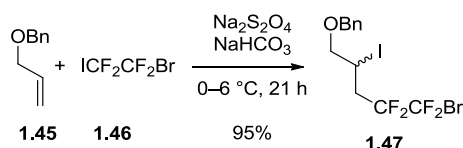


IR spectra were recorded as neat films on a Nicolet 380 FT-IR. Absorption peaks are given in cm⁻¹ and the intensities were designated as follows: w (weak), m (medium), s (strong), br (broad). Optical rotations were recorded on an Optical Activity Polaar 2001 polarimeter at 589 nm. Melting points were recorded on a Gallenkamp electrothermal

melting point apparatus. Low resolution ES mass spectra were recorded on a Waters ZMD single quadrupole system. High resolution mass spectra were recorded on the Bruker Apex III FT-ICR-MS.

8.2 Synthesis of Tetrafluoro Galactopyranose **1.57**

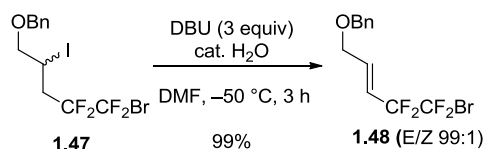
8.2.1 5-Benzyloxy-1-bromo-1,1,2,2-tetrafluoro-3-iodopentane (**1.47**)



A solution of allyl benzyl ether (29.5 g, 199 mmol) in MeCN/H₂O (1:1, 200 mL) was sonicated for 15 min under N₂ and then cooled to 0 °C. ICF₂CF₂Br (67.82 g, 221 mmol) was weighed into a separate flask then added to the first mixture. The residue was rinsed with MeCN/H₂O (1:1, 40 mL) (also sonicated). The reaction was then treated with NaHCO₃ (8.36 g, 99.5 mmol) and Na₂S₂O₄ (17.3 g, 99.5 mmol) and stirred at 4–6 °C for 21 h. H₂O (140 mL) was then added and the reaction mixture was extracted into Et₂O (3 × 240 mL). The combined organic extracts were washed with brine (2 × 400 mL), dried (MgSO₄), filtered and concentrated to give iodide **1.47** as an orange oil (86.3 g, 95%).

R_f 0.49 (petrol ether/Et₂O 96:4) **¹H NMR** (CDCl₃, 300 MHz) δ 7.28–7.43 (5H, m, H_{Ar}), 4.61 (2H, s, CH₂Ph), 4.39 (1H, m, CHI), 3.76 (1H, dd, *J* 10.7, 5.2 Hz, CHHOBn), 3.69 (1H, dd, *J* 10.5, 6.5 Hz, CHHOBn), 3.10 (1H, m, CF₂CHH), 2.72 (1H, m, CF₂CHH) (ppm); **¹³C NMR** (CDCl₃, 75 MHz) δ 137.4 (C_{Ar}), 128.5 (2 × CH_{Ar}), 128.0 (CH_{Ar}), 127.7 (2 × CH_{Ar}), 74.8 (CH₂Ph), 73.0 (CH₂OBn), 37.3 (t, *J* 22.1 Hz, CF₂CH₂), 15.3 (CHI) (ppm); **¹⁹F NMR** (CDCl₃, 282 MHz) δ -66.5 (2F, s), -111.8–111.3 (2F, m) (ppm). NMR spectra in agreement with reported data.⁶⁶

8.2.2 (*E*)-5-Benzyloxy-1-bromo-1,1,2,2-tetrafluoropent-3-ene (**1.48**)

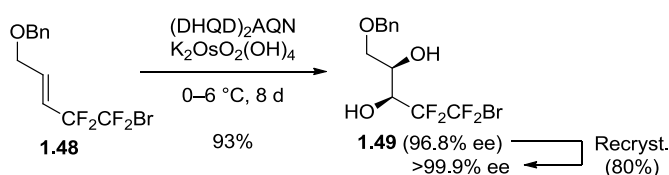


Iodide **1.47** (23.2 g, 50.9 mmol) was dissolved in laboratory reagent grade DMF (83 mL) and cooled to $-50\text{ }^\circ\text{C}$. DBU (23.6 mL, 158 mmol) was added slowly. Stirring was continued at -50 to $-55\text{ }^\circ\text{C}$ for 3 h. Aq. HCl (1M, 170 mL) was then added and the resultant mixture extracted quickly into Et₂O (4 × 230 mL). The combined organic phase was dried (Na₂SO₄), filtered and concentrated to give an orange oil. Column

chromatography (petrol ether/Et₂O 96:4) gave alkene **1.48** as a cloudy oil (16.41 g, 99%, *E/Z* 99:1).

R_f 0.41 (petrol ether/Et₂O 96:4) **¹H NMR** (CDCl₃, 300 MHz) δ 7.28–7.48 (5H, m, H_{Ar}), 6.49 (1H, dtt, *J* 15.8, 4.1, 2.1 Hz, CHCH₂), 6.01 (1H, m, CF₂CH), 4.59 (2H, app s, CH₂Ph), 4.17 (2H, m, CH₂OBn) (ppm); **¹³C NMR** (75 MHz, CDCl₃) δ (ppm) 138.9 (CHCH₂), 137.5 (C_{Ar}), 128.5 (2 × CH_{Ar}), 127.9 (CH_{Ar}), 127.7 (2 × CH_{Ar}), 117.1 (CHCF₂), 72.9 (CH₂Ph), 68.2 (CH₂OBn); **¹⁹F NMR** (CDCl₃, 282 MHz) δ (ppm) -66.0 (2F, t, *J* 5.4 Hz, CF₂Br), -109.8 (2F, m, CF₂CH) (ppm). NMR spectra correspond to reported data.⁶⁶

8.2.3 (3*S*,4*R*)-5-Benzyloxy-1-bromo-1,1,2,2-tetrafluoropentan-3,4-diol (**1.49**)



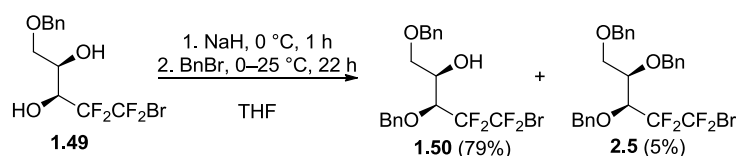
To a stirred solution of ^tBuOH/H₂O (1:1, 700 mL) was added (DHQD)₂AQN (1.33 g, 1.52 mmol), K₃Fe(CN)₆ (75.2 g, 229 mmol), K₂CO₃ (31.6 g, 229 mmol) and K₂OsO₂(OH)₄ (224 mg, 609 μmol). H₂O (30 mL) was added and most of the solids were dissolved. MeSO₂NH₂ (7.24 g, 76.2 mmol) was then added and the reaction mixture cooled to 0 °C. Alkene **1.48** (24.91 g, 76.2 mmol) was weighed in a separate flask and then added to the first mixture. The residue was rinsed in with ^tBuOH (30 mL) and the resultant mixture stirred at 4–6 °C for 8 days. Na₂SO₃ (100 g) was added and the reaction mixture stirred for 2 h, at 0 °C to r.t. before being treated with H₂O (175 mL). Extraction was carried out into EtOAc (3 × 350 mL). The combined organic phases were washed with HCl (2M, 2 × 75 mL) then brine (75 mL), before being dried (MgSO₄), filtered and concentrated to give a yellow solid (96.8% *e.e.*). Column chromatography (petrol ether/EtOAc 65:35) gave diol **1.49** as a white solid (25.61 g, 93%). This white solid was suspended in hexane and heated to 40 °C gently, then Et₂O was added until dissolution occurred. The solution was allowed to stand for 4 days at r.t. and the resultant crystals filtered and washed with hexane to give a white solid (20.54 g, 75%, >99.9% *e.e.*).

R_f 0.15 (petrol ether/EtOAc 80:20); **Mp** 96–97 °C (hexane/Et₂O); **[α]_D** -1.7 (c 0.54, CHCl₃, 23 °C); **¹H NMR** (CDCl₃, 300 MHz) δ (ppm) 7.29–7.44 (5H, m, H_{Ar}), 4.59 (2H, s, CH₂Ph), 4.29 (1H, m, CHCH₂), 4.16 (1H, app dddt, *J* 20.9, 8.6, 3.9, 1.2 Hz can be observed, CF₂CH), 3.63 (2H, d, *J* 5.9 Hz, CH₂OBn), 3.22 (1H, d, *J* 8.7 Hz, CF₂CHOH), 2.61 (1H, d, *J* 4.6 Hz, CHOHCH₂) (ppm); **¹³C NMR** (CDCl₃, 75 MHz) δ (ppm) 128.6 (2 × CH_{Ar}), 128.2 (CH_{Ar}), 127.9 (2 × CH_{Ar}), 73.7 (CH₂Ph), 71.0 (CH₂OBn), 68.4 (CF₂CH), 66.6

(CHCH₂) (ppm); ¹⁹F NMR (CDCl₃, 282 MHz) δ -62.7 (1F, dd, *J* 179.5, 8.6 Hz, CFFBr), -63.9 (1F, dd, *J* 179.5, 3.2 Hz, CFFBr), -113.8 (1F, d, *J* 269.7 Hz, CF₂CF₂Br), -125.7 (1F, ddd, *J* 269.7, 21.5, 8.6 Hz, CF₂CF₂Br) (ppm). NMR spectra in agreement with reported data.⁶⁶

The acidic extracts from the workup were combined and neutralised with NaOH (2M, aq) then extracted into EtOAc (2 × 270 mL). The combined organic phase was dried (MgSO₄), filtered and concentrated to give impure (DHQD)₂AQN as red solid. Column chromatography (DCM/MeOH 85:15) gave recovered (DHQD)₂AQN (1.29 g, 92%) as a yellow/orange solid.

8.2.4 (3S,4R)-3,5-Dibenzzyloxy-1-bromo-1,1,2,2-tetrafluoropentan-4-ol (1.50)



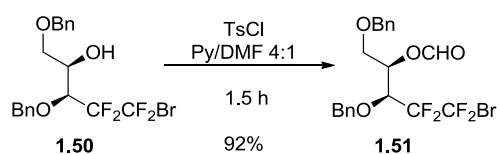
Diol **1.49** (11.7 g, 32.4 mmol) was dissolved in THF (200 mL) and cooled to 0 °C. NaH (60% in mineral oil, 1.30 g, 32.4 mmol) was added and stirred at 0 °C for 1 h. BnBr (3.85 mL, 32.4 mmol) was added and the resultant solution stirred from 0 °C to r.t. for 22 h. Aq. NH₄Cl (sat., 180 mL) was added and the resultant mixture stirred at r.t. for 30 min. Extraction was carried out into EtOAc (4 × 250 mL). The combined organic phase was washed with brine (2 × 800 mL), dried (MgSO₄), filtered and concentrated to give a pale yellow oil. Column chromatography (petrol ether/EtOAc 95:5) gave alcohol **1.50** as a colourless oil (11.54 g, 79%) and tris-benzyl ether **2.5** as a colourless oil (970 mg, 5%).

Data for 1.50: [α]_D -30.8 (c 0.5, CHCl₃, 25 °C) ¹H NMR (CDCl₃, 300 MHz) δ 7.29–7.41 (10H, m, H_{Ar}), 4.83 (1H, d, *J* 10.6 Hz, CHHPh), 4.54 (1H, d, *J* 11.8 Hz, CHHPh), 4.47 (1H, d, *J* 12.0 Hz, CHHPh), 4.28 (1 H, ddd, *J* 15.5, 8.4, 2.2 Hz, CF₂CH), 4.13 (1H, q, *J* 7.2 Hz, CHOH), 3.54 (1H, dd, *J* 9.5, 5.2 Hz, CHHOBn), 3.43 (1H, dd, *J* 8.8, 7.3 Hz, CHHOBn), 2.40 (1H, d, *J* 8.8 Hz, OH) (ppm); ¹³C NMR (75 MHz, CDCl₃) δ (ppm) 128.5 (2 × CH_{Ar}), 128.4 (CH_{Ar}), 128.3 (CH_{Ar}), 128.0 (CH_{Ar}), 127.9 (2 × CH_{Ar}), 75.8 (2 × CH₂Ph), 73.4 (CHOBn), 70.0 (CH₂Ph); ¹⁹F NMR (CDCl₃ 282 MHz) δ -63.1 (2F, app s, CF₂Br), -112.33 (1F, d, *J* 274.0 Hz, CF₂CF₂Br), -118.15 (1F, ddd, *J* 275.1, 15.0, 4.3 Hz, CF₂CF₂Br) (ppm). NMR spectra in agreement with reported data.⁶⁶

Data for (3S,4R)-3,4,5-Tribenzzyloxy-1-bromo-1,1,2,2-tetrafluoropentane (2.5): [α]_D -4.2 (c 0.5, CHCl₃, 24 °C) ¹H NMR (400 MHz, CDCl₃) δ (ppm) 7.28–7.48 (15H, m, H_{Ar}), 4.75 (1H, d, *J* 10.9 Hz, CHHPh), 4.72 (1H, d, *J* 9.0 Hz, CHHPh), 4.69 (1H, d, *J* 8.2

Hz, CHHPh), 4.64 (1H, d, J 11.7 Hz, CHHPh), 4.51 (1H, d, J 12.4 Hz, CHHPh), 4.46 (1H, d, J 12.5 Hz, CHHPh), 4.33 (1H, ddd, J 18.7, 6.1, 4.3 Hz, CHCF_2), 4.00 (1H, m, CHCH_2), 3.67 (1H, ddd, J 10.0, 5.8, 0.9 Hz, CHHOBn), 3.57 (1H, dd, J 10.0, 5.4 Hz, CHHOBn); ^{13}C NMR (101 MHz, CDCl_3) δ (ppm) 137.9 (C_{Ar}), 137.8 (C_{Ar}), 136.8 (C_{Ar}), 128.4 ($\text{CH}_{\text{Ar}} \times 2$), 128.34 ($\text{CH}_{\text{Ar}} \times 2$), 128.29 ($\text{CH}_{\text{Ar}} \times 2$), 128.27 ($\text{CH}_{\text{Ar}} \times 2$), 128.0 ($\text{CH}_{\text{Ar}} \times 4$), 127.6 - 127.8 ($\text{CH}_{\text{Ar}} \times 3$), 76.4 (CHCH_2), 75.5 (CH_2Ph), 75.0 (dd, J 28, 22 Hz, CHCF_2), 73.5 (CH_2Ph), 73.4 (CH_2Ph), 68.9 (CH_2OBn); ^{19}F NMR (282 MHz, CDCl_3) δ (ppm) -62.68 (2F, app. s, CF_2Br), -110.92 (1F, d, J 270.8 Hz, CFCH), -119.52 (1F, dd, J 270.8, 17.2 Hz, CFCH). NMR spectra in agreement with reported data.⁶⁶

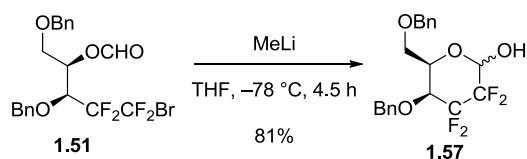
8.2.5 (3*S*,4*R*)-3,5-Dibenzyloxy-1-bromo-1,1,2,2-tetrafluoropentan-4-yl formate (**1.51**)



TsCl (6.94 g, 36.4 mmol) was dissolved in pyridine (66 mL) and cooled to 0 °C. DMF (22 mL) was added and the resultant solution stirred at r.t. for 20 min. The solution was then cooled to 0 °C and a solution of alcohol **1.50** (11.73 g, 26.0 mmol) in pyridine (22 mL) was added dropwise. The resultant solution was stirred at r.t. for 1.5 h before being cooled to 0 °C. H₂O (120 mL) was added and extraction carried out into hexane (3 × 120 mL). Combined organic phases were dried (MgSO_4), filtered and concentrated to give formate **1.51** as a pale yellow oil (11.44 g, 92%).

$[\alpha]_{\text{D}} -26.2$ (c 0.4, CHCl_3 , 23 °C); ^1H NMR (CDCl_3 , 300 MHz) δ 8.04 (1H, s, CHO), 7.28–7.42 (10H, m, H_{Ar}), 5.54 (1H, td, J 6.9, 3.1 Hz, CHCH_2), 4.82 (1H, d, J 10.8 Hz, CHHPh), 4.61 (1H, d, J 10.8 Hz, CHHPh), 4.53 (1H, d, J 12.0 Hz, CHHPh), 4.47 (1H, d, J 11.8 Hz, CHHPh), 4.45 (1H, m, CF_2CH), 3.57 - 3.70 (2H, m, CH_2OBn) (ppm); ^{13}C NMR (CDCl_3 , 75 MHz) δ 159.7 (CO), 137.2 (C_{Ar}), 136.3 (C_{Ar}), 128.6 ($4 \times \text{CH}_{\text{Ar}}$), 128.3 (CF_2CH), 128.3 ($2 \times \text{CH}_{\text{Ar}}$), 128.1 (CH_{Ar}), 127.9 ($2 \times \text{CH}_{\text{Ar}}$), 75.9 (CH_2Ph), 73.5 ($2 \times \text{CF}_2\text{CH}$ & CH_2Ph) (ppm); ^{19}F NMR (CDCl_3 , 282 MHz) δ -63.5 (2F, s, CF_2Br), -112.2 (1F, d, J 272.9 Hz, CF_2CH), -118.47 (1F, dd, J 274.0, 17.2 Hz, CF_2CH) (ppm). NMR spectra in agreement with reported data.⁶⁶

8.2.6 4,6-Di-*O*-benzyl-2,3-dideoxy-2,2,3,3-tetrafluorogalactopyranose (threohexopyranose) (**1.57**)

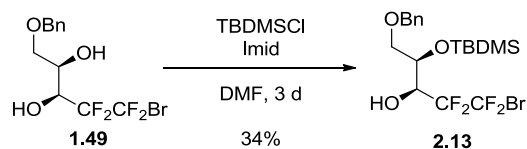


Formate **1.51** (10.69 g, 22.3 mmol) was dissolved in dry DCM (120 mL) and filtered through a pad of MgSO_4 directly into the reaction flask, while drying the filtrate with N_2 . The resultant oil was dried under high vacuum for 16 h before being dissolved in THF (210 mL) and cooled to $-78\text{ }^{\circ}\text{C}$. MeLi (1.6 M in Et_2O , 13.3 mL, 21.2 mmol) was added very slowly, dropwise. The resultant solution was stirred at $-78\text{ }^{\circ}\text{C}$ for 4.5 h. At $-78\text{ }^{\circ}\text{C}$, aq. NH_4Cl (sat., 75 mL) was added to the reaction mixture, which was then stirred for 30 min, while allowing to warm to r.t. The mixture was diluted with H_2O (150 mL) then extracted into EtOAc ($3 \times 520\text{ mL}$), dried (MgSO_4), filtered and concentrated to give a white solid. Column chromatography (petrol ether/acetone 90:10 then 75:25) gave pyranose **1.57** as a white solid (7.20 g, 81%).

Mp $98\text{--}103\text{ }^{\circ}\text{C}$ (CHCl_3); $^1\text{H NMR}$ (CDCl_3 , 300 MHz) δ (ppm) 7.18–7.39 (20H, m, H_{Ar}), 5.24 (1H, dd, J 14.6, 5.3 Hz, CHOH_α), 4.84 (1H, d, J 3.4 Hz, CHHPh), 4.81 (1H, d, J 3.4 Hz, CHOH), 4.32–4.56 (7H, m, $\text{CH}_2\text{Ph}_{\beta+\alpha}$, CHCH_2_α , $\text{CHHPh}_{\beta+\alpha}$), 3.78–3.95 (3H, m, CHCH_2_β , $\text{CF}_2\text{CH}_{\beta+\alpha}$), 3.46–3.62 (2H, m, $\text{CHHOBn}_{\alpha+\beta}$), 3.26–3.45 (2H, m, $\text{CHHOBn}_{\beta+\alpha}$); $^{19}\text{F NMR}$ (CDCl_3 , 282 MHz) α -**1.57**: -115.84 (1F, d, J 274.0 Hz), -119.4 (1F, m, J 271.9 Hz can be observed), -129.2 (1F, m, J 275.1 Hz can be observed), 134.5 (1F, d, J 270.8 Hz). β -**1.57**: -117.32 (1F, d, J 275.1 Hz), -130.7 (1F, dt, J 276.2, 11.8 Hz), -136.5 (1F, m, J 261.1 Hz can be observed), -138.8 (1F, m, J 261.1 Hz can be observed) (ppm). $^{13}\text{C NMR}$ (101 MHz, CDCl_3) δ (ppm) 137.1 (C_{Ar}), 136.9 (C_{Ar}), 136.4 ($\text{C}_{\text{Ar}} \times 2$), 127.8–128.8 ($\text{CH}_{\text{Ar}} \times 20$), 91.2–92.4 ($\text{C}-1_{\alpha+\beta}$), 74.4–75.4 ($\text{C}-4_{\alpha+\beta}$, $\text{CH}_2\text{Ph} \times 2$), 73.6 ($\text{CH}_2\text{Ph} \times 2$), 72.7 (d, J 7 Hz, $\text{C}-4_\beta$), 68.1 ($\text{C}-6_\alpha$), 68.0 (d, J 6 Hz, $\text{C}-4_\alpha$), 67.2 ($\text{C}-6_\beta$). NMR spectra in agreement with reported data.⁶⁶

8.3 Synthesis of Tetrafluoro Galactofuranoses **2.20** & **2.45**

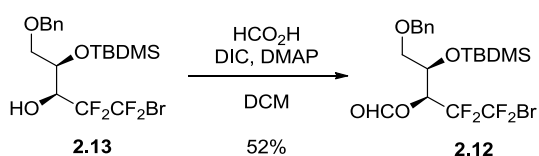
8.3.1 (3*S*, 4*R*)-5-(benzyloxy)-1-bromo-4-((*tert*-butyldimethylsilyl)oxy)-1,1,2,2-tetrafluoropentan-3-ol (**2.13**)



Diol **1.49** (250 mg, 0.69 mmol) was dissolved in DMF (1 mL) and treated with TBDMSCl (204 mg, 1.35 mmol) and imidazole (3.19 mmol). The reaction was stirred at r.t. for 3 days then diluted with DCM (15 mL) and washed with H₂O (10 mL) and brine (10 mL). The organic phase was dried (MgSO₄), filtered and concentrated to give a yellow oil. Column chromatography (petrol ether/EtOAc 98:2) gave TBDMS-ether **2.13** as a colourless oil (113 mg, 34%).

R_f 0.44 (petrol ether/EtOAc 90:10); [**α**]_D -13.1 (c 0.4, CHCl₃, 23.5 °C); **IR** (neat) 2954 (w), 2931 (w), 2361 (w), 2340 (w), 1257 (m), 1155 (m), 1132 (s), 1092 (s) cm⁻¹; **¹H NMR** (400 MHz, CDCl₃) δ (ppm) 7.28 - 7.41 (5H, m, H_{Ar}), 4.56 (1H, d, *J* 12.0 Hz, CHHPh), 4.53 (1H, d, *J* 11.9 Hz, CHHPh), 4.22 - 4.37 (2H, m, CHCF₂ & CHCH₂), 3.51 (1H, t, *J* 8.9 Hz, CHHOBn), 3.43 (1H, dd, *J* 9.2, 5.3 Hz, CHHOBn), 3.13 (1H, d, *J* 10.9 Hz, OH), 0.89 (9H, s, C(CH₃)₃), 0.10 (3H, d, *J* 0.6 Hz, SiCH₃), 0.09 (3H, s, SiCH₃); **¹³C NMR** (100 MHz, CDCl₃) δ (ppm) 137.6 (1C, C_{Ar}), 128.5 (2C, 2 × CH_{Ar}), 127.9 (1C, CH_{Ar}), 127.6 (2C, 2 × CH_{Ar}), 73.4 (1C, s, CH₂Ph), 70.1 (1C, CH₂OBn), 67.3 (1C, CHCH₂), 67.1 (1C, CHCF₂), 25.7 (3C, C(CH₃)₃), 17.9 (1C, C(CH₃)₃), -4.3 (1C, SiCH₃), -5.3 (1C, SiCH₃) CF₂CF₂ not observed; **¹⁹F NMR** (282 MHz, CDCl₃) δ (ppm) -62.7 (1F, dd, *J* 178, 9 Hz, CFFBn), -63.8 (1F, dd, *J* 178, 5 Hz, CFFBn), -114.6 (1F, d, *J* 269 Hz, CFFCH), -126.2 (1F, ddd, *J* 268, 23, 9 Hz, CFFCH); **ES⁺MS**: *m/z* 497.1 [M + Na]⁺ 497.1; **HRMS** (ES⁺) for C₁₈H₂₇BrF₄NaO₃Si⁺ [M + Na]⁺ calcd 497.0741, found 497.0733.

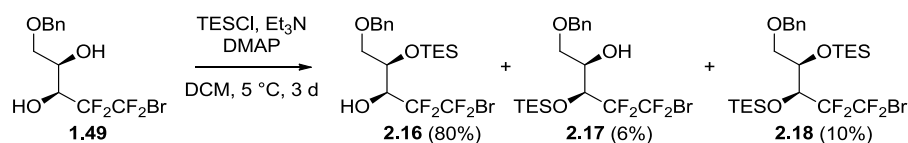
8.3.2 (3*S*,4*R*)-5-benzyloxy-1-bromo-4-((*tert*-butyldimethylsilyl)oxy)-1,1,2,2-tetrafluoropentane-3-yl formate (**2.12**)



Alcohol **2.13** (98 mg, 0.21 mmol) was dissolved in DCM (0.5 mL) and treated with DIC (39 μL, 0.25 mmol), DMAP (5 mg, 42 μmol) and formic acid (9.5 μL, 0.25 mmol). The reaction was stirred at r.t. for 16 h. The reaction was then diluted with DCM (2 mL) and washed with aq. HCl (1M, 4 × 3 mL) and brine (7 mL). The organic phase was dried (MgSO₄), filtered and concentrated then suspended in hexane and filtered too remove the urea by-product. Concentration of the hexane gave formate **2.12** as a colourless oil (55 mg, 52%).

R_f 0.30 (petrol ether/Et₂O 95:5); [**α**]_D -7.0 (c 0.5, CHCl₃, 23 °C); **IR** (neat) 2954 (w), 2930 (w), 2859 (w), 1744 (m), 1152 (s) cm⁻¹; **¹H NMR** (400 MHz, CDCl₃) δ (ppm) 8.13 (1H, s, CHO), 7.29 - 7.40 (5H, m, H_{Ar}), 5.87 (1H, ddd, *J* 19.8, 3.2 Hz, CHCF₂), 4.52 (1H, d, *J* 11.8 Hz, CHHPh), 4.47 (1H, d, *J* 11.8 Hz, CHHPh) 4.32 (1H, ddt, *J* 7.2, 4.9, 2.3, 2.3 Hz, CHCH₂), 3.49 (1H, dd, *J* 9.6, 5.3 Hz, CHHOBN), 3.39 (1H, ddd, *J* 9.7, 7.0, 0.9 Hz, CHHOBN), 0.88 (12H, s, C(CH₃)₃), 0.09 (3H, s, SiCH₃), 0.07 (3H, s, SiCH₃); **¹³C NMR** (101 MHz, CDCl₃) δ (ppm) 158.7 (1C, CHO), 137.5 (1C, C_{Ar}), 128.4 (2C, 2 × CH_{Ar}), 127.9 (2C, 2 × CH_{Ar}), 73.6 (1C, CH₂Ph), 70.2 (1C, CH₂OBn), 68.6 (2C, CHCH), 25.6 (3C, C(CH₃)₃), 17.9 (1C, C(CH₃)₃), -4.5 (1C, SiCH₃), -5.2 (1 C, SiCH₃), CF₂CF₂ not observed; **¹⁹F NMR** (282 MHz, CDCl₃) δ (ppm) -64.3 (1F, br. s, CF₂Br), -64.3 (1F, d, *J* 5 Hz, CF₂Br), -112.4 (1F, d, *J* 274 Hz, CF₂CH), -119.4 (1 F, ddd, *J*=274, 19, 6 Hz, CF₂CH); **ES⁺MS**: *m/z* 525.0 [M + Na]⁺ 525.1; **HRMS** (ES⁺) for C₁₉H₂₇BrF₄NaO₄Si⁺ [M + Na]⁺ calcd 525.0690, found 525.0679.

8.3.3 (3*S*,4*R*)-5-(Benzyloxy)-1-bromo-4-(triethylsilyloxy)-1,1,2,2-tetrafluoropentan-3-ol (**2.16**)



Diol **1.49** (20.4 g, 56.4 mmol) was dissolved in DCM (330 mL) and stirred at 0 °C. TESCl (10.41 mL, 62.0 mmol), Et₃N (9.44 mL, 67.7 mmol) and DMAP (689 mg, 5.64 mmol) were added. The reaction mixture was stirred at 4–6 °C for 70 h. DCM (150 mL) was then added and the resultant solution washed with H₂O (200 mL), then aq. NH₄Cl (sat., 200 mL) before being dried (MgSO₄), filtered and concentrated to give a yellow oil. Column chromatography (petrol ether/Et₂O 99:1 then 98:2 then 96:4) gave alcohol **2.16** as a colourless oil (21.6 g, 80%), alcohol **2.17** as a colourless oil (1.58 g, 6%) and bis-silyl ether **2.18** as a colourless oil (3.42 g, 10%).

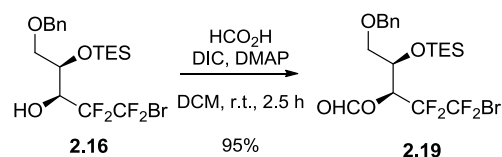
Data for 2.16: **R_f** 0.65 (petrol ether/EtOAc 80:20); [**α**]_D -38.2 (c 0.7, CHCl₃, 23.5 °C); **IR** (neat) 3516 (br, w), 2956 (m), 2878 (m), 1455 (w), 1130 (s), 1090 (s) (s) cm⁻¹; **¹H NMR** (400 MHz, CDCl₃) δ (ppm) 7.20–7.33 (5H, m, H_{Ar}), 4.48 (1H, d, *J* 11.9 Hz, CHHPh), 4.44 (1H, d, *J* 11.9 Hz, CHHPh), 4.14–4.23 (2H, m, CHCH), 3.42 (1H, t, *J* 9.0 Hz, CHHOBN), 3.34 (1H, dd, *J* 9.3, 5.4 Hz, CHHOBN), 3.12 (1H, d, *J* 10.8 Hz, OH), 0.86 (9H, t, *J* 8.0 Hz, CH₂CH₃ × 3), 0.54 (6H, q, *J* 7.9 Hz, CH₂CH₃ × 3); **¹³C NMR** (101 MHz, CDCl₃) δ (ppm) 137.6 (C_{Ar}), 128.5 (2C, CH_{Ar} × 2), 127.9 (CH_{Ar}), 127.7 (2C, CH_{Ar} × 2), 73.4 (CH₂Ph), 70.3 (CH₂OBn), 67.3 (CHCH₂), 67.4 (dd, *J* 29, 21 Hz, CHCF₂), 6.6 (3C, C(CH₃)₃), -4.5 (1C, SiCH₃), -5.2 (1C, SiCH₃).

$\underline{\text{CH}}_3 \times 3$), 4.8 (3C, $\underline{\text{CH}}_2\text{CH}_3 \times 3$). $\underline{\text{CF}}_2\underline{\text{CF}}_2$ not observed; ^{19}F NMR (282 MHz, CDCl_3) δ (ppm) -62.6 (1F, dd, J 178, 9 Hz, $\underline{\text{CF}}\underline{\text{F}}\underline{\text{Br}}$), -63.8 (1F, dd, J 178, 4 Hz, $\underline{\text{CF}}\underline{\text{F}}\underline{\text{Br}}$), -114.3 (1F, d, J 268 Hz, $\underline{\text{CF}}\underline{\text{F}}\underline{\text{CH}}$), -126.7 (1F, ddd, J 268, 23, 9 Hz, $\underline{\text{CF}}\underline{\text{F}}\underline{\text{CH}}$); ES^+MS : m/z 499 and 497 $[\text{M} + \text{Na}]^+$, 1:1 ratio; HRMS (ES^+) for $\text{C}_{18}\text{H}_{27}^{79}\text{BrF}_4\text{NaO}_3\text{Si}^+$ $[\text{M} + \text{Na}]^+$ calcd 497.0741, found 497.0750.

Data for (3*S*,4*R*)-5-(Benzyloxy)-1-bromo-3-(triethylsilyloxy)-1,1,2,2-tetrafluoropentan-4-ol (2.17): R_f 0.61 (petrol ether/EtOAc 80:20); $[\alpha]_D$ -14.9 (c 0.6, CHCl_3 , 24 °C); IR (neat) 3560 (w, br.), 2957 (m), 2879 (m), 1146 (s), 1097 (s) cm^{-1} ; ^1H NMR (400 MHz, CDCl_3) δ (ppm) 7.28–7.41 (5H, m, $\underline{\text{H}}_{\text{Ar}}$), 4.56 (1H, d, J 12.0 Hz, $\underline{\text{CH}}\underline{\text{H}}\underline{\text{Ph}}$), 4.53 (1H, d, J 11.9 Hz, $\underline{\text{CH}}\underline{\text{H}}\underline{\text{Ph}}$), 4.46 (1H, br. t, J 11.7 Hz, $\underline{\text{CH}}\underline{\text{CF}}_2$), 4.08 (1H, br. q, J 7.3 Hz, $\underline{\text{CH}}\underline{\text{CH}}_2$), 3.51 (1H, dd, J 9.3, 5.6 Hz, $\underline{\text{CH}}\underline{\text{HO}}\underline{\text{Bn}}$), 3.43 (1H, dd, J 8.9, 8.3 Hz, $\underline{\text{CH}}\underline{\text{HO}}\underline{\text{Bn}}$), 2.48 (1H, d, J 8.8 Hz), 0.96 (9H, t, J 8.0 Hz, $\text{CH}_2\underline{\text{CH}}_3 \times 3$), 0.59–0.74 (6H, m, $\underline{\text{CH}}_2\text{CH}_3 \times 3$); ^{13}C NMR (101 MHz, CDCl_3) δ (ppm) 137.6 ($\underline{\text{C}}_{\text{Ar}}$), 128.4 (2C, $\underline{\text{CH}}_{\text{Ar}} \times 2$), 127.9 ($\underline{\text{CH}}_{\text{Ar}}$), 127.8 (2C, $\underline{\text{CH}}_{\text{Ar}} \times 2$), 73.4 ($\underline{\text{CH}}_2\text{Ph}$), 69.9 (t, J 23 Hz, $\underline{\text{CH}}\underline{\text{CF}}_2$), 69.9 ($\underline{\text{CH}}_2\text{OBn}$), 67.5 (1C, $\underline{\text{CH}}\underline{\text{CH}}_2$), 6.6 (3C, $\underline{\text{CH}}_3 \times 3$), 4.8 (3C, $\underline{\text{CH}}_2\text{CH}_3 \times 3$), $\underline{\text{CF}}_2\underline{\text{CF}}_2$ not observed; ^{19}F NMR (282 MHz, CDCl_3) δ (ppm) -62.1 (1F, m, $\underline{\text{CF}}\underline{\text{F}}\underline{\text{Br}}$, J 181 Hz can be observed), -62.8 (1F, dd, J 178, 4 Hz, $\underline{\text{CF}}\underline{\text{F}}\underline{\text{Br}}$), -113.0 (1F, ddd, J 271, 11, 3 Hz, $\underline{\text{CF}}\underline{\text{F}}\underline{\text{CH}}$), -115.5 (1F, ddd, J 271, 12, 4 Hz, $\underline{\text{CF}}\underline{\text{F}}\underline{\text{CH}}$), ES^+MS : m/z 499 and 497 $[\text{M} + \text{Na}]^+$, 1:1 ratio; HRMS (ES^+) for $\text{C}_{18}\text{H}_{27}^{79}\text{BrF}_4\text{NaO}_3\text{Si}^+$ $[\text{M} + \text{Na}]^+$ calcd 497.0741, found 497.0742.

Data for (3*S*,4*R*)-5-(Benzyloxy)-1-bromo-3,4-di(triethylsilyloxy)-1,1,2,2-tetrafluoropentane (2.18): R_f 0.66 (petrol ether/ Et_2O 95:5); $[\alpha]_D$ +96.1 (c 0.5, CH_2Cl_2 , 25 °C); IR (neat) 2956 (m), 2878 (m), 1150 (s), 1073 (m), 1007 (m) cm^{-1} ; ^1H NMR (400 MHz, CDCl_3) δ (ppm) 7.28–7.40 (5H, m, H_{Ar}), 4.55 (1H, d, J 11.9 Hz, $\underline{\text{CH}}\underline{\text{H}}\underline{\text{Ph}}$), 4.51 (1H, d, J 11.9 Hz, $\underline{\text{CH}}\underline{\text{H}}\underline{\text{Ph}}$), 4.35 (1H, ddd, J 16.0, 9.9, 2.9 Hz, $\underline{\text{CH}}\underline{\text{CF}}_2$), 4.09 (1H, m, $\underline{\text{CH}}\underline{\text{CH}}_2$), 3.69 (1H, dd, J 9.6, 4.5 Hz, $\underline{\text{CH}}\underline{\text{HO}}\underline{\text{Bn}}$), 3.47 (1H, m, J 9.2 Hz can be observed, $\underline{\text{CH}}\underline{\text{HO}}\underline{\text{Bn}}$), 0.95 (18H, app q, J 8.0 Hz, $6 \times \text{CH}_2\underline{\text{CH}}_3$), 0.54–0.69 (12 H, m, $6 \times \underline{\text{CH}}_2\text{CH}_3$) ^{13}C NMR (101 MHz, CDCl_3) δ (ppm) 138.2 ($\underline{\text{C}}_{\text{Ar}}$), 128.3 ($2 \times \underline{\text{CH}}_{\text{Ar}}$), 127.6 ($2 \times \underline{\text{CH}}_{\text{Ar}}$), 127.5 ($\underline{\text{CH}}_{\text{Ar}}$), 73.2 ($\underline{\text{CH}}_2\text{Ph}$), 72.3 ($\underline{\text{CH}}\underline{\text{CH}}_2$), 70.8 ($\underline{\text{CH}}_2\text{OBn}$), 70.8 (t, J 24 Hz, $\underline{\text{CH}}\underline{\text{CF}}_2$), 6.7 ($3 \times \text{CH}_2\underline{\text{CH}}_3$), 6.6 ($3 \times \text{CH}_2\underline{\text{CH}}_3$), 4.93 ($3 \times \underline{\text{CH}}_2\text{CH}_3$), 4.89 ($3 \times \underline{\text{CH}}_2\text{CH}_3$) $\underline{\text{CF}}_2\underline{\text{CF}}_2$ not observed; ^{19}F NMR (282 MHz, CDCl_3) δ (ppm) -61.2 (1F, dd, J 175, 6 Hz, $\underline{\text{CF}}\underline{\text{F}}\underline{\text{Br}}$), -62.2 (1F, dd, J 175, 5 Hz, $\underline{\text{CF}}\underline{\text{F}}\underline{\text{Br}}$), -114.2 (1F, ddd, J 269, 10, 6 Hz, $\underline{\text{CF}}\underline{\text{F}}\underline{\text{CH}}$), -115.9 (1F, ddd, J 269, 16, 6 Hz, $\underline{\text{CF}}\underline{\text{F}}\underline{\text{CH}}$); ES^+MS : m/z 613 and 611 $[\text{M} + \text{Na}]^+$ 1:1 ratio; HRMS (ES^+) for $\text{C}_{24}\text{H}_{41}^{79}\text{BrF}_4\text{O}_3\text{Si}_2\text{Na}^+$ $[\text{M} + \text{Na}]^+$ calcd. 611.1606, found. 611.1600.

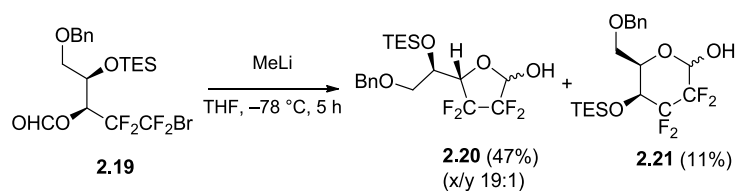
8.3.4 (3*S*,4*R*)-5-Benzyloxy-1-bromo-4-(triethylsilyloxy)-1,1,2,2-tetrafluoropentan-3-yl formate (**2.19**)



Alcohol **2.16** (9.74 g, 20.5 mmol) was dissolved in DCM (40 mL) and treated with DMAP (626 mg, 5.13 mmol) and DIC (5.08 mL, 32.8 mmol). The reaction mixture was then cooled to 0 °C before formic acid (1.24 mL, 32.8 mmol) was added slowly. The reaction mixture was then stirred at r.t. for 2.5 h before being diluted with DCM (60 mL) and washed with aq. HCl (1M, 50 mL). The aqueous phase was extracted into DCM (2 × 30 mL) and the combined DCM phases were washed with aq. HCl (1M, 3 × 50 mL) then brine (250 mL). The organic phase was dried (MgSO₄), filtered and concentrated; then suspended in hexane and filtered to remove the urea byproduct. The hexane filtrate was concentrated to give a cloudy oil. Column chromatography (petrol ether/Et₂O 95:5) gave formate **2.19** as a colourless oil (9.83 g, 95%).

R_f 0.48 (petrol ether/EtOAc 90:10); [**α**]_D −18.8 (c 0.4, CHCl₃, 25 °C); **IR** (neat) 2957 (m), 2878 (m), 1743 (s), 1456 (w), 1150 (s) cm^{−1}; **¹H NMR** (400 MHz, CDCl₃) δ (ppm) 8.13 (1H, s, CHO), 7.28–7.41 (5H, m, CH_{Ar}), 5.87 (1H, dt, *J* 19.5, 3.1 Hz, CHCF₂), 4.52 (1H, d, *J* 11.7 Hz, CHHPh), 4.47 (1H, d, *J* 11.7 Hz, CHHPh), 4.35 (1H, m, CHCH₂), 3.47 (1H, dd, *J* 9.5, 5.5 Hz, CHHOBn), 3.38 (1H, dd, *J* 9.0, 7.2 Hz, CHHOBn), 0.95 (9H, t, *J* 8.0 Hz, CH₃ × 3), 0.62 (6H, q, *J* 8.0 Hz, CH₂CH₃ × 3); **¹³C NMR** (101 MHz, CDCl₃) δ (ppm) 158.6 (CHO), 137.5 (C_{Ar}), 128.4 (2C, CH_{Ar} × 2), 127.93 (2C, CH_{Ar} × 2), 127.87 (CH_{Ar}), 73.6 (CH₂Ph), 70.2 (CH₂OBn), 68.6 (CHCH₂), 66.4 (dd, *J* 31, 20 Hz, CHCF₂), 6.6 (3C, CH₃ × 3), 4.8 (3C, CH₂CH₃ × 3) CF₂CF₂ not observed; **¹⁹F NMR** (282 MHz, CDCl₃) δ (ppm) −64.0 (1F, br. d, *J* 183 Hz, CFFBr), −64.7 (1F, dd, *J* 181, 5 Hz, CFFBr), −112.4 (1F, d, *J* 274 Hz, CFFCH), −119.6 (1F, ddd, *J* 274, 20, 4 Hz, CFFCH); **ES⁺MS**: *m/z* 527 and 525 [M + Na]⁺ 1:1 ratio; **HRMS** (ES⁺) for C₁₉H₂₇⁷⁹BrF₄O₄SiNa⁺ [M + Na]⁺ calcd 525.0690 found 525.0690.

8.3.5 6-*O*-Benzyl-5-*O*-(triethyl)silyl-2,3-dideoxy-2,2,3,3-tetrafluorogalactofuranose (threohexofuranose) (**2.20**)

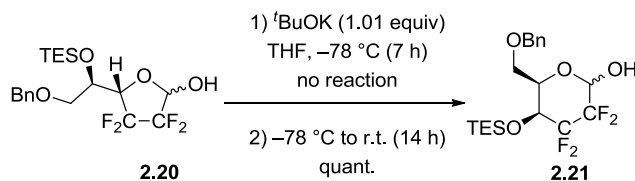


Formate **2.19** (1.36 g, 2.71 mmol) was dissolved in DCM (18 mL) and filtered through a pad of MgSO₄ directly into the reaction flask, while drying the filtrate with N₂. The resultant oil was dried under high vacuum for >16 h then dissolved in THF. The solution was cooled to -78 °C and MeLi (1.6M in Et₂O, 1.69 mL) was added very slowly, dropwise. Stirring was continued at -78 °C for 5 h. Aq. NH₄Cl (sat., 18 mL) was then added before the reaction was allowed to warm to r.t. H₂O (17 mL) was then added and the resultant mixture was extracted into EtOAc (60 mL). The aqueous phase was diluted with H₂O (50 mL) then extracted into EtOAc (2 × 100 mL). The combined organic phases were dried (MgSO₄), filtered and concentrated to give a colourless oil. Column chromatography (petrol ether/acetone 95:5, then 80:20) gave desired furanose **2.20** as a colourless oil (539 mg, 47%) and pyranose **2.21** as a colourless oil which eventually became an off-white amorphous solid, (132 mg, 11%).

Data for furanose 2.20 (ratio of anomers 19:1): R_f 0.26 (petrol ether/acetone 85:15); **IR** (neat) 3347 (br, w), 2958 (m), 2879 (m), 1455 (m), 1145 (s), 1109 (s), 1011 (s) cm⁻¹; **¹H NMR** (400 MHz, CDCl₃) δ (ppm) 7.29–7.42 (5H, m, H_{Ar}), 5.20–5.32 (2H, m, OH, H-1), 4.62 (1H, ddt, *J* 18.3, 3.0, 1.6, Hz, H-4), 4.57 (1H, d, *J* 11.8 Hz, CHHPh), 4.51 (1H, d, *J* 11.7 Hz, CHHPh), 4.09 (1H, td, *J* 7.3, 1.4 Hz, H-5), 3.59 (1H, t, *J* 8.9 Hz, H-6), 3.47 (1H, ddd, *J* 9.2, 5.4, 0.9 Hz, H-6), 0.95 (9H, t, *J* 8.3 Hz, CH₃ × 3), 0.67 (6H, q, *J* 7.8 Hz, CH₂CH₃ × 3), [D₂O exchange: 5.25 (2 H, br. d, *J* 7.5 Hz, H-1)]; **¹³C NMR** (101 MHz, CDCl₃) δ (ppm) 137.3 (C_{Ar}), 128.5 (2C, CH_{Ar} × 2), 128.0 (CH_{Ar}), 127.8 (2C, CH_{Ar} × 2), 96.6 (dd, *J* 40, 24 Hz, C-1), 81.4 (app dd, *J* 28, 25 Hz can be observed, C-4), 73.6 (CH₂Ph), 69.0 (C-6), 68.4 (d, *J* 7 Hz, C-5), 6.4 (3C, CH₃ × 3), 4.5 (3C, CH₂CH₃ × 3), CF_{2CF₂ not observed; **¹⁹F NMR** (282 MHz, CDCl₃) δ (ppm) -115.4 (1F, dd, *J* 248, 17 Hz), -122.4 (1F, dt, *J* 249, 5 Hz), -123.6 (1F, d, *J* 247 Hz), -124.9 (1F, d, *J* 249 Hz) **¹⁹F (-H) NMR** (282 MHz, CDCl₃) δ (ppm) -115.4 (1F, d, *J* 247 Hz), -122.4 (1F, dt, *J* 248, 5 Hz), -123.6 (1F, dt, *J* 248, 6 Hz), -124.9 (1F, d, *J* 249 Hz); **ES⁺MS**: *m/z* 447 [M + Na]⁺; **HRMS** (ES⁺) for C₁₉H₂₈F₄NaO₄Si⁺ [M + Na]⁺ calcd. 447.1585; found 447.1593.}

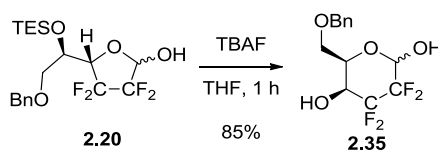
Data for 6-*O*-benzyl-4-*O*-triethylsilyl-2,3-dideoxy-2,2,3,3-tetrafluorogalactopyranose (threohexopyranose) (2.21, α/β 1:1): R_f 0.21 (petrol ether/Me₂CO 95:5); **Mp** 40–44 °C (Et₂O); **IR** (neat) 3412 (br., w), 2956 (m), 2879 (m), 1456 (w), 1197 (m), 1151 (s), 1123 (s), 1079 (s) cm⁻¹; **¹H NMR** (400 MHz, CDCl₃) δ (ppm) 7.29–7.42 (10H, m, H_{Ar} \times 10), 5.30 (1H, dd, J 8.7, 6.1 Hz, H-1 _{α}), 4.86 (1H, dd, J 13.9, 3.6 Hz, H-1 _{β}), 4.55–4.61 (3H, m, CHHPh \times 3), 4.53 (1H, d, J 11.8 Hz, CHHPh), 4.49 (1H, m, H-5 _{α}), 4.12 (2H, m, H-4 _{$\alpha+\beta$}), 3.91 (1H, m, H-5 _{β}), 3.60–3.70 (4H, m, H-6 _{$\alpha+\beta$} and H-6' _{$\alpha+\beta$}), 0.96 (9H, t, J 8.0 Hz, CH₃ _{α/β} \times 3), 0.95 (9H, t, J 7.9 Hz, CH₃ _{β/α}), 0.58–0.73 (12H, m, CH₃CH₂ \times 6); **¹³C NMR** (101 MHz, CDCl₃) δ (ppm) 137.4 (C_{Ar} α/β), 137.3 (C_{Ar} β/α), 128.5 (4C, CH_{Ar} \times 4), 128.0 (4C, CH_{Ar} \times 4), 128.0 (2C, CH_{Ar} \times 2), 91.3–92.5 (2C, m, C-1 _{$\alpha+\beta$}), 73.7 (2C, CH₂Ph _{$\alpha+\beta$}), 73.2 (d, J 6 Hz, C-5 _{β}), 69.6–70.9 (2C, m, C-4 _{$\alpha+\beta$}), 68.8 (d, J 5 Hz, C-5 _{α}), 67.8 (C-6 _{α/β}), 67.2 (C-6 _{β/α}), 6.5 (6C, CH₃ \times 6), 4.6 (6C, s, CH₃CH₂ \times 6), CF₂CF₂ not observed; **¹⁹F NMR** (282 MHz, CDCl₃) δ (ppm) -118.8 (1F, ddt, J 271, 16, 9 Hz), -119.3 (1F, ddt, J 269, 14, 8 Hz), -120.4 (1F, dt, J 271, 5 Hz), -128.1 (1F, m, J 269 Hz can be observed), -129.8 (1F, m, J 270 Hz can be observed), -134.1 (1F, m, J 271 Hz can be observed), -135.9 (1F, br. d, J 260 Hz), -137.8 (1F, m, J 260 Hz can be observed); **ES⁺MS**: m/z 447 [M + Na]⁺; **HRMS** (ES⁺) for C₁₉H₂₈F₄NaO₄Si⁺ [M + Na]⁺ calcd. 447.1585; found 447.1577.

8.3.6 Isomerisation of furanose 2.20 to pyranose 2.21



Furanose **2.20** (130 mg, 0.31 mmol) was dissolved in THF (6 mL) and cooled to -78 °C. To the reaction mixture was added *t*BuOK (38 mg, 0.313 mmol). The resultant mixture was stirred at -78 °C for 7 h then allowed to warm to r.t. for 14 h. To the reaction was added aq. HCl (1M, 0.33 mL) then H₂O (1 mL). The volatile components were removed under reduced pressure and the resultant aqueous phase was extracted into EtOAc (3 \times 8 mL). The combined organic phase was washed with aq. NaHCO₃ (sat., 10 mL) then brine (10 mL), before being dried (MgSO₄), filtered and concentrated to give a colourless oil. Column chromatography (petrol ether/acetone 80:20) gave **2.21** as a white waxy solid (130 mg, quant.).

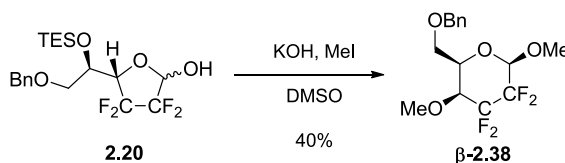
8.3.7 6-*O*-Benzyl-2,3-dideoxy-2,2,3,3-tetrafluorogalactopyranose (threohexopyranose) (**2.35**)



Furanose **2.20** (128 mg, 0.30 mmol) was dissolved in THF (0.4 mL) at r.t. and treated with TBAF (1M in THF, 300 μ L, 0.30 mmol), dropwise. The reaction was stirred at r.t. for 1 h, then concentrated under reduced pressure. The resultant oil was purified by column chromatography (hexane/Me₂CO 70:30) to give pyranose **2.24** as a white solid (79 mg, 85%).

R_f 0.05 (petrol ether/EtOAc 85:15); **Mp** 120–126 °C (CH₂Cl₂); **IR** (neat) 3383 (m, br.), 2931 (w), 2876 (w), 1454 (w), 1117 (s), 1063 (s) cm⁻¹ **¹H NMR** (400 MHz, acetone-*d*₆) [OH peaks only] δ (ppm) 6.71 (1H, m, OH-1 _{α}), 4.94–5.21 (2H, m, OH-4 _{$\alpha+\beta$}), 2.83 (1H, br. s, OH-1 _{β}) [D₂O exchange] δ (ppm) 7.23–7.42 (10H, m, H_{Ar}), 5.30 (1H, dd, *J* 9.2, 6.5 Hz, H-1 _{α}), 5.00 (1H, dt, *J* 13.1, 3.6 Hz, H-1 _{β}), 4.52–4.62 (5H, m, CH₂Ph _{$\alpha+\beta$} , H-5 _{α}), 4.09–4.23 (2H, m, H-4 _{$\alpha+\beta$}), 4.02 (1H, dtd, *J* 8.0, 4.0, 2.0 Hz, H-5 _{β}), 3.81 (2H, dd, *J* 9.8, 6.0 Hz, H-6 _{$\alpha+\beta$}), 3.71 (1H, ddd, *J* 9.9, 6.3, 1.4 Hz, H-6' _{β}), 3.67 (1H, ddd, *J* 9.9, 6.4, 1.5 Hz, H-6' _{α}), **¹³C NMR** (101 MHz, acetone-*d*₆) δ (ppm) 139.5 (C_{Ar}), 139.4 (C_{Ar}), 129.2 (4C, CH_{Ar} \times 4), 128.5 (4C, CH_{Ar} \times 4), 128.4 (2C, CH_{Ar} \times 2), 93.2–92.2 (m, C-1 _{$\alpha+\beta$}), 73.91 (CH₂Ph _{α/β}), 73.86 (CH₂Ph _{β/α}), 73.6 (d, *J* 7 Hz, C-5 _{β}), 70.1 (t, *J* 21 Hz, C-4 _{α/β}), 69.8 (t, *J* 20 Hz, C-4 _{β/α}), 69.0 (C-6 _{α/β}), 68.8 (C-6 _{β/α}), 68.6 (d, *J* 6 Hz, C-5 _{α}); **¹⁹F NMR** (282 MHz, acetone-*d*₆) δ (ppm) -117.6 (1F, ddt, *J* 265, 17, 9 Hz), -118.4 (1F, ddt, *J* 266, 15, 8, Hz), -119.8 (1F, d, *J* 268 Hz), -129.4 (1F, dd, *J* 268, 8 Hz), -131.6 (1F, dt, *J* 268, 11 Hz), -133.2 (1F, dtt, *J* 267, 10, 4 Hz), -136.0 (1F, br. d, *J* 259 Hz), -137.1 (1F, dt, *J* 258, 13 Hz). **ES⁺MS**: *m/z* 333 [M + Na]⁺; **HRMS** (ES⁺) for C₁₃H₁₄F₄NaO₄⁺ [M + Na]⁺ calcd 333.0720, found 333.0717.

8.3.8 Methyl 6-*O*-benzyl-1,4-di-2,3-dideoxy-2,2,3,3-tetrafluoro- β -galactopyranoside (threohexopyranoside) (β -**2.38**)

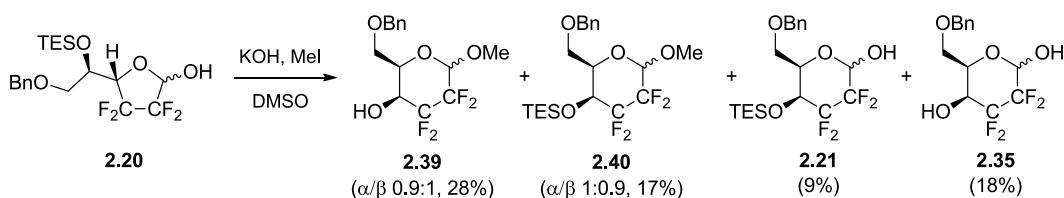


Furanose **2.20** (65 mg, 0.15 mmol) was dissolved in DMSO (0.6 mL). Ground KOH (34 mg, 0.61 mmol) was added and the reaction was stirred at r.t. for 20 min. MeI (76 μ L,

1.22 mmol) was added dropwise and stirring was continued for 15 h. Aq. HCl (1M, 5 mL) was added and the resultant mixture extracted into EtOAc (4 × 7 mL). The combined organic phase was dried (Na₂SO₄), filtered and concentrated to give a brown oil. Column chromatography (petrol ether/acetone 85:15) followed by HPLC (hexane/acetone 90:10) gave methyl glycoside **β-2.38** as a colourless oil (21 mg, 40%).

R_f 0.48 (petrol ether/acetone 70:30); [**α**]_D -45.4 (c 0.5, CHCl₃, 25 °C); **IR** (neat) 2940 (w), 2851 (w), 1113 (s), 1074 (s) cm⁻¹; **¹H NMR** (400 MHz, CDCl₃) δ (ppm) 7.12–7.40 (5H, m, H_{Ar}), 4.43–4.55 (3H, m, CHHPh, CHHPh, H-1), 3.84 (1H, m, H-5), 3.70 (1H, dd, *J* 9.1, 7.6 Hz, H-6), 3.58–3.66 (2H, m, H-6, H-4), 3.53 (3H, s, C1OCH₃), 3.47 (3H, s, C4OCH₃) **¹³C NMR** (101 MHz, CDCl₃) δ (ppm) 137.5 (C_{Ar}), 128.5 (CH_{Ar} × 2), 128.0 (CH_{Ar}), 127.8 (CH_{Ar} × 2), 98.4 (td, *J* 23, 4 Hz, C-1), 77.5 (dd, *J* 29, 18 Hz, C-4), 73.7 (CH₂Ph), 72.5 (d, *J* 7 Hz, C-5), 66.8 (C-6), 61.4 (d, *J* 3 Hz, CH₃OC4), 57.8 (CH₃OC1). **¹⁹F NMR** (282 MHz, CDCl₃) -117.4 (1F, d, *J* 275 Hz), -131.9 (1F, dt, *J* 275, 13 Hz), -136.9 (2F, br. s.). **ES⁺MS**: *m/z* 361.2 [M + Na]⁺; **HRMS** (ES⁺) for C₁₅H₁₈F₄O₄Na⁺ [M + Na]⁺ Calcd 361.1033 found 361.1031

8.3.9 Methyl 6-*O*-benzyl-2,3-dideoxy-2,2,3,3-tetrafluorogalactopyranoside (threohexopyranoside) (**2.39**) and methyl 6-*O*-benzyl-4-*O*-triethylsilyl-2,3-dideoxy-2,2,3,3-tetrafluorogalactopyranoside (threohexopyranoside) (**2.40**)



10.2, 5.4 Hz, H-6), 3.76 (1H, dd, J 10.2, 5.7 Hz, H-6), 3.51 (3H, s, CH_3), 2.80 (1H, d, J 6.1 Hz, OH). ^{13}C NMR (101 MHz, CDCl_3) δ (ppm) 137.3 (C_{Ar}), 128.5 (CH_{Ar}), 128.0 (CH_{Ar}), 127.7 (CH_{Ar}), 98.2 (dd, J 38, 23 Hz, C-1), 73.8 (CH_2Ph), 70.3 (dd, J 31, 20 Hz, C-4), 68.3 (C-6), 67.5 (d, J 4 Hz, C-5), 56.2 (CH_3). ^{19}F NMR (282 MHz, CDCl_3) δ (ppm) -116.6 (1F, ddt, J 275, 21, 9, Hz), -119.9 (1F, ddt, J 271, 17, 9, Hz), -131.0 (1F, d, J 271 Hz), -134.3 (1F, dt, J 275, 17 Hz); **EIMS**: m/z 324.0 [M^+]; **HRMS** (ES+) for $\text{C}_{14}\text{H}_{16}\text{F}_4\text{O}_4\text{Na}^+$ [$\text{M} + \text{Na}$] $^+$ calcd 347.0877, found 347.0877.

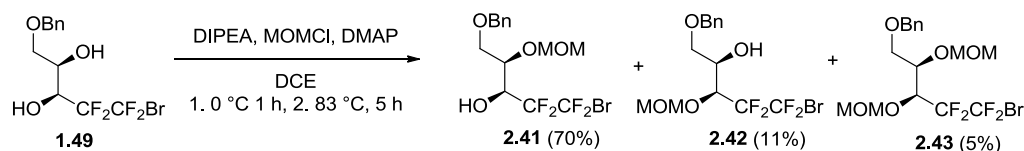
Data for β -2.39: R_f 0.34 (petrol ether/acetone 70:30); $[\alpha]_D -34.1$ (c 0.5, CHCl_3 , 25 °C); **IR** (neat) 3405 (br, w), 2942 (w), 2879 (w), 1110 (s), 1053 (s) cm^{-1} ; ^1H NMR (400 MHz, CDCl_3) δ (ppm) 7.21–7.36 (5H, m, H_{Ar}), 4.48–4.57 (3H, m, CH_2Ph , H-1), 4.05 (1H, m, H-4), 3.86 (1H, tdt, J 5.7, 4.2, 1.8 Hz, H-5), 3.74 (1H, dd, J 9.9, 5.9 Hz, H-6), 3.69 (1H, ddd, J 10.0, 5.7, 0.8 Hz, H-6), 3.57 (3H, s, CH_3), 2.65 (1H, br. s., OH). ^{13}C NMR (101 MHz, CDCl_3) δ (ppm) 137.3 (C_{Ar}), 128.6 (CH_{Ar}), 128.1 (CH_{Ar}), 127.8 (CH_{Ar}), 98.6 (ddd, J 28, 19, 4 Hz, C-1), 73.9 (CH_2Ph), 72.5 (d, J 4 Hz, C-5), 69.9 (dd, J 29, 19 Hz, C-4), 67.6 (C-6), 58.1 (CH_3). ^{19}F NMR (282 MHz, CDCl_3) δ (ppm) -120.9 (1F, d, J 275 Hz), -133.0 (1F, d, J 271 Hz), -135.2 (1F, dt, J 266, 17 Hz), -136.9 (1F, d, J 266 Hz); **ESI-MS**: m/z 323.0 [$\text{M} - \text{H}$] $^-$ **HRMS** (ES+) for $\text{C}_{14}\text{H}_{16}\text{F}_4\text{O}_4\text{Na}^+$ [$\text{M} + \text{Na}$] $^+$ calcd 347.0877, found 347.0880.

Data for α -2.40: R_f 0.32 (hexane/acetone 95:5); $[\alpha]_D +71.6$ (c 0.5, CHCl_3 , 26 °C); **IR** (neat) 2656 (w), 2913 (w), 2879 (w), 1130 (s), 1065 (s) cm^{-1} ; ^1H NMR (400 MHz, CDCl_3) δ (ppm) 7.17–7.32 (5H, m, H_{Ar}), 4.78 (1H, dd, J 9.1, 6.1 Hz, H-1), 4.51 (1H, d, J 11.6 Hz, CHHPh), 4.48 (1H, d, J 12.1 Hz, CHHPh), 4.21 (1H, m, H-5), 4.06 (1H, dd, J 13.1, 6.1 Hz, H-4), 3.63 (1H, dd, J 9.1, 6.6 Hz, H-6), 3.55 (1H, ddd, J 9.6, 6.1, 1.0 Hz, H-6), 3.41 (3H, s, CH_3O), 0.89 (9H, t, J 8.1 Hz, $\text{CH}_3\text{CH}_2 \times 3$), 0.59 (6H, qd, J 7.9, 3.5 Hz, $\text{CH}_3\text{CH}_2 \times 3$); ^{13}C NMR (101 MHz, CDCl_3) δ (ppm) 137.6 (C_{Ar}), 128.4 ($\text{CH}_{\text{Ar}} \times 2$), 127.9 (CH_{Ar}), 127.8 ($\text{CH}_{\text{Ar}} \times 2$), 98.2 (ddd, J 38, 25, 3 Hz, C-1), 73.6 (CH_2Ph), 70.5 (1C, dd, J 32, 20 Hz, C-4), 68.4 (3C, d, J 4 Hz, C-5), 67.7 (C-6), 56.0 (CH_3O), 6.6 ($\text{CH}_3\text{CH}_2 \times 3$), 4.7 ($\text{CH}_3\text{CH}_2 \times 3$); ^{19}F NMR (282 MHz, CDCl_3) δ (ppm) -117.1 (1F, ddt, J 271, 21, 9, 9 Hz), -119.5 (1F, dquin, J 275, 9 Hz), -128.2 (1F, d, J 275 Hz), -134.2 (1F, dt, J 271, 17 Hz).

Data for β -2.40: R_f 0.26 (hexane/acetone 95:5); $[\alpha]_D -16.8$ (c 0.5, CHCl_3 , 26 °C); **IR** (neat) 2956 (w), 2915 (w), 2879 (w), 1118 (s), 1078 (s) cm^{-1} ; ^1H NMR (400 MHz, CDCl_3) δ (ppm) 7.17–7.34 (5H, m, H_{Ar}), 4.52 (1H, d, J 11.1 Hz, CHHPh), 4.51 (1H, m, H-1), 4.47 (1H, d, J 11.6 Hz, CHHPh), 4.08 (1H, m, H-4), 3.82 (1H, ddt, J 11.1, 6.1, 2.0 Hz, H-5), 3.67 (1H, dd, J 9.1, 6.6 Hz, H-6), 3.61 (1H, ddd, J 9.1, 6.1, 1.5 Hz, H-6), 3.57 (3H, s, CH_3O), 0.89 (9H, t, J 8.1 Hz, $\text{CH}_3\text{CH}_2 \times 3$), 0.58 (6H, ddd, J 16.2, 8.1, 3.0 Hz, $\text{CH}_3\text{CH}_2 \times 3$); ^{13}C NMR (101 MHz, CDCl_3) δ (ppm) 137.5 (C_{Ar}), 128.5 (CH_{Ar}), 127.9 (CH_{Ar}), 127.9

(CH_{Ar}), 98.5 (td, J 23, 4 Hz, C-1), 73.7 (CH_2Ph), 73.3 (d, J 6 Hz, C-5), 70.2 (dd, J 31, 19 Hz, C-4), 67.4 (C-6), 58.0 (CH_3O), 6.5 ($\text{CH}_3\text{CH}_2 \times 3$), 4.6 ($\text{CH}_3\text{CH}_2 \times 3$); ^{19}F NMR (282 MHz, CDCl_3) δ (ppm) -120.5 (1F, d, J 266 Hz), -130.3 (1F, d, J 271 Hz), -135.5 (1F, d, J 262 Hz), -136.5 (1F, d, J 271 Hz); ES^+MS : m/z 461.2 $[\text{M} + \text{Na}]^+$; HRMS (ES^+) for $\text{C}_{20}\text{H}_{30}\text{F}_4\text{O}_4\text{SiNa}^+ [\text{M} + \text{Na}]^+$ calcd 461.1742, found 461.1745.

8.3.10 (3*S*,4*R*)-5-(Benzyloxy)-1-bromo-4-((methoxymethyl)oxy)-1,1,2,2-tetrafluoropentane-3-ol (**2.41**)



Diol **2.41** (933 mg, 2.58 mmol) was dissolved in DCE (10 mL) then cooled to 0 °C. The resultant mixture was treated with MOMCl (235 μL , 3.10 mmol), DIPEA (540 μL , 3.10 mmol) & DMAP (32 mg, 258 μmol). The reaction mixture was stirred at 0 °C for 1 h, then 83 °C for 5 h. The brown reaction mixture was then washed with aq. NaHCO_3 (sat., 9 mL), which was extracted into DCM (3×9 mL). Combined organic phases were dried (MgSO_4), filtered and concentrated to give a brown oil. Column chromatography (petrol ether/EtOAc 97:3, 95:5, 90:10, 78:22) gave a pale yellow oil (306 mg) containing bis-MOM ether **2.43** (55 mg, 5%) and desired alcohol **2.41** (251 mg, 24%), a second pale yellow oil, which was desired alcohol **2.42** (46%), an oil/solid mixture (226 mg) containing undesired alcohol **2.42** (120 mg, 11%) and starting diol **1.49** (106 mg, 11%).

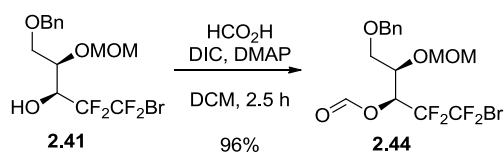
Data for 2.41: R_f 0.40 (petrol ether/EtOAc 70:30); $[\alpha]_D +0.2$ (c 0.5, CHCl_3 , 25 °C); **IR** (neat) 3421 (br, w), 2941 (w), 2900 (w), 1152 (s), 1128 (s), 1078 (s), 1033 (s) cm^{-1} ; ^1H NMR (400 MHz, CDCl_3) δ (ppm) 7.16–7.38 (5H, m, H_{Ar}), 4.64–4.70 (2H, m, OCH_2HO , OCH_2HO), 4.47–4.54 (2H, m, CHHPh , CHHPh), 4.31 (1H, dddt, J 22.2, 10.1, 3.0, 1.5 Hz, CHOH), 4.11 (1H, tt, J 6.6, 2.0 Hz, CHCH_2), 3.53–3.69 (2H, m, CHHOBn , CHHOBn), 3.32 (3H, s, CH_3), 3.05 (1H, d, J 10.1 Hz, OH); ^{13}C NMR (101 MHz, CDCl_3) δ (ppm) 137.5 (C_{Ar}), 128.5 (CH_{Ar}), 127.9 (CH_{Ar}), 127.6 (CH_{Ar}), 96.7 (OCH_2O), 73.5 (CH_2Ph), 72.4 (CHCH_2), 68.7 (CH_2OBn), 67.7 (dd, J 29, 20 Hz, CHOH), 56.2 (CH_3); ^{19}F NMR (282 MHz, CDCl_3) δ (ppm) -62.7 (1F, dd, J 176, 9 Hz), -63.8 (1F, d, J 176 Hz), -113.6 (1F, d, J 266 Hz), -126.4 (1F, ddd, J 271, 21, 9 Hz); ES^+MS : m/z 427.1 $[\text{M} + \text{Na}]^+$; HRMS (ES^+) for $\text{C}_{14}\text{H}_{17}\text{BrF}_4\text{O}_4\text{Na}^+ [\text{M} + \text{Na}]^+$ calcd 427.0139, found 427.0134.

Data for (3*S*,4*R*)-5-Benzyloxy-1-bromo-3-((methoxy)methoxy)-1,1,2,2-tetrafluoropentane-4-ol (2.42): R_f 0.29 (petrol ether/EtOAc 70:30); $[\alpha]_D -28.9$ (c 0.5,

CHCl₃, 25.5 °C); **IR** (neat) 3465 (br., w), 2905 (w), 2867 (w), 1130 (s), 1095 (s), 1028 (s) cm⁻¹; **¹H NMR** (400 MHz, CDCl₃) δ (ppm) 7.28–7.42 (5H, m), 4.74 (2H, s, CHHOMe + CHHOMe), 4.57 (2H, s, CHHPh + CHHPh), 4.37 (1H, dd, *J* 21.7, 8.6 Hz, CHCF₂), 4.18 (1H, t, *J* 6.3 Hz, CHCH₂), 3.66 (1H, s, CHHOBn), 3.65 (1H, s, CHHOBn), 3.39 (3H, s, CH₃), 3.12 (1H, d, *J* 10.1 Hz, OH); **¹³C NMR** (101 MHz, CDCl₃) δ (ppm) 137.6 (C_{Ar}), 128.5 (CH_{Ar} × 2), 127.9 (CH_{Ar}), 127.8 (CH_{Ar} × 2), 98.7 (CH₂OMe), 74.5 (dd, *J* 26, 23 Hz, CHCF₂), 73.4 (CH₂Ph), 70.0 (CH₂OBn), 67.8 (CHCH₂), 56.8 (CH₃); **¹⁹F NMR** (282 MHz, CDCl₃) δ (ppm) -62.7 (1F, d, *J* 181 Hz), -63.4 (1 F, d, *J* 176 Hz), -112.5 (1 F, d, *J* 275 Hz), -117.5 (1 F, dd, *J* 275, 13 Hz); **ES⁺MS**: *m/z* 427.1 [M + Na]⁺; **HRMS** (ES+) for C₁₄H₁₇BrF₄O₄Na⁺ [M + Na]⁺ calcd 427.0139, found 427.0134.

Data for (3S,4R)-5-Benzyloxy-1-bromo-3,4-di-((methoxy)methoxy)-1,1,2,2-tetrafluoropentane (2.43): *R_f* 0.46 (petrol ether/EtOAc 70:30); [α]_D: +6.1 (c 0.5, CHCl₃, 24.5 °C); **IR** (neat) 2936 (w), 2898 (w), 1134 (s), 1107 (s), 1075 (s), 1025 (s) cm⁻¹; **¹H NMR** (400 MHz, CDCl₃) δ (ppm) 7.28–7.40 (5H, m), 4.79 (1H, d, *J* 7.1 Hz, CHHOMe), 4.74–4.77 (2H, m, CHHOMe + CHHOMe), 4.73 (1H, d, *J* 6.6 Hz, CHHOMe), 4.58 (1H, d, *J* 12.1 Hz, CHHPh), 4.55 (1H, d, *J* 12.1 Hz, CHHPh), 4.45 (1H, ddd, *J* 17.3, 7.5, 2.0 Hz, CHCF₂), 4.15 (1H, td, *J* 6.1, 1.5 Hz, CHCH₂), 3.70 (2H, d, *J* 6.1 Hz, CHHOBn + CHHOBn), 3.44 (3H, s, CH₃), 3.39 (3H, s, CH₃); **¹³C NMR** (101 MHz, CDCl₃) δ (ppm) 137.7 (C_{Ar}), 128.4 (CH_{Ar} × 2), 127.8 (CH_{Ar}), 127.7 (CH_{Ar} × 2), 98.7 (CH₂OMe), 97.3 (CH₂OMe), 74.5 (CHCH₂), 73.4 (CH₂Ph), 73.5 (dd, *J* 26, 20 Hz, CHCF₂), 68.7 (CH₂OBn), 56.8 (CH₃), 55.9 (CH₃); **¹⁹F NMR** (282 MHz, CDCl₃) δ (ppm) -62.7 (1F, d, *J* 185 Hz), -63.4 (1F, d, *J* 181 Hz), -112.2 (1F, d, *J* 271 Hz), -118.2 (1F, dd, *J* 275, 17 Hz); **ES⁺MS**: *m/z* 471.1 [M + Na]⁺; **HRMS** (ES+) for C₁₆H₂₁BrF₄O₅Na⁺ [M + Na]⁺ calcd 471.0401, found 471.0402.

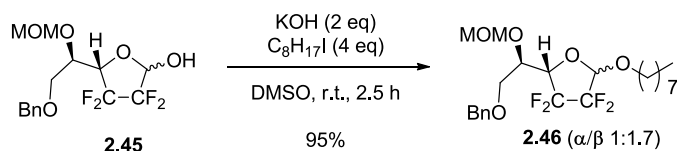
8.3.11 (3S,4R)-5-Benzyloxy-1-bromo-4-(methoxymethoxy)-1,1,2,2-tetrafluoropentane-3-yl formate (2.44)



Alcohol **2.44** (3.16 g, 7.79 mmol) was dissolved in DCM (15 mL) and treated with DMAP (238 mg, 1.95 mmol) and DIC (1.93 mL, 12.5 mmol). The resultant mixture was cooled to 0 °C then treated with formic acid (470 µL, 12.5 mmol) dropwise. The mixture was then stirred at r.t. for 2.5 h before being diluted with DCM (25 mL) and aq. HCl (1M,

R_f 0.24 (petrol ether/acetone 80:20); **IR** (neat) 3344 (w, br.) 2901 (w), 1139 (s), 1103 (m), 1018 (s) cm⁻¹; **¹H NMR** (400 MHz, CDCl₃) δ (ppm) 7.28–7.42 (6.5H, m, H_{Ar}), 5.48 (0.3H, d, *J* 6.6 Hz, H-1_y), 5.31 (1H, d, *J* 8.1 Hz, H-1_x), 4.70–4.80 (2.6H, m, CHHOMe_{x+y} + CHHOMe_{x+y}), 4.65 (1.3H, m, H-4_{x+y}), 4.52–4.60 (2.6H, m, CHHPh_{x+y} + CHHPh_{x+y}), 4.05 (0.3H, q, *J* 5.1 Hz, H-5_y), 4.00 (1H, t, *J* 6.6 Hz, H-5_x), 3.62–3.77 (2.6H, m, 2 × H-6_{x+y}), 3.40 (3H, s, CH_{3x}), 3.38 (0.9H, s, CH_{3y}); **¹³C NMR** (101 MHz, CDCl₃) δ (ppm) 137.4 (C_{Arx}), 137.3 (C_{Arx}), 128.4, 128.4, 127.9, 127.8, 127.7, 127.7 (CH_{Arx+y}), 97.3 (CH₂OMe_x), 96.8 (CH₂OMe_y), 96.2 (ddd, *J* 38, 25, 3 Hz, C-1_x), 94.7 (dd, *J* 38, 22 Hz, C-1_y), 79.5 (dd, *J* 29, 22 Hz, C-4_x), 77.2 (dd, *J* 29, 23 Hz, C-4_y) 73.6 (CH₂Ph_x), 73.5 (CH₂Ph_y), 73.3 (C-5_y), 73.1 (d, *J* 6 Hz, C-5_x), 68.5 (C-6_y), 67.8 (C-6_x), 56.4 (CH_{3x}), 55.8 (CH_{3y}); **¹⁹F NMR** (282 MHz, CDCl₃) δ (ppm) -115.9 (0.3F, dd, *J* 246, 11 Hz, F_y), -116.9 (1F, dd, *J* 249, 17 Hz, F_x), -124.8 (1F, d, *J* 247 Hz, F_x), -125.0 (1F, dd, *J* 241, 5 Hz, F_x), -125.9 (1F, m, *J* 247 Hz can be observed, F_x), -127.7 (0.3F, d, *J* 247 Hz, F_y), -130.5 (0.3F, d, *J* 246 Hz, F_y), -131.2 (0.3F, dd, *J* 246, 14 Hz, F_y); **ES⁺MS**: *m/z* 377.1 [M + Na]⁺; **HRMS** (ES⁺) for C₁₅H₁₈F₄O₅Na⁺ [M + Na]⁺ Calcd 377.0983 found 377.0985.

8.3.13 n-Octyl 6-*O*-benzyl-5-*O*-(methoxy)methyl-2,3-dideoxy-2,3,3-tetrafluorogalactofuranoside (threohexofuranoside) (**2.46**)

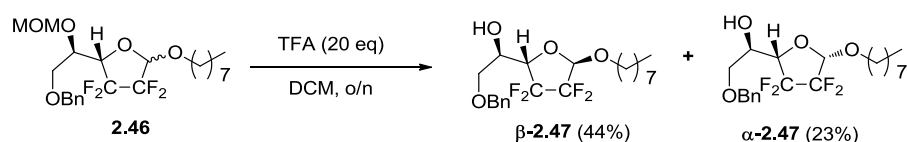


Furanose **2.45** (1.45 g, 4.10 mmol) was dissolved in DMSO (16 mL) and treated with ground KOH (460 mg, 8.20 mmol). The resultant mixture was stirred for 20 min at r.t. as it became dark yellow. 1-Iodooctane (1.02 mL, 16.4 mmol) was then added, dropwise. The mixture was stirred for 2.5 h before being treated with aq. HCl (1M, 35 mL). The resultant solution was extracted into EtOAc (4 × 50 mL). Combined organic phases were dried (Na₂SO₄), filtered and concentrated to give a brown oil. Column chromatography (petrol ether/acetone 95:5) gave octyl glycoside **2.46** as a pale yellow oil (1.82 g, 95%, β/α 1:0.6).

R_f 0.45 (petrol ether/acetone 80:20); **IR** (neat) 2927 (m), 2857 (w), 1142 (s), 1107 (m), 1011 (s) cm⁻¹; **¹H NMR** (400 MHz, CDCl₃) δ (ppm) 7.27–7.46 (8H, m, H_{Ar}), 5.12 (1H, dd, *J* 8.1, 2.5 Hz, H-1_β), 5.02 (0.6H, dd, *J* 9.1, 2.0 Hz, H-1_α), 4.82 (0.6H, d, *J* 7.1 Hz, CHHOMe_α), 4.78–4.80 (0.6H, m, CHHOMe_α), 4.78 (1H, d, *J* 5.1 Hz, CHHOMe_β), 4.74 (1H, d, *J* 6.6 Hz, CHHOMe_β), 4.58 (3.2H, app. s, CHHOPh_{β+α} + CHHOPh_{β+α}), 4.34–4.56 (1.6H, m, H-4_{β+α}), 4.07 (1H, q, *J* 5.1 Hz, H-5_β), 4.02 (0.6H, dt, *J* 7.7, 4.0 Hz, H-5_α), 3.62–

3.89 (4.8H, m, $2 \times \text{H-6}_{\beta+\alpha} + \text{H-1}'_{\beta+\alpha}$), 3.49–3.61 (1.6H, m, $\text{H-1}'_{\beta+\alpha}$), 3.40 (1.8H, s, $\text{CH}_3\text{O}_\alpha$), 3.39 (3H, s, $\text{CH}_3\text{O}_\beta$), 1.57–1.74 (3.2H, m, $2 \times \text{H-2}'_{\beta+\alpha}$), 1.21–1.43 (16H, m, $\text{H-3'-7}'_{\beta+\alpha}$), 0.89 (4.8H, t, J 6.6 Hz, $\text{H-8}'_{\beta+\alpha}$); ^{13}C NMR (101 MHz, CDCl_3) δ (ppm) 137.7 (C_{Ar}), 128.4, 127.7, 127.7, (CH_{Ar}), 99.5 (dd, J 40, 20 Hz, C-1_α), 99.4 (dd, J 40, 20 Hz, C-1_β), 97.0 ($\text{CH}_2\text{OMe}_\beta$), 96.8 ($\text{CH}_2\text{OMe}_\alpha$), 77.0–77.8 (m, $\text{C-4}_{\beta+\alpha}$), 74.6 (C-5_α), 73.6 ($\text{CH}_2\text{Ph}_\alpha$), 73.6 ($\text{CH}_2\text{Ph}_\beta$), 73.1 (C-5_β), 69.7, 69.0, 68.9, 68.8 ($\text{C-6}_{\beta+\alpha} + \text{C-1}'_{\beta+\alpha}$), 55.8 ($\text{CH}_3\text{O}_\beta$), 55.7 ($\text{CH}_3\text{O}_\alpha$), 31.8, 29.2, 25.8, 25.8, 22.6, ($\text{C-3'-7}'$) 29.1 ($\text{C-2}'$), 14.0 ($\text{C-8}'$); ^{19}F NMR (282 MHz, CDCl_3) δ (ppm) -113.7 (1F, dd, J 245, 9 Hz, F_β), -125.1 (dt, J 245, 9 Hz, F_α), -125.2 (d, J 245 Hz, F_β), -126.7 (ddd, J 245, 17, 9 Hz, F_α), -128.2 (d, J 249 Hz, F_α), -130.0 (d, J 245 Hz, F_β), -132.9 (dd, J 245, 13 Hz, F_β), -137.0 (dt, J 249, 9 Hz, F_α); ES^+MS : m/z 489.2 $[\text{M} + \text{Na}]^+$; HRMS (ES^+) for $\text{C}_{23}\text{H}_{34}\text{F}_4\text{O}_5\text{Na}^+$ $[\text{M} + \text{Na}]^+$ calcd 489.2235, found 489.2230.

8.3.14 n-Octyl 6-*O*-benzyl-2,3-dideoxy-2,2,3,3-tetrafluorogalactofuranoside (threohexofuranoside) (**2.47**)



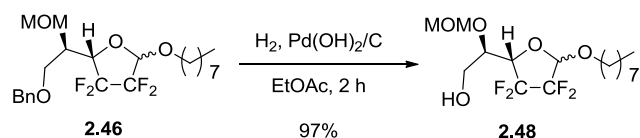
Galactofuranoside **2.46** (1.03 g, 2.21 mmol) was dissolved in DCM (15 mL), TFA (3.4 mL, 44.2 mmol) was added and the mixture was stirred at r.t. for 16 h. The reaction mixture was then concentrated to give a brown oil. Column chromatography (petrol ether/acetone 90:10) gave the product as a pale yellow oil (931 mg, quant, β/α 1:0.6). HPLC (hexane/acetone 90:10) gave α -**2.47** as a pale yellow oil (212 mg, 23%) and β -**2.47** as a pale yellow oil (414 mg, 44%).

Data for α -2.47: R_f 0.26 (petrol ether/acetone 80:20); $[\alpha]_D^{25} +37.4$ (c 0.5, CHCl_3 , 25 °C); IR (neat) 3459 (br., w), 2927 (m), 2858 (m), 1139 (s), 1012 (s) cm^{-1} ; ^1H NMR (400 MHz, CDCl_3) δ (ppm) 7.27–7.46 (5H, m, H_{Ar}), 5.07 (1H, d, J 8.6 Hz, H-1), 4.61 (1H, d, J 11.6 Hz, CHHPh), 4.57 (1H, d, J 12.1 Hz, CHHPh), 4.41 (1H, td, J 12.8, 6.8 Hz, H-4), 4.06 (1H, quin, J 4.5 Hz, H-5), 3.86 (1H, dt, J 9.2, 6.8 Hz, $\text{H-1}'$), 3.69–3.56 (3H, m, $\text{H-1}'$, $2 \times \text{H-6}$), 2.63 (1H, d, J 4.5 Hz, OH), 1.55–1.71 (2H, m, $\text{H-2}'$), 1.40–1.20 (10H, m, $\text{H-3'-H-7}'$), 0.89 (3H, t, J 6.3 Hz, $\text{H-8}'$); ^{13}C NMR (101 MHz, CDCl_3) δ (ppm) 137.5 (C_{Ar}), 128.5 ($2 \times \text{CH}_{\text{Ar}}$), 127.9 (CH_{Ar}), 127.7 ($2 \times \text{CH}_{\text{Ar}}$), 99.9 (dd, J 38, 20 Hz, C-1), 78.8 (t, J 26 Hz, C-4), 73.6 (CH_2Ph), 70.0 ($\text{C-1}'$), 69.4 (C-6), 68.3 (t, J 3 Hz, C-5), 31.7, 29.2, 25.7, 22.6 ($\text{C-3'-C-7}'$), 29.1 ($\text{C-2}'$), 14.0 ($\text{C-8}'$); ^{19}F NMR (282 MHz, CDCl_3) δ (ppm) -125.4 (2F, app.

d, J 13 Hz), -125.3 (1F, d, J 249 Hz), -134.8 (1F, br. dt, J 249, 9, Hz); **ES⁺MS**: m/z 445.1 $[M + Na]^+$; **HRMS** (ES⁺) for $C_{21}H_{30}F_4O_4Na^+$ $[M + Na]^+$ calcd 445.1972, found 445.1973.

Data for β -2.47: **R_f** 0.21 (petrol ether/acetone 80:20); **[α]_D** -65.4 (c 0.5, $CHCl_3$, 25 °C); **IR** (neat) 3455 (w, br.), 2928 (w), 2858 (w), 1149 (s), 1022 (m) cm^{-1} ; **¹H NMR** (400 MHz, $CDCl_3$) δ (ppm) 7.29–7.45 (5H, m, H_{Ar}), 5.13 (1H, dd, J 7.8, 2.8 Hz, H-1), 4.60 (2H, s, CH_2Ph), 4.35 (1H, ddd, J 14.3, 11.5, 6.1 Hz, H-4), 4.14 (1H, quin, J 5.4 Hz, H-5), 3.79 (1H, dt, J 9.5, 6.6 Hz, H-1'), 3.67 (1H, dd, J 10.1, 5.1 Hz, H-6), 3.63 (1H, dd, J 10.1, 5.6 Hz, H-6), 3.58 (1H, dt, J 9.6, 6.6 Hz, H-1'), 2.39 (1H, d, J 6.1 Hz, OH_H), 1.66 (1H, t, J 6.6 Hz, H-2'), 1.63 (1H, t, J 6.6 Hz, H-2'), 1.17–1.43 (10H, m, H-3'–7'), 0.89 (3H, t, J 6.6 Hz, H-8'); **¹³C NMR** (101 MHz, $CDCl_3$) δ (ppm) 137.4 (C_{Ar}), 128.5 ($CH_{Ar} \times 2$), 127.9 (CH_{Ar}), 127.8 ($CH_{Ar} \times 2$), 99.5 (dd, J 40, 20 Hz, C-1), 77.8 (dd, J 29, 22 Hz, C-4), 73.6 (CH_2Ph), 69.6 (C-6), 69.0 (C-1'), 67.6 (C-5), 31.7, 29.2, 29.1, 25.8, 22.6 (C-2'–7'), 14.0 (C-8'); **¹⁹F NMR** (282 MHz, $CDCl_3$) δ (ppm) -113.2 (1F, dd, J 245, 9 Hz), -125.3 (1F, dd, J 245, 9 Hz), -130.8 (1F, d, J 245 Hz), -133.5 (1F, dd, J 245, 1 Hz); **ES⁺MS**: m/z 445.2 $[M + Na]^+$; **HRMS** (ES⁺) for $C_{21}H_{30}F_4O_4Na^+$ $[M + Na]^+$ calcd 445.1972, found 445.1973.

8.3.15 n-Octyl 5-*O*-(methoxy)methyl-2,3-dideoxy-2,2,3,3-tetrafluorogalactofuranoside (threohexofuranoside) (**2.48**)

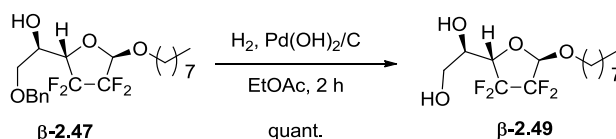


Galactofuranoside **2.46** (76 mg, 0.16 mmol) was dissolved in EtOAc (1.3 mL) and $Pd(OH)_2/C$ (26 mg, 48 μ mol) was added. The reaction was flushed with H_2 then stirred at r.t. under H_2 for 2 h. The resultant mixture was filtered through Celite[®], which was washed with plenty of EtOAc. The EtOAc was concentrated to give **2.48** as a colourless oil (59 mg, 97%, β/α 1:0.6).

R_f 0.25 (petrol ether/acetone 80:20); **IR** (neat) 3439 (w, br.), 2928 (m), 2857 (w), 1141 (s), 1012 (s) cm^{-1} ; **¹H NMR** (400 MHz, $CDCl_3$) δ (ppm) 5.11 (1H, dd, J 8.1, 2.5 Hz, H-1 $_{\beta}$), 5.03 (0.6H, dd, J 8.8, 2.3 Hz, H-1 $_{\alpha}$), 4.79–4.82 (1.2H, m, $CHHOMe_{\alpha}$ + $CHHOMe_{\beta}$), 4.75–4.79 (2H, m, $CHHOMe_{\beta}$ + $CHHOMe_{\alpha}$), 4.23–4.44 (1.6H, m, H-4 $_{\beta+\alpha}$), 3.64–3.97 (6.4H, m, H-5 $_{\beta+\alpha}$, 2 \times H-6 $_{\beta+\alpha}$, H-1' $_{\beta+\alpha}$), 3.52–3.63 (1.6H, m, H-1' $_{\beta+\alpha}$), 3.43–3.48 (4.8H, m, $CH_3O_{\beta+\alpha}$), 2.65 (1H, t, J 5.1 Hz, OH_{β}), 2.63 (0.6H, t, J 4.0 Hz, OH_{α}) (1.6H, dt, J 7.1, 5.1 Hz, $OH_{\beta+\alpha}$), 1.55–1.73 (3.2H, m, H-2' $_{\beta+\alpha}$), 1.16–1.45 (16H, m, H-3'–7'), 0.82–1.03 (4.8H, m, H-8'); **¹³C NMR** (101 MHz, $CDCl_3$) δ (ppm) 99.7 (dd, J 38, 20 Hz, C-1 $_{\alpha}$), 99.6 (dd, J 40, 20 Hz,

C-1_β), 97.5 (CH₂OMe_β), 97.3 (CH₂OMe_α), 78.3 (C-5_α), 77.0–77.8 (C-4_{β+α}), 77.0 (C-5_β), 69.8 (C-1'_α), 69.0 (C-1'_β), 61.8 (C-6_β), 61.7 (C-6_α), 56.0 (CH₃O_{β+α}), 56.0, 31.8, 29.3, 29.2, 29.2, 29.1, 25.8, 22.6 (C-2'-7'), 14.0 (C-8'); **¹⁹F NMR** (282 MHz, CDCl₃) δ (ppm) -113.6 (1F, dd, *J* 245, 9 Hz, F_β), -125.1 (1.6F, d, *J* 245 Hz, F_{β+α}), -126.5 (0.6F, ddd, *J* 249, 17, 9 Hz, F_α), -127.7 (0.6F, d, *J* 245 Hz, F_α), -129.8 (1F, d, *J* 245 Hz, F_β), -133.0 (1F, dd, *J* 245, 13 Hz, F_β), -136.8 (1F, br. dt, *J* 245, 9, 9 Hz, F_α); **ES⁺MS**: *m/z* 399.2 [M + Na]⁺; **HRMS** (ES⁺) for C₁₆H₂₈F₄O₅Na⁺ [M + Na]⁺ calcd 399.1765, found 399.1769.

8.3.16 n-Octyl 2,3-dideoxy-2,2,3,3-tetrafluoro-β-galactofuranoside (threohexofuranoside) (β-2.49)

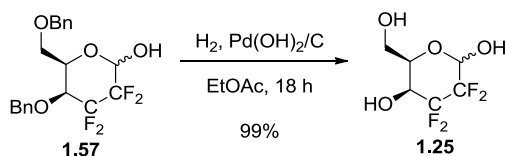


Galactofuranoside β-2.47 (57 mg, 0.13 mmol) was dissolved in EtOAc (1.1 mL) and Pd(OH)₂/C (21 mg, 39 μmol) was added. The reaction was flushed with H₂ then stirred at r.t. under H₂ for 2 h. The resultant mixture was filtered through Celite[®], which was washed with plenty of EtOAc. The EtOAc was concentrated to give **2.49** a colourless oil (44 mg, quant), which was used immediately without further purification.

R_f 0.13 (petrol ether/acetone 80:20); [**α**]_D -34.4 (c 0.2, CHCl₃, 23 °C); **IR** (neat) 3370 (w, br.), 2927 (m), 2857 (w), 1145 (s), 1014 (s) cm⁻¹; **¹H NMR** (300 MHz, CDCl₃) δ (ppm) 5.13 (1H, dd, *J* 8.1, 2.6 Hz, H-1), 4.30 (1H, ddd, *J* 3.5, 11.9, 6.4 Hz, H-4), 4.06 (1H, dt, *J* 9.9, 4.9 Hz, H-5), 3.89–3.69 (3H, m, *J* 15.7, 6.6 Hz, H-1', H-6, H-6), 3.59 (2H, dt, *J* 9.5, 6.6 Hz, H-1'), 2.38 (1H, d, *J* 4.8 Hz, OH-5), 1.93 (1H, t, *J* 5.5 Hz, OH-6), 1.65 (2H, quin, *J* 7.0 Hz, H-2'), 1.43–1.23 (10H, m, H-3'-7'), 0.89 (3H, t, *J* 6.4 Hz, H-8'); **¹³C NMR** (75 MHz, CDCl₃) δ (ppm) 99.6 (dd, *J* 39, 20 Hz, C-1), 77.8 (dd, *J* 31, 25 Hz, C-4), 69.2 (C-1'), 68.8 (C-5), 62.4 (C-6), 31.8 (s), 29.2 (br. s.), 29.2 (s), 25.8 (s), 22.6 (C-2'-7'), 14.1 (C-8'); **¹⁹F NMR** (282 MHz, CDCl₃) δ ppm -113.1 (1F, dd, *J* 245, 13 Hz), -125.3 (1F, dd, *J* 245, 9 Hz), -130.9 (1F, d, *J* 249 Hz), -133.8 (1F, dd, *J* 245, 13 Hz); **ES⁺MS**: *m/z* 355.2 [M + Na]⁺; **HRMS** (ES⁺) for C₁₄H₂₄F₄O₄Na⁺ [M+Na]⁺ calcd 355.1503, found 355.1501.

8.4 Synthesis of galactopyranosides discussed in chapter 3

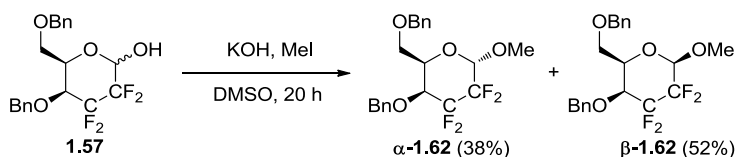
8.4.1 2,3-Dideoxy-2,2,3,3-tetrafluorogalactopyranose (threohexopyranose) (1.25)



Pyranose **1.57** (1.2 g, 3.0 mmol) was dissolved in EtOAc (24 mL). Pd(OH)₂/C (20% wt, 958 mg, 1.8 mmol) was added and the resultant mixture flushed with H₂. Stirring under H₂ at r.t. was continued for 18 h before the reaction mixture was filtered through Celite[®], which was washed with plenty of EtOAc. The solvent was concentrated to give galactopyranose **1.25** as a white foam (654 mg, 99%).

¹H NMR (400 MHz, D₂O) δ (ppm) 5.44 (1H, dd, *J* 9.1, 6.3 Hz, H-1_α), 5.13 (1H, dt, *J* 13.6, 3.1 Hz, H-1_β), 4.42 (1H, m, H-5_α), 4.20–4.31 (2H, m, H-4_{α+β}), 3.99 (1H, m, H-5_β), 3.75–3.87 (4H, m, H-6_{α+β}); ¹³C NMR (101 MHz, Acetone-*d*₆) δ (ppm) 91.3–94.4 (m, C-1_{α+β}), 75.3 (d, *J* 6 Hz, C-5_β), 69.5–70.4 (m, C-4_{α+β}), 61.0 (C-6), 60.8 (C-6); ¹⁹F NMR (282 MHz, D₂O) δ (ppm) **α anomer**: -118.89 (1F, ddt, *J* 271.9, 18.3, 9.7, Hz), -119.67 (1F, ddt, *J* 270.8, 16.1, 7.5, Hz), -130.39 (1F, m, *J* 270.8 Hz can be observed), -132.64 (1F, dddd, *J* 270.8, 17.2, 11.8, 5.4 Hz), **β anomer**: -121.00 (1F, m, *J* 270.8 Hz can be observed), -134.12 (1F, dddd, *J* 271.9, 16.1, 10.7, 5.4 Hz); -136.69 (1F, m, *J* 260.0 Hz can be observed), -137.82 (1F, dt, *J* 260.0, 15.0 Hz). NMR corresponded to the reported data.⁶⁶

8.4.2 Methyl 4,6-di-*O*-benzyl-2,3-dideoxy-2,2,3,3-tetrafluorogalactopyranoside (threohexopyranoside) (1.62)

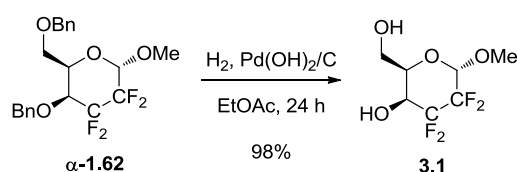


To a stirred solution of pyranose **1.57** (2.00 g, 5.00 mmol) in DMSO (20 mL) was added ground KOH (1.12 g, 20.0 mmol). The reaction mixture was stirred for 20 mins before the dropwise addition of MeI (2.48 mL, 40.0 mmol). Stirring was continued for 20 h. HCl (1M, 60 mL) was added and extraction was carried out into EtOAc (4 × 80 mL). The combined organic extracts were then dried (Na₂SO₄), filtered and concentrated to give a brown oil. Column chromatography (petrol ether/acetone 90:10) then HPLC (hexane/acetone 90:10) gave α-pyranoside **α-1.62** as a colourless oil (793 mg, 38%) and β-pyranoside **β-1.62** as a colourless oil (1.078 g, 52%).

Data for α -1.62: $[\alpha]_D +40.9$ (c 0.5, CHCl_3 , 25 °C); $^1\text{H NMR}$ (CDCl_3 , 600 MHz) δ 4.92 (1H, d, J 11.4 Hz, CHHPh), 4.88 (1H, dd, J 9.0, 5.9 Hz, H-1), 4.56 (1H, d, J 11.5 Hz, CHHPh), 4.51 (1H, d, J 11.8 Hz, CHHPh), 4.44 (1H, d, J 11.8 Hz, CHHPh), 4.31 (1H, br. t, J 6.6 Hz, H-5), 3.93 (1H, dd, J 6.0, 5.7 Hz, H-4), 3.63 (1H, dd, 9.4, 6.3 Hz, H-6), 3.57 (1H, dd, 9.3, 6.9 Hz, H-6'), 3.53 (3H, s, CH_3) (ppm); $^{13}\text{C NMR}$ (CDCl_3 , 151 MHz) δ 137.6 (C_{Ar}), 136.7 (C_{Ar}), 128.47 (CH_{Ar}), 128.23 (CH_{Ar}), 127.89 (CH_{Ar}), 127.71 (CH_{Ar}), 98.2 (dd, J 38, 26 Hz, C-1), 75.2 (dd, J 30, 17 Hz, C-4), 75.0 (CH_2Ph), 73.6 (CH_2Ph), 68.0 (d, J 6 Hz, C-5), 67.6 (C-6), 56.1 (CH_3); $^{19}\text{F NMR}$ (CDCl_3 , 565 MHz) δ -115.99 (1F, ddt, J 272.7, 13.5, 6.9 Hz), -118.02 (1F, ddt, J 272.9, 17.1, 8.3 Hz), -129.20 (1F, m, J 273.1 Hz can be observed), -134.46 (1F, dddd, J 272.7, 15.2, 9.3, 5.1 Hz) (ppm).

Data for β -1.62: $[\alpha]_D -39.4$ (c 0.5, CHCl_3 , 25 °C); $^1\text{H NMR}$ (CDCl_3 , 600 MHz) δ 7.27–7.40 (10H, m, H_{Ar}), 4.92 (1H, d, J 11.5 Hz, CHHPh), 4.60 (1H, ddd, J 7.5, 7.2, 4.3 Hz, H-1), 4.57 (1H, d, J 11.5 Hz, CHHPh), 4.48 (1H, d, J 11.8 Hz, CHHPh), 4.45 (1H, d, J 11.8 Hz, CHHPh), 3.96–3.91 (2H, m, H-4, H-5), 3.69 (1H, ddd, J 9.4, 5.9, 1.4 Hz, H-6) 3.66–3.61 (4H, m, H-6', CH_3) (ppm). $^{13}\text{C NMR}$ (CDCl_3 , 151 MHz) 137.5 (C_{Ar}), 136.7 (C_{Ar}), 128.5 ($\text{CH}_{\text{Ar}} \times 2$), 128.4 ($\text{CH}_{\text{Ar}} \times 2$), 128.4 (CH_{Ar}), 128.2 (CH_{Ar}), 128.0 ($\text{CH}_{\text{Ar}} \times 2$), 127.8 ($\text{CH}_{\text{Ar}} \times 2$), 98.5 (t, J 23 Hz, C-1), 74.9 (dd, J 23, 18 Hz, C-4), 74.8 (CH_2Ph), 74.6 (CH_2Ph), 72.8 (d, J 6 Hz, C-5), 67.3 (C-6), 57.9 (CH_3). $^{19}\text{F NMR}$ (CDCl_3 , 565 MHz) δ -117.09 (1F, d, J 273.7 Hz), -131.04 (1F, dt, J 273.5, 10.0 Hz), -136.58 (2F, br. s) (ppm). NMR for both anomers corresponded to the reported data.⁶⁶

8.4.3 2,3-Dideoxy-2,2,3,3-tetrafluoro- α -galactopyranose (threohexopyranoside) (3.1)

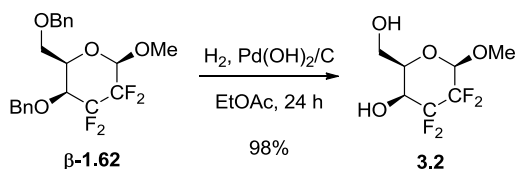


To a stirred solution of pyranoside **α -1.62** (140 mg, 0.34 mmol) in EtOAc (2.6 mL) was added $\text{Pd(OH)}_2/\text{C}$ (108 mg, 0.20 mmol). The resultant mixture was flushed with H_2 then stirred under H_2 for 24 h. EtOAc (10 mL) was added followed by filtration through Celite[®]. The filtrate was concentrated to give pyranoside **3.1** as a white solid (78 mg, 98%).

R_f 0.4 (EtOAc); **Mp** 107–116 °C (Et₂O); $[\alpha]_D +118.2$ (c 0.5, acetone, 22 °C); **IR** (neat) 3381 (br, w), 2947 (w), 1404 (w), 1118 (s), 1049 (s) cm^{-1} ; $^1\text{H NMR}$ (CDCl_3 , 600 MHz) δ 4.91 (1H, dd, $^3J_{\text{H1-F2ax}}$ 9.0 Hz, $^4J_{\text{H1-F3eq}}$ 5.7 Hz, H-1), 4.23 (1H, m, H-5), 4.15 (1H, m, H-4), 3.96 (2H, m, H-6), 3.52 (3H, s, CH_3), 2.89 (1H, d, $^3J_{\text{OH4-H4}}$ 5.4 Hz, OH-4), 2.07 (1H, t,

$^3J_{\text{OH6-H6}}$ 5.6 Hz, OH-6). $^1\text{H}(-^{19}\text{F})$ NMR (CDCl_3 , 600 MHz) δ 4.91 (1H, s, H1), 4.23 (1H, td, $^3J_{\text{H5-H6}}$ 5.4 Hz, $^4J_{\text{H5-H1}}$ 1.1 Hz, H-5), 4.15 (1H, d, $^3J_{\text{H4-OH4}}$ 5.4 Hz, H4), all other peaks as in ^1H . ^{13}C NMR (CDCl_3 , 125 MHz) δ 98.3 (dddd, $^2J_{\text{C1-F2ax}}$ 37.9 Hz, $^2J_{\text{C1-F2eq}}$ 25.4 Hz, $^3J_{\text{C1-F3eq}}$ 2.8 Hz, $^3J_{\text{C1-F3ax}}$ 2.1 Hz, C-1), 70.6 (dddd, $^2J_{\text{C4-F3ax}}$ 31.4 Hz, $^2J_{\text{C4-F3eq}}$ 20.8 Hz, $^3J_{\text{C4-F2eq}}$ 2.4 Hz, $^3J_{\text{C4-F2eq}}$ 1.6 Hz, C4), 68.4 (d, $J_{\text{C5-F}}$ 5.0 Hz, C-5), 61.8 (C-6), 56.3 (CH_3), 111.7 and 109.8 (m, C-2 and C-3). ^{19}F NMR (CDCl_3 , 565 MHz) δ -116.58 (1F, dddd, $^2J_{\text{F2ax-F2eq}}$ 275.5 Hz, $^3J_{\text{F2ax-F3eq}}$ 18.3 Hz, $^3J_{\text{F2ax-H1}}$ 9.0 Hz, $^3J_{\text{F2ax-F3ax}}$ 7.5 Hz, F2ax), -119.70 (1F, ddddd, $^2J_{\text{F3ax-F3eq}}$ 272.0 Hz, $^3J_{\text{F3ax-F2eq}}$ 15.0 Hz, $^4J_{\text{F3ax-H4}}$ 7.8 Hz, $^3J_{\text{F3ax-F2ax}}$ 7.5 Hz, $^4J_{\text{F3ax-H5}}$ 2.2 Hz, F3ax), -131.05 (1F, ddddd, $^2J_{\text{F3eq-F3ax}}$ 272.0 Hz, $^3J_{\text{F3eq-F2ax}}$ 18.3 Hz, $^3J_{\text{F3eq-F2eq}}$ 10.7 Hz, $^4J_{\text{F3eq-H1}}$ 5.7 Hz, $^3J_{\text{F3eq-H4}}$ 5.0 Hz, F3eq), -134.12 (1F, dddd, $^2J_{\text{F2eq-F2ax}}$ 275.5 Hz, $^3J_{\text{F2eq-F3ax}}$ 15.0 Hz, $^3J_{\text{F2eq-F3eq}}$ 10.7 Hz, $^4J_{\text{F2eq-H4}}$ 5.0 Hz, F2eq). $^{19}\text{F}(-^1\text{H})$ NMR (CDCl_3 , 565 MHz) δ -116.58 (1F, ddd, $^2J_{\text{F2ax-F2eq}}$ 275.5 Hz, $^3J_{\text{F2ax-F3eq}}$ 18.3 Hz, $^3J_{\text{F2ax-F3ax}}$ 7.5 Hz, F2ax), -119.70 (1F, ddd, $^2J_{\text{F3ax-F3eq}}$ 272.0 Hz, $^3J_{\text{F3ax-F2eq}}$ 15.0 Hz, $^3J_{\text{F3ax-F2ax}}$ 7.5 Hz, F3ax), -131.05 (1F, ddd, $^2J_{\text{F3eq-F3ax}}$ 272.0 Hz, $^3J_{\text{F3eq-F2ax}}$ 18.3 Hz, $^3J_{\text{F3eq-F2eq}}$ 10.7 Hz, F3eq), -134.12 (1F, ddd, $^2J_{\text{F2eq-F2ax}}$ 275.5 Hz, $^3J_{\text{F2eq-F3ax}}$ 15.0 Hz, $^3J_{\text{F2eq-F3eq}}$ 10.7 Hz, F2eq); **ES⁺MS**: m/z 233.1 [$\text{M} - \text{H}$]⁻; **HRMS** (ES⁺) for $\text{C}_7\text{H}_{10}\text{F}_4\text{O}_4\text{Na}$ [$\text{M} + \text{Na}$]⁺ calcd 257.0407, found 257.0408. Assignment of NMR coupling constants was achieved by the use of higher resolution spectroscopy in combination with additional experiments (see section 3.1).

8.4.4 2,3-Dideoxy-2,2,3,3-tetrafluoro- β -galactopyranose (threohexopyranoside) (3.2)

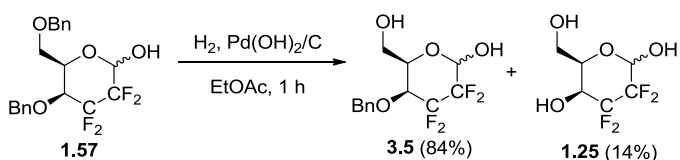


To a stirred solution of pyranoside **β-1.62** (184 mg, 0.44 mmol) in EtOAc (3.4 mL) was added $\text{Pd}(\text{OH})_2/\text{C}$ (142 mg, 0.27 mmol). The resultant mixture was flushed with H_2 then stirred under H_2 for 24 h. EtOAc (11 mL) was added followed by filtration through Celite[®]. The filtrate was concentrated to give pyranoside **3.2** as a white solid (101 mg, 98%).

R_f 0.13 (hexane/EtOAc 1:1); **Mp** 114–123 °C (Et_2O); **[α]_D** -40.2 (c 0.5, acetone, 24 °C); **IR** (neat) 3373 (br, m), 2951 (w), 1383 (w), 1119 (s), 1047 (s) cm^{-1} ; ^1H NMR (CDCl_3 , 600 MHz) δ 4.64 (1H, dd, $^3J_{\text{H1-F2ax}}$ 14.3, $^4J_{\text{H1-F3ax}}$ 4.0 Hz, H-1), 4.15 (1H, m, H-4), 3.99 (2H, m, H-6), 3.86 (1H, m, H-5), 3.68 (3H, s, CH_3), 2.87 (1H, d, $^3J_{\text{OH4-H4}}$ 7.2 Hz, OH-4), 2.06 (1H, t, $^3J_{\text{OH6-H6}}$ 6.2 Hz, OH-6). $^1\text{H}(-^{19}\text{F})$ NMR (CDCl_3 , 600 MHz) δ 4.64 (1H, s, H-1), 4.15 (1H, d, $^3J_{\text{H4-OH4}}$ 7.2 Hz, H-4), 3.86 (1H, td, $^3J_{\text{H5-H6}}$ 5.5 Hz, $^3J_{\text{H5-H4}}$ or $^4J_{\text{H5-H1}}$ 1.1 Hz, H-5), all

others as in ^1H . ^{13}C NMR (CDCl_3 , 125 MHz) δ 98.6 (ddd, $^2J_{\text{C1-F2ax}}$ 26.6 Hz, $^2J_{\text{C1-F2eq}}$ 18.9 Hz, $^3J_{\text{C1-F3eq}}$ 4.1 Hz, C-1), 73.3 (d, $J_{\text{C5-F}}$ 5.2 Hz, C-5), 70.2 (dd, $^2J_{\text{C4-F3ax}}$ 31.1 Hz, $^2J_{\text{C4-F3eq}}$ 20.1 Hz, C-4), 61.3 (d, $J_{\text{C6-F}}$ 2.05 Hz, C-6), 58.4 ($\underline{\text{CH}}_3$), 113.0 and 110.7 (m, C-2 and C-3). ^{19}F NMR (CDCl_3 , 565 MHz) δ -120.69 (1F, dddddd, $^2J_{\text{F3ax-F3eq}}$ 272.6, $^3J_{\text{F3ax-F2eq}}$ 14.0, $^3J_{\text{F3ax-F2ax}}$ 7.0 Hz, $^3J_{\text{F3ax-H4}}$ 6.5 Hz, $^4J_{\text{F3ax-H5}}$ 4.0 Hz, $^4J_{\text{F3ax-H1}}$ 4.6 Hz, F3ax), -133.14 (1F, dddd, $^2J_{\text{F3eq-F3ax}}$ 272.6 Hz, $^3J_{\text{F3eq-F2ax}}$ 16.4 Hz, $^3J_{\text{F3eq-F2eq}}$ 10.3 Hz, $^3J_{\text{F3eq-H4}}$ 5.1 Hz, F3eq), -135.32 (ddd, $^2J_{\text{F2ax-F2eq}}$ 264.7 Hz, $^3J_{\text{F2ax-F3eq}}$ 16.4 Hz, $^3J_{\text{F2ax-H1}}$ 14.3 Hz, $^3J_{\text{F2ax-F3ax}}$ 7.0 Hz, F2ax), -136.74 (ddd, $^2J_{\text{F2eq-F2ax}}$ 264.7 Hz, $^3J_{\text{F2eq-F3ax}}$ 14.0 Hz, $^3J_{\text{F2eq-F3eq}}$ 10.3 Hz, $^4J_{\text{F2eq-H4}}$ 5.0 Hz, F2eq). ^{19}F (^1H) NMR (CDCl_3 , 565 MHz) δ -120.69 (1F, ddd, $^2J_{\text{F3ax-F3eq}}$ 272.6 Hz, $^3J_{\text{F3ax-F2eq}}$ 14.0 Hz, $^3J_{\text{F3ax-F2ax}}$ 7.0 Hz, F3ax), -133.14 (1F, ddd, $^2J_{\text{F3eq-F3ax}}$ 272.6 Hz, $^3J_{\text{F3eq-F2ax}}$ 16.4 Hz, $^3J_{\text{F3eq-F2eq}}$ 10.3 Hz, F3eq), -135.32 (ddd, $^2J_{\text{F2ax-F2eq}}$ 264.7 Hz, $^3J_{\text{F2ax-F3eq}}$ 16.4 Hz, $^3J_{\text{F2ax-F3ax}}$ 7.0 Hz, F2ax), -136.74 (ddd, $^2J_{\text{F2eq-F2ax}}$ 264.7 Hz, $^3J_{\text{F2eq-F3ax}}$ 14.0 Hz, $^3J_{\text{F2eq-F3eq}}$ 10.3 Hz, F2eq); **ES⁺MS**: m/z 233.1 [$\text{M} - \text{H}$]⁻; **HRMS** (ES⁺) for $\text{C}_7\text{H}_{10}\text{F}_4\text{O}_4\text{Na}$ [$\text{M} + \text{Na}$]⁺ calcd 257.0407, found 257.0410. Assignment of NMR coupling constants was achieved by the use of higher resolution spectroscopy in combination with additional experiments (see section 3.1).

8.4.5 4-O-Benzyl-2,3-dideoxy-2,2,3,3-tetrafluorogalactopyranose (threohexopyranoside) (3.5)



To a stirred solution of pyranose **1.57** (405 mg, 1.01 mmol) in EtOAc (8 mL) was added $\text{Pd(OH)}_2/\text{C}$ (107 mg, 0.20 mmol). The resultant mixture was flushed with H_2 then stirred under H_2 for 1 h. EtOAc (11 mL) was added followed by filtration through Celite[®] to give a colourless oil. Column chromatography (petrol ether/acetone 60:40) gave pyranose **3.5** as a foam (264 mg, 84%) and pyranose **1.25** as a colourless residue (32 mg, 14%). Recrystallisation of **3.5** was achieved by dissolution in acetone and subsequently allowing to stand for several weeks. X-Ray diffraction crystallography revealed the β - anomer. Data for the anomeric mixture (1:1) was achieved after equilibration in solvent.

R_f 0.27 (petrol ether/acetone 60:40); **Mp** 138–142 °C (acetone); **IR** (neat) 3320 (w, br.), 2892 (w), 1692 (m), 1116 (s), 1074 (s), 1046 (s) cm^{-1} ;

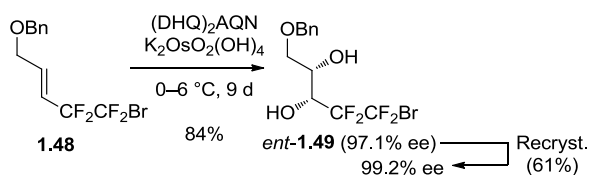
(β - only): ^1H NMR (400 MHz, Acetone- d_6) δ (ppm) 7.25–7.45 (5H, m, H_{Ar}), 6.67 (1H, br. s, $\text{OH}_{\text{H-1}}$), 4.99 (1H, d, J 13.6 Hz, H-1), 4.88 (1H, d, J 11.1 Hz, $\underline{\text{CH}}\text{HPh}$), 4.72 (1H, d, J

11.1 Hz, CHHPh), 4.18 (1H, m, H-4), 4.12 (1H, br. t, J 5.3 Hz, OH-6), 3.92 (1H, m, H-6), 3.73 - 3.82 (2 H, m); ^{13}C NMR (101 MHz, Acetone- d_6) δ (ppm) 138.8 (C_{Ar}), 129.2 ($\text{CH}_{\text{Ar}} \times 2$), 128.9 ($\text{CH}_{\text{Ar}} \times 2$), 128.7 (CH_{Ar}), 93.1 (ddd, J 26, 20, 3 Hz, C-1), 76.7 (dd, J 29, 19 Hz, C-4), 76.0 (d, J 3 Hz, CH_2Ph), 75.3 (d, J 6 Hz, C-5), 60.4 (C-6); ^{19}F NMR (282 MHz, Acetone- d_6) δ (ppm) -116.9 (1F, d, J 272 Hz), -130.8 (1F, dt, J 272, 10 Hz), -136.4 (1F, dt, J 259, 9 Hz), -137.7 (1F, dtd, J 259, 15, 15, 5 Hz);

(α/β 1:1): ^1H NMR (400 MHz, Acetone) δ (ppm) 7.27–7.44 (10H, m, H_{Ar}), 6.62–6.75 (2H, m, OH-1 $_{\alpha+\beta}$), 5.31 (1H, m, H-1 $_{\alpha}$), 4.99 (1H, br. d, J 14.1 Hz, H-1 $_{\beta}$), 4.88 (1H, d, J 11.1 Hz, CHHPh $_{\alpha/\beta}$), 4.87 (1H, d, J 11.1 Hz, CHHPh $_{\beta/\alpha}$), 4.72 (2H, d, J 11.1 Hz, CHHPh $_{\alpha+\beta}$), 4.45 (1H, m, H-5 $_{\alpha}$), 4.12–4.21 (3H, m, H-4 $_{\alpha+\beta}$, OH-6 $_{\beta}$), 4.05 (1H, dd, J 6.6, 5.1 Hz, OH-6 $_{\alpha}$), 3.92 (1H, tdt, J 6.4, 4.7, 2.1 Hz, H-5 $_{\beta}$), 3.67–3.82 (4H, m, H-6 $_{\alpha+\beta}$, H-6' $_{\alpha+\beta}$); ^{13}C NMR (101 MHz, Acetone) δ (ppm) 138.9 ($\text{C}_{\text{Ar}\alpha}$), 138.8 ($\text{C}_{\text{Ar}\beta}$), 129.2, 128.8, 128.8, 128.7, 128.7 ($\text{CH}_{\text{Ar}} \times 10$), 92.1–93.5 (m, C-1 $_{\alpha+\beta}$), 76.3–77.4 (m, C-4 $_{\alpha+\beta}$), 75.9 (d, J 3 Hz, $\text{CH}_2\text{Ph}_{\alpha+\beta}$), 75.3 (d, J 6 Hz, C-5 $_{\beta}$), 70.3 (J 6 Hz, C-5 $_{\alpha}$), 60.4 (C-6 $_{\alpha}$), 60.4 (C-6 $_{\beta}$); ^{19}F NMR (282 MHz, Acetone) δ (ppm) -115.3 (1F, ddt, J 270, 13, 8 Hz, F $_{\alpha}$), -116.9 (1F, dspt, J 271, 6, 6 Hz, F $_{\beta}$), -118.7 (1F, ddt, J 266, 17, 9 Hz, F $_{\alpha}$), -128.8 (1F, m, J 270 Hz can be observed, F $_{\alpha}$), -130.8 (1F, app. dt, J 272, 11 Hz, F $_{\beta}$), -133.7 (1F, dddd, J 266, 16, 10, 6 Hz, F $_{\alpha}$), -136.4 (1F, m, J 259 Hz can be observed, F $_{\beta}$), -137.7 (1F, dtd, J 259, 15, 5 Hz, F $_{\beta}$); **ES⁺MS**: m/z 374.1 [$\text{M} + \text{MeCN} + \text{Na}$] $^+$; **HRMS** (ES $^+$) for $\text{C}_{13}\text{H}_{14}\text{F}_4\text{O}_4\text{Na}^+$ [$\text{M} + \text{Na}$] $^+$ calcd 333.0720, found 333.0720.

8.5 Synthesis of Tetrafluoro Glucopyranose 1.24

8.5.1 (3R,4S)-5-Benzyloxy-1-bromo-1,1,2,2-tetrafluoropentan-3,4-diol (*ent*-1.49)



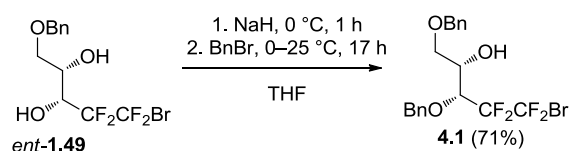
To a stirred solution of $t\text{BuOH}/\text{H}_2\text{O}$ (1:1, 400 mL) was added (DHQ) $_2$ AQN (655 mg, 0.84 mmol), $\text{K}_3\text{Fe}(\text{CN})_6$ (41.6 g, 126 mmol), K_2CO_3 (17.4 g, 126 mmol) and $\text{K}_2\text{OsO}_2(\text{OH})_4$ (124 mg, 337 μmol). H_2O (15 mL) was added and most of the solids were dissolved. MeSO_2NH_2 (4.00 g, 42.1 mmol) was added and the reaction mixture cooled to 0 $^\circ\text{C}$. Alkene **1.48** (13.8 g, 42.1 mmol) was added and washed in with $t\text{BuOH}$ (15 mL). The resultant mixture was stirred at 4–6 $^\circ\text{C}$ for 9 days. Na_2SO_3 (60 g) was added and the reaction mixture stirred for 2 h at 5 $^\circ\text{C}$ to r.t. H_2O (40 mL) was then added and extraction carried out into Et_2O (3 \times 210 mL). The combined organic phases were washed with aq.

HCl (2M, 2 × 40 mL) then brine (40 mL), before being dried (MgSO₄), filtered and concentrated to give a yellow solid. Column chromatography (petrol ether/EtOAc 70:30) gave diol *ent*-**1.49** as a white solid (3.57 g, 84%, 97.1% *e.e.*). This was suspended in hexane and heated to 40 °C, then Et₂O was added until dissolution occurred. The solution was allowed to stand for 7 days, after which time crystals were filtered and washed with a small amount of hexane to give a white solid (7.73 g, 51%, 99.2% *e.e.*).

Mp 84–86 °C (hexane/Et₂O); [α]_D +1.7 (c 0.5, CHCl₃, 25 °C); NMR corresponded to the reported data.⁶⁶

The acidic extracts from the workup were combined and neutralised with aq. NaOH (2M) then extracted into EtOAc (2 × 150 mL). The combined organic phase was dried (MgSO₄), filtered and concentrated to give impure (DHQ)₂AQN as an orange solid

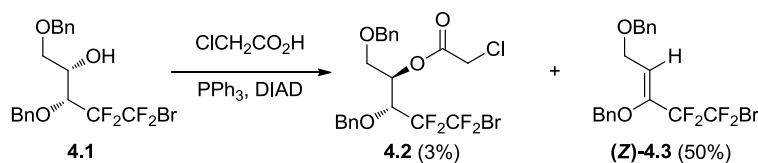
8.5.2 (3*R*,4*S*)-3,5-Dibenzyloxy-1-bromo-1,1,2,2-tetrafluoropentan-4-ol (**4.1**)



A stirred solution of diol *ent*-**1.49** (1.87 g, 5.17 mmol) in THF (33 mL) was cooled to 0 °C. NaH (60% in mineral oil, 207 mg, 5.17 mmol) was added and stirring continued at 0 °C for 1 h. BnBr (615 μ L, 5.17 mmol) was added and stirring continued at 0 °C to r.t. for 17 h. Aq. NH₄Cl (sat., 44 mL) was then added and the resultant mixture stirred at r.t. for 30 min. Extraction was carried out into EtOAc (4 × 65 mL). The combined organic phase was washed with brine (2 × 200 mL), dried (MgSO₄), filtered and concentrated to give an orange oil. Column chromatography (petrol ether/EtOAc 90:10) gave alcohol **4.1** as a slightly yellow oil (1.66 g, 71%).

[α]_D +43.4 (c 0.5, CHCl₃, 24 °C). NMR spectra in agreement with reported data.⁶⁶

8.5.3 (3*R*,4*R*)-3,5-Dibenzyloxy-1-bromo-1,1,2,2-tetrafluoropentan-4-yl chloroacetate (**4.2**)



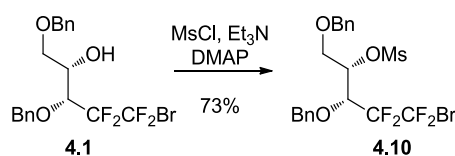
Alcohol **4.1** (131 mg, 0.29 mmol) was dissolved in toluene (2.9 mL) and treated with PPh₃ (152 mg, 0.58 mmol) and chloroacetic acid (55 mg, 0.58 mmol). The reaction was stirred until dissolution, DIAD (114 μ L, 0.58 mmol) was then added and stirring continued

at r.t. overnight. The reaction mixture was then concentrated to give a residue, which was purified by column chromatography (petrol ether/EtOAc 95:5, 70:30, 0:100) to give (**Z**)-**4.3** as a colourless oil (63 mg, 50%) and ester **4.2** as a colourless oil (5 mg, 3%).

Data for 4.2: R_f 0.38 (petrol ether/EtOAc 90:10), $[\alpha]_D$ not calculated as low *e.e.* material. **IR** (neat) 3033 (w), 2952 (w), 2875 (w), 1768 (m), 1152 (s) cm^{-1} , **^1H NMR** (400 MHz, CDCl_3) δ (ppm) 7.27 – 7.43 (10H, m, H_{Ar}), 5.50 (1H, td, J 5.5, 2.8 Hz, CHCH_2), 4.75 (1H, d, J 10.7 Hz, CHHPh), 4.69 (1H, d, J 10.8 Hz, CHHPh), 4.56 (1H, d, J 11.9 Hz, CHHPh), 4.50 (1H, d, J 11.9 Hz, CHHPh), 4.38 (1H, dt, J 16.6, 5.9 Hz, CHCF_2), 4.05 (1H, d, J 14.9 Hz, CHHCl), 3.99 (1H, d, J 14.9 Hz, CHHCl), 3.86 (1H, dd, J 11.3, 6.0 Hz, CHHOBn), 3.78 (1H, dd, J 11.3, 2.8 Hz, CHHOBn), **^{13}C NMR** (101 MHz, CDCl_3) δ (ppm) 166.2 (C=O), 137.4 (C_{Ar}), 136.1 (C_{Ar}), 128.5 (4C, $4 \times \text{CH}_{\text{Ar}}$), 128.4 (CH_{Ar}), 128.2 (2C, $2 \times \text{CH}_{\text{Ar}}$), 127.9 (CH_{Ar}), 127.7 (2C, $2 \times \text{CH}_{\text{Ar}}$), 75.4 (CH_2Ph), 75.3 (dd, J 27, 21 Hz, CHCF_2), 73.4 (CH_2Ph), 72.3 (CHCH_2), 67.6 (CH_2OBn), 40.6 (CH_2Cl); **^{19}F NMR** (282 MHz, CDCl_3) δ (ppm) -63.1 (1F, d, J 5 Hz, CFBr), -63.2 (1F, s, CFBr), -111.0 (1F, d, J 274 Hz, CFCH), -119.3 (1F, ddd, J 274, 17, 6 Hz, CFCH), **ES^+MS** : m/z 549.1 [$\text{M} + \text{Na}$] $^+$ 549.0, **HRMS** (ES^+) for $\text{C}_{21}\text{H}_{20}\text{BrClF}_4\text{O}_4\text{Na}^+$ [$\text{M} + \text{Na}$] $^+$ calcd 549.0062; found 549.0062.

Data for (Z)-3,5-Dibenzyloxy-1-bromo-1,1,2,2-tetrafluoropent-3-ene (4.3): **^1H NMR** (400 MHz, CDCl_3) δ (ppm) 7.28–7.63 (10H, m, H_{Ar}), 6.00 (1H, t, J 6.6 Hz, CHCH_2), 4.88 (2H, s, $\text{CHHPh} + \text{CHHPh}$), 4.47 (2 H, s, $\text{CHHPh} + \text{CHHPh}$), 4.12 (1H, t, J 2.2 Hz, CHHOBn), 4.11 (1H, t, J 2.2 Hz, CHHOBn); **^{13}C NMR** (101 MHz, CDCl_3) δ (ppm) 137.2 (C_{Ar}), 136.4 (C_{Ar}), 128.6 ($\text{CH}_{\text{Ar}} \times 2$), 128.5 ($\text{CH}_{\text{Ar}} \times 2$), 128.3 (CH_{Ar}), 128.1 (CH_{Ar}), 127.94 ($\text{CH}_{\text{Ar}} \times 2$), 127.88 ($\text{CH}_{\text{Ar}} \times 2$), 123.5 (CHCH_2), 75.8 ($\text{CH}_2\text{Ph} \times 2$), (dd, J 26, 22 Hz, CCF_2), 73.5 (CH_2Ph), 66.5 (CH_2OBn); **^{19}F NMR** (282 MHz, CDCl_3) δ (ppm) -64.08 (2F, t, J 5.4 Hz, $\text{CF}_2\text{CF}_2\text{Br}$), -110.87 (2 F, br. s, CF_2Br); NMR spectra in agreement with reported data.⁹⁶

8.5.4 (3*R*,4*S*)-3,5-Dibenzyloxy-1-bromo-1,1,2,2-tetrafluoropentan-4-yl methanesulfonate (**4.10**)

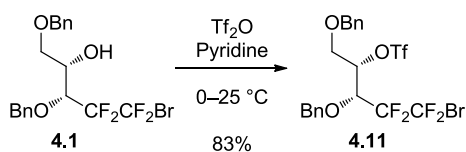


Alcohol **4.1** (774 mg, 1.72 mmol) was dissolved in DCM (8.6 mL) and treated with Et_3N (598 μL , 4.29 mmol) and DMAP (21 mg, 0.17 mmol). The reaction was cooled to 0 °C and

MsCl (173 μ L, 2.23 mmol) was added dropwise. The reaction mixture was stirred at 0 °C to r.t. for 2.5 h before being filtered. The filtrate was washed with H₂O (8 mL) and brine (2 \times 8 mL). The organic phase was dried (Na₂SO₄), filtered and concentrated to give mesylate **4.10** as an orange oil (664 mg, 72%).

[α]_D not calculated as low *e.e.* material. ¹H NMR (300 MHz, CDCl₃) δ (ppm) 7.31–7.57 (10H, m, H_{Ar}), 5.19 (1H, app td, *J* 5.6, 3.8 Hz, CHCH₂), 4.84 (1H, d, *J* 11.0 Hz, CHHPh), 4.76 (1H, d, *J* 10.9 Hz, CHHPh), 4.51–4.68 (3H, m, CHHPh, CHHPh, CHCF₂), 3.83–4.02 (2H, m, CHHOBn, CHHOBn), 3.00 (3H, s, CH₃); ¹³C NMR (101 MHz, CDCl₃) δ (ppm) 136.8 (C_{Ar}), 135.7 (C_{Ar}), 128.3 (CH_{Ar} \times 2), 128.24 (CH_{Ar} \times 2), 128.15 (CH_{Ar}), 128.0 (CH_{Ar} \times 2), 127.8 (CH_{Ar}), 127.6 (CH_{Ar} \times 2), 76.2–76.9 (CHCH₂), 76.0 (CH₂Ph), 75.3 (1 C, s), 73.7 (1 C, dd, *J* 28, 20 Hz, CHCF₂), 73.2 (CH₂Ph), 67.5 (CH₂OBn) 38.1 (CH₃); ¹⁹F NMR (282 MHz, CDCl₃) δ (ppm) -63.23 (2F, s, CF₂Br), -111.02 (1F, d, *J* 275.1 Hz, CFFCH), -120.21 (1F, dd, *J* 270.8, 17.2 Hz, CFFCH). NMR spectra in agreement with reported data.⁹⁶

8.5.5 (3*R*,4*S*)-3,5-Dibenzoyloxy-1-bromo-1,1,2,2-tetrafluoropentan-4-yl trifluoromethanesulfonate (**4.11**)

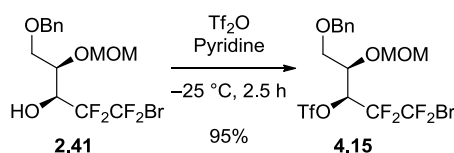


Alcohol **4.1** (480 mg, 1.06 mmol) was dissolved in DCM (1.7 mL) and treated with pyridine (172 μ L, 2.12 mmol). The reaction was cooled to 0 °C then Tf₂O (357 μ L, 2.12 mmol) was added dropwise while stirring vigorously. The mixture was stirred for 2 h at 0 °C then at r.t. for 14.5 h. The reaction was diluted with DCM (9 mL) and the solid pyridinium trifluoromethane sulfonate filtered off. The resultant solution was washed with cold (~0 °C) water (3 \times 8 mL), dried (MgSO₄), filtered and concentrated to give a brown liquid. Chromatographic purification (petrol ether/Et₂O 90:10) gave triflate **4.11** as a colourless oil (512 mg, 83%).

R_f 0.20 (petrol ether/EtOAc 70:30); [α]_D not calculated as low *e.e.* material; **IR** (neat) 3034 (w), 2928 (br., w), 2881 (w), 2362 (w), 1416 (m), 1212 (s), 1144 (s), 925 (m) cm⁻¹; ¹H NMR (400 MHz, CDCl₃) δ (ppm) 7.28–7.43 (10H, m, H_{Ar}), 5.20 (1H, dd, *J* 10.0, 4.5 Hz, CHCH₂), 4.75 (1H, d, *J* 11.0 Hz, CHHPh), 4.69 (1H, d, *J* 11.0 Hz, CHHPh), 4.58 (1 H, d, *J* 11.5 Hz, CHHPh), 4.53 (2H, d, *J* 12.0 Hz, CHHPh), 4.51 (1H, dt, *J* 17.6, 4.5 Hz, CHCF₂), 3.83 (1H, dd, *J* 11.0, 4.5 Hz, CHHOBn), 3.77 (1H, dd, *J* 11.5, 6.0 Hz, CHHOBn);

¹³C NMR (101 MHz, CDCl₃) δ (ppm) 129.0 (CH_{Ar} × 3), 129.0 (CH_{Ar} × 2), 129.0 (CH_{Ar} × 2), 128.8 (CH_{Ar} × 2), 128.7 (CH_{Ar}), 128.3 (CH_{Ar} × 2), 83.2 (CHCH₂), 76.3 (CH₂Ph), 74.1 (CH₂Ph), 67.4 (CH₂OBn); **¹⁹F NMR** (282 MHz, CDCl₃) δ (ppm) -63.3 (2F, s, CF₂Br), -75.1 (3F, s, CF₃), -110.9 (1F, d, *J* 275 Hz, CFFCH), -120.4 (1 F, dd, *J* 274, 18 Hz, CFFCH); **HRMS** (ES⁺): for C₂₀H₁₈BrF₇O₅SNa⁺ [M + Na]⁺ calcd.604.9839; found 604.9823.

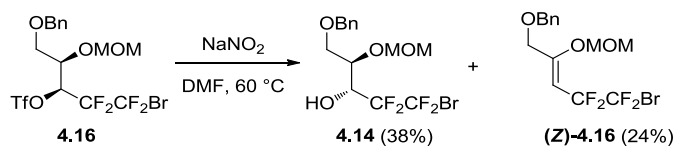
8.5.6 (3S,4R)-5-Benzyloxy-4-((methoxy)methoxy)-1-bromo-1,1,2,2-tetrafluoropentan-3-yl trifluoromethanesulfonate (**4.15**)



Alcohol **2.41** (420 mg, 1.04 mmol) was dissolved in DCM (6 mL) and treated with pyridine (168 μL, 2.07 mmol). The reaction was then cooled to -35 °C before the dropwise addition of Tf₂O (1M in DCM, 1.56 mL, 1.56 mmol). Stirring was continued at -25 °C for 2.5 h, after which time the reaction was allowed to warm to room temperature. H₂O (12 mL) and aq. NaHCO₃ (12 mL) were then added and the resultant mixture was extracted into DCM (2 × 24 mL). The combined organic phase was dried (Na₂SO₄), filtered and concentrated to give a yellow oil, which was diluted in DCM and filtered through silica. The silica plug was washed with plenty of DCM and the resultant combined DCM was concentrated to give triflate **4.15** as a pale yellow oil (527 mg, 95%).

R_f 0.47 (petrol ether/EtOAc 80:20); [**α**]_D not calculated as low *e.e.* material; **IR** (neat) 2900 (w), 1418 (m), 1212 (s), 1135 (s), 1086 (s) cm⁻¹; **¹H NMR** (400 MHz, CDCl₃) δ (ppm) 7.28–7.43 (5H, m, H_{Ar}), 5.66 (1H, td, *J* 10.4, 4.0 Hz, CHCF₂), 4.74 (1H, d, *J* 7.1 Hz, CHHOMe), 4.70 (1H, d, *J* 7.1 Hz, CHHOMe), 4.64 (1H, d, *J* 11.6 Hz, CHHPh), 4.53 (1H, d, *J* 11.6 Hz, CHHPh), 4.23 (1H, dd, *J* 11.1, 5.1 Hz, CHCH₂), 3.77 (1H, dd, *J* 10.1, 5.1 Hz, CHHOBn), 3.67 (1H, dd, *J* 10.1, 6.6 Hz, CHHOBn), 3.38 (3H, s, CH₃); **¹³C NMR** (101 MHz, CDCl₃) δ (ppm) 137.2 (C_{Ar}), 128.5 (CH_{Ar} × 2), 128.0 (CH_{Ar}), 127.8 (CH_{Ar} × 2), 97.4 (CH₂OMe), 77.8 (t, *J* 26 Hz, CHCF₂), 73.6 (CH₂Ph), 72.7 (CHCH₂), 67.7 (CH₂OBn), 56.2 (CH₃); **¹⁹F NMR** (282 MHz, CDCl₃) δ (ppm) -63.8 (1F, d, *J* 185 Hz, CFFBr), -64.6 (1F, d, *J* 185 Hz, CFFBr), -74.0 (3F, br. s., CF₃), -112.7 (1F, d, *J* 275 Hz, CFFCH), -113.9 (1F, d, *J* 279 Hz, CFFCH); **EIMS**: *m/z* 490.9 [M-MOM]⁺; **HRMS** (ES⁺) for C₁₅H₁₆⁷⁹BrF₇O₆SNa⁺ [M + Na]⁺ calcd 558.9631, found 560.9623.

8.5.7 (3R,4R)-5-(Benzyloxy)-1-bromo-4-((methoxymethyl)oxy)-1,1,2,2-tetrafluoropentan-3-ol (**4.14**)



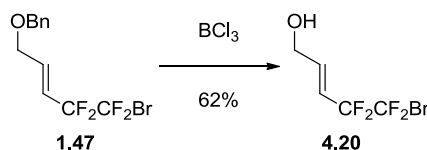
Triflate **4.15** (69 mg, 0.13 mmol) was dissolved in DMF (1 mL) and cooled to 0 °C. NaNO₂ (89 mg, 1.28 mmol) was then added and the reaction stirred at 60 °C for 17 h. The resultant mixture was diluted with H₂O (2 mL) and extracted into DCM (4 × 2 mL). Combined organic phases were dried (Na₂SO₄), filtered and concentrated to give a pale yellow oil. Column chromatography (petrol ether/EtOAc 90:10, 80:20) gave alkene (**Z**)-**4.16** as a colourless oil (12 mg, 24%) and alcohol **4.14** as a pale yellow oil (20 mg, 38%).

Data for 4.14: **R_f** 0.19 (petrol ether/EtOAc 80:20); [α]_D: *low e.e. material*; **IR** (neat) 3415 (w, br.), 2940 (w), 2360 (w), 1152 (s), 1101 (s), 1030 (s) cm⁻¹; **¹H NMR** (400 MHz, CDCl₃) δ (ppm) 7.29–7.44 (5H, m), 4.77 (1H, d, *J* 7.1 Hz, OCHHO), 4.74 (1H, d, *J* 7.1 Hz, OCHHO), 4.59 (2H, s, CHHPh, CHHPh), 4.47 (1H, ddt, *J* 22.2, 8.6, 3.5 Hz, CHCF₂), 4.28 (1H, d, *J* 8.6 Hz, OH), 4.02 (1H, q, *J* 3.5 Hz, CHCH₂), 3.89 (1H, dd, *J* 10.6, 4.0 Hz, CHHOBn), 3.83 (1H, dd, *J* 10.1, 3.5 Hz, CHHOBn), 3.43 (3H, s, CH₃); **¹³C NMR** (101 MHz, CDCl₃) δ (ppm) 137.0 (C_{Ar}), 128.6 (CH_{Ar} × 2), 128.1 (CH_{Ar}), 127.9 (CH_{Ar} × 2), 96.8 (OCH₂O), 75.6 (CHCH₂), 74.0 (CH₂Ph), 70.7 (t, *J* 3 Hz, CH₂OBn), 70.6 (dd, *J* 28, 22 Hz, CHCF₂), 56.1 (CH₃); **¹⁹F NMR** (282 MHz, CDCl₃) δ (ppm) -62.7 (1F, dd, *J* 181, 9 Hz, CFFBr), -63.9 (1F, d, *J* 176 Hz, CFFBr), -114.7 (1F, d, *J* 271 Hz, CFFCH), -124.7 (1F, dt, *J* 266, 9 Hz, CFFCH); **ES⁺MS**: *m/z* 468.0 [⁷⁹BrM+MeCN+Na]⁺; **HRMS** (ES⁺) for C₁₄H₁₇BrF₄O₄Na⁺ [*M* + Na]⁺ calcd 427.0139, found 427.0148.

Data for (Z)-5-Benzyloxy-1-bromo-4-(methoxy)methoxy-1,1,2,2-tetrafluoro-pent-3-ene (4.16): **R_f** 0.47 (petrol ether/EtOAc 80:20); **IR** (neat) 2919 (w), 1675 (m), 1153 (s), 1082 (s), 1002 (s), 914 (s) cm⁻¹; **¹H NMR** (400 MHz, CDCl₃) δ (ppm) 7.29–7.43 (5H, m, H_{Ar}), 5.13 (2H, s, CH₂OMe), 5.01 (1H, t, *J* 14.1 Hz, CH), 4.57 (2H, s, CH₂Ph), 4.21 (2H, t, *J* 1.8 Hz, CH₂OBn), 3.49 (3H, s, CH₃); **¹³C NMR** (101 MHz, CDCl₃) δ (ppm) 159.9 (t, *J* 5 Hz, COMOM), 137.1 (C_{Ar}), 128.6 (CH_{Ar} × 2), 128.1 (CH_{Ar}), 127.9 (CH_{Ar} × 2), 96.7 (t, *J* 25 Hz, CH), 93.9 (CH₂OMe), 72.2 (CH₂Ph), 67.6 (CH₂OBn), 56.8 (CH₃); **¹⁹F NMR** (282 MHz, CDCl₃) δ (ppm) -66.2 (2F, t, *J* 9 Hz, CF₂Br), -104.4 (2F, m, CF₂CH); **ES⁺MS**: *m/z*

409.0 $[M + Na]^+$; **HRMS** (ES+) for $C_{14}H_{15}BrF_4O_3Na^+$ $[M + Na]^+$ calcd 409.0033, found 409.0034.

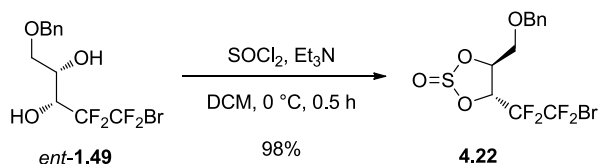
8.5.8 (E)-1-Bromo-1,1,2,2-tetrafluoropent-3-en-5-ol (4.20)



Alkene **1.47** (3.00 g, 3.8 mmol) was dissolved in DCM (80 mL) and treated with BCl_3 (1M in DCM, 40 mL). The reaction was stirred at r.t. for 2 h then concentrated to give a dark green oil. Column chromatography (petrol ether/EtOAc 90:10, 80:20, 70:30) gave a brown oil, which was again purified by column chromatography (petrol ether/EtOAc 90:10, 80:20) to give allylic alcohol **4.20** as a yellow oil (1.36 g, 62%).

R_f 0.24 (petrol ether/EtOAc 80:20); **IR** (neat) 3326 (w, br.), 2924 (w), 1680 (w), 1235 (m), 1148 (s), 1078 (s) cm^{-1} ; **¹H NMR** (400 MHz, CDCl_3) δ (ppm) 6.55 (1H, dtt, J 15.8, 3.9, 1.9 Hz, CHCH_2), 6.00 (1H, m, CHCF_2), 4.36 (2H, br. s, CH_2), 1.65 (1H, t, J 5.6 Hz, OH); **¹³C NMR** (101 MHz, CDCl_3) δ (ppm) 139.1 (t, J 7 Hz), 114.1 (t, J 23 Hz), 59.3 (s); **¹⁹F NMR** (282 MHz, CDCl_3) δ (ppm) -66.1 (2F, br. s, CF_2Br), -109.6 (2 F, br. s, CF_2CH).

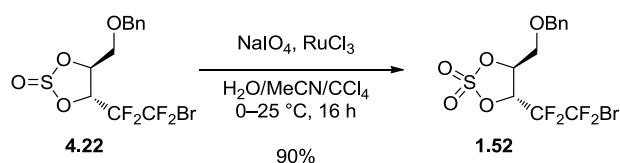
8.5.9 (4S,5R)-4-((Benzyloxy)methyl)-5-(2-bromo-1,1,2,2-tetrafluoroethyl)-2-oxo-1,3,2-dioxathiolane (4.22)



Diol *ent*-**1.49** (4.79 g, 13.3 mmol) was dissolved in DCM (60 mL) and cooled to 0 °C. Et_3N (7.42 mL, 53.2 mmol) was added, followed by SOCl_2 (1.94 mL, 26.6 mmol), dropwise over 9 mins. The reaction was stirred at 0 °C for 25 min then diluted with cold Et_2O (90 mL). H_2O (180 mL) was added and the layers separated. The aqueous phase was extracted into Et_2O (4×180 mL) and the resultant organic phases combined and washed with brine (4×180 mL). Drying (Na_2SO_4) was followed by filtration and concentration to give a dark brown oil. The oil was dissolved in Et_2O and filtered through silica, which was washed with plenty of Et_2O . Concentration of the filtrate gave a brown oil. Column chromatography (petrol ether/ Et_2O 90:10) gave sulfite **4.22** as an oil (5.265 g, 98%).

¹H NMR (300 MHz, CDCl₃) δ (ppm) 7.28–7.48 (10H, m, H_{Ar}), 5.30–5.41 (2H, m, CHCF₂, CHCH₂'), 5.10 (1H, dd, *J* 10.2, 5.5 Hz, CHCH₂), 5.04 (1H, ddd, *J* 19.8, 7.0, 4.0 Hz, CHCF₂'), 4.67 (2H, d, *J* 12.1 Hz, CHHPh, CHHPh'), 4.63 (1H, d, *J* 8.4 Hz, CHHPh), 4.60 (1H, d, *J* 12.1 Hz, CHHPh'), 3.93 (1H, dd, *J* 11.7, 2.2 Hz, CHHOBn'), 3.90–3.86 (2H, m, CHHOBn + CHHOBn'), 3.73 (1H, dd, *J* 11.7, 2.6 Hz, CHHOBn'); **¹³C NMR** (101 MHz, CDCl₃) δ (ppm) 136.9 (C_{Ar}), 136.7 (C_{Ar}'), 128.6 (CH_{Ar}' × 2), 128.5 (CH_{Ar} × 2), 128.2 (CH_{Ar}'), 128.1 (CH_{Ar}), 127.7 (CH_{Ar} × 2, CH_{Ar}' × 2), 81.8 (CHCH₂), 80.3 (CHCH₂'), 77.6 (dd, *J* 34, 23 Hz, CHCF₂), 76.2 (dd, *J* 35, 23 Hz, CHCF₂'), 73.7 (CH₂Ph'), 73.6 (CH₂Ph), 69.3 (CH₂OBn), 67.0 (CH₂OBn'); **¹⁹F NMR** (282 MHz, CDCl₃) δ ppm -64.4–-63.5 (3F, m, CFFCH, CFFCH', CFFCH), -64.8 (1F, d, *J* 189 Hz, CFFCH'), -116.0 (1F, d, *J* 271 Hz, CFFBr), -116.0 (1F, d, *J* 271 Hz, CFFBr'), -121.9 (1F, ddd, *J* 271, 21, 9 Hz, CFFBr'), -125.7 (1F, dd, *J* 266, 17 Hz, CFFBr). NMR spectra in agreement with reported data.⁹⁶

8.5.10 (4*S*,5*R*)-4-((Benzyloxy)methyl)-5-(2-bromo-1,1,2,2-tetrafluoroethyl)-2,2-dioxo-1,3,2-dioxathiolane (**1.52**)

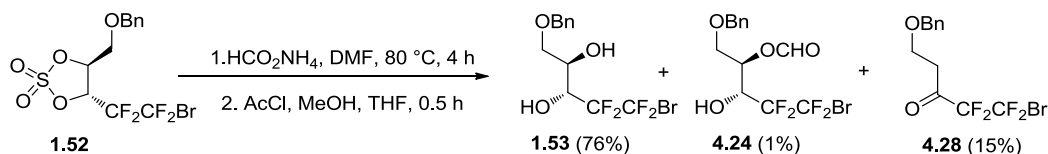


Sulfite **4.22** (4.3 g, 10.6 mmol) was dissolved in H₂O (25 mL), MeCN (17 mL) and CCl₄ (17 mL) and then immediately cooled to 0 °C. NaIO₄ (2.71 g, 12.67 mmol) and RuCl₃·xH₂O (55 mg) were added, followed by vigorous stirring at 0 °C to r.t. for 16 h. The resultant mixture was diluted with Et₂O (50 mL) then stirred for 5 min. The aqueous phase was then separated and extracted into Et₂O (3 × 80 mL). Combined organics were washed with H₂O (80 mL), dried (Na₂SO₄), filtered and concentrated to give a red oil. Column chromatography (petrol ether/Et₂O 75:25) gave sulfate **1.52** as a colourless oil, which after storage in the fridge for several days became a solid (4.00 g, 90%).

[α]_D -37.1 (c 0.5, CHCl₃, 27 °C); **¹H NMR** (300 MHz, CDCl₃) δ (ppm) 7.30–7.41 (5H, m, H_{Ar}), 5.37 (1H, ddd, *J* 18.0, 6.4, 2.9 Hz, CF₂CH), 5.18 (1H, dt, *J* 6.5, 3.4 Hz, CH₂CH), 4.71 (1H, d, *J* 12.0 Hz, CHHPh), 4.62 (1H, d, *J* 12.0 Hz, CHHPh), 3.95 (1H, ddd, *J* 12.0, 3.5, 1.0 Hz, CHHOBn), 3.80 (1H, ddd, *J* 12.2, 3.8, 1.1 Hz, CHHOBn). **¹³C NMR** (75 MHz, CDCl₃) δ (ppm) 136.3 (C_{Ar}), 128.7 (2 × CH_{Ar}), 128.4 (CH_{Ar}), 127.9 (2 × CH_{Ar}), 78.9 (CCH₂), 74.8 (CCF₂), 74.0 (CH₂Ph), CF₂CF₂ and CH₂OBn not observed; **¹⁹F NMR** (282

MHz, CDCl₃) δ (ppm) -65.1 (2F, s, CF₂Br), -118.1 (1F, d, *J* 277 Hz, CFFCH), -123.8 (1F, dd, *J* 277, 17 Hz, CFFCH). NMR spectra in agreement with reported data.⁶⁶

8.5.11 (3R,4R)-5-Benzyloxy-1-bromo-1,1,2,2-tetrafluoropentan-3,4-diol (1.50)



Sulfate **1.52** (3.52 g, 8.32 mmol) was dissolved in DMF (65 mL) and treated with HCO₂NH₄ (1.05 g, 16.6 mmol). The reaction was stirred at 80 °C for 4 h before being concentrated under reduced pressure. The resultant oil was dissolved in THF (45 mL) and treated with acetyl chloride (2M in MeOH, 12.5 mL, 25.0 mmol). The reaction mixture was stirred at r.t. for 30 min before being quenched with NaHCO₃. Stirring was continued for 20 min before the reaction was filtered and washed through with EtOAc. Concentration of the filtrate gave a yellow residue. Column chromatography (petrol ether/EtOAc 85:15 then 70:30) gave ketone **4.27** as a yellow oil (439 mg, 15%), sulfate **1.49** as a yellow oil (82 mg, 2.3%), formate **4.23** as a yellow oil (38 mg, 1.2%) and desired diol **1.50** as an oily solid (2.27 g, 76%).

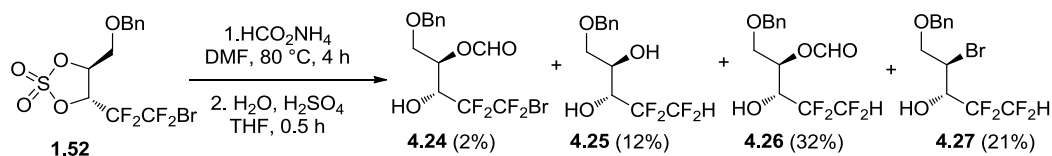
Data for 1.53: $[\alpha]_D^{25} +21.7$ (c 0.5, CHCl₃, 26 °C); *R*_f 0.27 (petrol ether/EtOAc 70:30); ¹H NMR (400 MHz, CDCl₃) δ (ppm) 7.28–7.45 (5H, m, H_{Ar}), 4.59 (1H, d, *J* 12.6 Hz, CHHPh), 4.56 (1H, d, *J* 11.6 Hz, CHHPh), 4.44 (1H, ddt, *J* 21.7, 8.6, 4.0 Hz, CHCF₂), 4.06 (1H, m, CHCH₂), 3.91 (1H, dd, *J* 10.1, 4.0 Hz, CHHOBN), 3.81 (1H, dd, *J* 10.1, 3.0 Hz, CHHOBN), 3.75 (1H, d, *J* 8.6 Hz, CF₂CHOH), 3.06 (1H, d, *J* 8.1 Hz, CH₂CHOH); ¹³C NMR (101 MHz, CDCl₃) δ (ppm) 136.7 (C_{Ar}), 128.7 (CH_{Ar} × 2), 128.3 (CH_{Ar}), 128.0 (CH_{Ar} × 2), 74.1 (CH₂Ph), 71.9 (CH₂OBn), 71.6 (dd, *J* 26, 22 Hz, CHCF₂), 67.7 (d, *J* 3 Hz, CHCH₂); ¹⁹F NMR (282 MHz, CDCl₃) δ (ppm) -63.2 (1F, dd, *J* 181, 9 Hz, CFFBr), -64.0 (1F, d, *J* 176 Hz, CFFBr), -116.0 (1F, d, *J* 271 Hz, CFFCH), -124.5 (1F, ddd, *J* 271, 21, 9 Hz, CFFCH).). NMR spectra in agreement with reported data.⁶⁶

Data for (3R,4R)-5-Benzyloxy-1-bromo-3-hydroxy-1,1,2,2-tetrafluoropentan-4-yl formate (4.24): *R*_f 0.24 (hexane/EtOAc 80:20); $[\alpha]_D^{25} -3.0$ (c 0.6, CHCl₃, 24 °C); ¹H NMR (400 MHz, CDCl₃) δ (ppm) 8.10 (1H, s, CHO), 7.30–7.43 (H, m, H_{Ar}), 5.38 (1H, m, *J* 1.5 Hz can be observed, CHCH₂), 4.50–4.65 (3H, m, CHCF₂, CHHPh, CHHPh), 4.13 (1H, d, *J* 8.6 Hz, OH), 4.02 (1H, dd, *J* 11.4, 3.3 Hz, CHHOBN), 3.85 (1H, dd, *J* 11.1, 2.5 Hz, CHHOBN); ¹³C NMR (101 MHz, CDCl₃) δ (ppm) 159.7 (C=O), 136.4 (C_{Ar}), 128.7 (CH_{Ar} × 2), 128.4 (CH_{Ar}), 128.0 (CH_{Ar} × 2), 74.2 (CH₂Ph), 70.0 (dd, *J* 28, 22 Hz, CHCF₂), 69.8

(CHCH₂), 68.8 (CH₂OBn); ¹⁹F NMR (282 MHz, CDCl₃) δ (ppm) -63.0 (1F, dd, *J* 180, 10 Hz, CFFBr), -64.0 (1F, d, *J* 176 Hz, CFFBr), -115.1 (1F, d, *J* 266 Hz, CFFCH₂), -124.9 (1F, ddd, *J* 266, 21, 9 Hz, CFFCH₂).). NMR spectra in agreement with reported data.⁶⁶

Data for 5-Benzyloxy-1-Bromo-1,1,2,2-tetrafluoropentan-3-one (4.28): *R*_f 0.54 (hexane/EtOAc 80:20); IR (neat) 2873 (w), 1756 (m), 1163 (s), 1098 (s) cm⁻¹; ¹H NMR (400 MHz, CDCl₃) δ (ppm) 7.28–7.40 (5H, m, H_{Ar}), 4.55 (2H, s, CH₂Ph), 3.82 (2H, t, *J* 6.1 Hz, CH₂OBn), 3.07 (2H, t, *J* 6.1 Hz, CH₂C=O); ¹³C NMR (101 MHz, CDCl₃) δ (ppm) 192.4 (t, *J* 28 Hz, C=O), 137.7 (C_{qAr}), 128.4 (CH_{Ar} × 2), 127.8 (CH_{Ar}), 127.7 (CH_{Ar} × 2), 73.4 (CH₂Ph), 63.4 (CH₂OBn), 38.7 (CH₂C=O); ¹⁹F NMR (282 MHz, CDCl₃) δ (ppm) -64.8 (2F, br. s.), -116.8 (2F, br. s.); **CI⁺MS**: *m/z* 344.1 [M + H]⁺; **HRMS** (ESI⁻) for C₁₂H₁₀BrF₄O₂ [M – H]⁻ calcd 340.9806, found 340.9802.

8.5.12 (3*R*,4*R*)-5-(Benzyloxy)-1,1,2,2-tetrafluoropentan-3,4-diol (4.25), (3*R*,4*R*)-5-benzyloxy-3-hydroxy-1,1,2,2-tetrafluoropentan-4-yl formate (4.26) and (4*S*,5*R*)-4-((benzyloxy)methyl)-5-(1,1,2,2-tetrafluoroethyl)-2,2-dioxo-1,3,2-dioxathiolane (4.27)



Sulfate **1.52** (110 mg, 0.26 mmol) was dissolved in DMF (2 mL) and treated with HCO₂NH₄ (33 mg, 0.52 mmol). The reaction was stirred at 80 °C for 4 h before being concentrated under reduced pressure. The resultant oil was dissolved in THF (1.3 mL) and treated with H₂O (1M in THF, 260 μL, 0.26 mmol) and H₂SO₄ (1M in THF, 260 μL, 0.26 mmol). The reaction mixture was stirred at r.t. for 1 h before being quenched with NaHCO₃. Stirring was continued for 10 min before the reaction was filtered through a pad of silica and washed through with Et₂O. Concentration of the filtrate gave an orange oil. Column chromatography (petrol ether/EtOAc 85:15 then 70:30) gave formate **4.24** as a colourless residue (2 mg, 2%), diol **4.25** as a colourless oil (9 mg, 12%), formate **4.26** as a colourless oil (26 mg, 32%) and bromide **4.27** as a colourless oil (19 mg, 21%).

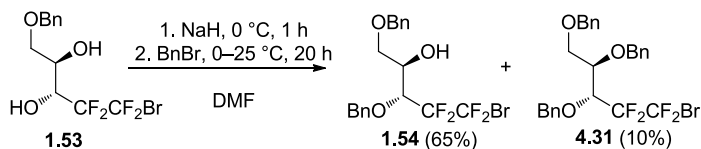
Data for 4.25: *R*_f 0.25 (hexane/EtOAc 70:30); [α]_D -2.7 (c 0.2, CHCl₃, 26 °C); IR (neat) 3405 (br, m), 2929 (w), 2873 (w), 1101 (s) cm⁻¹; ¹H NMR (400 MHz, CDCl₃) δ (ppm) 7.30–7.43 (5H, m, H_{Ar}), 6.11 (1H, tdd, *J* 53.2, 7.4, 4.6 Hz), 4.59 (2H, s, CHHPh × 2), 4.16

(1H, td, *J* 16.2, 6.1 Hz, $\underline{\text{CHCF}_2}$), 3.98 - 4.08 (1H, m, $\underline{\text{CHCH}_2}$), 3.86 (1H, dd, *J* 9.9, 4.4 Hz, $\underline{\text{CHHOBn}}$), 3.79 (1H, ddd, *J* 9.9, 3.1, 1.3 Hz, $\underline{\text{CHHOBn}}$), 3.26 (1H, d, *J* 6.7 Hz, $\underline{\text{CF}_2\text{CHOH}}$), 2.79 (1H, d, *J* 7.2 Hz, $\underline{\text{CH}_2\text{CHOH}}$), **¹³C NMR** (101 MHz, CDCl₃) δ (ppm) 136.9 ($\underline{\text{C}_{\text{Ar}}}$), 128.7 (2C, $2\times \underline{\text{CH}_{\text{Ar}}}$), 128.2 ($\underline{\text{CH}_{\text{Ar}}}$), 127.9 (2C, $2\times \underline{\text{CH}_{\text{Ar}}}$), 109.2 (tdd, *J* 253, 34, 31 Hz, $\underline{\text{CF}_2\text{H}}$), 73.9 ($\underline{\text{CH}_2\text{Ph}}$), 71.4 ($\underline{\text{CH}_2\text{OBn}}$), 71.1 (dd, *J* 26, 22 Hz, $\underline{\text{CHCF}_2}$), 67.7 ($\underline{\text{CHCH}_2}$); **¹⁹F NMR** (282 MHz, CDCl₃) δ (ppm) -131.0 (1F, m, *J* 269 Hz can be observed), -132.3 (1F, dd, *J* 270, 8 Hz), -137.6 (1F, ddd, *J* 300, 53, 10 Hz), -141.9 (1F, ddd, *J* 300, 54, 10 Hz). **ES⁺MS**: *m/z* 281.2 [*M* - H]⁺; **HRMS** (ES⁺): for C₁₂H₁₃F₄O₃⁺ [*M* - H]⁺; Calcd.281.0806; Found 281.0803.

Data for 4.26: *R_f* 0.32 (petrol ether/EtOAc 70:30); [α]_D -15.1 (c 0.5, CHCl₃, 24 °C); **IR** (neat) 3425 (w, br.), 2933 (w), 1727 (m), 1167 (m), 1101 (s) cm⁻¹; **¹H NMR** (400 MHz, CDCl₃) δ (ppm) 8.10 (1H, s, $\underline{\text{CHO}}$), 7.28–7.44 (5H, m, *H_{Ar}*), 6.05 (1H, dddd, *J* 54.1, 52.5, 9.6, 1.5 Hz, $\underline{\text{CF}_2\text{H}}$), 5.38 (1H, q, *J* 3.5 Hz, $\underline{\text{CHCH}_2}$), 4.61 (1H, d, *J* 11.6 Hz, $\underline{\text{CHHPh}}$), 4.57 (1H, d, *J* 12.1 Hz, $\underline{\text{CHHPh}}$), 4.26–4.44 (1H, m, $\underline{\text{CHOH}}$), 4.09 (1H, d, *J* 7.6 Hz, $\underline{\text{OH}}$), 4.03 (1H, dd, *J* 11.1, 3.5 Hz, $\underline{\text{CHHOBn}}$), 3.85 (1H, dd, *J* 11.1, 3.0 Hz, $\underline{\text{CHHOBn}}$); **¹³C NMR** (101 MHz, CDCl₃) δ (ppm) 159.7 ($\underline{\text{CHO}}$), 136.4 (*C_{Ar}*), 128.7 ($\underline{\text{CH}_{\text{Ar}}} \times 2$), 128.4 ($\underline{\text{CH}_{\text{Ar}}}$), 128.0 ($\underline{\text{CH}_{\text{Ar}}} \times 2$), 74.1 ($\underline{\text{CH}_2\text{Ph}}$), 70.0 ($\underline{\text{CH}_2\text{OBn}}$), 70.1 (dd, *J* 28, 23 Hz, $\underline{\text{CHOH}}$), 68.4 ($\underline{\text{CHCH}_2}$); **¹⁹F NMR** (282 MHz, CDCl₃) δ (ppm) -131.0 (1F, d, *J* 266 Hz, $\underline{\text{CF}_2\text{CH}}$), -132.3 (1F, ddd, *J* 271, 17, 9 Hz, $\underline{\text{CF}_2\text{CH}}$), -136.5 (1F, ddd, *J* 301, 52, 9 Hz, $\underline{\text{CF}_2\text{H}}$), -145.1 (1F, ddt, *J* 301, 52, 9 Hz, $\underline{\text{CF}_2\text{H}}$); **HRMS** (ES⁺) for C₁₃H₁₄F₄O₄Na⁺ [*M* + Na]⁺ calcd 333.0717, found 333.0717.

Data for 4.27: [α]_D +4.63 (c 0.27, CHCl₃, 24 °C); **IR** (neat) 3420 (w, br.), 2873 (w), 1099 (s), 1065 (s) cm⁻¹; **¹H NMR** (400 MHz, CDCl₃) δ (ppm) 7.31–7.42 (5H, m, *H_{Ar}*), 6.06 (1H, ddd, *J* 53.6, 52.5, 10.6 Hz, $\underline{\text{CF}_2\text{H}}$), 4.63 (2H, s, $\underline{\text{CHHPh}}$, $\underline{\text{CHHPh}}$), 4.34–4.46 (2H, m, $\underline{\text{CHBr}}$, $\underline{\text{CHOH}}$), 4.31 (1H, d, *J* 7.6 Hz, $\underline{\text{OH}}$), 4.24 (1H, dd, *J* 11.1, 3.5 Hz, $\underline{\text{CHHOBn}}$), 3.95 (1H, dd, *J* 11.1, 3.5 Hz, $\underline{\text{CHHOBn}}$); **¹³C NMR** (101 MHz, CDCl₃) δ (ppm) 136.4 (*C_{Ar}*), 128.7 ($\underline{\text{CH}_{\text{Ar}}} \times 2$), 128.4 ($\underline{\text{CH}_{\text{Ar}}}$), 127.9 ($\underline{\text{CH}_{\text{Ar}}} \times 2$), 74.1 ($\underline{\text{CH}_2\text{Ph}}$), 73.5 (dd, *J* 26, 20 Hz, $\underline{\text{CHOH}}$), 73.1 ($\underline{\text{CH}_2\text{OBn}}$), 44.8 ($\underline{\text{CHBr}}$); **¹⁹F NMR** (282 MHz, CDCl₃) δ (ppm) -130.5 (1F, app. dd, *J* 267, 9 Hz, $\underline{\text{CF}_2\text{CH}}$), -132.2 (1F, ddd, *J* 262, 21, 9 Hz, $\underline{\text{CF}_2\text{CH}}$), -136.2 (1F, dd, *J* 301, 52 Hz, $\underline{\text{CF}_2\text{H}}$), -145.3 (1F, ddt, *J* 301, 56, 9 Hz, $\underline{\text{CF}_2\text{H}}$); **CI-MS**: *m/z* 344.1 [⁷⁹Br*M*]⁺; **HRMS** (ES⁺) for C₁₂H₁₃BrF₄O₂Na⁺ [*M* + Na]⁺ calcd 366.9927, found 366.9932.

8.5.13 (3*R*,4*R*)-3,5-Dibenzyloxy-1-bromo-1,1,2,2-tetrafluoropentan-4-ol (**1.54**)



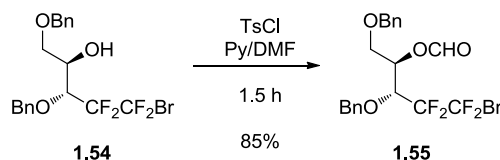
Diol **1.53** (1.88 g, 5.19 mmol) was dissolved in DMF (200 mL) and cooled to 0 °C. NaH (60% in mineral oil, 208 mg, 5.19 mmol) was added and stirring continued at 0 °C for 1 h. BnBr (617 μ L, 5.19 mmol) was added and stirring continued at 0 °C to r.t. for 20 h. aq. NH₄Cl (sat., 25 mL) was added and the resultant mixture stirred at r.t. for 30 min. Extraction was carried out into EtOAc (4 \times 40 mL). The combined organic phase was washed with brine (2 \times 130 mL), dried (MgSO₄), filtered and concentrated to give a yellow oil. Column chromatography (petrol ether/EtOAc 90:10 then 70:30) gave alcohol **1.51** as a colourless oil (1.53 g, 65%), tris-benzyl ether **4.30** as a colourless oil (288 mg, 10%) and starting diol **1.50** as a colourless oil (394 mg, 21%).

Data for 1.54: [α]_D +21.7 (c 0.3, CHCl₃, 26 °C); **R_f** 0.20 (petrol ether/EtOAc 90:10); **¹H NMR** (400 MHz, CDCl₃) δ (ppm) 7.27–7.44 (10H, m), 4.78 (1H, d, *J* 11.1 Hz, CHHPh), 4.74 (1H, d, *J* 11.1 Hz, CHHPh), 4.60 (1H, d, *J* 12.1 Hz, CHHPh'), 4.55 (1H, d, *J* 11.6 Hz, CHHPh'), 4.22–4.35 (2H, m, CHCH₂, CHCF₂), 3.71–3.80 (2H, m, CHHOBn, CHHOBn), 2.72 (1H, d, *J* 4.5 Hz, OH); **¹³C NMR** (101 MHz, CDCl₃) δ (ppm) 137.5 (C_{Ar}), 136.7 (C_{Ar}), 128.5, 128.4, 128.1, 128.1, 128.0, 127.9 (CH_{Ar} \times 8), 77.6 (dd, *J* 26, 22 Hz, CHCF₂), 75.7 (CH₂Ph), 73.6 (CH₂Ph), 69.9 (CH₂OBn), 69.6 (CHCH₂); **¹⁹F NMR** (282 MHz, CDCl₃) δ (ppm) -62.4 (1F, dd, *J* 176, 9 Hz, CFFBr), -63.1 (1F, d, *J* 176 Hz, CFFBr), -110.7 (1F, d, *J* 275 Hz, CFFCH), -119.3 (1F, ddd, *J* 275, 17, 9 Hz, CFFCH).). NMR spectra in agreement with reported data.⁶⁶

Data for (3*R*,4*R*)-3,4,5-Tribenzyloxy-1-bromo-1,1,2,2-tetrafluoropentane (4.31): [α]_D +11.6 (c 0.4, CHCl₃, 25 °C); **R_f** 0.70 (petrol ether/EtOAc 70:30); **¹H NMR** (400 MHz, CDCl₃) δ (ppm) 7.23–7.39 (15H, m, H_{Ar}), 4.77 (1H, d, *J* 10.6 Hz, CHHPh), 4.75 (1H, d, *J* 12.1 Hz, CHHPh), 4.70 (1H, d, *J* 10.6 Hz, CHHPh'), 4.65 (1H, d, *J* 11.6 Hz, CHHPh'), 4.57 (1H, d, *J* 12.1 Hz, CHHPh''), 4.54 (1H, d, *J* 12.1 Hz, CHHPh'''), 4.33 (1H, ddd, *J* 19.2, 6.1, 3.5 Hz, CHCF₂), 4.06 (1H, br. quin, *J* 2.5 Hz, CHCH₂), 3.84 (1H, dd, *J* 11.1, 2.5 Hz, CHHOBn), 3.79 (1H, dd, *J* 10.6, 6.1 Hz, CHHOBn); **¹³C NMR** (101 MHz, CDCl₃) δ (ppm) 138.1 (C_{Ar}), 137.9 (C_{Ar}), 136.7 (C_{Ar}), 128.4 (CH_{Ar} \times 6), 128.2 (CH_{Ar} \times 2), 128.1 (CH_{Ar}), 127.9 (CH_{Ar} \times 2), 127.7 (CH_{Ar}), 127.6 (CH_{Ar} \times 3), 77.8 (CHCH₂), 76.9 (dd, *J* 28, 20 Hz, CHCF₂), 75.2 (CH₂Ph), 73.5 (CH₂Ph), 72.9 (CH₂Ph), 69.8 (CH₂OBn); **¹⁹F NMR**

NMR (282 MHz, CDCl₃) δ (ppm) -62.2 (1F, dd, J 176, 9 Hz, CFFBr), -63.1 (1F, d, J 176 Hz, CFFBr), -110.6 (1F, d, J 275 Hz, CFFCH), -120.6 (1F, ddd, J 275, 17, 9 Hz, CFFCH). NMR spectra in agreement with reported data.⁶⁶

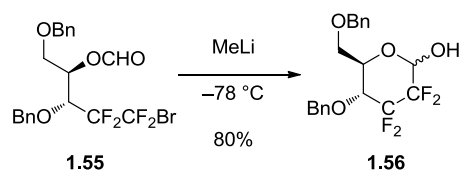
8.5.14 (3*R*,4*R*)-3,5-Dibenzyloxy-1-bromo-1,1,2,2-tetrafluoropentan-4-yl formate (1.55)



TsCl (1.02 g, 3.82 mmol) was dissolved in pyridine (9.8 mL) and cooled to 0 °C. DMF (3.25 mL) was added and the resultant solution stirred at 0 °C for 15 min then r.t. for 30 min. The solution was then cooled to 0 °C and a solution of alcohol **1.54** (1.72 g, 3.82 mmol) in pyridine (3 mL) was added dropwise and washed in with pyridine (0.25 mL). The resultant solution was stirred at r.t. for 1.5 h before being cooled to 0 °C. H₂O (20 mL) was added and extraction carried out into hexane (4 × 20 mL). Combined organic phases were dried (Na₂SO₄), filtered and concentrated to give a pale yellow oil. Column chromatography (petrol ether/EtOAc 95:5 then 80:20) gave formate **1.55** as a colourless oil (1.56 g, 85%) and starting alcohol **1.54** as a colourless oil (165 mg, 10%).

R_f 0.34 (petrol ether/EtOAc 90:10); [α]_D +15.2 (c 0.66, CHCl₃, 25 °C); **¹H NMR** (400 MHz, CDCl₃) δ (ppm) 7.95 (1H, s, CHO), 7.10–7.31 (10H, m, H_{Ar}), 5.46 (1H, dddt, J 6.1, 5.0, 2.9, 0.8 Hz, CHCHO), 4.65 (1H, d, J 10.7 Hz, CHHPh), 4.61 (1H, d, J 10.6 Hz, CHHPh), 4.47 (1H, d, J 11.9 Hz, CHHPh), 4.41 (1H, d, J 11.9 Hz, CHHPh), 4.30 (1H, dt, J 16.9, 5.7 Hz, CHCF₂), 3.76 (1H, dd, J 11.4, 6.2 Hz, CHHOBn), 3.69 (1H, dd, J 11.2, 2.8 Hz, CHHOBn); **¹³C NMR** (101 MHz, CDCl₃) δ (ppm) 159.6 (CHO), 137.4 (C_{Ar}), 136.1 (C_{Ar}), 128.5 (CH_{Ar}), 128.3 (CH_{Ar}), 128.2 (CH_{Ar}), 127.9 (CH_{Ar}), 127.7 (CH_{Ar}), 75.5 (dd, J 28, 22 Hz, CHCF₂), 75.3 (CH₂Ph), 73.4 (CH₂Ph), 70.2 (CHCHO), 67.7 (CH₂OBn); **¹⁹F NMR** (282 MHz, CDCl₃) δ (ppm) -62.7 (dd, J 181, 9 Hz), -63.4 (d, J 181 Hz), -110.7 (d, J 271 Hz), -119.5 (ddd, J 275, 17, 9 Hz). NMR spectra in agreement with reported data.⁶⁶

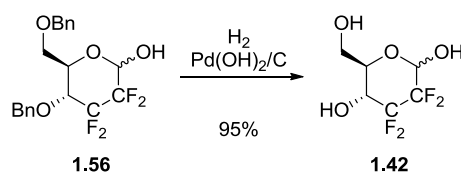
8.5.15 4,6-Di-O-benzyl-2,3-dideoxy-2,2,3,3-tetrafluoroglucopyranose (erythrohexopyranose) (1.56)



Formate **1.55** (1.46 g, 3.23 mmol) was dissolved in dry DCM (20 mL) and filtered through a pad of MgSO_4 directly into the reaction flask, while drying the filtrate with argon. The resultant oil was dried under high vacuum for 16 h before being dissolved in THF (30 mL) and cooled to -78°C . MeLi (1.22 M in Et_2O , 2.65 mL, 3.23 mmol) was added very slowly, dropwise. The resultant solution was stirred at -78°C for 4.5 h. At -78°C , aq. NH_4Cl (sat., 10 mL) was added to the reaction mixture, which was then stirred for 20 min, while allowing to warm to r.t. The mixture was diluted with H_2O (20 mL) then extracted into EtOAc (3×75 mL), dried (MgSO_4), filtered and concentrated to give a white solid. Column chromatography (petrol ether/acetone 90:10 then 75:25) gave pyranose **1.56** as a colourless oil (1.04 g, 80%).

R_f 0.38 (petrol ether/acetone 70:30); $^1\text{H NMR}$ (400 MHz, Acetone- d_6) δ (ppm) 7.24–7.40 (34H, m, H_{Ar}), 6.87 (0.7H, br. s, OH_β), 6.77 (1H, br. s, OH_α), 5.37 (1H, dd, J 8.1, 5.6 Hz, H-1_α), 5.05 (0.7H, d, J 15.7 Hz, H-1_β), 4.86 (1.7H, d, J 11.1 Hz, $\text{CHHPh}_{\alpha+\beta}$), 4.74 (1.7H, d, J 11.1 Hz, $\text{CHHPh}_{\alpha+\beta}$), 4.51–4.64 (3.4H, m, $\text{CHHPh}_{\alpha+\beta}$, $\text{CHHPh}_{\alpha+\beta}$), 4.27 (1H, d, J 10.1 Hz, H-5_α), 4.02–4.17 (1.7H, m, $\text{H-4}_{\alpha+\beta}$), 3.68–3.88 (4.1H, m, H-5_β , $\text{CHHOBn}_{\alpha+\beta}$, $\text{CHHOBn}_{\alpha+\beta}$); $^{13}\text{C NMR}$ (101 MHz, Acetone- d_6) δ (ppm) 139.4 (C_{Ar}), 139.3 (C_{Ar}), 138.5 (C_{Ar}), 138.4 (C_{Ar}), 129.3, 129.2, 129.0, 129.0, 128.9, 128.7, 128.7, 128.5, 128.5 ($\text{CH}_{\text{Ar}} \times 20$), 92.5 (dd, J 26, 20 Hz, C-1_β), 92.2 (dd, J 37, 25 Hz, C-1_α), 76.0 ($\text{CH}_2\text{Ph}_\beta$), 76.0 ($\text{CH}_2\text{Ph}_\alpha$), 74.6–75.2 ($\text{C-4}_{\alpha+\beta}$), 74.0 ($\text{CH}_2\text{Ph}_\alpha$), 74.0 ($\text{CH}_2\text{Ph}_\beta$), 69.8 ($\text{C-5}_{\alpha/\beta}$), 69.7 ($\text{C-5}_{\beta/\alpha}$), 69.1 (C-6_α), 69.0 (C-6_β); $^{19}\text{F NMR}$ (282 MHz, CDCl_3) δ (ppm) -120.3 (1F, m, J 269 Hz observed, F_α), -126.5 (1F, m, J 259 Hz observed, F_α), -128.2 (1F, dtd, J 258, 17, 6 Hz, F_α), -129.7 (0.7F, ddd, J 260, 20, 10 Hz, F_β), -130.8 (0.7F, dt, J 260, 16 Hz, F_β), -134.6 (1F, ddd, J 270, 16, 9 Hz, F_α), -136.9 (0.7F, ddd, J 259, 14, 10 Hz, F_β), -140.2 (1F, dt, J 259, 13 Hz, F_β); $^{19}\text{F (-H) NMR}$ (282 MHz, CDCl_3) δ (ppm) -120.3 (1F, ddd, J 269, 16, 6 Hz, F_α), -126.5 (1F, ddd, J 259, 16, 9 Hz, F_α), -128.2 (1F, ddd, J 258, 16, 6 Hz, F_α), -129.7 (0.7F, dt, J 260, 11 Hz, F_β), -130.8 (0.7F, ddd, J 259, 13, 4 Hz, F_β), -134.6 (1F, ddd, J 269, 16, 9 Hz, F_α), -136.9 (0.7F, ddd, J 259, 15, 10 Hz, F_β), -140.2 (0.7F, ddd, J 259, 12, 4 Hz, F_β). NMR spectra in agreement with reported data.⁶⁶

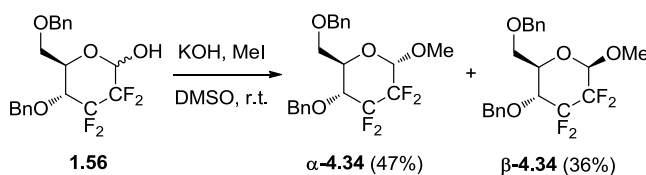
8.5.16 2,3-Dideoxy-2,2,3,3-tetrafluoroglucopyranose (erythrohexopyranose) (**1.24**)



Pyranose **1.56** (470 mg, 1.17 mmol) was dissolved in EtOAc (9 mL) and treated with $\text{Pd(OH)}_2/\text{C}$ (249 mg, 0.47 mmol). The resultant mixture was flushed with H_2 then stirred under H_2 for 3.5 h before being filtered through Celite[®]. The Celite[®] was washed with plenty of EtOAc, which was concentrated to give a colourless oil. Column chromatography (petrol ether/acetone 55:45) followed by HPLC (hexane/acetone 50:50) gave pyranose **1.24** as a colourless oil (244 mg, 95%, α/β 1:1).

R_f 0.05 (petrol ether/acetone 70:30); $^1\text{H NMR}$ (300 MHz, D_2O) δ (ppm) 5.43 (1H, dt, J 8.1, 2.6 Hz, H-1 $_{\alpha}$), 5.16 (1H, app d, J 15.4 Hz, H-1 $_{\beta}$), 3.98–4.19 (3H, m), 3.75–3.96 (4H, m), 3.72 (1H, ddd, J 10.0, 4.8, 1.6 Hz); $^{13}\text{C NMR}$ (101 MHz, D_2O) δ (ppm) 91.3 (dd, J 28, 19 Hz, C-1 $_{\alpha}$), 91.4 (dd, J 37, 26 Hz, C-1 $_{\beta}$), 74.5 (t, J 3 Hz, C-5), 70.4 (t, J 3 Hz, C-5), 66.9 (t, J 19 Hz, C-4), 66.6 (t, J 19 Hz, C-4), 60.4 (C-6), 60.2 (C-6); $^{19}\text{F NMR}$ (282 MHz, D_2O) δ (ppm) -121.2 (1F, d, J 266 Hz), -129.9 (2F, br. s.), -132.4 (2F, t, J 13 Hz), -134.5 (1F, dt, J 266, 13 Hz), -136.8 (1F, dt, J 262, 13 Hz), -139.8 (1F, dd, J 258, 17 Hz). NMR spectra in agreement with reported data.⁶⁶

8.5.17 Methyl 4,6-Di-O-benzyl-2,3-dideoxy-2,2,3,3-tetrafluoroglucopyranoside (erythrohexopyranoside) (**4.34**)



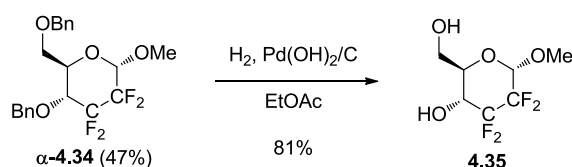
Pyranose **1.56** (227 mg, 0.57 mmol) was dissolved in DMSO and treated with ground KOH (64 mg, 1.14 mmol). The reaction was stirred at r.t. for 20 min, then MeI (142 μL , 2.28 mmol) was added, dropwise. Stirring was continued for 2.5 h, before the reaction was quenched with aq. HCl (1M, 5 mL). Extraction was then carried out into EtOAc (4×7 mL). Combined organic extracts were dried (Na_2SO_4), filtered and concentrated to give an orange oil. Column chromatography (petrol ether/acetone 90:10) followed by HPLC

(toluene/hexane 75:25) gave pyranose **α -4.34** as a colourless oil (110 mg, 47%) and **β -4.34** as a colourless oil (84 mg, 36%).

Data for α -4.34: R_f 0.31 (toluene); $[\alpha]_D$: +122.1 (c 0.4, CHCl_3 , 26 °C); **IR** (neat) 2936 (w), 2870 (w), 1684 (w), 1210 (m), 1117 (s), 1064 (s) cm^{-1} ; **^1H NMR** (400 MHz, CDCl_3) δ (ppm) 7.15–7.43 (10H, m), 4.85 (1H, m, H-1), 4.85 (1H, d, J 11.1 Hz, CHHPh), 4.64 (1H, d, J 12.1 Hz, CHHPh), 4.58 (1H, d, J 11.1 Hz, CHHPh), 4.51 (1H, d, J 12.1 Hz, CHHPh), 4.00–4.09 (2H, m, H-4, H-5), 3.78 (1H, dd, J 10.6, 3.0 Hz, H-6), 3.70 (1H, d, J 11.1 Hz, H-6'), 3.47 (3H, s, CH_3); **^{13}C NMR** (101 MHz, CDCl_3) δ (ppm) 137.6 (C_{Ar}), 136.8 (C_{Ar}), 128.4, 128.1, 128.0, 127.8, 127.8 ($\text{CH}_{\text{Ar}} \times 10$), 97.9 (dd, J 35, 25 Hz, C-1), 75.2 (CH_2Ph), 73.6 (CH_2Ph), 73.3 (t, J 18 Hz, C-4), 69.0 (d, J 6 Hz, C-5), 67.6 (C-6), 56.0 (CH_3); **^{19}F NMR** (282 MHz, CDCl_3) δ (ppm) -119.0 (1F, ddt, J 272, 15, 8, Hz), -126.6 (1F, d, J 260 Hz), -128.7 (1F, d, J 260 Hz), -134.9 (1F, ddd, J 272, 16, 9 Hz); **^{19}F (-H) NMR** (282 MHz, CDCl_3) δ (ppm) -119.0 (1F, ddd, J 272, 16, 7 Hz), -126.6 (1F, ddd, J 256, 16, 9 Hz), -128.7 (1F, ddd, J 257, 15, 7 Hz), -134.9 (1F, ddd, J 272, 16, 9 Hz); **HRMS** (ES+) for $\text{C}_{21}\text{H}_{22}\text{F}_4\text{O}_4\text{Na}^+$ $[\text{M} + \text{Na}]^+$ calcd 437.1346, found 437.1352.

Data for β -4.34: R_f 0.23 (toluene); $[\alpha]_D$: +27.4 (c 0.8, CHCl_3 , 26 °C); **IR** (neat) 2940 (w), 2872 (w), 1108 (s), 1065 (s) cm^{-1} ; **^1H NMR** (400 MHz, CDCl_3) δ (ppm) 7.16–7.44 (10H, m), 4.87 (1H, d, J 10.6 Hz, CHHPh), 4.66 (1H, d, J 12.1 Hz, CHHPh), 4.61 (1H, d, J 10.6 Hz, CHHPh), 4.58–4.62 (1H, m, H-1), 4.55 (1H, d, J 12.1 Hz, CHHPh), 4.05 (1H, app td, J 12.1, 10.6 Hz, H-4), 3.73–3.80 (2H, m, H-6, H-6'), 3.67–3.73 (1H, m, H-5), 3.66 (3H, s, CH_3); **^{13}C NMR** (101 MHz, CDCl_3) δ (ppm) 137.7 (C_{Ar}), 136.6 (C_{Ar}), 128.5, 128.4, 128.2, 128.2, 127.8 ($\text{CH}_{\text{Ar}} \times 10$), 97.9 (t, J 22 Hz, C-1), 75.3 (CH_2Ph), 73.6 (CH_2Ph), 73.7 (t, J 18 Hz, C-4), 73.2 (t, J 4 Hz, C-5), 67.7 (C-6), 58.0 (CH_3); **^{19}F NMR** (282 MHz, CDCl_3) δ (ppm) -130.5–130.3 (2F, m), -138.0–137.8 (2F, m); **ES⁺MS**: 437.2 $[\text{M} + \text{Na}]^+$, 453.2 $[\text{M} + \text{K}]^+$; **HRMS** (ES+) for $\text{C}_{21}\text{H}_{22}\text{F}_4\text{O}_4\text{Na}^+$ $[\text{M} + \text{Na}]^+$ calcd 437.1346, found 437.1349, for $\text{C}_{21}\text{H}_{26}\text{F}_4\text{O}_4\text{N}^+$ $[\text{M} + \text{NH}_4]^+$ calcd 432.1792, found 432.1797.

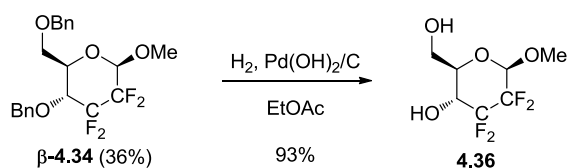
8.5.18 Methyl 2,3-dideoxy-2,2,3,3-tetrafluoro- α -glucopyranoside (erythrohexopyranoside) (4.35)



Pyranose ***α*-4.34** (96 mg, 0.23 mmol) was dissolved in EtOAc (1.8 mL) and treated with Pd(OH)₂/C (49 mg, 92 μmol). The resultant mixture was flushed with H₂ then stirred under H₂ for 22 h before being filtered through Celite[®]. The Celite[®] was washed with plenty of EtOAc, which was concentrated to give a colourless oil. Column chromatography (petrol ether/acetone 70:30) gave pyranose **4.35** as a colourless oil (44 mg, 81%).

R_f 0.14 (petrol ether/acetone 70:30); [**α**]_D +126.0 (c 0.4, CH₃OH, 27 °C); **¹H NMR** (400 MHz, Acetone-*d*₆) δ (ppm) 5.35 (1H, d, *J* 7.1 Hz, OH-4), 4.97 (1H, dd, *J* 8.3, 3.8 Hz, H-1), 4.04 (1H, m, H-4), 3.98 (1H, t, *J* 5.6 Hz, OH-6), 3.75–3.93 (3H, m, H-5, H-6, H-6'), 3.47 (3H, s, CH₃); **¹³C NMR** (101 MHz, Acetone-*d*₆) δ (ppm) 98.5 (dd, *J* 37, 26 Hz, C-1), 72.0 (d, *J* 3 Hz, C-5), 67.6 (t, *J* 19 Hz, C-4), 61.2 (C-6), 56.0 (CH₃); **¹⁹F NMR** (282 MHz, Acetone-*d*₆) δ (ppm) -118.9 (1F, dtd, *J* 269, 9, 4 Hz), -130.3–129.8 (2F, m), -134.5 (1F, dt, *J* 270, 13 Hz); **ES⁺MS**: 233.2 [M – H][–]; **HRMS** (ES⁺) for C₇H₉F₄O₄[–] [M – H][–] calcd 233.0442, found 233.0441.

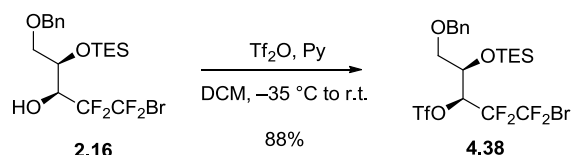
8.5.19 Methyl 2,3-dideoxy-2,2,3,3-tetrafluoro-*β*-glucopyranoside (erythrohexopyranoside) (**4.36**)



Pyranose ***β*-4.34** (76 mg, 0.18 mmol) was dissolved in EtOAc (1.5 mL) and treated with Pd(OH)₂/C (38 mg, 72 μmol). The resultant mixture was flushed with H₂ then stirred under H₂ for 3.5 h before being filtered through Celite[®]. The Celite[®] was washed with plenty of EtOAc, which was concentrated to give a colourless oil. Column chromatography (petrol ether/acetone 70:30) gave pyranose **4.36** as a colourless oil (40 mg, 93%).

R_f 0.10 (petrol ether/acetone 70:30); [**α**]_D –21.2 (c 0.5, CH₃OH, 26 °C); **IR** (neat) 3337 (w, br.), 2949 (w), 1232 (m), 1079 (s), 1037 (s), 1007 (s), 960 (s); **¹H NMR** (400 MHz, Acetone-*d*₆) δ (ppm) 5.44 (1H, m, OH-4), 4.80 (1H, m, H-1), 3.96–4.12 (2H, m, OH-6, H-4), 3.91 (1H, m, H-6), 3.80 (1H, m, H-6'), 3.54–3.64 (4H, m, CH₃, H-5); **¹³C NMR** (101 MHz, Acetone-*d*₆) δ (ppm) 98.6 (td, *J* 22, 3 Hz, C-1), 75.7 (d, *J* 4 Hz, C-5), 67.9 (t, *J* 19 Hz, C-5), 61.3 (C-6), 57.9 (CH₃); **¹⁹F NMR** (282 MHz, Acetone) δ (ppm) -131.9 (1F, ddd, *J* 252, 15, 10 Hz), -132.9 (1F, ddd, *J* 254, 19, 10 Hz), -138.7–136.5 (2F, m); **ES⁺MS**: 233.2 [M – H][–]; **HRMS** (ES⁺) for C₇H₉F₄O₄[–] [M – H][–] calcd 233.0442, found 233.0441.

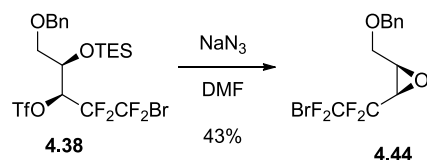
8.5.20 (3*S*,4*R*)-5-Benzyloxy-1-bromo-4-(triethylsilyloxy)-1,1,2,2-tetrafluoropentan-3-yl trifluoromethanesulfonate (**4.38**)



Alcohol **2.16** (1.25 g, 2.63 mmol) was dissolved in DCM (8 mL) and treated with pyridine (425 μ L, 5.26 mmol). The reaction mixture was cooled to -35°C before adding TiF_2O (665 μ L, 3.95 mmol), dropwise. Stirring was continued at approximately -25°C for 1.5 h then stirred at r.t. for 18 h. H_2O (15 mL) and NaHCO_3 (sat., aq, 15 mL) were added to the reaction mixture, which was extracted into DCM (2×30 mL). Organic phase was dried (Na_2SO_4), filtered and concentrated to give an orange oil. Column chromatography (petrol ether/ EtOAc 95:5) gave triflate **4.38** as a colourless oil (1.41 g, 88%).

R_f 0.31 (petrol ether/EtOAc 95:5); $[\alpha]_D^{+25} +5.1$ (c 0.5, CHCl_3 , 23.5°C) **IR** (neat) 2959 (w), 2915 (w), 2880 (w), 2361 (w), 1417 (m), 1216(s), 1139 (s), 1093 (m) cm^{-1} ; **^1H NMR** (400 MHz, CDCl_3) δ (ppm) 7.28–7.46 (5H, m, H_{Ar}), 5.55 (1H, td, J 10.9, 2.4 Hz, CHCF_2), 4.64 (1H, d, J 11.6 Hz, CHHPh), 4.49 (1H, d, J 11.6 Hz, CHHPh), 4.33–4.41 (1H, m, CHCH_2), 3.49–3.63 (2H, m, CH_2OBn), 0.95 (9H, t, J 7.9 Hz, $\text{CH}_3 \times 3$), 0.62 (2H, q, J 7.8 Hz, $\text{CH}_2\text{CH}_3 \times 3$); **^{13}C NMR** (101 MHz, CDCl_3) δ (ppm) 137.2 (C_{Ar}), 128.5 ($\text{CH}_{\text{Ar}} \times 2$), 127.9 (CH_{Ar}), 127.8 ($\text{CH}_{\text{Ar}} \times 2$), 78.3 (t, J 25 Hz, CHCF_2), 73.5 (CH_2Ph), 69.3 (CH_2OBn), 68.1 (CHCH_2), 6.5 ($\text{CH}_3 \times 3$), 4.8 ($\text{CH}_2\text{CH}_3 \times 3$); **^{19}F NMR** (282 MHz, CDCl_3) δ (ppm) -64.14 (1F, s), -73.96 (3F, s, CF_3), -112.55 (1F, d, J 275.1 Hz), -114.23 (1F, d, J 275.1 Hz); **ES $^+$ MS**: m/z 607.5 $[\text{M} + \text{H}]^+$; **HRMS** (ESI $^+$) for $\text{C}_{19}\text{H}_{26}\text{BrF}_7\text{O}_5\text{SSiNa}^+$ ($\text{M} + \text{Na}$) $^+$ calcd. 629.0234; found 629.0246.

8.5.21 (2*R*,3*R*)-2-((Benzyloxy)methyl)-3-(2-bromo-1,1,2,2-tetrafluoroethyl)oxirane (**4.44**)

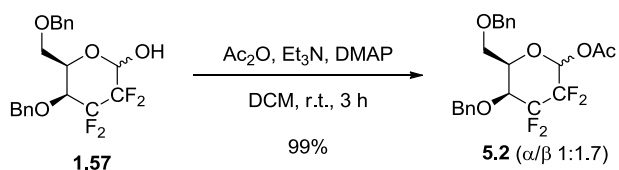


Triflate **4.38** (218 mg, 0.36 mmol) was dissolved in DMF (1 mL) and cooled to 0°C . NaN_3 (107 mg, 1.65 mmol) was added portionwise, followed by stirring at 0°C to r.t. for 19 h. The reaction mixture was then quenched with H_2O (1 mL) and extracted into DCM (10 mL), which was washed with brine (10 mL), dried (Na_2SO_4), filtered and concentrated to give a yellow oil. Column chromatography (petrol ether/EtOAc 90:10) gave epoxide **4.44** as a colourless oil (53 mg, 43%).

R_f 0.41 (hexane/EtOAc 85:15); [α]_D *low e.e. material*; **IR** (neat) 3033 (w), 2863 (w), 2361 (w), 1455 (m), 1256 (m), 1140 (s), 1084 (s), 917 (s) cm⁻¹; **¹H NMR** (400 MHz, CDCl₃) δ (ppm) 7.30–7.41 (5H, m, H_{Ar}), 4.68 (1H, d, *J* 11.7 Hz, CHHPh), 4.57 (1H, d, *J* 11.6 Hz, CHHPh), 3.95 (1H, dd, *J* 11.9, 2.5 Hz, CHHOBN), 3.69 (1H, ddt, *J* 12.1, 6.9, 2.3 Hz, CHHOBN), 3.52 (1H, ddt, *J* 10.5, 4.2, 1.0, Hz, CHCH₂) 3.47 (1H, m, CHCH₂); **¹³C NMR** (101 MHz, CDCl₃) δ (ppm) 137.4 (C_{Ar}), 128.5 (CH_{Ar} × 2), 127.9 (CH_{Ar}), 127.8 (CH_{Ar} × 2), 73.4 (CH₂Ph), 67.0 (t, *J* 4 Hz, CH₂OBn), 56.0 (CHCH₂), 50.4 (dd, *J* 31, 25 Hz, CHCF₂); **¹⁹F NMR** (282 MHz, CDCl₃) δ (ppm) -66.52 (2F, s), -114.13 (1F, dd, *J* 262.2, 12.9 Hz), -116.74 (1F, d, *J* 262.2 Hz); **CIMS**: *m/z* 91.0 (46%), 108.1 ([PhCH₂O⁻ + H⁺] 66%), 163.0 (20%), 343.0 ([⁷⁹BrM + H]⁺ 25%), 345.0 ([⁸¹BrM + H]⁺ 20%), 360.1 ([⁷⁹BrM + NH₄]⁺, 100%), 362.1 ([⁸¹BrM + NH₄]⁺ 49%); **HRMS** (EI⁺) for C₁₂H₁₁BrF₄O₂ [M+•] calcd.341.9879; Found 341.9876.

8.6 Towards the Glycosylation of Tetrafluoro Pyranose 1.57

8.6.1 Acetyl 4,6-di-*O*-benzyl-2,3-dideoxy-2,2,3,3-tetrafluorogalactopyranoside (threohexopyranoside) (5.2)

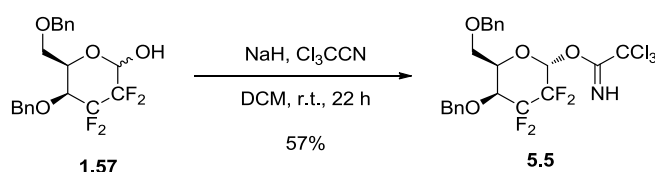


Pyranose **1.57** (1.94 g, 4.84 mmol) was dissolved in DCM (15 mL) and treated with Et₃N (1.01 mL, 7.26 mmol) then DMAP (119 mg, 0.97 mmol). Ac₂O (686 μ L, 7.26 mmol) was then added, dropwise and stirring continued at r.t. for 3 h. The solution was then concentrated to remove DCM before being re-dissolved in EtOAc. The EtOAc was filtered through celite then concentrated to give a red oil. Column chromatography (cyclohexane/EtOAc 85:15) gave pyranosyl acetate **5.2** as a colourless oil (2.11 g, 99%).

R_f (cyclohexane/EtOAc 70:30): 0.44; **IR** (neat) 3033 (w), 2926 (w), 2879 (w), 1773 (s), 1117 (s), 1097 (s) cm⁻¹; **¹H NMR** (β/α 1:0.57 sample) (400 MHz, CDCl₃) δ (ppm) 7.27–7.50 (16H, m, H_{Ar}), 6.33 (0.57H, dd, *J* 8.7, 5.8 Hz, H-1 _{α}), 5.90 (1H, dd, *J* 15.2, 3.6 Hz, H-1 _{β}), 4.94 (0.57H, d, *J* 11.2 Hz, CHHPh _{α}), 4.94 (1H, d, *J* 11.4 Hz, CHHPh _{β}), 4.61 (1H, d, *J* 11.4 Hz, CHHPh _{β}), 4.59 (0.57H, d, *J* 11.2 Hz, CHHPh _{α}), 4.47–4.53 (1.57H, m, CHHPh _{$\alpha+\beta$}), 4.41–4.47 (1.57H, m, CHHPh _{$\alpha+\beta$}), 4.38–4.43 (0.57H, m, H-5 _{α}), 4.07–4.15 (1H, m, H-5 _{β}), 4.00–4.08 (1.57H, m, H-4 _{$\alpha+\beta$}), 3.59–3.72 (3.14H, m, H-6 _{$\alpha+\beta$}), 2.21 (3H, s, CH₃ _{β}), 2.18 (1.71H, s, CH₃ _{α}); **¹³C NMR** (101 MHz, CDCl₃) δ (ppm) 168.2 (C=O), 168.0 (C=O), 137.4 (C_{Ar}), 137.3 (C_{Ar}), 136.6 (C_{Ar}), 136.6 (C_{Ar}), 128.4, 128.4, 128.3, 128.1, 127.9, 127.8

(CH_{Ar} × 20) 89.2 (dd, *J* 40, 28 Hz, C-1_α), 88.7 (ddd, *J* 29, 18, 4 Hz, C-1_β), 74.9–75.3 (CH₂Ph_{α+β}), 74.8 (dd, *J* 29, 18 Hz, C-4_{α+β}), 73.6 (CH₂Ph_α), 73.5 (CH₂Ph_β), 73.5 (d, *J* 6 Hz, C-5_β), 70.5 (d, *J* 6 Hz, C-5_α), 66.9 (C-6_α), 66.5 (C-6_β), 20.6 (CH_{3α}), 20.5 (CH_{3β}); ¹⁹F NMR (282 MHz, CDCl₃) δ (ppm) -117.4–-116.1 (0.6F, m, F_α), -117.4 (1F, d, *J* 275 Hz, F_β), -118.3 (0.6F, ddt, *J* 275, 17, 9 Hz, F_α), -130.0 (0.6F, d, *J* 266 Hz, F_α), -131.3 (1F, d, *J* 275 Hz, F_β), -134.9 – -133.4 (0.6F, m, F_α), -134.7 (1F, m, *J* 267 Hz can be observed, F_β), -136.6 (1F, d, *J* 258 Hz, F_β); **ES⁺MS**: *m/z* 465.2 [M + Na]⁺; **HRMS** (ES⁺) for C₂₂H₂₂F₄O₅Na [M + Na]⁺ calcd 465.1296, found 465.1293.

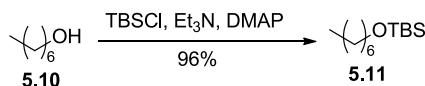
8.6.2 2,2,2-Trichloroethanimidoyl 4,6-Di-*O*-benzyl-2,3-dideoxy-2,2,3,3-tetrafluoro- α -galactopyranoside (threohexopyranoside) (**5.5**)



NaH (60% in mineral oil, 17 mg, 0.43 mmol) was suspended in DCM (0.6 mL) and cooled to 0 °C. To this was added pyranose **1.57** (173 mg, 0.43 mmol) as a solution in DCM (3.2 mL). The mixture was stirred at r.t. for 10 min, before dropwise addition of Cl₃CCN (0.54 mL, 5.4 mmol). The reaction was stirred at r.t. for 22 h then filtered through Celite[®], which was washed with plenty of DCM and concentrated to give a yellow residue. Column chromatography (petrol ether/acetone 90:10 then 80:20) gave trichloroacetimidate **5.5** as a colourless oil (134 mg, 57%) and pyranose **1.57** as a colourless oil (35 mg, 20%).

R_f 0.5 (cyclohexane/EtOAc 80:20); **IR** (neat) 3344 (w), 2876 (w), 1679 (m), 1158 (s), 1119 (s), 1045 (s), 1001 (s) cm⁻¹; ¹H NMR (400 MHz, CDCl₃) δ (ppm) 8.82 (1H, s, NH), 7.18–7.40 (10H, m, H_{Ar}), 6.51 (1H, dd, *J* 8.1, 6.1 Hz, H-1), 4.93 (1H, d, *J* 11.1 Hz, CHHPh), 4.58 (1H, d, *J* 11.6 Hz, CHHPh), 4.53 (1H, m, H-5), 4.48 (1H, d, *J* 12.1 Hz, CHHPh), 4.42 (1H, d, *J* 12.1 Hz, CHHPh), 4.06 (1H, dd, *J* 11.6, 5.6 Hz, H-4), 3.58–3.71 (2H, m, H-6, H-6'); ¹³C NMR (101 MHz, CDCl₃) δ (ppm) 160.1 (C=N), 137.4 (C_{Ar}), 136.6 (C_{Ar}), 128.5, 128.3, 128.2, 127.9, 127.7 (CH_{Ar}), 92.8 (dd, *J* 41, 28 Hz, C-1), 90.2 (CCl₃), 75.2 (d, *J* 4 Hz, CH₂Ph), 74.9 (dd, *J* 29, 16 Hz, C-4), 73.5 (CH₂Ph), 70.8 (d, *J* 7 Hz, C-5), 66.8 (C-6); ¹⁹F NMR (282 MHz, CDCl₃) δ (ppm) -116.8 (1F, ddtd, *J* 272, 15, 7, 3 Hz), -117.9 (1F, ddt, *J* 274, 16, 9, Hz), -130.0 (1F, dtd, *J* 274, 11, 6 Hz), -134.1 (1F, dddd, *J* 274, 15, 9, 6 Hz); **ES⁺MS**: *m/z* 566.1 [³⁵ClM + Na]⁺; **HRMS** (ES⁺) for C₂₂H₂₀Cl₃F₄NONa⁺ [M + Na]⁺ calcd 566.0286, found 566.0287.

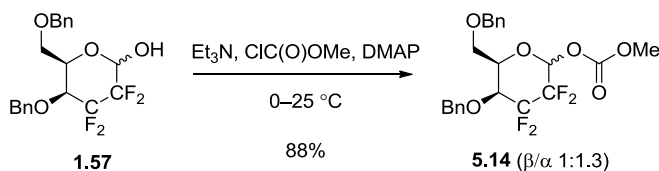
8.6.3 1-*tert*-Butyldimethylsilyloxyheptane (**5.11**)



DMAP (95 mg, 0.78 mmol) was dissolved in DCM (25 mL) and treated with heptan-1-ol (**5.10**) (1 mL, 7.1 mmol) was added to the solution, followed by Et₃N (1.09 mL, 7.8 mmol). A solution of TBDMSCl (1.28 g, 8.5 mmol) in DCM (10 mL) was then added to the reaction mixture, which was stirred at r.t. for 2 h. The reaction mixture was then concentrated before being dissolved in pentane (40 mL) and washed with H₂O (2 × 40 mL). The resultant organic phase was dried (MgSO₄), filtered and concentrated to give a colourless oil, which was filtered through silica. The silica was washed with plenty of pentane, which was concentrated to give silyl ether **5.11** as a colourless oil (1.57 g, 96%);

¹H NMR (300 MHz, CDCl₃) δ (ppm) 3.61 (2H, t, *J* 6.6 Hz, CH₂-1), 1.52 (2H, quin, *J* 6.4 Hz, CH₂-2), 1.29 (8H, br. s., CH₂-3–6), 0.80–1.02 (12H, CH₃-7, 3 × CH₂-10), 0.00 – 0.15 (6H, m, 2 × CH₃-8); ¹³C NMR (75 MHz, CDCl₃) δ (ppm) 63.3 (C-1), 32.9 (C-2), 31.9 (C-5), 29.1 (C-4), 26.0 (C-10), 25.8 (C-3), 22.6 (C-6), 18.4 (C-9), 14.1 (C-7), -5.3 (C-8). NMR spectra in agreement with reported data.¹⁷¹

8.6.4 Methyl carbonoyl 4,6-di-*O*-benzyl-2,3-dideoxy-2,2,3,3-tetrafluorogalactopyranoside (threohexopyranoside) (**5.14**)

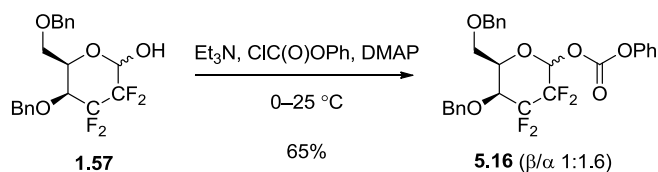


Pyranose **1.57** (100 mg, 0.25 mmol) was dissolved in DCM (0.8 mL) and cooled to 0 °C. Et₃N (70 μL, 0.5 mmol) was added, followed by DMAP (6 mg, 50 μmol). Methyl chloroformate (42 μL, 0.54 mmol) was then added, dropwise. The resultant solution was stirred at 0 °C to r.t. for 1 h before being concentrated to give a white solid, which was suspended in EtOAc and filtered through Celite. The Celite was washed with plenty of EtOAc, which was concentrated to give a colourless oil. Column chromatography (cyclohexane/EtOAc 80:20) gave methyl carbonate **5.14** as a colourless oil (101 mg, 88%, β/α 1:1.3).

R_f 0.5 (cyclohexane/EtOAc 70:30); IR (neat) 3033 (w), 2959 (w), 2876 (w), 1769 (s), 1280 (s), 1125 (s) cm⁻¹; NMR for α-6: ¹H NMR (400 MHz, CDCl₃) δ (ppm) 7.21–7.44 (10H, m), 6.16 (1H, dd, *J* 8.6, 5.7 Hz, H-1), 4.91 (1H, d, *J* 11.2 Hz, CHHPh), 4.56 (1H, d,

J 11.2 Hz, CHHPh), 4.47 (1H, d, J 11.9 Hz, CHHPh), 4.42 (1H, d, J 11.9 Hz, CHHPh), 4.39–4.45 (1 H, m, H-5), 4.03 (1H, q, J 5.3 Hz, H-4), 3.86 (3H, s, CH₃), 3.57–3.67 (2H, m, H-6); ¹³C NMR (101 MHz, CDCl₃) δ (ppm) 153.3 (C=O), 137.4 (C_{Ar}), 136.6 (C_{Ar}), 128.5, 128.3, 128.2, 127.9, 127.8 (CH_{Ar} \times 8), 92.8 (dd, J 41, 28 Hz, C-1), 75.2 (d, J 3 Hz, CH₂Ph), 74.7 (dd, J 31, 19 Hz, H-4), 73.6 (CH₂Ph), 70.6 (d, J 6 Hz, C-5), 66.7 (C-6), 55.7 (CH₃); ¹⁹F NMR (282 MHz, CDCl₃) δ (ppm) -117.5 – -116.2 (1F, m), -118.1 (1F, ddt, J 275, 17, 9, Hz), -130.2 (1F, d, J 275 Hz), -134.0 (1F, m, J 275 Hz can be observed); **NMR for β -6:** ¹H NMR (400 MHz, CDCl₃) δ (ppm) 7.14–7.58 (10H, m, H_{Ar}), 5.75 (1H, dd, J 14.9, 3.4 Hz, H-1), 4.91 (1H, d, J 11.4 Hz, CHHPh), 4.58 (1H, d, J 11.4 Hz, CHHPh), 4.48 (1H, d, J 11.9 Hz, CHHPh), 4.43 (1H, d, J 11.7 Hz, CHHPh), 3.96–4.22 (2H, m, H-4, H-5), 3.88 (3H, s, CH₃), 3.65–3.74 (2H, m, 2 \times H-6); ¹³C NMR (101 MHz, CDCl₃) δ (ppm) 153.5 (C=O), 137.3 (C_{Ar}), 136.6 (C_{Ar}), 128.5, 128.4, 128.2, 128.0, 127.8 (CH_{Ar} \times 8), 92.0 (t, J 23 Hz, C-1), 75.1 (d, J 3 Hz, CH₂Ph), 74.7 (dd, J 28, 18 Hz, C-4), 73.6 (CH₂Ph, C-5), 66.6 (C-6), 55.8 (CH₃); ¹⁹F NMR (282 MHz, CDCl₃) δ (ppm) -117.7 (1F, d, J 275 Hz), -131.2 (1F, d, J 275 Hz), -134.9 (1F, dt, J 258, 13 Hz), -136.3 (1F, d, J 258 Hz); **ES⁺MS:** m/z 481.2 [M + Na]⁺; **HRMS** (ES⁺) for C₂₂H₂₂F₄O₆Na [M + Na]⁺ calcd 481.1245, found 481.1252.

8.6.5 Phenyl carbonyl 4,6-di-*O*-benzyl-2,3-dideoxy-2,2,3,3-tetrafluorogalactopyranoside (threohexopyranoside) (**5.16**)

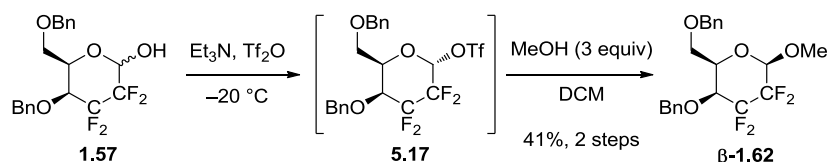


Pyranose **1.57** (100 mg, 0.8 mmol) was dissolved in DCM (0.8 mL) and cooled to 0 °C. Et₃N (70 μ L, 0.5 mmol) was added, followed by DMAP (6 mg, 50 μ mol). Phenyl chloroformate (69 μ L, 0.55 mmol) was then added, dropwise. The resultant solution was stirred at 0 °C to r.t. for 5.5 h before being concentrated to give a white solid, which was suspended in EtOAc and filtered through Celite. The Celite was washed with plenty of EtOAc, which was concentrated to give a pale yellow oil. Column chromatography (cyclohexane/EtOAc 80:20) gave phenyl carbonate **5.16** as a colourless oil (84 mg, 65%).

R_f 0.5 (cyclohexane/EtOAc 70:30); **IR** (neat) 3065 (w), 3033 (w), 2934 (w), 2877 (w), 1781 (s), 1246 (s), 1121 (s) cm⁻¹; ¹H NMR (400 MHz, CDCl₃) δ (ppm) 7.11–7.68 (23.4H, m, H_{Ar}), 6.25 (1H, dd, J 8.5, 5.7 Hz, H-1_α), 5.82 (0.56H, dd, J 14.7, 3.5 Hz, H-1_β), 4.94 (1.56H, d, J 11.4 Hz, CHHPh_{α+β}), 4.60 (0.56H, d, J 11.2 Hz, CHHPh_β), 4.58 (1H, d, J 11.4

Hz, CHHPh_α), 4.40–4.54 (4.12H, m, CHHPh_{α+β}, CHHPh_{α+β}, H-5_α), 4.01–4.17 (2.12H, m, H-5_β, H-4_{α+β}), 3.61–3.75 (3.12H, m, H-6_{α+β}); ¹³C NMR (101 MHz, CDCl₃) δ (ppm) 151.6 (C=O), 151.4 (C=O), 150.7 (C_{Ar}-O × 2), 137.4 (C_{Ar} × 2), 136.5 (C_{Ar} × 2), 129.6, 128.5, 128.3, 128.2, 128.0, 127.8, 126.6, 126.5, 126.3, 120.9, 120.7, (CH_{Ar} × 30) 92.8–93.8 (m, C-1_{α+β}), 75.2 (CH₂Ph), 74.3–75.0 (m, C-4_{α+β}), 73.7 (CH₂Ph + C-5_β), 71.0 (d, *J* 6 Hz, C-5_α), 66.9 (C-6), 66.5 (C-6); ¹⁹F NMR (282 MHz, CDCl₃) δ (ppm) -117.3 – -115.8 (m), -118.3 – -117.2 (m), -117.9 (ddt, *J* 279, 17, 9, Hz), -130.1 (d, *J* 275 Hz), -131.1 (d, *J* 271 Hz), -133.9 (d, *J* 279 Hz), -134.6 (7 F, dt, *J* 262, 13 Hz), -136.0 (d, *J* 262 Hz); **ES⁺MS**: *m/z* 543.4 [M + Na]⁺; **HRMS** (ES⁺) for C₂₇H₂₄F₄O₆Na [M + Na]⁺ calcd 543.1401, found 543.1407.

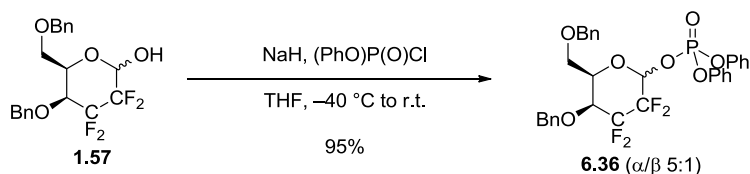
8.6.6 Glycosylation via Glycosyl Triflate 5.17



Pyranose **1.57** (500 mg, 1.25 mmol) was dissolved in DCM (20 mL) and cooled to $-20\text{ }^{\circ}\text{C}$. Et₃N was then added and stirring continued for 10 min. Tf₂O (1M in DCM, 2.5 mL) was added, followed by stirring at $-20\text{ }^{\circ}\text{C}$ for 4 h. The reaction was then allowed to warm to r.t. before being filtered through a pad of silica to give crude triflate as an orange oil. A sample of this oil (21%) was carried forward without further purification. The crude triflate ($\leq 140\text{ mg}$, $\leq 0.26\text{ mmol}$) was dissolved in DCM (4.4 mL) and treated with MeOH (35 μL , 0.89 mmol). The reaction was stirred at r.t. for 3 d then concentrated to give a red oil. Column chromatography (petrol ether/acetone 80:20 then 60:40) gave β -methyl glycoside **1.62** as a colourless oil (45 mg, 41% overall).

8.7 Synthesis of Tetrafluoro Galactosyl Phosphates

8.7.1 Diphenyl 4,6-di-*O*-benzyl-2,3-dideoxy-2,2,3,3-tetrafluorogalactopyranosyl (threohexopyranosyl) phosphate (6.36)



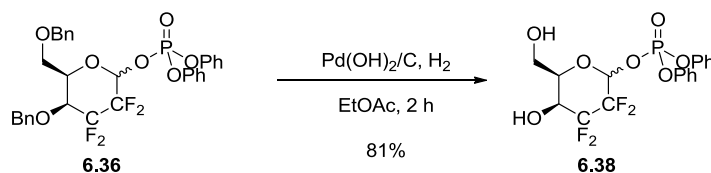
Pyranose **1.57** (1.5 g, 3.7 mmol) was dissolved in THF (24 mL) and cooled to $-40\text{ }^{\circ}\text{C}$. NaH (60% in mineral oil, 300 mg, 7.4 mmol) was added and stirring at $-40\text{ }^{\circ}\text{C}$ continued

for 10 min. (PhO)₂P(O)Cl (1.16 mL, 5.6 mmol) was added, dropwise. Stirring was continued for 24 h at -40 °C to r.t. before adding aq. NH₄Cl (sat., 50 mL). Stirring was continued for 30 min at r.t. before extraction into EtOAc (3 × 50 mL). The combined organic extracts were washed with brine (100 mL), dried (MgSO₄), filtered and concentrated to give a cloudy oil. Column chromatography (petrol ether/acetone 80:20) gave pyranosyl phosphates **6.36** as a colourless oil (2.22 g, 95%, α/β (5:1)).

Data for anomeric mixture (α,β-6.36): R_f 0.38 (petrol ether/acetone 80:20); **IR** (neat) 3065 (w), 3032 (w), 2921 (w), 2876 (w), 1590 (w), 1489 (m), 1298 (m), 1187(s), 1163 (m), 1128 (s), 1011 (m) 954 (s) cm⁻¹; **ES⁺MS**: m/z 655.3 [M + Na]⁺; **HRMS** (ES⁺) for C₃₂H₂₉F₄O₇PNa⁺ [M + Na]⁺ calcd 655.1479, found 655.1477. **Data for α-6.36** (isolated for analytical purposes): [α]_D +12.9 (c 0.5, CHCl₃, 27 °C) **¹H NMR** (400 MHz, CDCl₃) δ (ppm) 7.03–7.54 (20H, m, H_{Ar}), 5.95 (1H, app q, *J* 6.9 Hz, H-1), 4.87 (1H, d, *J* 11.1 Hz, CHHPh), 4.53 (1H, d, *J* 11.2 Hz, CHHPh), 4.38–4.32 (3H, m, CHHPh × 2, H-5), 4.01 (1H, m, H-4), 3.56 (1H, t, *J* 8.6 Hz, H-6), 3.30 (1H, ddd, *J* 8.7, 5.6, 1.6 Hz, H-6); **¹³C NMR** (101 MHz, CDCl₃) δ (ppm) 150.1 (d, *J* 7 Hz, C_{Ar}OP), 150.0 (d, *J* 7 Hz, C_{Ar}OP), 137.3 (C_{Ar}CH₂), 136.6 (C_{Ar}CH₂), 129.9 (CH_{Ar} × 2), 129.8 (CH_{Ar} × 2), 128.4 (CH_{Ar} × 6), 128.2 (CH_{Ar} × 2), 127.9 (CH_{Ar}), 127.8 (CH_{Ar}), 125.8 (CH_{Ar}), 125.7 (CH_{Ar}), 120.2 (d, *J* 4 Hz, CH_{Ar}OP × 2), 119.9 (d, *J* 6 Hz, CH_{Ar}OP × 2), 94.5 (dd, *J* 42, 29 Hz, C-1), 75.2 (d, *J* 2.9 Hz, CH₂Ph), 74.6 (dd, *J* 29, 19 Hz, C-4), 73.5 (CH₂Ph), 70.0 (d, *J* 6 Hz, C-5), 66.3 (C-6); **¹⁹F NMR** (282 MHz, CDCl₃) -116.31 (1F, ddt, *J* 275, 15, 8 Hz), -118.61 (1F, ddt, *J* 274, 17, 8 Hz), -129.57 (1F, dddt, *J* 275, 17, 12, 5 Hz), -133.08 (1F, dddd, *J* 274, 15, 10, 5 Hz); **³¹P NMR** (121 MHz, CDCl₃) δ (ppm) -13.59 (1P, d, *J* 6.7 Hz).

NMR for β-6.36 (synthesised as the racemate): **¹H NMR** (400 MHz, CDCl₃) δ (ppm) 7.13–7.51 (20H, m, H_{Ar}), 5.57 (1H, m, H-1), 4.90 (1H, d, *J* 11.4 Hz, CHHPh), 4.57 (1H, d, *J* 11.4 Hz, CHHPh), 4.43 (1H, d, *J* 12.1 Hz, CHHPh), 4.40 (1H, d, *J* 11.7 Hz, CHHPh), 3.93–4.09 (2H, m, H-4, H-5), 3.59 (1H, m, H-6), 3.50 (1H, m, H-6); **¹³C NMR** (101 MHz, CDCl₃) δ (ppm) 150.0 (d, *J* 7 Hz, C_{Ar}OP), 149.9 (d, *J* 7 Hz, C_{Ar}OP), 137.3 (C_{Ar}CH₂), 136.5 (C_{Ar}CH₂), 129.8 (CH_{Ar} × 2), 129.6 (CH_{Ar} × 2), 128.4 (CH_{Ar} × 4), 128.4 (CH_{Ar} × 2), 128.2 (CH_{Ar} × 2), 127.9 (CH_{Ar}), 127.7 (CH_{Ar}), 125.8 (CH_{Ar}), 125.6 (CH_{Ar}), 120.3 (d, *J* 4 Hz, CH_{Ar}OP × 2), 120.2 (d, *J* 4 Hz, CH_{Ar}OP × 2), 93.6 (t, *J* 25 Hz, C-1), 75.1 (d, *J* 2.9 Hz, CH₂Ph), 74.6 (dd, *J* 29, 18 Hz, C-4), 73.49 (CH₂Ph), 73.45 (C-5), 66.3 (C-6); **¹⁹F NMR** (282 MHz, CDCl₃) δ (ppm) -117.26 (1F, d, *J* 275.1 Hz), -130.95 (1F, dt, *J* 275.1, 12.9 Hz), -135.77 (1F, dt, *J* 257.9, 12.9 Hz), -136.75 (1F, d, *J* 266.5 Hz); **³¹P NMR** (121 MHz, CDCl₃) δ (ppm) -12.82 (1P, d, *J* 6.7 Hz)

8.7.2 Diphenyl 2,3-Dideoxy-2,2,3,3-tetrafluorogalactopyranosyl (threohexopyranosyl) phosphate (6.38)

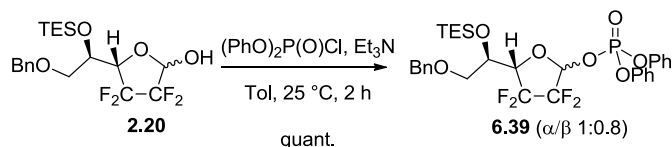


Pyranoside **6.36** (α/β 5:1) (2.33 g, 3.68 mmol) was dissolved in EtOAc (29 mL). Pd(OH)₂/C (20% wt, 1.18 g, 2.21 mmol) was added and the resultant mixture flushed with H₂. Stirring under H₂ at r.t. was continued for 2 h before the reaction mixture was filtered through Celite, which was washed with plenty of EtOAc. The solvent was concentrated to give pyranoside **6.38** as a pale yellow oil (α/β 5:1, 1.35 g, 81%).

R_f 0.15 (petrol ether/acetone 70:30); **IR** (neat) 3372 (br., s), 1590 (w), 1488 (m), 1281 (m), 1183 (s), 1157 (s), 1131 (s), 1011 (s), 951 (s) cm⁻¹; **¹H NMR** (α/β 1:1) (400 MHz, CDCl₃) δ (ppm) 7.01–7.49 (20H, m, H_{Ar}), 5.86 (1H, dd, *J* 13.3, 7.1 Hz, H-1 _{α}), 5.43 (1H, ddd, *J* 12.9, 7.2, 3.4 Hz, H-1 _{β}), 4.07 (3H, br. s., H-5 _{α} , H-4 _{α} , OH-4 _{α}), 4.02 (1H, s, H-4 _{β}), 3.88 (1H, br. s., OH-4 _{β}), 3.72–3.81 (1H, H-5 _{β}), 3.68 (2H, br. s., H-6 _{β} × 2), 3.63 (2H, br. s., H-6 _{α} × 2), 3.07 (1H, br. s., OH-6 _{α}), 2.97 (1H, br. s., OH-6 _{α}); **¹³C NMR** (101 MHz, CDCl₃) δ (ppm) 149.7–150.0 (C_{Ar} × 4), 130.0 (*m*-CH_{Ar} × 2), 123.0 (*m*-CH_{Ar} × 2), 129.9 (*m*-CH_{Ar} × 2), 129.8 (*m*-CH_{Ar} × 2), 126.2–125.9 (m, *p*-CH_{Ar} × 4), 120.4 (d, *J* 4 Hz, *o*-CH_{Ar} × 2), 120.1 (d, *J* 4 Hz, *o*-CH_{Ar} × 4), 120.0 (d, *J* 4 Hz, *o*-CH_{Ar} × 2), 94.6 (dd, *J* 44, 29 Hz, C-1 _{α}), 93.68 (dd, *J* 26, 21 Hz, C-1 _{β}), 74.7 (C-5 _{β}), 71.0 (C-5 _{α}), 69.6 (dd, *J* 48, 28 Hz, C-4 _{$\alpha+\beta$}), 60.94 (C-6 _{α}), 60.58 (C-6 _{β}); **¹⁹F NMR** (282 MHz, CDCl₃) δ (ppm) -117.46 (1F, ddt, *J* 275.1, 17.2, 8.6 Hz, α -F), -119.87 (1F, d, *J* 266.5 Hz, α -F), -120.83 (1F, d, *J* 275.1 Hz, β -F), -131.40 (1F, d, *J* 270.8 Hz, α -F), -132.61 (1F, d, *J* 270.8 Hz, β -F), -133.15 (1F, d, *J* 275.1 Hz, α -F), -134.90 (1F, dt, *J* 262.2, 12.9 Hz, β -F), -136.43 (1F, d, *J* 262.2 Hz, β -F); **³¹P NMR** (121 MHz, CDCl₃) δ (ppm) -13.1 (1P, d, *J* 6.7 Hz, β -P), -13.9 (1P, d, *J* 4.5 Hz, α -P); **ES⁺MS**: *m/z* 475.1 [M + Na]⁺; **HRMS** (ES⁺) for C₁₈H₁₇F₄O₇PNa⁺ [M + Na]⁺ calcd 475.0540, found 475.0526.

8.7.3 Diphenyl

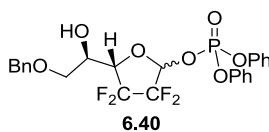
6-*O*-benzyl-5-*O*-triethylsilyl-2,3-dideoxy-2,2,3,3-tetrafluorogalactofuranosyl phosphate (threohexofuranosyl) (**6.39**)



Furanose **2.20** (3.03 g, 7.14 mmol) was dissolved in toluene (35 mL). $(\text{PhO})_2\text{P}(\text{O})\text{Cl}$ (1.78 mL, 8.57 mmol) was added, followed by Et_3N (1.19 mL, 8.57 mmol), dropwise. The reaction was stirred at r.t. for 2 h before quenching with aq. HCl (1M, 9 mL). The organic layer was extracted and washed with H_2O (18 mL) then aq. NaHCO_3 (sat, 18 mL). The organic extract was dried (MgSO_4), filtered and concentrated to give a pale yellow oil. Column chromatography (petrol ether/acetone 90:10) gave a colourless oil (4.90 g), which was a mixture (1:0.1) of desired glycosyl phosphate **6.39** (4.70 g, quant., α/β 1:0.8) and $(\text{PhO})_2\text{P}(\text{O})\text{Cl}$ (0.2 g).

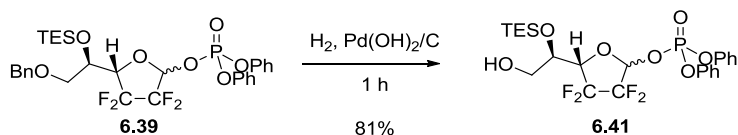
R_f 0.21 (hexane/acetone 90:10); **IR** (neat) 2955 (w), 2912 (w), 2877 (w), 1489 (m), 1185 (m), 1158 (m), 1101 (m), 1007 (m), 944 (s) cm^{-1} ; **¹H NMR** (performed on 3:1 mixture of unassigned anomers β/α) (400 MHz, CDCl_3) δ (ppm) 7.14–7.47 (20H, m, H_{Ar}), 6.08 (1H, td, J 6.3, 2.4 Hz, $\text{H}-1_\beta$), 6.04 (0.33H, td, J 6.9, 1.8 Hz, $\text{H}-1_\alpha$), 4.50–4.55 (3H, m, $\text{CH}_2\text{Ph}_{\beta+\alpha}$, $\text{H}-4_\alpha$), 4.47 (1H, dd, J 13.4, 4.4 Hz, $\text{H}-4_\beta$), 4.14–4.18 (0.33H, m, $\text{H}-5_\alpha$), 4.13 (1H, q, J 5.1 Hz, $\text{H}-5_\beta$), 3.49–3.64 (2.66H, $\text{H}-6_{\beta+\alpha}$) 0.86–1.02 (12H, m, $4 \times \text{CH}_3$), 0.60 (8H, q, J 8.0 Hz, $4 \times \text{CH}_2\text{CH}_3$); **¹³C NMR** (101 MHz, CDCl_3) δ (ppm) 150.1 (d, J 7 Hz, $\text{C}_{\text{ArOP}_{\beta+\alpha}}$), 149.9 (d, J 7 Hz, $\text{C}_{\text{ArOP}_{\beta+\alpha}}$), 137.7 ($\text{C}_{\text{ArCH}_{2\alpha}}$), 137.6 ($\text{C}_{\text{ArCH}_{2\beta}}$), 129.8, 128.4, 127.5–128.0 ($\text{CH}_{\text{Ar}\beta+\alpha}$), 125.5–126.1 ($p\text{-CH}_{\text{Ar}\beta+\alpha}$), 119.9–120.3 ($o\text{-CH}_{\text{Ar}\beta+\alpha}$), 96.7 (dd, J 44, 23 Hz, $\text{C}-4_{\beta+\alpha}$), 80.4 (dd, J 28, 23 Hz, $\text{C}-1_{\beta+\alpha}$), 73.6 ($\text{CH}_2\text{Ph}_\alpha$), 73.5 ($\text{CH}_2\text{Ph}_\beta$), 70.6 ($\text{C}-6_\alpha$), 70.4 ($\text{C}-6_\beta$), 69.8 ($\text{C}-5_\beta$), 68.6 ($\text{C}-5_\alpha$), 6.6 ($\text{CH}_{3\beta+\alpha}$), 4.8 ($\text{CH}_2\text{CH}_{3\beta}$), 4.7 ($\text{CH}_2\text{CH}_{3\alpha}$); **¹⁹F NMR** (282 MHz, CDCl_3) δ (ppm) -111.34 (dd, J 249.3, 12.9 Hz, F_β), -125.29 (d, J 245.0 Hz, F_β), -126.09 (d, J 249.3 Hz, F_α), -127.29 (ddd, J 245.0, 12.9, 12.7 Hz, F_α), -128.87 (d, J 245.0 Hz, F_β), -129.79 (dd, J 249.3, 8.6 Hz, F_α), -132.84 (dd, J 249.3, 8.6 Hz, F_β), -134.01 (m, J 249.3 Hz can be observed, F_β); **³¹P NMR** (121 MHz, CDCl_3) δ (ppm) -13.7 (d, J 6.7 Hz, P_α), -13.8 (d, J 4.5 Hz, P_β); **ES⁺MS**: m/z 679.2 $[\text{M} + \text{Na}]^+$; **HRMS** (ES⁺) for $\text{C}_{31}\text{H}_{37}\text{F}_4\text{O}_7\text{PSiNa}^+ [\text{M} + \text{Na}]^+$ calcd 679.1875, found 679.1849.

8.7.4 Diphenyl 6-*O*-benzyl-2,3-dideoxy-2,2,3,3-tetrafluorogalactofuranosyl (threohexofuranosyl) phosphate (6.40)



(β/α 1:0.5): **IR** (neat) 3431 (w, br.), 3066 (w), 2869 (w), 1590 (m), 1488 (m), 1288 (m), 1183 (m), 1158 (m), 9457 (s) cm^{-1} ; **^1H NMR** (400 MHz, CDCl_3) δ 7.15–7.44 (22.5H, m, H_{Ar}), 6.09 (1H, td, J 6.2, 2.5 Hz, H-1_β), 5.98–6.04 (0.5H, m, H-1_α), 4.49–4.62 (3.5H, m, $\text{CHHPh}_{\beta+\alpha}$, $\text{CHHPh}_{\beta+\alpha}$, H-4_y), 4.40 (1H, td, J 12.7, 5.1 Hz, H-4_β), 4.10 (1H, quin, J 5.4 Hz, H-5_β), 4.01 (0.5H, tt, J 6.3, 4.5 Hz, H-5_α), 3.60 (1H, t, J 3.7 Hz, H-6_α), 3.57 (2H, d, J 5.1 Hz, H-6_β), 3.01 (0.5H, d, J 6.2 Hz, OH_α), 2.52 (1H, d, J 6.3 Hz, OH_β) (ppm); **^{13}C NMR** (101 MHz, CDCl_3) δ 149.6–150.1 (m, $\text{C}_{\text{ArOP}} \times 4$), 137.4 ($\text{C}_{\text{ArCH}_2} \times 2$), 137.3, 129.9, 129.8, 129.8, 128.4, 128.3, 127.8, 127.7, 127.6 ($\text{CH}_{\text{Ar}} \times 18$), 125.7–126.0 ($p\text{-CHAr} \times 4$), 119.9–120.2 ($o\text{-CHAr} \times 8$), 96.6 (t, J 22 Hz, C-1_x), 96.2 (t, J 21 Hz, C-1_α), 80.3 (dd, J 29, 23 Hz, C-4_α), 80.0 (t, J 23 Hz, C-4_β), 73.5 ($\text{CH}_2\text{Ph}_{\beta/\alpha}$), 73.5 ($\text{CH}_2\text{Ph}_{\alpha/\beta}$), 69.3 ($\text{C-6}_{\beta+\alpha}$), 68.0 (C-5_α), 67.0 (C-5_β) (ppm) **^{19}F NMR** (282 MHz, CDCl_3) δ 112.0 (1F, dd, J 245, 13 Hz, F_β), -125.0 (0.5F, m, J 245 Hz can be observed, F_α), -125.6 (1F, d, J 245 Hz, F_β), -126.9 (0.5F, d, J 254 Hz, F_α), -128.3 (0.5F, dq, J 249, 9 Hz, F_α), -128.9 (1F, d, J 249 Hz, F_β), -133.3 (1F, dd, J 245, 9 Hz, F_β), -133.8 (0.5F, d, J 249 Hz, F_α); **^{31}P NMR** (121 MHz, CDCl_3) δ -13.8 (1P, s, P_β), -14.2 (0.3P, s, P_α) (ppm); **ES^+MS** : 565.2 m/z [$\text{M} + \text{Na}$] $^+$; **HRMS** (ES^+) for $\text{C}_{25}\text{H}_{23}\text{F}_4\text{O}_7\text{PNa}$ [$\text{M} + \text{Na}$] $^+$ calcd 565.1010, found 565.1003.

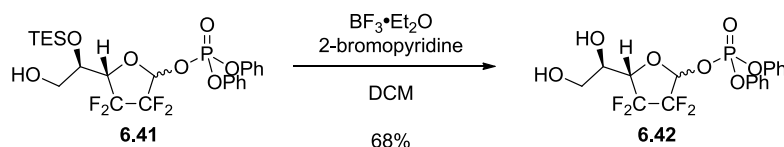
8.7.5 Diphenyl 5-*O*-Triethylsilyl-2,3-dideoxy-2,2,3,3-tetrafluorogalactofuranosyl (threohexofuranosyl) phosphate (6.41)



Furanoside **6.39** (787 mg, 1.20 mmol) was dissolved in EtOAc (10 mL) at r.t. and treated with $\text{Pd}(\text{OH})_2/\text{C}$ (20% wt, 192 mg, 0.36 mmol). The flask was flushed with H_2 then stirred under H_2 positive pressure for 1 h. The resultant reaction mixture was filtered through Celite[®], which was washed with plenty of EtOAc. Concentration gave a brown oil which was purified by column chromatography (petrol ether/acetone 80:20) to give furanoside **6.41** as a colourless oil (538 mg, 81%) (β/α 1:0.3).

R_f 0.36 (hexane/acetone 70:30); **IR** (neat) 3464 (w, br.), 2956 (w), 2879 (w) 1591 (m), 1489 (m), 1184 (m), 1156 (m), 947 (s) cm⁻¹; **¹H NMR** (400 MHz, CDCl₃) δ 7.17–7.40 (13H, m, H_{Ar}), 6.06 (1H, td, *J* 6.2, 2.5 Hz, H-4_β), 6.01–6.06 (0.3H, m, H-1_α), 4.46 (1H, ddd, *J* 14.0, 12.0, 7.1 Hz, H-4_β), 4.36–4.44 (0.3H, m, H-4_α), 4.05 (1H, dt, *J* 8.0, 3.7, 3.7 Hz, H-5_α), 4.02 (1H, dt, *J* 6.8, 4.2 Hz, H-5_β), 3.56–3.80 (2.6H, m, H-6_{β+α}), 2.17 (1H, br. s, OH_β), 1.77 (0.3H, br. s, OH_α), 0.95 (9H, t, *J* 8.0 Hz, CH_{3β}), 0.92 (2.7H, t, *J* 7.9 Hz, CH_{3α}), 0.57–0.69 (7.8H, m, SiCH_{2β+α}) (ppm); **¹³C NMR** (101 MHz, CDCl₃) δ 149.7–150.2 (4C, m, C_{Ar} × 4), 129.8 (*m*-CH_{Arβ}), 129.7 (*m*-CH_{Arα}), 125.6–125.9 (m, *p*-CH_{Arβ+α}), 120.0 (t, *J* 5 Hz, *o*-CH_{Arα}), 119.8 (d, *J* 4 Hz, *o*-CH_{Arβ}), 96.7 (dd, *J* 42, 23 Hz, C-1_β), 96.0 (dd, *J* 41, 22 Hz, C-1_α), 79.7 (dd, *J* 28, 23 Hz, C-4_{β+α}), 71.0 (C-5_α), 69.6 (C-5_β), 62.5 (C-6_α), 62.4 (C-6_β), 6.5 (CH_{3β+α}), 4.7 (SiCH_{2β}), 4.6 (SiCH_{2α}) (ppm); **¹⁹F NMR** (282 MHz, CDCl₃) δ -112.9 (1F, dd, *J* 245, 9 Hz, F_β), -125.2 (1F, d, *J* 245 Hz, F_β), -126.2 (0.3F, dt, *J* 249, 9 Hz, F_α), -127.6 (1F, d, *J* 245 Hz, F_β), -128.0 (0.3F, ddd, *J* 249, 17, 9 Hz, F_α), -131.1 (0.3F, d, *J* 245 Hz, F_β), -133.3 (1F, dd, *J* 249, 13 Hz, F_β), -134.9 (0.3F, d, *J* 249 Hz, F_α); **³¹P NMR** (121 MHz, CDCl₃) δ -14.1 (1.3P, br. s) (ppm); **ES⁺MS** *m/z* 589.3 [M + Na]⁺; **HRMS** (ES⁺) for C₂₄H₃₁F₄O₇PSiNa⁺ [M + Na]⁺ calcd 589.1405, found 589.1391.

8.7.6 Diphenyl 4,6-di-*O*-benzyl-2,3-dideoxy-2,2,3,3-tetrafluorogalactofuranosyl (threohexofuranosyl) phosphate (6.42)



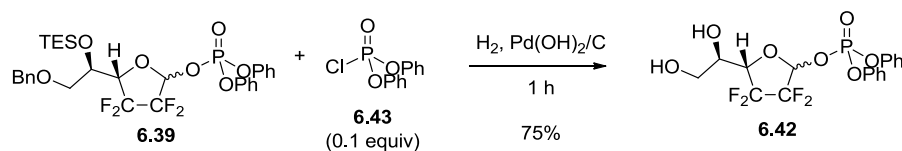
Furanoside **7.8** (278 mg, 0.51 mmol) was dissolved in DCM (5 mL) and treated with 2-bromopyridine (97 μL, 1.02 mmol), followed by BF₃·Et₂O (31 μL, 0.26 mmol). The reaction mixture was stirred at r.t. for 40 h before being concentrated under reduced pressure to give an oil. Column chromatography (petrol/acetone 80:20, 70:30, 60:40) gave furanoside **6.42** as a colourless oil (156 mg, 68%). The anomers could be separated by HPLC (DCM/MeOH 95:5).

Data for β-6.42: **R_f** 0.20 (DCM/MeOH 93:7); [α]_D -58.5 (c 0.5, CHCl₃, 29.5 °C); **IR** (neat) 3417 (m, br.), 1590 (m), 1488 (m), 1285 (m), 1182 (m), 1010 (m), 942 (s) cm⁻¹; **¹H NMR** (400 MHz, CDCl₃) δ (ppm) 7.15–7.44 (10H, m, H_{Ar}), 6.04 (1H, td, *J* 5.9, 2.3 Hz, H-1), 4.29 (1H, td, *J* 12.8, 5.4 Hz, H-4), 3.94 (1H, br. quin, *J* 4.5 Hz, H-5), 3.46–3.69 (2H, m, H-6 × 2), 2.62 (1H, d, *J* 5.2 Hz, OH-5), 2.20 (1H, t, *J* 6.2 Hz, OH-6); **¹H (-F) NMR** (400 MHz, CDCl₃) δ (ppm) 7.15–7.40 (10H, m, H_{Ar}), 6.00 (1H, d, *J* 5.6 Hz, H-1), 4.26 (1 H, d,

J 5.6 Hz, H-4), 3.94 (1H, br. quin, J 5.1 Hz, H-5), 3.55–3.69 (3H, m, H-6 \times 2), 2.62 (1H, d, J 5.1 Hz, OH-5), 2.20 (1H, t, J 6.3 Hz, OH-6); ^{13}C NMR (101 MHz, CDCl_3) δ 149.9 (d, J 7 Hz, $\underline{\text{C}}_{\text{Ar}}$), 149.8 (d, J 9 Hz, $\underline{\text{C}}_{\text{Ar}}$), 130.0 ($m\text{-CH}_{\text{Ar}}$), 130.0 ($m\text{-CH}_{\text{Ar}}$), 126.1 ($p\text{-CH}_{\text{Ar}}$), 126.0 ($p\text{-CH}_{\text{Ar}}$), 120.1 (d, J 4 Hz, $o\text{-CH}_{\text{Ar}}$), 120.1 (d, J 4 Hz, $o\text{-CH}_{\text{Ar}}$), 96.6 (dd, J 42, 22 Hz, C-1), 80.0 (dd, J 29, 23 Hz, C-4), 68.3 (C-5), 62.1 (C-6) (ppm); ^{19}F NMR (282 MHz, CDCl_3) δ 112.6 (1F, dd, J 245, 13 Hz), -125.6 (1F, d, J 249 Hz), -128.8 (1F, d, J 249 Hz), -133.4 (1F, t, J 249 Hz) (ppm); ^{31}P NMR (121 MHz, CDCl_3) δ -14.1 (1P, br. s.) (ppm); ES^+MS m/z 475.1 $[\text{M} + \text{Na}]^+$; **HRMS** (ESI+) for $\text{C}_{18}\text{H}_{17}\text{F}_4\text{O}_7\text{PNa}^+$ $[\text{M} + \text{Na}]^+$ calcd 475.0540, found 475.0544.

Data for α -6.42: R_f 0.26 (DCM/MeOH 93:7) 0.26; $[\alpha]_D^{25} +54.0$ (c 0.5, CHCl_3 , 29.5 $^\circ\text{C}$); **IR** (neat) 3419 (m, br.), 1590 (m), 1488 (m), 1287 (m), 1183 (m), 1011 (m), 950 (s) cm^{-1} ; ^1H NMR (400 MHz, CDCl_3) δ (ppm) 7.13–7.49 (10H, m, H_{Ar}), 5.98 (1H, ddt, J 6.2, 4.2, 1.9, Hz, H-1), 4.45 (1H, dddd, J 13.1, 12.1, 8.6, 1.5 Hz, H-4), 3.86 (1H, dq, J 8.1, 4.0 Hz, H-5), 3.78 (1H, app dt, J 11.9, 3.0 Hz, H-6), 3.60 (1H, app dt, J 11.9, 4.0 Hz, H-6), 3.36 (1H, d J 3.5 Hz, OH-5), 2.12 (1H, t, J 6.3 Hz, OH-6); ^1H (-F) NMR (400 MHz, CDCl_3) δ (ppm) 7.14–7.47 (10H, m, H_{Ar}), 5.98 (1H, d, J 4.5 Hz, H-1), 4.45 (1H, d, J 8.6 Hz, H-4), 3.86 (1H, dq, J 8.1, 4.0 Hz, H-5), 3.78 (6 H, app ddd, J 11.6, 5.1, 3.5 Hz, H-6), 3.59 (1H, ddd, J 11.7, 6.7, 4.8 Hz, H-6), 3.36 (1H, d, J 4.0 Hz, OH-5), 2.11 (1H, t, J 6.3 Hz, OH-6); ^{13}C NMR (101 MHz, CDCl_3) δ 149.9 (d, J 4 Hz, $\underline{\text{C}}_{\text{Ar}}$), 149.8 (d, J 3 Hz, $\underline{\text{C}}_{\text{Ar}}$), 130.0 ($m\text{-CH}_{\text{Ar}}$), 126.2 ($p\text{-CH}_{\text{Ar}}$), 120.1 (d, J 4 Hz, $o\text{-CH}_{\text{Ar}}$), 120.0 (d, J 4 Hz, $o\text{-CH}_{\text{Ar}}$), 96.6 (dd, J 42, 20 Hz, C-1), 80.4 (dd, J 28, 23 Hz, C-4), 69.0 (C-5), 62.0 (C-6) (ppm); ^{19}F NMR (282 MHz, CDCl_3) δ (ppm) -124.8 (1F, dt, J 249, 11 Hz), -126.4 (1F, d, J 245 Hz), -127.1 (1F, d, J 245 Hz), -133.1 (1F, d, J 249 Hz); ^{31}P NMR (121 MHz, CDCl_3) δ -14.4 (1P, br. s) (ppm); ES^+MS m/z 475.1 $[\text{M} + \text{Na}]^+$; **HRMS** (ESI+) for $\text{C}_{18}\text{H}_{17}\text{F}_4\text{O}_7\text{PNa}^+$ $[\text{M} + \text{Na}]^+$ calcd 475.0540, found 475.0530.

8.7.7 Galactofuranosyl phosphate 6.42 from 6.39

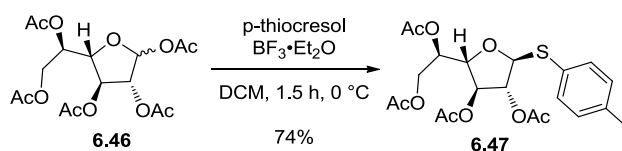


The inseparable mixture of furanoside **6.39** (4.70 g, 7.14 mmol) and $(\text{PhO})_2\text{P}(\text{O})\text{Cl}$ (0.2 g, 0.7 mmol) was dissolved in EtOAc (50 mL) and treated with $\text{Pd}(\text{OH})_2/\text{C}$ (20% wt, 1.14 g, 2.1 mmol). The flask was flushed with H_2 then stirred under H_2 positive pressure for 1 h. The resultant reaction mixture was filtered through Celite[®], which was washed

with plenty of EtOAc. Concentration gave a yellow oil which was purified by column chromatography (petrol ether/acetone 80:20 then 50:50) to give the deprotected furanoside **6.42** as a pale yellow oil (2.41 g, 75%). HPLC (DCM/MeOH 95:5) allowed separation of the anomers.

8.8 Synthesis of Galactofuranosyl Tetrafluoro Galactofuranosides

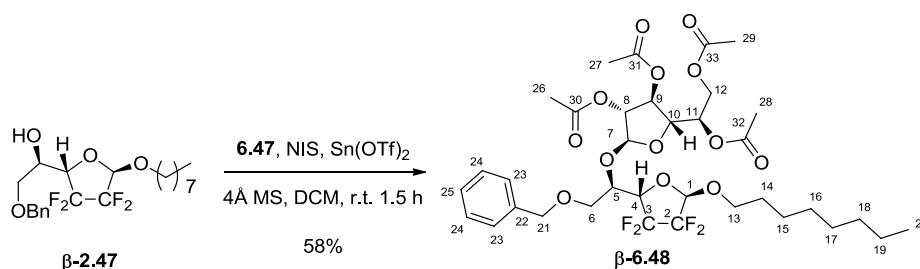
8.8.1 *p*-Tolyl-2,3,5,6-tetra-*O*-acetyl-1-thio- β -galactofuranoside (**6.47**)



Galactofuranose pentaacetate (**6.46**)¹⁶⁹ (200 mg, 0.49 mmol) was dissolved in DCM (2.5 mL) and cooled to 0°C . *p*-Thiocresol (75 mg, 0.6 mmol) was added and the reaction stirred for 20 min. $\text{BF}_3 \cdot \text{Et}_2\text{O}$ (0.15 mL, 1.2 mmol) was then added dropwise and the reaction was stirred for 90 min before being neutralised with Et_3N (0.17 mL, 1.2 mmol). The solution was diluted with DCM (5 mL) and washed with water (5 mL) then brine (5 mL). The organic phase was dried (Na_2SO_4), filtered and concentrated to give a pale yellow oil. Column chromatography (petrol ether/EtOAc 90:10) gave thioglycoside **6.47** as a pale yellow oil (170 mg, 74%).

R_f 0.11 (petrol ether/EtOAc 90:10); ^1H NMR (300 MHz, CDCl_3) δ (ppm) 7.39 (2H, app. d, J 8.4 Hz, $2 \times \text{H}_{\text{Ar}}$), 7.13 (2H, app. d, J 8.1 Hz, $2 \times \text{H}_{\text{Ar}}$), 5.44 (1H, d, J 2.6 Hz, H-1), 5.40 (1H, dt, J 6.8, 4.3 Hz, H-5), 5.22 (1H, t, J 2.6 Hz, H-2), 5.09 (1H, dd, J 6.2, 2.6 Hz, H-3), 4.47 (1H, dd, J 6.0, 3.8 Hz, H-4), 4.33 (1H, dd, J 11.7, 4.8 Hz, H-6), 4.19 (1H, dd, J 11.7, 7.0 Hz, H-6'), 2.35 (3H, s, CH_3Ar), 2.13 (3H, s, CH_3CO), (3H, s, CH_3CO), 2.11 (3H, s, CH_3CO), 2.06 (3H, s, CH_3CO); ^{13}C NMR (75 MHz, CDCl_3) δ (ppm) 170.5 (C=O), 170 (C=O), 169.9 (C=O), 169.6 (C=O), 138.3 (C_{Arq}), 132.9 ($2 \times \text{C}_{\text{Ar}}$), 129.8 ($2 \times \text{C}_{\text{Ar}}$), 90.7 (C-1), 81.1 (C-2), 79.5 (C-4), 76.5 (C-3), 69.1 (C-5), 62.5 (C-6), 21.1 (CH_3Ar), 20.8 (CH_3CO), 20.7 ($3 \times \text{CH}_3\text{CO}$). Spectra consistent with the reported data¹⁵⁷

8.8.2 n-Octyl 6-*O*-benzyl-5-*O*-(2,3,5,6-tetra-*O*-acetyl- β -galactofuranosyl)-2,3-dideoxy-2,2,3,3-tetrafluoro- β -galactofuranoside (threohexofuranoside) (β -6.48)

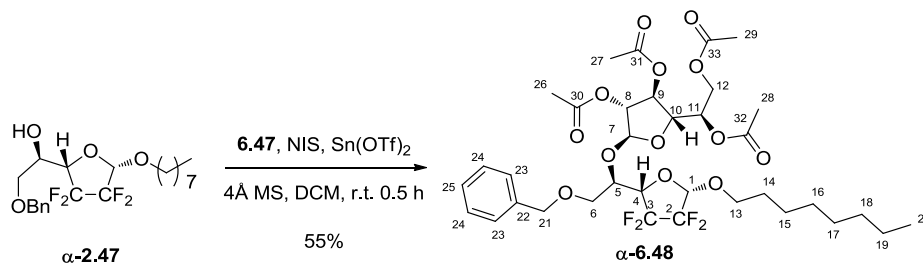


Furanoside β -2.47 (132 mg, 0.31 mmol) in DCM (6 mL) was added to a flask containing powdered molecular sieves (4Å, 62 mg) and the residue was rinsed with DCM (0.3 mL). The resultant solution was cooled to 0 °C then treated with donor **6.47** (185 mg, 0.41 mmol) in DCM (3 mL), which was then rinsed in with DCM (0.2 mL). The resultant mixture was stirred for 15 min before being treated with NIS (90 mg, 0.40 mmol) and $\text{Sn}(\text{OTf})_2$ (17 mg, 41 μmol). Stirring was continued at r.t. for 1.5 h before the reaction was quenched with Et_3N (0.7 mL). The reaction mixture was diluted with DCM (7 mL) and filtered through Celite[®], which was washed with DCM (6 mL). Combined DCM was washed with aq. $\text{Na}_2\text{S}_2\text{O}_3$ (10%, 6 mL) then aq. NaHCO_3 (sat., 6 mL). Combined organic phases were dried (Na_2SO_4), filtered and concentrated to give an orange oil. Column chromatography (petrol ether/acetone 95:5, 90:10, 80:20) gave disaccharide β -6.48 as a pale yellow oil (136 mg, 58%).

R_f 0.37 (petrol ether/acetone 70:30); **[α]_D** –68.8 (c 0.5, CHCl_3 , 25 °C); **IR** (neat) 2930 (w), 2858 (w), 1748 (s), 1371 (w), 1228 (s), 1149 (m), 1029 (m) cm^{-1} ; **¹H NMR** (400 MHz, CDCl_3) δ (ppm) 7.26–7.43 (5H, m, H-23–25), 5.41 (1H, dt, J 7.3, 3.9 Hz, H-11), 5.10–5.17 (2H, m, H-1, H-8), 4.98 (1H, dd, J 6.1, 2.0 Hz, H-9), 4.58 (1H, d, J 12.1 Hz, H-21), 4.55 (1H, d, J 12.1 Hz, H-21'), 4.31–4.45 (3H, m, H-4, H-10, H-12), 4.15–4.27 (2H, m, H-5, H-12'), 3.77 (1H, dt, J 9.6, 6.6 Hz, H-13), 3.65–3.74 (2H, m, H-6, H-6'), 3.58 (1H, dt, J 9.5, 6.6 Hz, H-13'), 2.14, 2.09, 2.06, 2.05 (4 \times 3H, s, H-26–29), 1.67 (1H, t, J 6.6 Hz, H-14), 1.63 (1H, t, J 6.6 Hz, H-14'), 1.19–1.43 (10H, m, H-15–19), 0.90 (3H, t, J 7.1 Hz, H-20); **¹³C NMR** (101 MHz, CDCl_3) δ (ppm) 170.4 (C=O), 169.9 (2 \times C=O), 169.4 (C=O), 137.6 (C-22), 128.3 (C-23/24), 127.7 (C-25), 127.5 (C-24/23), 104.4 (C-7), 99.3 (dd, J 38, 20 Hz, C-1), 81.3 (C-8), 80.2 (C-10), 77.0 (dd, J 29, 23 Hz, C-4), 76.4 (C-9), 73.5 (C-21), 71.5 (C-5), 69.1 (C-11), 68.8 (C-13), 68.3 (C-6), 62.6 (C-12), 31.7, 29.1, 29.1, 25.8, 22.5 (C-14–19), 20.7, 20.6, 20.5, 20.4 (C-26–29), 14.0 (C-20); **¹⁹F NMR** (282 MHz, CDCl_3) δ (ppm) –112.3 (1F, dd, J 244, 11 Hz), –125.0 (1F, dd, J 245, 8 Hz), –130.8 (1F, d, J 245 Hz),

-132.7 (1F, dd, J 244, 14 Hz); **ES⁺MS**: m/z 775.2 $[M + Na]^+$; **HRMS** (ES+) for $C_{35}H_{48}F_4O_{13}Na^+$ $[M + Na]^+$ calcd 775.2923, found 775.2911.

8.8.3 *n*-Octyl 6-*O*-benzyl-5-*O*-(2,3,5,6-tetra-*O*-acetyl- β -galactofuranosyl)-2,3-dideoxy-2,2,3,3-tetrafluoro- α -galactofuranoside (threohexofuranoside) (α -6.48)

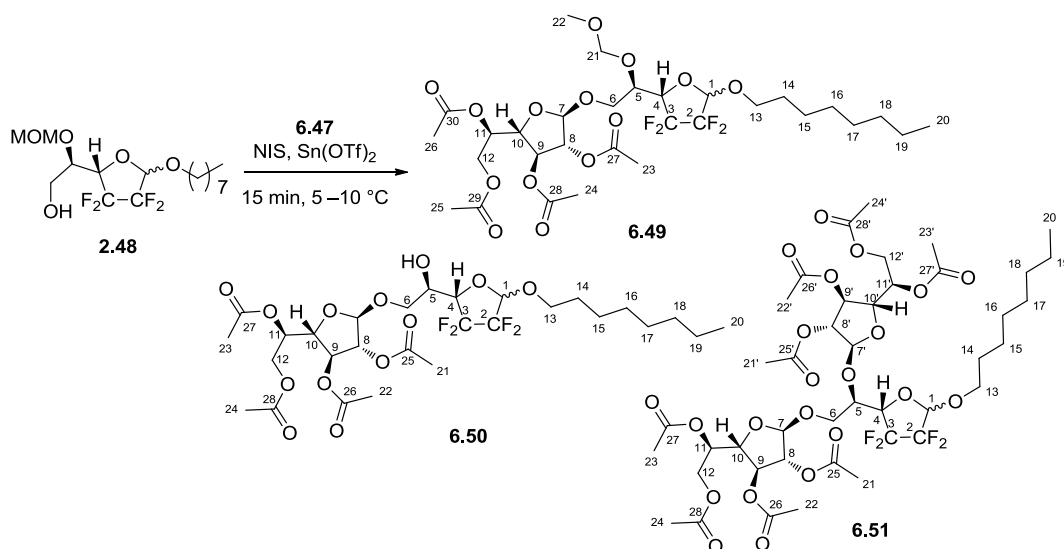


Furanoside α -2.47 (93 mg, 0.22 mmol) in DCM (4 mL) was added to a flask containing powdered molecular sieves (4Å, 44 mg) and the residue was rinsed with DCM (0.5 mL). The resultant solution was cooled to 0 °C then treated with donor **6.47** (120 mg, 0.26 mmol) in DCM (2 mL), which was then rinsed in with DCM (0.3 mL). The resultant mixture was stirred for 15 min before being treated with NIS (58 mg, 0.26 mmol) and $Sn(OTf)_2$ (11 mg, 26 μ mol). Stirring was continued at r.t. for 0.5 h before the reaction was quenched with Et_3N (0.5 mL). The reaction mixture was diluted with DCM (5 mL) and filtered through Celite[®], which was washed with DCM (4 mL). Combined DCM was washed with aq. $Na_2S_2O_3$ (10%, 4 mL) then aq. $NaHCO_3$ (sat., 4 mL). Combined organic phases were dried (Na_2SO_4), filtered and concentrated to give a brown oil. Column chromatography (petrol ether/acetone 95:5, 90:10, 80:20) followed by HPLC (hexane/acetone 80:20) gave disaccharide α -6.48 as a pale yellow oil (91 mg, 55%).

R_f 0.38 (petrol ether/acetone 70:30); **[α]_D** -6.6 (c 0.5, $CHCl_3$, 24 °C); **IR** (neat) 2929 (w), 2858 (w), 1747 (s), 1371 (w), 1223 (s), 1146 (m), 1044 (m) cm^{-1} ; **¹H NMR** (400 MHz, $CDCl_3$) δ (ppm) 7.23–7.39 (5H, m, H-23–25), 5.39 (1H, dt, J 7.5, 4.1 Hz, H-11), 5.34 (1H, s, H-7), 5.14 (1H, d, J 2.0 Hz, H-8), 4.96–5.04 (2H, m, H-9, H-1), 4.57 (1H, d, J 12.1 Hz, H-21), 4.53 (1H, d, J 12.1 Hz, H-21'), 4.36 (1H, dd, J 5.8, 3.8 Hz, H-10) 4.25–4.34 (2H, m, H-12, H-4), 4.12–4.23 (2H, m, H-12', H-5), 3.83 (1H, dt, J 9.5, 6.6 Hz, H-13), 3.75 (1H, dd, J 10.6, 3.0 Hz, H-6), 3.67 (1H, dd, J 10.6, 6.6 Hz, H-6'), 3.54 (1H, dt, J 9.5, 6.6 Hz, H-13'), 2.12, 2.08, 2.06, 2.04 (4 \times 3H, s, H-26–29), 1.55–1.66 (2H, m, H-14, H-14'), 1.19–1.39 (10H, m, H-15–19), 0.88 (3H, t, J 7.1 Hz, H-20); **¹³C NMR** (101 MHz, $CDCl_3$) δ (ppm) 170.4, 170.0, 169.9, 169.4 (C-30–33), 137.7 (C-22), 128.3, 127.6, 127.5 (C-23–25), 104.9 (C-7), 99.4 (dd, J 38, 19 Hz, C-1), 81.2 (C-5), 80.3 (C-10), 76.7 (td, J 23, 3 Hz, C-4), 76.4 (C-9), 73.8 (C-5), 73.5 (C-21), 69.6 (C-13), 69.1 (C-11), 68.5 (C-6), 62.5 (C-

12), 31.7, 29.2, 29.1, 25.7, 22.5 (C-14–19), 20.7, 20.6, 20.5 (C-26–29), 14.0 (s, C-20); ^{19}F NMR (282 MHz, CDCl_3) δ (ppm) -125.1 (1F, d, J 245 Hz), -126.5 (2F, br. s.), -136.8 (1F, d, J 249 Hz); ES^+MS : m/z 775.2 $[\text{M} + \text{Na}]^+$; HRMS (ES^+) for $\text{C}_{35}\text{H}_{48}\text{F}_4\text{O}_{13}\text{Na}$ $[\text{M} + \text{Na}]^+$ calcd 775.2923, found 775.2916.

8.8.4 n-Octyl 5-O-(methoxymethyl)-6-O-(2,3,5,6-tetra-O-acetyl- β -galactofuranosyl)-2,3-dideoxy-2,2,3,3-tetrafluorogalactofuranoside (threohexofuranoside) (**6.49**)



Octyl glycoside **2.48** (558 mg, 1.48 mmol) in DCM (28 mL) was transferred to a flask containing powdered molecular sieves (4\AA , 296 mg) then washed in with DCM (3 mL). The reaction was cooled to 0 °C before being treated with donor **6.47** (637 mg, 1.40 mmol) in DCM (14 mL), which was washed in with DCM (1 mL). The reaction was stirred at 0 °C for 15 min at 0 °C then treated with NIS (333 mg, 1.48 mmol) and $\text{Sn}(\text{OTf})_2$ (62 mg, 148 μmol). Stirring was continued at 5 – 10 °C for 15 min before the reaction was quenched with Et_3N (3.4 mL). The mixture was then diluted with DCM (30 mL) and filtered through Celite[®], which was washed with DCM (25 mL). The filtrate was washed with aq. $\text{Na}_2\text{S}_2\text{O}_3$ (10%, 30 mL) and aq. NaHCO_3 (sat., 30 mL) then dried (Na_2SO_4), filtered and concentrated to give a brown oil. Column chromatography (petrol ether/acetone 95:5, 80:20, 70:30) gave disaccharide **6.49** as a yellow oil (502 mg, 48%), disaccharide **6.50** as a yellow oil (161 mg, 16%) and trisaccharide **6.51** as an orange oil (110 mg, 7%).

Data for 6.49: R_f 0.31 (petrol ether/acetone 70:30); IR (neat) 2931 (w), 2857 (w), 1748 (s), 1372 (m), 1224 (s), 1145 (m), 1309 (s) cm^{-1} ; ^1H NMR (400 MHz, CDCl_3) δ (ppm) 5.40 (0.6H, q, J 4.0 Hz, H-11 $_{\alpha}$), 5.38 (1H, q, J 3.5 Hz, H-11 $_{\beta}$), 4.99–5.16 (6.4H, m, H-1 $_{\alpha+\beta}$, H-7–9 $_{\alpha+\beta}$), 4.81 (0.6H, d, J 7.1 Hz, H-21 $_{\alpha}$), 4.76–4.79 (1.6H, m, H-21' $_{\alpha}$, H-21 $_{\beta}$), 4.75 (1H, d, J 6.6 Hz, H-21' $_{\beta}$), 4.25–4.46 (4.8H, m, H-4 $_{\alpha+\beta}$, H-10 $_{\alpha+\beta}$, H-12 $_{\alpha+\beta}$), 4.22 (1H, d, J 7.1 Hz,

H-12'_β), 4.20 (0.6H, d, *J* 7.1 Hz, H-12'_α), 4.07 (1H, q, *J* 5.6 Hz, H-5_β), 4.01 (0.6H, ddd, *J* 8.0, 4.7, 3.5 Hz, H-5_α), 3.93 (0.6H, dd, *J* 11.1, 3.0 Hz, H-6_α), 3.89 (1H, dd, *J* 10.6, 4.5 Hz, H-6_β), 3.85 (0.6H, dt, *J* 9.6, 2.5 Hz, H-13_α), 3.79 (1H, dt, *J* 9.6, 6.6 Hz, H-13_β), 3.62–3.71 (1.6H, m, H-6'_{α+β}), 3.57 (1.6H, dt, *J* 9.6, 6.8 Hz, H-13'_{α+β}), 3.43 (1.8H, s, H-22_α), 3.42 (3H, s, H-22_β), 2.14, 2.11, 2.08, 2.06 (4 × 4.8H, s, H-23–26_{α+β}), 1.59–1.71 (3.2H, m, H-14_{α+β}), 1.24–1.40 (16H, m, H-15–19_{α+β}), 0.89 (4.8H, t, *J* 6.8 Hz, H-20_{α+β}); ¹³C NMR (101 MHz, CDCl₃) δ (ppm) 170.3, 169.8, 169.8, 169.4 (C-27–30), 105.6 (C-7_α), 105.5 (C-7_β), 99.5 (m, C-1_α), 99.5 (dd, *J* 38, 19 Hz, C-1_β), 97.0 (C-21_β), 96.7 (C-21_α), 80.8 (C-8_{α+β}), 80.4 (C-10_β), 80.1 (C-10_α), 77.4 (dd, *J* 28, 22 Hz, C-4_β), 77.2 (m, C-4_α), 76.3 (C-9_β), 76.2 (C-9_α), 74.1 (C-5_α), 72.9 (C-5_β), 69.6 (C-13_α), 69.2 (C-11_{α+β}), 69.1 (C-13_β), 66.3 (C-6_α), 66.0 (C-6_β), 62.5 (C-12_{α+β}), 55.7 (C-22_β), 55.6 (C-22_α), 31.6, 29.1, 29.0, 25.7, 22.5 (C-14–19), 20.6, 20.6, 20.5, 20.4 (C-23–26), 13.9 (C-20); ¹⁹F NMR (282 MHz, CDCl₃) δ (ppm) -113.3 (1F, dd, *J* 245, 11 Hz, F_β), -125.8 – -124.4 (1.6F, m, F_{α+β}), -126.3 (0.6F, ddd, *J* 247, 17, 9 Hz, F_α), -128.0 (0.6F, dq, *J* 247, 8 Hz, F_α), -130.2 (1F, d, *J* 245 Hz, F_β), -132.6 (1F, dd, *J* 245, 15 Hz, F_β), -137.0 (0.6F, dt, *J* 247, 7 Hz, F_α); **ES⁺MS**: *m/z* 729.1 [M + Na]⁺; **HRMS** (ES+) for C₃₀H₄₆F₄O₁₄Na⁺ [M + Na]⁺ calcd 729.2716, found 729.2711.

Data for β-6.50: *R*_f 0.19 (petrol ether/acetone 70:30); [α]_D: -59.4 (c 0.5, CHCl₃, 25 °C);

IR (neat) 3481 (w, br.), 2930 (w), 1743 (s), 1371 (m), 1218 (s), 1145 (m), 1018 (s) cm⁻¹; ¹H NMR (400 MHz, CDCl₃) δ (ppm) 5.37 (1H, dt, *J* 6.8, 4.4 Hz, H-11), 5.14 (1H, dd, *J* 8.1, 2.5 Hz, H-1), 5.10 (1H, s, H-7), 5.08 (1H, m, H-8), 5.06 (1H, dd, *J* 5.6, 1.5 Hz, H-9), 4.36 (1H, dd, *J* 11.9, 4.3 Hz, H-12), 4.29 (1H, dd, *J* 5.1, 4.0 Hz, H-10), 4.26 (1H, m, H-4), 4.21 (1H, dd, *J* 11.6, 6.6 Hz, H-12'), 4.15 (1H, quin, *J* 5.4 Hz, H-5), 3.85 (1H, dd, *J* 10.6, 4.0 Hz, H-6), 3.81 (1H, dt, *J* 9.6, 7.1 Hz, H-13), 3.67 (1H, dd, *J* 10.9, 5.8 Hz, H-6'), 3.59 (1H, dt, *J* 9.6, 6.6 Hz, H-13'), 2.57 (1H, d, *J* 5.6 Hz, OH), 2.14, 2.13, 2.09, 2.07 (4 × 3H, s), 1.65 (2H, quin, *J* 6.6 Hz, H-14), 1.23–1.42 (10H, m, H-15–19), 0.89 (3H, t, *J* 6.8 Hz, H-20); ¹³C NMR (101 MHz, CDCl₃) δ (ppm) 170.4, 169.9, 169.8, 169.6 (C25–28), 105.8 (C-7), 99.5 (dd, *J* 40, 20 Hz, C-1), 81.0 (C-8), 80.5 (C-10), 77.8 (dd, *J* 28, 23 Hz, C-4), 76.2 (C-9), 69.2 (C-13, C-11), 67.5 (C-6), 67.4 (C-5), 62.4 (C-12), 31.7, 29.1, 29.1, 25.7, 22.5 (C-14–19), 20.7, 20.6, 20.6, 20.5 (C-21–24), 14.0 (C-20); ¹⁹F NMR (282 MHz, CDCl₃) δ (ppm) -112.9 (1F, dd, *J* 245, 11 Hz), -125.4 (1F, dd, *J* 246, 7 Hz), -131.1 (1F, d, *J* 247 Hz), -133.3 (1F, dd, *J* 245, 13 Hz); **ES⁺MS**: *m/z* 685.1 [M + Na]⁺; **HRMS** (ES+) for C₂₈H₄₂F₄O₁₃Na⁺ [M + Na]⁺ calcd 685.2454, found 685.2442.

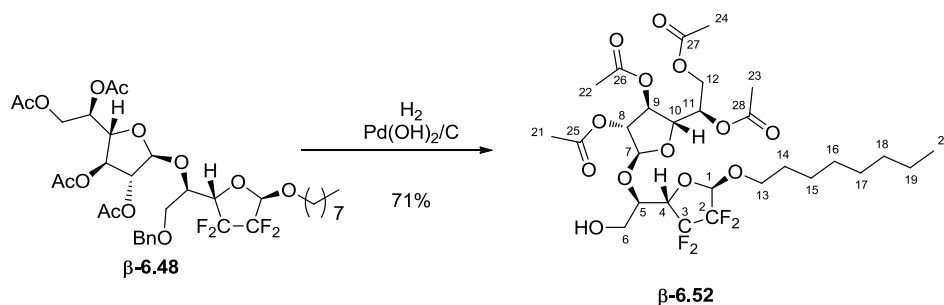
Data for α-6.50: *R*_f 0.21 (petrol ether/acetone 70:30); [α]_D: -17.2 (c 0.4, CHCl₃, 25 °C);

IR (neat) 3483 (w, br.), 2930 (w), 1744 (s), 1371 (m), 1219 (s), 1141 (m), 1029 (s) cm⁻¹; ¹H

NMR (400 MHz, CDCl₃) δ (ppm) 5.39 (1H, dt, J 6.6, 4.5 Hz, H-11), 5.00–5.18 (4H, m, H-1, H-7, H-8, H-9), 4.31–4.44 (2H, m, H-4, H-12), 4.28 (1H, t, J 4.5 Hz, H-10), 4.21 (1H, dd, J 11.6, 7.1 Hz, H-12'), 4.06 (1H, quin, J 5.6 Hz, H-5), 3.88 (1H, dt, J 9.2, 7.0 Hz, H-13), 3.81 (1H, dd, J 10.6, 5.6 Hz, H-6), 3.59–3.67 (2H, m, H-6', H-13'), 2.75 (1H, d, J 6.1 Hz, OH), 2.14, 2.12, 2.09, 2.07 (4 \times 3H, s), 1.65 (2H, t, J 6.7 Hz, H-14), 1.41–1.23 (10H, m, H-15–19), 0.89 (3H, t, J 6.8 Hz, H-20); **¹³C NMR** (101 MHz, CDCl₃) δ (ppm) 170.5, 169.9, 169.8, 169.6 (C-25–28), 105.6 (C-7), 99.9 (dd, J 38, 20 Hz, C-1), 80.9 (C-8), 80.6 (C-10), 78.7 (td, J 25, 3 Hz, C-4), 76.2 (C-9), 70.1 (C-6), 69.2 (C-11), 67.9 (t, J 3 Hz, C-5), 66.8 (C-13), 62.5 (C-12), 31.7, 29.2, 29.1, 25.7, 22.5 (C-14–19), 20.7, 20.6, 20.6, 20.5 (C-21–24), 14.0 (C-20); **¹⁹F NMR** (282 MHz, CDCl₃) δ (ppm) -125.3–-124.9 (2F, m), -125.3 (1F, dd, J 248, 8 Hz), -134.5 (1F, dt, J 248, 6 Hz); **ES⁺MS**: m/z 685.1 [M + Na]⁺; **HRMS** (ES⁺) for C₂₈H₄₂F₄O₁₃Na⁺ [M + Na]⁺ calcd 685.2454, found 685.2446.

Data for n-Octyl 5,6-di-O-(2,3,5,6-tetra-O-acetyl- β -galactofuranosyl)-2,3-dideoxy-2,2,3,3-tetrafluoro-galactofuranoside (threohexofuranoside) (6.51): **R_f** 0.11 (petrol ether/acetone 70:30); **IR** (neat) 2932 (w), 1745 (s), 1372 (m), 1223 (s), 1044 (s) cm⁻¹; **¹H NMR** (β/α 1:0.2, peaks from major anomer reported) (400 MHz, CDCl₃) δ (ppm) 5.40 (2H, dt, J 11.1, 4.5 Hz, H-11, H-11'), 5.31–5.36 (1H, m, H-7'), 5.13 (1H, dd, J 8.1, 2.5 Hz, H-1), 4.94–5.10 (5H, m, H-7, H-8, H-8', H-9, H-9'), 4.29–4.43 (4H, m, H-12, H-12', H-10, H-4), 4.13–4.29 (4H, m, H-5, H-10', H-12, H-12'), 3.91 (1H, dd, J 10.6, 3.5 Hz, H-6), 3.79 (1H, dt, J 9.5, 6.6 Hz, H-13), 3.67 (1H, dd, J 10.6, 7.1 Hz, H-6'), 3.58 (1H, dt, J 9.7, 6.8 Hz, H-13'), 2.14, 2.14, 2.11, 2.10, 2.10, 2.06, 2.06, 2.06 (8 \times 3H, s, H-21–24, H21'–24'), 1.65 (2H, quin, J 6.8 Hz, H-14), 1.25–1.40 (10H, m, H-15–19), 0.89 (3H, t, J 6.8 Hz, H-20); **¹³C NMR** (β/α 1:0.2, peaks from major anomer reported) (101 MHz, CDCl₃) δ (ppm) 170.4, 170.3, 169.8, 169.8, 169.5, 169.4 (C-25–28, C-25'–28'), 105.7 (C-7), 104.9 (C-7'), 99.4 (dd, J 38, 19 Hz, C-1), 81.2 (C-8), 80.8 (C-8'), 80.5 (C-10'), 80.4 (C-10), 77.0 (dd, J 29, 23 Hz, C-4), 76.4 (C-9, C-9'), 71.7 (C-5), 69.2 (C-11), 69.1 (C-11', C-13), 65.9 (C-6), 62.5 (C-12'), 62.5 (C-12), 31.6, 29.1, 29.0, 25.7, 22.5 (C-14–19), 20.6, 20.6, 20.5, 20.4, 20.4 (C-21–24, C-21'–24'), 13.9 (C-20); **¹⁹F NMR** (282 MHz, CDCl₃) Major (β): δ (ppm) -112.0 (1F, dd, J 245, 11 Hz), -125.0 (1F, dd, J 245, 7 Hz), -130.7 (1F, d, J 246 Hz), -132.4 (1F, dd, J 245, 13 Hz); Minor (α): δ (ppm) -125.2 (1F, d, J 248 Hz), -126.3 (m, J 7 Hz), -136.8 (dt, J 248, 6 Hz); **ES⁺MS**: m/z 1015.1 [M + Na]⁺; **HRMS** (ES⁺) for C₄₂H₆₀F₄O₂₂Na⁺ [M + Na]⁺ calcd 1015.3405, found 1015.3409.

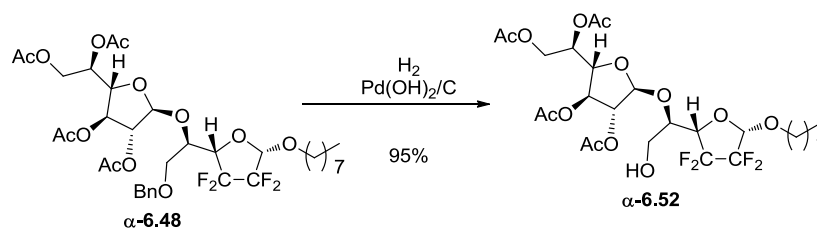
8.8.5 n-Octyl 5-*O*-(2,3,5,6-tetra-*O*-acetyl- β -galactofuranosyl)-2,3-dideoxy-2,2,3,3-tetrafluoro- β -galactofuranoside (threohexofuranoside) (β -6.52)



Disaccharide **β -6.48** (103 mg, 137 μmol) was dissolved in EtOAc (1.2 mL) and treated with $\text{Pd(OH)}_2/\text{C}$ (22 mg, 40 μmol). The reaction was flushed with H_2 then stirred under H_2 at r.t. for 19 h. The reaction mixture was diluted with EtOAc and filtered through Celite[®], which was washed with plenty of EtOAc. Concentration gave a colourless oil, which was chromatographed (petrol ether/acetone 80:20) to give disaccharide **β -6.52** as a colourless oil (64 mg, 71%).

R_f 0.26 (petrol ether/acetone 70:30); **$[\alpha]_{\text{D}}$** -55.3 (c 0.49, CHCl_3 , 26 °C); **IR** (neat) 3516 (w, br.), 2930 (m), 2858 (w), 1743 (s), 1371 (m), 1219 (s), 1144 (s), 1015 (s) cm^{-1} ; **^1H NMR** (400 MHz, CDCl_3) δ (ppm) 5.36 (1H, dt, J 7.3, 3.9 Hz, H-11), 5.25 (1H, s, H-7), 5.11 (1H, dd, J 8.1, 2.5 Hz, H-1), 5.06 (1H, dd, J 6.6, 2.5 Hz, H-9), 5.02 (1H, d, J 2.5 Hz, H-8), 4.38 (1H, dd, J 6.8, 3.3 Hz, H-10), 4.26–4.36 (1H, m, H-4), 4.33 (1H, dd, J 11.9, 4.3 Hz, H-12), 4.16 (1H, dd, J 11.9, 7.3 Hz, H-12'), 4.05 (1H, td, J 6.4, 3.8 Hz, H-5), 3.79–3.88 (2H, m, H-6 + H-6'), 3.76 (1H, dt, J 9.6, 6.6 Hz, H-13), 3.57 (1H, dt, J 9.6, 6.6 Hz, H-13'), 2.51 (1H, br. t, J 5.6, 5.6 Hz, OH), 2.13, 2.12, 2.07, 2.04 ($4 \times 3\text{H}$, s, H-21–24), 1.63 (2H, quin, J 6.9 Hz, H-14), 1.18–1.43 (10H, m, H-15–19), 0.87 (3H, t, J 6.6 Hz, H-20); **^{13}C NMR** (101 MHz, CDCl_3) δ (ppm) 170.6, 170.5, 170.0, 169.9 (C-25–28), 105.3 (C-7), 99.5 (dd, J 38, 20 Hz, C-1), 82.5 (C-8), 79.6 (C-10), 76.9 (dd, J 29, 23 Hz, C-4), 75.6 (C-9), 74.7 (C-5), 69.0 (C-13), 68.8 (C-11), 62.7 (C-12), 60.9 (d, J 3 Hz, C-6), 31.7, 29.2, 29.1, 25.8, 22.6 (C-14–19), 20.7, 20.5, 20.5 (C-21–24), 14.0 (C-20); **^{19}F NMR** (282 MHz, CDCl_3) δ (ppm) -112.9 (1F, dd, J 245, 9 Hz), -124.9 (1F, dd, J 245, 9 Hz), -129.9 (1F, d, J 245 Hz), -132.5 (1F, dd, J 245, 13 Hz); **HRMS** (ES⁺) for $\text{C}_{28}\text{H}_{42}\text{F}_4\text{O}_{13}\text{Na}^+$ $[\text{M} + \text{Na}]^+$ calcd 685.2454, found 685.2444.

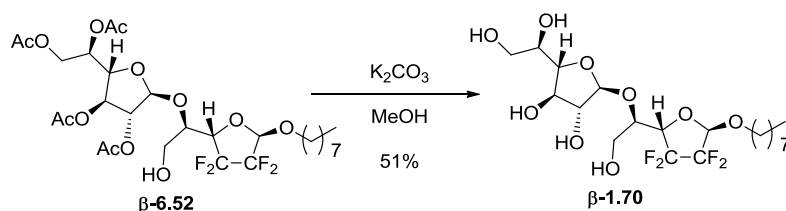
8.8.6 n-Octyl 5-*O*-(2,3,5,6-tetra-*O*-acetyl- β -galactofuranosyl)-2,3-dideoxy-2,2,3,3-tetrafluoro- α -galactofuranoside (threohexofuranoside) (**α -6.52)**



Disaccharide **α -8.7** (47 mg, 62 μ mol) was dissolved in EtOAc (1 mL) and treated with Pd(OH)₂/C (10 mg, 19 μ mol). The reaction was flushed with H₂ then stirred under H₂ at r.t. for 22 h. The reaction mixture was diluted with EtOAc and filtered through Celite[®], which was washed with plenty of EtOAc. Concentration gave a colourless oil, which was chromatographed (petrol ether/acetone 80:20) to give **α -6.52** as a colourless oil (39 mg, 95%).

R_f 0.38 (petrol ether/acetone 70:30); [α]_D +9.5 (c 0.7, CHCl₃, 28 °C); **¹H NMR** (400 MHz, CDCl₃) δ (ppm) 5.35 (1H, dt, *J* 7.2, 3.7 Hz, H-11), 5.23 (1H, s, H-7), 5.11 (1H, dd, *J* 6.6, 2.5 Hz, H-9), 4.97–5.05 (2H, m, H-8, H-1), 4.38 (1H, dd, *J* 6.1, 3.5 Hz, H-10), 4.32 (3H, dd, *J* 11.6, 4.5 Hz, H-12), 4.24–4.35 (1H, m, H-4), 4.17 (1H, dd, *J* 11.6, 7.1 Hz, H-12'), 4.00 (1H, td, *J* 6.8, 3.0 Hz, H-5), 3.81–3.92 (2H, m, H-13, H-6), 3.71–3.81 (1 H, m, H-6'), 3.56 (1H, dt, *J* 9.0, 6.6 Hz, H-13'), 2.57 (1H, br. t, *J* 6.1, 6.1 Hz, OH), 2.13, 2.13, 2.09, 2.05 (4 \times 3H, s, H-26–29), 1.62 (2H, quin, *J* 7.1 Hz, H-14), 1.21–1.42 (10H, m, H-15–19), 0.88 (3H, t, *J* 6.3 Hz, H-20); **¹³C NMR** (101 MHz, CDCl₃) δ (ppm) 170.7, 170.5, 169.9, 169.9 (C-30–33), 106.0 (C-7), 99.5 (dd, *J* 38, 20 Hz, C-1), 82.7 (C-8), 79.5 (C-10), 77.5 (C-5), 76.6 (t, *J* 23 Hz, C-4), 75.4 (C-9), 69.7 (C-13), 68.8 (C-11), 62.5 (C-12), 60.8 (d, *J* 3 Hz, C-6), 31.7, 29.2, 29.2, 29.1, 25.8, 22.6 (C-14–19), 20.7, 20.6 (C-26–29), 14.0 (C-20); **¹⁹F NMR** (282 MHz, CDCl₃) δ (ppm) -125.2 (1F, dt, *J* 248, 9Hz), -125.7 (1F, ddd, *J* 247, 18, 8 Hz), -127.2 (1F, dq, *J* 247, 8 Hz), -137.3 (1F, dt, *J* 247, 7 Hz); **ES⁺MS**: *m/z* 685.1 [M + Na]⁺; **HRMS** (ES⁺) for C₂₈H₄₂F₄O₁₃Na [M + Na]⁺ calcd 685.2454, found 685.2443.

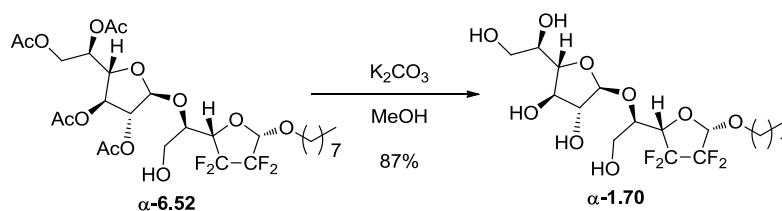
8.8.7 n-Octyl 5-*O*-(β -galactofuranosyl)-2,3-dideoxy-2,2,3,3-tetrafluoro- β -galactofuranoside (threohexofuranoside) (β -1.70)



Disaccharide **β -6.52** (57 mg, 86 μ mol) was dissolved in MeOH (4 mL) and treated with K_2CO_3 (71 mg, 520 μ mol). The reaction was stirred at r.t. for 2 h then diluted with MeOH and filtered through a thin pad of Dowex (50WX8, 50–100 mesh). The pad was washed with plenty of MeOH, which was concentrated to give an off-white waxy solid. Column chromatography (DCM/MeOH 85:15) gave disaccharide **β -1.70** as an off-white solid (22 mg, 51%).

R_f 0.25 (DCM/MeOH 85:15); **M_p** : 92–95 °C (acetone); **$[\alpha]_D$** : –113.7 (c 0.5, CH_3OH , 23 °C); **IR** (neat) 3356 (m, br.), 2928 (m), 2858 (w), 1146 (s), 1017 (s) cm^{-1} ; **1H NMR** (400 MHz, Acetone- d_6) δ (ppm) 5.37 (1H, dd, J 8.3, 2.8 Hz, H-1), 5.23 (1H, s, H-7), 4.67 (1H, d, J 8.1 Hz, OH-8), 4.48 (1H, ddd, J 16.2, 10.1, 7.6 Hz, H-4), 4.35 (1H, d, J 4.5 Hz, OH-11), 4.18 (1H, t, J 3.5 Hz, H-10), 4.15 (1H, t, J 6.1 Hz, OH-6), 4.11 (1H, ddd, J 7.6, 5.1, 3.5 Hz, H-5), 4.00 (1H, m, J 8.8 Hz can be observed, H-9), 3.96 (1H, d, J 8.1 Hz, H-8), 3.88 (1H, ddd, J 12.1, 5.1, 3.5 Hz, H-6), 3.78–3.84 (2H, m, H-11, H-13), 3.58–3.78 (6H, m, OH-9, OH-12, H-12, H-6', H-12', H-13'), 1.63 (2H, quin, J 6.6 Hz, H-14), 1.16–1.47 (10H, m, H-15–19), 0.88 (3H, t, J 7.1 Hz, H-20); **^{13}C NMR** (101 MHz, Acetone- d_6) δ (ppm) 107.6 (C-7), 100.0 (dd, J 40, 20 Hz, C-1), 87.2 (C-10), 81.2 (C-8), 79.4 (C-9), 77.6 (dd, J 29, 23 Hz, C-4), 73.3 (C-5), 72.6 (C-11), 69.5 (C-13), 64.3 (C-12), 60.4 (C-6), 32.6, 30.0, 26.7, 23.4 (C-14–19), 14.4 (C-10); **^{19}F NMR** (282 MHz, Acetone- d_6) δ (ppm) –113.6 (1F, dd, J 243, 10 Hz), –124.7 (1F, dd, J 244, 8 Hz), –129.1 (1F, d, J 245 Hz), –132.4 (1F, dd, J 243, 16 Hz); **ES^+MS** : m/z 517.2 $[M + Na]^+$; **HRMS** (ES^+) for $C_{20}H_{34}F_4O_9Na^+$ $[M + Na]^+$ calcd 517.2031, found 517.2030.

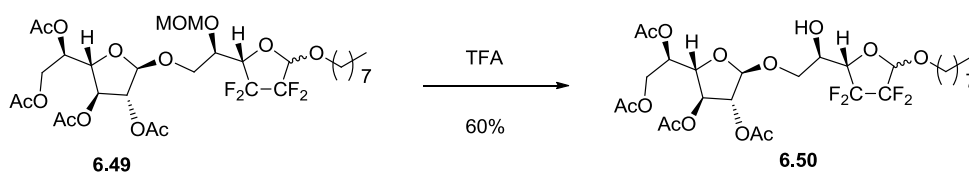
8.8.8 n-Octyl 5-*O*-(β -galactofuranosyl)-2,3-dideoxy-2,2,3,3-tetrafluoro- α -galactofuranoside (threohexofuranoside) (α -1.70)



Disaccharide **α -6.52** (37 mg, 56 μ mol) was dissolved in MeOH (2.8 mL) and treated with K_2CO_3 (46 mg, 330 μ mol). The reaction was stirred at r.t. for 45 min then diluted with MeOH and filtered through a thin pad of Dowex (50WX8, 50–100 mesh). The pad was washed with plenty of MeOH, which was concentrated to give a colourless residue. Column chromatography (DCM/MeOH 90:10) gave disaccharide **α -1.70** as a white solid (24 mg, 87%).

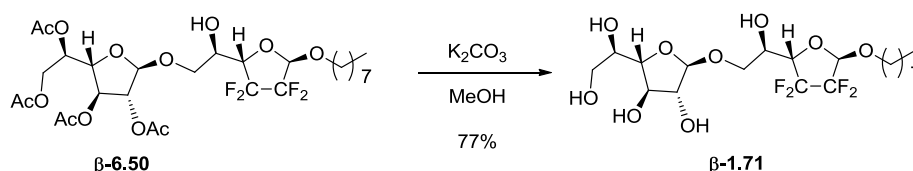
R_f 0.15 (DCM/MeOH 90:10); **Mp** 112–119 °C (CH₃OH); **[α]_D** –15.0 (c 0.4, CH₃OH, 22 °C); **IR** (neat) 3408 (m, br.), 3334 (m), 2925 (m), 2859 (m), 1114 (m), 1026 (s), 975 (s) cm^{–1}; **¹H NMR** (400 MHz, Acetone-*d*₆) δ (ppm) 5.21–5.34 (2H, m, H-1, H-7), 4.74 (1H, dd, *J* 8.1, 3.0 Hz, OH-8), 4.37–4.53 (2H, m, OH-11, H-4), 4.21 (1H, quin, *J* 3.0 Hz, H-10), 4.15 (1H, br. dd, *J* 9.6, 5.1 Hz, OH-6), 4.06 (1H, m, H-5), 3.95–4.02 (3H, m, H-9, H-8, H-13), 3.92 (1H, m, H-6), 3.77–3.87 (2H, m, H-11, OH-12), 3.74 (1H, dd, *J* 9.6, 3.0 Hz, OH-9), 3.58–3.71 (4H, m, H-6', H-13', H-12, H-12'), 1.64 (2H, quin, *J* 6.8 Hz, H-14), 1.21–1.45 (10H, m, H-15–19), 0.80–0.96 (3H, m, H-20); Peaks that resolved after D₂O shake: 4.43 (1H, dt, *J* 17.2, 9.6 Hz, H-4), 4.19 (1H, t, *J* 2.8 Hz, H-10), 4.04 (1H, dt, *J* 7.7, 4.0 Hz, H-5), 3.89 (1H, dd, *J* 12.4, 2.3 Hz, H-6), 3.79 (1H, td, *J* 6.2, 2.8 Hz, H-11); **¹³C NMR** (101 MHz, Acetone-*d*₆) δ (ppm) 107.4 (C-7), 100.2 (ddd, *J* 38, 20, 3 Hz, C-1), 87.7 (C-10), 80.9 (C-8), 79.5 (C-9), 77.4 (t, *J* 23 Hz, C-4), 74.6 (C-5), 72.8 (C-11), 70.5 (C-13), 64.2 (C-12), 60.1 (C-6), 32.6, 30.1, 30.1, 26.7, 23.4 (C-14–19), 14.4 (C-20); **¹⁹F NMR** (282 MHz, Acetone-*d*₆) δ (ppm) –125.0 (1F, dt, *J* 246, 7 Hz), –125.9 (1F, ddd, *J* 246, 17, 7 Hz), –127.2 (1F, dd, *J* 245, 5 Hz), –136.6 (1F, dt, *J* 246, 6 Hz); **ES⁺MS**: *m/z* 517.2 [M + Na]⁺; **HRMS** (ES⁺) for C₂₀H₃₄F₄O₉Na⁺ [M + Na]⁺ calcd 517.2031, found 517.2031.

8.8.9 n-Octyl 6-O-(2,3,5,6-tetra-O-acetyl- β -galactofuranosyl)-2,3-dideoxy-2,2,3,3-tetrafluorogalactofuranoside (threohexofuranoside) (**6.50**)



Disaccharide **6.49** (119 mg, 0.18 mmol) was dissolved in DCM (1.5 mL) and treated with TFA (140 μ L, 1.8 mmol). The reaction was stirred at r.t. overnight then concentrated to give a yellow oil. Column chromatography (petrol ether/acetone 90:10 then 80:20) gave disaccharide **6.50** as a colourless oil (67 mg, 60%). Separation of the anomers was achieved by preparative HPLC (hexane/acetone 80:20).

8.8.10 n-Octyl 6-O-(β -galactofuranosyl)-2,3-dideoxy-2,2,3,3-tetrafluoro- β -galactofuranoside (threohexofuranoside) (β -**1.71**)

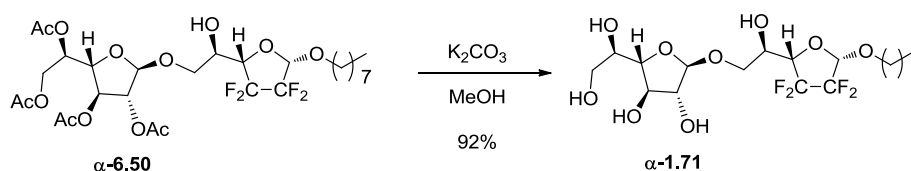


Disaccharide β -**6.50** (35 mg, 53 μ mol) was dissolved in MeOH (2.7 mL) and treated with K_2CO_3 (44 mg, 320 μ mol). The reaction was stirred at r.t. for 45 min then diluted with MeOH and filtered through a thin pad of Dowex (50WX8, 50–100 mesh). The pad was washed with plenty of MeOH, which was concentrated to give a colourless residue. Column chromatography (DCM/MeOH 90:10) followed by HPLC (MeOH/DCM 90:10) gave disaccharide β -**1.71** as a colourless oil (20 mg, 77%).

R_f 0.13 (DCM/MeOH 90:10); $[\alpha]_D -109.9$ (c 0.4, CH_3OH , 23 $^\circ\text{C}$); **IR** (neat) 3354 (m, br.), 2928 (m), 1697 (m), 1240 (m), 1148 (s), 1013 (s) cm^{-1} ; **^1H NMR** (400 MHz, Acetone- d_6) δ (ppm) 5.33 (1H, m, H-1), 4.95 (1H, m, H-7), 4.63 (1H, br. dd, J 7.1, 4.0 Hz, OH-8), 4.28–4.45 (2H, m, OH-5, H-4), 4.20 (1H, t, J 5.1 Hz, OH-11), 4.16 (1H, dd, J 6.6, 4.0 Hz, OH-9), 4.00–4.13 (3H, m, H-10, H-5, H-9), 3.97 (1H, m, H-8), 3.74–3.90 (4H, m, OH-12, H-11, H-6, H-13), 3.52–3.69 (4H, m, H-6', H-13', H-12, H-12'), 1.55–1.70 (2H, m, H-14), 1.19–1.45 (10H, m, H-15–19), 0.80–0.98 (3H, m, H-20); Peaks which resolved upon D_2O shake: δ (ppm) 5.32 (1H, dt, J 8.1, 2.5 Hz, H-1), 4.94 (1H, s, H-7), 4.36 (1H, tt, J 14.1, 4.5 Hz, H-4), 3.95 (1H, br. s, H-8); **^{13}C NMR** (101 MHz, Acetone- d_6) δ (ppm) 109.6 (C-7), 100.1 (dd, J 40, 20 Hz, C-1), 86.3 (C-10), 82.1 (C-8), 79.3 (C-9), 79.1 (dd, J 29, 25 Hz, C-4), 72.6 (C-11), 69.4, 68.4 (C-6, C-13), 68.2 (t, J 3 Hz, C-5), 64.3 (C-12), 32.6, 30.1, 30.1,

26.7, 23.4 (C-14–19), 14.4 (C-20); ^{19}F NMR (282 MHz, Acetone- d_6) δ (ppm) -111.9 (1F, dd, J 243, 12 Hz), -125.0 (1F, dd, J 243, 8 Hz), -130.9 (1F, d, J 243 Hz), -132.6 (1F, dd, J 242, 14 Hz); ES^+MS : m/z 517.2 $[\text{M} + \text{Na}]^+$; HRMS (ES+) for $\text{C}_{20}\text{H}_{34}\text{F}_4\text{O}_9\text{Na}^+ [\text{M} + \text{Na}]^+$ calcd 517.2031, found 517.2025.

8.8.11 n-Octyl 6-O-(β -galactofuranosyl)-2,3-dideoxy-2,2,3,3-tetrafluoro- α -galactofuranoside (threohexofuranoside) (α -8.2)



Disaccharide **α -6.50** (62 mg, 90 μmol) was dissolved in MeOH (4.5 mL) and treated with K_2CO_3 (75 mg, 540 μmol). The reaction was stirred at r.t. for 45 min then diluted with MeOH and filtered through a thin pad of Dowex (50WX8, 50–100 mesh). The pad was washed with plenty of MeOH, which was concentrated to give a pale yellow residue. Column chromatography (DCM/MeOH 90:10) gave disaccharide **α -1.71** as a colourless oil (41 mg, 92%).

R_f 0.09 (DCM/MeOH 90:10); $[\alpha]_D -14.7$ (c 0.7, CH_3OH , 23 $^\circ\text{C}$); IR (neat) 3352 (w, br.), 2927 (w), 2858 (w), 1140 (m), 1009 (s), 956 (s) cm^{-1} ; ^1H NMR (400 MHz, Acetone- d_6) δ (ppm) 5.27 (H, d, J 8.6 Hz, H-1), 4.95 (1H, s, H-7), 4.65 (1H, d, J 7.6 Hz, OH-8), 4.27–4.40 (2H, m, OH-5, H-4), 4.18–4.25 (2H, m, OH-11, OH-9), 4.10 (1H, dd, J 4.0, 3.0 Hz, H-10), 4.05 (1H, ddd, J 6.9, 4.4, 2.3 Hz, H-9), 4.01 (1H, m, H-5), 3.91–3.98 (2H, m, H-8, H-13), 3.89 (1H, dd, J 10.9, 3.8 Hz, H-6), 3.74–3.84 (2H, m, OH-12, H-11), 3.60–3.68 (3H, m, H-13', H-12, H-12'), 3.57 (1H, dd, J 10.6, 5.1 Hz, H-6'), 1.63 (2H, tt, J 7.6, 6.6 Hz, H-14), 1.23–1.43 (10 H, m, H-15–19), 0.88 (3H, t, J 7.1 Hz, H-20); Peaks resolved after D_2O shake: 4.33 (1H, tdd, J 14.0, 7.5, 1.5 Hz, H-4), 4.09 (1H, dd, J 4.5, 3.0 Hz, H-10), 4.04 (1H, dd, J 4.5, 2.5 Hz, H-9), 3.98 (1H, dt, J 7.8, 4.2 Hz, H-5), 3.93 (1H, dt, J 9.6, 3.0 Hz, H-13), 3.89 (1H, dd, J 11.1, 3.5 Hz, H-6), 3.75 (1H, td, J 6.1, 3.0 Hz, H-11); ^{13}C NMR (101 MHz, Acetone- d_6) δ (ppm) 109.5 (C-7), 100.2 (dd, J 38, 19 Hz, C-1), 86.4 (C-10), 82.0 (C-8), 79.3 (C-9), 79.3 (dd, J 28, 20 Hz, C-4), 72.6 (C-11), 70.0 (C-13), 69.4 (C-5), 68.0 (C-6), 64.3 (C-12), 32.6, 30.1, 30.1, 30.0, 26.7, 23.4 (C-14–19), 14.4 (C-20); ^{19}F NMR (282 MHz, Acetone- d_6) δ (ppm) -125.3–125.1 (2F, m), -125.3 (1F, m, J 245, 7 Hz can be observed), -135.6 (1F, dt, J 245, 6 Hz); ES^+MS : m/z 517.2 $[\text{M} + \text{Na}]^+$; HRMS (ES+) for $\text{C}_{20}\text{H}_{34}\text{F}_4\text{O}_9\text{Na}^+ [\text{M} + \text{Na}]^+$ calcd 517.2031, found 517.2033.

Chapter 9. References

- (1) Pauling, L. *J. Am. Chem. Soc.* **1932**, *54*, 3570-3582.
- (2) Bondi, A. *J. Phys. Chem.* **1964**, *68*, 441-451.
- (3) O'Hagan, D. *J. Org. Chem.* **2012**, *77*, 3689-3699.
- (4) Morgenthaler, M.; Schweizer, E.; Hoffmann-Röder, A.; Benini, F.; Martin, R. E.; Jaeschke, G.; Wagner, B.; Fischer, H.; Bendels, S.; Zimmerli, D.; Schneider, J.; Diederich, F.; Kansy, M.; Müller, K. *ChemMedChem* **2007**, *2*, 1100-1115.
- (5) Mukherjee, L. H.; Grunwald, E. *J. Phys. Chem.* **1958**, *62*, 1311-1314.
- (6) Arrowsmith, C. H.; Kresge, A. J.; Tang, Y. C. *J. Am. Chem. Soc.* **1991**, *113*, 179-182.
- (7) Purser, S.; Moore, P. R.; Swallow, S.; Gouverneur, V. *Chem. Soc. Rev.* **2008**, *37*, 320-330.
- (8) Graton, J.; Wang, Z.; Brossard, A.-M.; Gonçalves Monteiro, D.; Le Questel, J.-Y.; Linclau, B. *Angew. Chem., Int. Ed.* **2012**, *51*, 6176-6180.
- (9) Harrell, S. A.; McDaniel, D. H. *J. Am. Chem. Soc.* **1964**, *86*, 4497-4497.
- (10) Emsley, J. *Chem. Soc. Rev.* **1980**, *9*, 91-124.
- (11) West, R.; Powell, D. L.; Whatley, L. S.; Lee, M. K. T.; von R. Schleyer, P. *J. Am. Chem. Soc.* **1962**, *84*, 3221-3222.
- (12) Quioco, F. A. *Biochem. Soc. Trans.* **1993**, *21*, 442-448.
- (13) Dunitz, J. D.; Taylor, R. *Chem. Eur. J.* **1997**, *3*, 89-98.
- (14) Howard, J. A. K.; Hoy, V. J.; O'Hagan, D.; Smith, G. T. *Tetrahedron* **1996**, *52*, 12613-12622.
- (15) Barbarich, T. J.; Rithner, C. D.; Miller, S. M.; Anderson, O. P.; Strauss, S. H. *J. Am. Chem. Soc.* **1999**, *121*, 4280-4281.
- (16) Carosati, E.; Sciabola, S.; Cruciani, G. *J. Med. Chem.* **2004**, *47*, 5114-5125.
- (17) Fröhlich, R.; Rosen, T. C.; Meyer, O. G. J.; Rissanen, K.; Haufe, G. *J. Mol. Struct.* **2006**, *787*, 50-62.
- (18) Bernet, B.; Vasella, A. *Helv. Chim. Acta* **2000**, *83*, 995-1021.
- (19) Bernet, B.; Vasella, A. *Helv. Chim. Acta* **2007**, *90*, 1874-1888.
- (20) Chandler, D. *Nature* **2005**, *437*, 640-647.
- (21) Gao, J. M.; Qiao, S.; Whitesides, G. M. *J. Med. Chem.* **1995**, *38*, 2292-2301.
- (22) Mecinovic, J.; Snyder, P. W.; Mirica, K. A.; Bai, S.; Mack, E. T.; Kwant, R. L.; Moustakas, D. T.; Heroux, A.; Whitesides, G. M. *J. Am. Chem. Soc.* **2011**, *133*, 14017-14026.
- (23) Olsen, J. A.; Banner, D. W.; Seiler, P.; Wagner, B.; Tschopp, T.; Obst-Sander, U.; Kansy, M.; Müller, K.; Diederich, F. *ChemBioChem* **2004**, *5*, 666-675.
- (24) Olsen, J. A.; Banner, D. W.; Seiler, P.; Obst Sander, U.; D'Arcy, A.; Stihle, M.; Müller, K.; Diederich, F. *Angew. Chem., Int. Ed.* **2003**, *42*, 2507-2511.
- (25) Vulpetti, A.; Hommel, U.; Landrum, G.; Lewis, R.; Dalvit, C. *J. Am. Chem. Soc.* **2009**, *131*, 12949-12959.
- (26) Vulpetti, A.; Schiering, N.; Dalvit, C. *Proteins: Struct., Funct., Bioinf.* **2010**, *78*, 3281-3291.
- (27) Dalvit, C.; Vulpetti, A. *ChemMedChem* **2011**, *6*, 104-114.
- (28) Dalvit, C.; Vulpetti, A. *ChemMedChem* **2012**, *7*, 262-272.
- (29) Muller, K.; Faeh, C.; Diederich, F. *Science* **2007**, *317*, 1881-1886.
- (30) O'Hagan, D. *Chem. Soc. Rev.* **2008**, *37*, 308-319.
- (31) Chenoweth, M. B.; McCarty, L. P. *Pharmacol. Rev.* **1963**, *15*, 673-707.
- (32) O'Hagan, D.; S. Rzepa, H. *Chem. Commun.* **1997**, 645-652.
- (33) Patani, G. A.; LaVoie, E. J. *Chem. Rev.* **1996**, *96*, 3147-3176.
- (34) Phillipps, G. H.; Bailey, E. J.; Bain, B. M.; Borella, R. A.; Buckton, J. B.; Clark, J. C.; Doherty, A. E.; English, A. F.; Fazakerley, H. *J. Med. Chem.* **1994**, *37*, 3717-3729.

- (35) Millan, D. S.; Ballard, S. A.; Chunn, S.; Dybowski, J. A.; Fulton, C. K.; Glossop, P. A.; Guillabert, E.; Hewson, C. A.; Jones, R. M.; Lamb, D. J.; Napier, C. M.; Payne-Cook, T. A.; Renery, E. R.; Selby, M. D.; Tutt, M. F.; Yeadon, M. *Bioorg. Med. Chem. Lett.* **2011**, *21*, 5826-5830.
- (36) London, R. E.; Gabel, S. A. *Biophys. J.* **1995**, *69*, 1814-1818.
- (37) Allman, S. A.; Jensen, H. H.; Vijayakrishnan, B.; Garnett, J. A.; Leon, E.; Liu, Y.; Anthony, D. C.; Sibson, N. R.; Feizi, T.; Matthews, S.; Davis, B. G. *ChemBioChem* **2009**, *10*, 2522-2529.
- (38) Bessell, E. M.; Westwood, J. H.; Foster, A. B. *Biochem. J.* **1972**, *128*, 199-&.
- (39) Glaudemans, C. P. J. *Chem. Rev.* **1991**, *91*, 25-33.
- (40) Street, I. P.; Armstrong, C. R.; Withers, S. G. *Biochemistry* **1986**, *25*, 6021-6027.
- (41) McCarter, J. D.; Adam, M. J.; Hartman, N. G.; Withers, S. G. *Biochem. J.* **1994**, *301*, 343-348.
- (42) Xia, Z.; Azurmendi, H. F.; Lairson, L. L.; Withers, S. G.; Gabelli, S. B.; Bianchet, M. A.; Amzel, L. M.; Mildvan, A. S. *Biochemistry* **2005**, *44*, 8989-8997.
- (43) Forconi, M.; Schwans, Jason P.; Porecha, Rishi H.; Sengupta, Raghuvir N.; Piccirilli, Joseph A.; Herschlag, D. *Chem. Biol.* **2011**, *18*, 949-954.
- (44) Sen, A. K.; Widdas, W. F. *J. Physiol. (London)* **1962**, *160*, 392-403.
- (45) Riley, G. J.; Taylor, N. F. *Biochem. J.* **1973**, *135*, 773-777.
- (46) Kim, H. W.; Rossi, P.; Shoemaker, R. K.; DiMagno, S. G. *J. Am. Chem. Soc.* **1998**, *120*, 9082-9083.
- (47) Bresciani, S.; Lebl, T.; Slawin, A. M. Z.; O'Hagan, D. *Chem. Commun.* **2010**, *46*, 5434-5436.
- (48) Varki, A. *Glycobiology* **1993**, *3*, 97-130.
- (49) Varki, A. *Essentials of Glycobiology*; Cold Spring Harbor Laboratory Press, 2009.
- (50) Stallforth, P.; Lepenies, B.; Adibekian, A.; Seeberger, P. H. *J. Med. Chem.* **2009**, *52*, 5561-5577.
- (51) Weymouth-Wilson, A. C. *Nat. Prod. Rep.* **1997**, *14*, 99-110.
- (52) Langenhan, J. M.; Griffith, B. R.; Thorson, J. S. *J. Nat. Prod.* **2005**, *68*, 1696-1711.
- (53) Cipolla, L.; Peri, F. *Mini-Rev. Med. Chem.* **2011**, *11*, 39-54.
- (54) Sears, P.; Wong, C.-H. *Angew. Chem., Int. Ed.* **1999**, *38*, 2300-2324.
- (55) McCarter, J. D.; Adam, M. J.; Withers, S. G. *Biochem. J.* **1992**, *286*, 721-727.
- (56) Angus, D. I.; Kiefel, M. J.; Itzstein, M. v. *Bioorg. Med. Chem.* **2000**, *8*, 2709-2718.
- (57) Quiocho, F. A. *Pure Appl. Chem.* **1989**, *61*, 1293-1306.
- (58) Davis, A. M.; Teague, S. J. *Angew. Chem., Int. Ed.* **1999**, *38*, 736-749.
- (59) Engelsen, S. B.; Monteiro, C.; Hervé de Penhoat, C.; Pérez, S. *Biophys. Chem.* **2001**, *93*, 103-127.
- (60) Toone, E. J. *Curr. Opin. Struct. Biol.* **1994**, *4*, 719-728.
- (61) Lemieux, R. U. *Acc. Chem. Res.* **1996**, *29*, 373-380.
- (62) Lemieux, R. U. *Chem. Soc. Rev.* **1989**, *18*, 347-374.
- (63) Davis, A. P. *Org. Biomol. Chem.* **2009**, *7*, 3629-3638.
- (64) Barwell, N. P.; Davis, A. P. *J. Org. Chem.* **2011**, *76*, 6548-6557.
- (65) Biffinger, J. C.; Kim, H. W.; DiMagno, S. G. *ChemBioChem* **2004**, *5*, 622-627.
- (66) Timofte, R. S.; Linclau, B. *Org. Lett.* **2008**, *10*, 3673-3676.
- (67) McNaught, A. D. *Adv. Carbohydr. Chem. Biochem.* **1997**, *52*, 43-177.
- (68) Shelling, J. G.; Dolphin, D.; Wirz, P.; Cobbledick, R. E.; Einstein, F. W. B. *Carbohydr. Res.* **1984**, *132*, 241-259.
- (69) Pacak, J.; Tocik, Z.; Podesva, J.; Cerny, M. *Collect. Czech. Chem. Commun.* **1972**, *37*, 2589-&.
- (70) Sarda, P.; Escribano, F. C.; José Alves, R.; Olesker, A.; Lukacs, G. *J. Carbohydr. Chem.* **1989**, *8*, 115-123.
- (71) Bresciani, S.; Slawin, A. M. Z.; O'Hagan, D. *J. Fluorine Chem.* **2009**, *130*, 537-543.
- (72) Gassman, P. G.; O'Reilly, N. J. *J. Org. Chem.* **1987**, *52*, 2481-2490.
- (73) Boydell, A. J.; Vinader, V.; Linclau, B. *Angew. Chem., Int. Ed.* **2004**, *43*, 5677-5679.
- (74) Linclau, B.; Boydell, A. J.; Timofte, R. S.; Brown, K. J.; Vinader, V.; Weymouth-Wilson, A. C. *Org. Biomol. Chem.* **2009**, *7*, 803-814.

- (75) Demchenko, A. V. *Synlett* **2003**, 1225-1240.
- (76) Kempton, J. B.; Withers, S. G. *Biochemistry* **1992**, *31*, 9961-9969.
- (77) Bucher, C.; Gilmour, R. *Angew. Chem., Int. Ed.* **2010**, *49*, 8724-8728.
- (78) Gabius, H.-J.; Siebert, H.-C.; André, S.; Jiménez-Barbero, J.; Rüdiger, H. *ChemBioChem* **2004**, *5*, 740-764.
- (79) Wu, F.-H.; Huang, W.-Y. *J. Fluorine Chem.* **1998**, *92*, 85-87.
- (80) Kolb, H. C.; VanNieuwenhze, M. S.; Sharpless, K. B. *Chem. Rev.* **1994**, *94*, 2483-2547.
- (81) Morelli, C. F.; Fornili, A.; Sironi, M.; Duri, L.; Speranza, G.; Manitto, P. *Tetrahedron: Asymmetry* **2002**, *13*, 2609-2618.
- (82) Vilsmeier, A.; Haack, A. *Ber. Dtsch. Chem. Ges.* **1927**, *60*, 119-122.
- (83) Mizutani, K.; Yamazaki, T.; Kitazume, T. *J. Chem. Soc., Chem. Commun.* **1995**, 51-52.
- (84) Yamazaki, T.; Oniki, T.; Kitazume, T. *Tetrahedron* **1996**, *52*, 11753-11762.
- (85) Yamazaki, T.; Mizutani, K.; Kitazume, T. *J. Org. Chem.* **1993**, *58*, 4346-4359.
- (86) Mackie, W.; Perlin, A. S. *Can. J. Chem.* **1966**, *44*, 2039-2049.
- (87) Stork, G.; Takahashi, T. *J. Am. Chem. Soc.* **1977**, *99*, 1275-1276.
- (88) Sato, K.-i.; Sakai, K.; Tsushima, K.; Akai, S. *Tetrahedron Lett.* **2007**, *48*, 3745-3748.
- (89) Olson, S. H.; Balkovec, J. M.; Zhu, Y.; Merck and Co Inc: 2007; Vol. US 07179802.
- (90) Linclau, B.; Golten, S.; Light, M.; Sebban, M.; Oulyadi, H. *Carbohydr. Res.* **2011**, *346*, 1129-1139.
- (91) Wray, V. J. *J. Chem. Soc., Perkin Trans. 2* **1976**, 1598-1605.
- (92) Lemieux, R. U.; Stevens, J. D. *Can. J. Chem.* **1965**, *43*, 2059-2070.
- (93) Jeffrey, G. *Acta Crystallogr., Sect. B* **1990**, *46*, 89-103.
- (94) Linclau, B.; Golten, S.; Light, M. *J. Carbohydr. Chem.* **2011**, *30*, 618-625.
- (95) Boydell, A. J. Ph. D. Thesis, University of Southampton, 2007.
- (96) Timofte, R. S. Ph. D. Thesis, University of Southampton, 2007.
- (97) Martin, S. F.; Dodge, J. A. *Tetrahedron Lett.* **1991**, *32*, 3017-3020.
- (98) Saïah, M.; Bessodes, M.; Antonakis, K. *Tetrahedron Lett.* **1992**, *33*, 4317-4320.
- (99) Perlmutter, P.; Vounatsos, F. J. *Carbohydr. Chem.* **2003**, *22*, 719-732.
- (100) Camp, D.; Jenkins, I. D. *J. Org. Chem.* **1989**, *54*, 3045-3049.
- (101) Hughes, D. L.; Reamer, R. A. *J. Org. Chem.* **1996**, *61*, 2967-2971.
- (102) Zhao, Y.-R.; Guang, B.; Bouillon, R.; Verstuyf, A.; De Clercq, P.; Vandewalle, M. *Eur. J. Org. Chem.* **2005**, *2005*, 4414-4427.
- (103) Crosignani, S.; Young, A. C.; Linclau, B. *Tetrahedron Lett.* **2004**, *45*, 9611-9615.
- (104) Chighine, A.; Crosignani, S.; Arnal, M. C.; Bradley, M.; Linclau, B. *J. Org. Chem.* **2009**, *74*, 4753-4762.
- (105) Paulsen, H.; Rutz, V.; Brockhausen, I. *Liebigs Ann. Chem.* **1992**, 735-745.
- (106) Hederos, M.; Konradsson, P. J. *Carbohydr. Chem.* **2005**, *24*, 297-320.
- (107) Errey, J. C.; Mann, M. C.; Fairhurst, S. A.; Hill, L.; McNeil, M. R.; Naismith, J. H.; Percy, J. M.; Whitfield, C.; Field, R. A. *Org. Biomol. Chem.* **2009**, *7*, 1009-1016.
- (108) Kysilka, O.; Rybackova, M.; Skalicky, M.; Kvicálová, M.; Cvacka, J.; Kvicál, J. *Collect. Czech. Chem. Commun.* **2008**, *73*, 1799-1813.
- (109) Katagiri, T.; Irie, M.; Uneyama, K. *Tetrahedron: Asymmetry* **1999**, *10*, 2583-2589.
- (110) Li, K. Q.; Leriche, C.; Liu, H. W. *Bioorg. Med. Chem. Lett.* **1998**, *8*, 1097-1100.
- (111) Yue, X.; Wu, Y.-Y.; Qing, F.-L. *Tetrahedron* **2007**, *63*, 1560-1567.
- (112) Nakai, K.; Takagi, Y.; Ogawa, S.; Tsuchiya, T. *Carbohydr. Res.* **1999**, *320*, 8-18.
- (113) Bell, A. A.; Pickering, L.; Finn, M.; de la Fuente, C.; Krülle, T. M.; Davis, B. G.; Fleet, G. W. J. *Synlett* **1997**, *1997*, 1077,1078.
- (114) Xu, X.-H.; Qiu, X.-L.; Zhang, X.; Qing, F.-L. *J. Org. Chem.* **2006**, *71*, 2820-2824.
- (115) Katsuki, T.; Sharpless, K. B. *J. Am. Chem. Soc.* **1980**, *102*, 5974-5976.

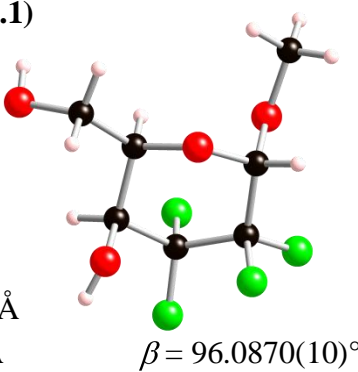
- (116) Gao, Y.; Klunder, J. M.; Hanson, R. M.; Masamune, H.; Ko, S. Y.; Sharpless, K. B. *J. Am. Chem. Soc.* **1987**, *109*, 5765-5780.
- (117) Carlsen, P. H. J.; Katsuki, T.; Martin, V. S.; Sharpless, K. B. *J. Org. Chem.* **1981**, *46*, 3936-3938.
- (118) Oldendorf, J.; Haufe, G. *Eur. J. Org. Chem.* **2006**, *2006*, 4463-4472.
- (119) Hunter, L.; Kirsch, P.; Slawin, A. M. Z.; O'Hagan, D. *Angew. Chem., Int. Ed.* **2009**, *48*, 5457-5460.
- (120) Jiang, Z. X.; Qing, F. L. *J. Org. Chem.* **2004**, *69*, 5486-5489.
- (121) Ogawa, S.; Watanabe, M.; Maruyama, A.; Hisamatsu, S. *Bioorg. Med. Chem. Lett.* **2002**, *12*, 749-752.
- (122) Takahashi, T.; Tsukamoto, H.; Yamada, H. *Org. Lett.* **1999**, *1*, 1885-1887.
- (123) Ben Othman, R.; Affani, R.; Tranchant, M.-J.; Antoniotti, S.; Dalla, V.; Duñach, E. *Angew. Chem., Int. Ed.* **2010**, *49*, 776-780.
- (124) Zhu, X.; Schmidt, R. R. *Angew. Chem., Int. Ed.* **2009**, *48*, 1900-1934.
- (125) Schmidt, R. R.; Michel, J. *Angewandte Chemie International Edition in English* **1980**, *19*, 731-732.
- (126) Larsen, K.; Olsen, C. E.; Motawia, M. S. *Carbohydr. Res.* **2008**, *343*, 383-387.
- (127) Inaba, S.; Yamada, M.; Yoshino, T.; Ishido, Y. *J. Am. Chem. Soc.* **1973**, *95*, 2062-2063.
- (128) Imori, T.; Shibazaki, T.; Ikegami, S. *Tetrahedron Lett.* **1996**, *37*, 2267-2270.
- (129) Azumaya, I.; Niwa, T.; Kotani, M.; Imori, T.; Ikegami, S. *Tetrahedron Lett.* **1999**, *40*, 4683-4686.
- (130) Nokami, T.; Nozaki, Y.; Saigusa, Y.; Shibuya, A.; Manabe, S.; Ito, Y.; Yoshida, J.-i. *Org. Lett.* **2011**, *13*, 1544-1547.
- (131) Crich, D.; Sun, S. *J. Org. Chem.* **1997**, *62*, 1198-1199.
- (132) Crich, D. *Acc. Chem. Res.* **2010**, *43*, 1144-1153.
- (133) Berg, S.; Kaur, D.; Jackson, M.; Brennan, P. J. *Glycobiology* **2007**, *17*, 35R-56R.
- (134) Peltier, P.; Euzen, R.; Daniellou, R.; Nugier-Chauvin, C.; Ferrieres, V. *Carbohydr. Res.* **2008**, *343*, 1897-1923.
- (135) Richards, M. R.; Lowary, T. L. *ChemBioChem* **2009**, *10*, 1920-1938.
- (136) Pedersen, L. L.; Turco, S. J. *Cell. Mol. Life Sci.* **2003**, *60*, 259-266.
- (137) Houseknecht, J. B.; Lowary, T. L. *Curr. Opin. Chem. Biol.* **2001**, *5*, 677-682.
- (138) Beláňová, M.; Dianišková, P.; Brennan, P. J.; Completo, G. C.; Rose, N. L.; Lowary, T. L.; Mikušová, K. *J. Bacteriol.* **2008**, *190*, 1141-1145.
- (139) Rose, N. L.; Completo, G. C.; Lin, S.-J.; McNeil, M.; Palcic, M. M.; Lowary, T. L. *J. Am. Chem. Soc.* **2006**, *128*, 6721-6729.
- (140) Barlow, J. N.; Girvin, M. E.; Blanchard, J. S. *J. Am. Chem. Soc.* **1999**, *121*, 6968-6969.
- (141) Barlow, J. N.; Blanchard, J. S. *Carbohydr. Res.* **2000**, *328*, 473-480.
- (142) Burton, A.; Wyatt, P.; Boons, G. J. *J. Chem. Soc., Perkin Trans. 1* **1997**, 2375-2382.
- (143) Zhang, Q.; Liu, H.-w. *J. Am. Chem. Soc.* **2001**, *123*, 6756-6766.
- (144) Zhang, Q.; Liu, H.-w. *J. Am. Chem. Soc.* **2000**, *122*, 9065-9070.
- (145) Yuan, Y.; Bleile, D. W.; Wen, X.; Sanders, D. A. R.; Itoh, K.; Liu, H.-w.; Pinto, B. M. *J. Am. Chem. Soc.* **2008**, *130*, 3157-3168.
- (146) Soltero-Higgin, M.; Carlson, E. E.; Gruber, T. D.; Kiessling, L. L. *Nat. Struct. Mol. Biol.* **2004**, *11*, 539-543.
- (147) Gruber, T. D.; Westler, W. M.; Kiessling, L. L.; Forest, K. T. *Biochemistry* **2009**, *48*, 9171-9173.
- (148) Sun, H. G.; Ruszczycky, M. W.; Chang, W. C.; Thibodeaux, C. J.; Liu, H. W. *J. Biol. Chem.* **2012**, *287*, 4602-4608.
- (149) Itoh, K.; Huang, Z.; Liu, H.-w. *Org. Lett.* **2007**, *9*, 879-882.
- (150) Caravano, A.; Mengin-Lecreulx, D.; Brondello, J.-M.; Vincent, S. P.; Sinaÿ, P. *Chem. Eur. J.* **2003**, *9*, 5888-5898.
- (151) Caravano, A.; Vincent, S. P. *Eur. J. Org. Chem.* **2009**, *2009*, 1771-1780.
- (152) Zhang, Q.; Liu, H.-w. *Bioorg. Med. Chem. Lett.* **2001**, *11*, 145-149.
- (153) Caravano, A.; Dohi, H.; Sinaÿ, P.; Vincent, S. P. *Chem. Eur. J.* **2006**, *12*, 3114-3123.

- (154) Szczepina, M. G.; Zheng, R. B.; Completo, G. C.; Lowary, T. L.; Pinto, B. M. *ChemBioChem* **2009**, *10*, 2052-2059.
- (155) Brown, C. D.; Rusek, M. S.; Kiessling, L. L. *J. Am. Chem. Soc.* **2012**, *134*, 6552-6555.
- (156) Poulin, M. B.; Zhou, R.; Lowary, T. L. *Org. Biomol. Chem.* **2012**, *10*, 4074-4087.
- (157) Pathak, A. K.; Pathak, V.; Seitz, L.; Maddry, J. A.; Gurcha, S. S.; Besra, G. S.; Suling, W. J.; Reynolds, R. C. *Bioorg. Med. Chem.* **2001**, *9*, 3129-3143.
- (158) Pallanca, J. E.; Turner, N. J. *J. Chem. Soc., Perkin Trans. 1* **1993**, 3017-3022.
- (159) Maeda, T.; Nishimura, S. I. *Chem. Eur. J.* **2008**, *14*, 478-487.
- (160) Vincent, S. P.; Gastinel, L. N. *Carbohydr. Res.* **2002**, *337*, 1039-1042.
- (161) Chang, Y.-K.; Lee, J.; Park, G.-S.; Lee, M.; Park, C. H.; Kim, H. K.; Lee, G.; Lee, B.-Y.; Baek, J. Y.; Kim, K. S. *Tetrahedron* **2010**, *66*, 5687-5691.
- (162) Zhang, W.; Robins, M. J. *Tetrahedron Lett.* **1992**, *33*, 1177-1180.
- (163) Zhang, Y.; Fechter, E. J.; Wang, T.-S. A.; Barrett, D.; Walker, S.; Kahne, D. E. *J. Am. Chem. Soc.* **2007**, *129*, 3080-3081.
- (164) Illarionov, P. A.; Torgov, V. I.; Hancock, I. I.; Shibaev, V. N. *Russ. Chem. Bull.* **2001**, *50*, 1303-1308.
- (165) Kelly, D. R.; Roberts, S. M.; Newton, R. F. *Synth. Commun.* **1979**, *9*, 295-299.
- (166) Hattori, K.; Sajiki, H.; Hirota, K. *Tetrahedron* **2001**, *57*, 2109-2114.
- (167) Leung, L. M. H.; Gibson, V.; Linclau, B. *J. Org. Chem.* **2008**, *73*, 9197-9206.
- (168) Ferrières, V.; Bertho, J.-N.; Plusquellec, D. *Carbohydr. Res.* **1998**, *311*, 25-35.
- (169) Ferrières, V.; Gelin, M.; Boulch, R.; Toupet, L. c.; Plusquellec, D. *Carbohydr. Res.* **1998**, *314*, 79-83.
- (170) Yang, Y.; Li, Y.; Yu, B. *J. Am. Chem. Soc.* **2009**, *131*, 12076-12077.
- (171) Prabhakaran, P. C.; Gould, S. J.; Orr, G. R.; Coward, J. K. *J. Am. Chem. Soc.* **1988**, *110*, 5779-5784.

Chapter 10. Appendices

10.1 Appendix A: X-Ray Crystal Structure Data

Table 1. Crystal data and structure refinement details.

Identification code	2010sot0050 (3.1)	
Empirical formula	C ₇ H ₁₀ F ₄ O ₄	
Formula weight	234.15	
Temperature	120(2) K	
Wavelength	0.71073 Å	
Crystal system	Monoclinic	
Space group	<i>P</i> 2 ₁	
Unit cell dimensions	<i>a</i> = 12.2256(5) Å <i>b</i> = 8.2904(2) Å <i>c</i> = 13.8049(5) Å	$\beta = 96.0870(10)^\circ$
Volume	1391.31(8) Å ³	
<i>Z</i>	6 (<i>Z'</i> = 3)	
Density (calculated)	1.677 Mg / m ³	
Absorption coefficient	0.182 mm ⁻¹	
<i>F</i> (000)	720	
Crystal	Rod; Colourless	
Crystal size	0.40 × 0.10 × 0.04 mm ³	
θ range for data collection	2.97 – 27.48°	
Index ranges	–15 ≤ <i>h</i> ≤ 15, –10 ≤ <i>k</i> ≤ 10, –17 ≤ <i>l</i> ≤ 17	
Reflections collected	19386	
Independent reflections	3399 [<i>R</i> _{int} = 0.0607]	
Completeness to $\theta = 27.48^\circ$	99.8 %	
Absorption correction	Semi-empirical from equivalents	
Max. and min. transmission	0.9927 and 0.9306	
Refinement method	Full-matrix least-squares on <i>F</i> ²	
Data / restraints / parameters	3399 / 1 / 415	
Goodness-of-fit on <i>F</i> ²	1.109	
Final <i>R</i> indices [<i>F</i> ² > 2σ(<i>F</i> ²)]	<i>R</i> 1 = 0.0393, <i>wR</i> 2 = 0.0852	
<i>R</i> indices (all data)	<i>R</i> 1 = 0.0562, <i>wR</i> 2 = 0.0930	
Absolute structure parameter	10(10)	
Largest diff. peak and hole	0.252 and –0.313 e Å ⁻³	

Diffraction: Nonius KappaCCD area detector (ϕ scans and ω scans to fill *asymmetric unit*). **Cell determination:** DirAx (Duisenberg, A.J.M.(1992). *J. Appl. Cryst.* 25, 92-96.) **Data collection:** Collect (Collect: Data collection software, R. Hooft, Nonius B.V., 1998). **Data reduction and cell refinement:** Denzo (Z. Otwinowski & W. Minor, *Methods in Enzymology* (1997) Vol. 276: *Macromolecular Crystallography*, part A, pp. 307–326; C. W. Carter, Jr. & R. M. Sweet, Eds., Academic Press). **Absorption correction:** Sheldrick, G. M. SADABS - Bruker Nonius area detector scaling and absorption correction - V2.10 **Structure solution:** SHELXS97 (G. M. Sheldrick, *Acta Cryst.* (1990) A46 467–473). **Structure refinement:** SHELXL97 (G. M. Sheldrick (1997), University of Göttingen, Germany). **Graphics:** Cameron - A Molecular Graphics Package. (D. M. Watkin, L. Pearce and C. K. Prout, Chemical Crystallography Laboratory, University of Oxford, 1993).

Special details: All hydrogen atoms were placed in idealised positions and refined using a riding model.

Table 2. Atomic coordinates [$\times 10^4$], equivalent isotropic displacement parameters [$\text{\AA}^2 \times 10^3$] and site occupancy factors. U_{eq} is defined as one third of the trace of the orthogonalized U_{ij} tensor.

Atom	x	y	z	U_{eq}	$S.o.f.$
F101	935(2)	7232(2)	8965(2)	38(1)	1
F102	178(2)	6074(3)	7642(2)	40(1)	1
F103	788(2)	4589(3)	10007(1)	33(1)	1
F104	-782(2)	5055(3)	9159(2)	46(1)	1
O101	2733(2)	5232(3)	9053(2)	22(1)	1
O102	-434(2)	2707(3)	7871(2)	36(1)	1
O103	1397(2)	2481(2)	8549(2)	21(1)	1
O104	3280(2)	3554(3)	6802(2)	30(1)	1
C101	2880(3)	2741(4)	7591(2)	26(1)	1
C102	1822(3)	3507(4)	7833(2)	22(1)	1
C103	1954(3)	5220(4)	8223(2)	21(1)	1
C104	848(3)	5799(4)	8486(2)	27(1)	1
C105	264(3)	4578(5)	9080(2)	28(1)	1
C106	301(3)	2849(4)	8712(2)	26(1)	1
C107	-603(4)	1047(5)	7585(3)	46(1)	1
F201	7602(2)	2118(2)	5497(1)	26(1)	1
F202	8810(1)	1907(2)	4451(1)	28(1)	1
F203	7680(1)	3789(2)	3178(1)	24(1)	1
F204	6604(1)	1977(2)	3705(1)	24(1)	1
O201	9388(2)	5036(3)	4599(2)	23(1)	1
O202	5779(2)	4085(2)	4904(2)	19(1)	1
O203	7077(2)	6021(2)	4562(1)	17(1)	1
O204	8836(2)	8071(3)	4954(2)	24(1)	1
C201	8325(3)	7332(4)	5725(2)	22(1)	1
C202	7804(2)	5711(4)	5435(2)	18(1)	1
C203	8657(2)	4429(4)	5247(2)	21(1)	1
C204	8070(2)	2945(4)	4789(2)	20(1)	1
C205	7182(2)	3331(3)	3969(2)	19(1)	1
C206	6420(2)	4686(4)	4229(2)	18(1)	1
C207	4860(3)	5113(4)	5042(3)	26(1)	1
F301	3129(2)	4483(2)	1568(1)	30(1)	1
F302	2276(2)	2310(2)	1973(1)	29(1)	1
F303	5068(1)	3230(2)	2043(1)	25(1)	1
F304	4039(2)	2706(2)	3199(1)	27(1)	1
O301	3981(2)	2959(2)	61(2)	23(1)	1
O302	3724(2)	-328(3)	2619(2)	25(1)	1
O303	4511(2)	176(2)	1175(2)	18(1)	1
O304	3707(2)	-2080(2)	-264(2)	24(1)	1
C301	3505(3)	-387(4)	-364(2)	22(1)	1
C302	3446(2)	374(4)	625(2)	18(1)	1

C303	3183(3)	2165(4)	558(2)	21(1)	1
C304	3193(3)	2844(4)	1583(2)	21(1)	1
C305	4205(3)	2333(4)	2264(2)	20(1)	1
C306	4502(3)	553(4)	2169(2)	19(1)	1
C307	3919(3)	-2045(4)	2606(3)	32(1)	1

Table 3. Bond lengths [Å] and angles [°].

F101–C104	1.359(4)	C106–O102–C107	111.7(3)
F102–C104	1.370(4)	C106–O103–C102	113.5(2)
F103–C105	1.369(4)	O104–C101–C102	110.2(3)
F104–C105	1.354(4)	O103–C102–C101	106.5(3)
O101–C103	1.410(4)	O103–C102–C103	109.9(2)
O102–C106	1.395(4)	C101–C102–C103	114.1(3)
O102–C107	1.441(5)	O101–C103–C104	110.3(3)
O103–C106	1.415(4)	O101–C103–C102	109.4(2)
O103–C102	1.441(4)	C104–C103–C102	108.4(3)
O104–C101	1.411(4)	F101–C104–F102	106.1(2)
C101–C102	1.510(4)	F101–C104–C103	111.5(3)
C102–C103	1.522(4)	F102–C104–C103	108.5(3)
C103–C104	1.515(5)	F101–C104–C105	109.6(3)
C104–C105	1.527(5)	F102–C104–C105	107.2(3)
C105–C106	1.523(5)	C103–C104–C105	113.5(3)
F201–C204	1.367(3)	F104–C105–F103	106.0(3)
F202–C204	1.366(3)	F104–C105–C106	111.3(3)
F203–C205	1.360(3)	F103–C105–C106	106.9(3)
F204–C205	1.355(3)	F104–C105–C104	110.4(3)
O201–C203	1.422(4)	F103–C105–C104	107.3(3)
O202–C206	1.374(4)	C106–C105–C104	114.4(3)
O202–C207	1.438(4)	O102–C106–O103	112.7(3)
O203–C206	1.415(4)	O102–C106–C105	108.5(3)
O203–C202	1.443(4)	O103–C106–C105	108.5(3)
O204–C201	1.429(4)	C206–O202–C207	112.6(2)
C201–C202	1.522(4)	C206–O203–C202	114.2(2)
C202–C203	1.530(4)	O204–C201–C202	112.8(3)

C203–C204	1.527(4)	O203–C202–C201	105.4(2)
C204–C205	1.518(4)	O203–C202–C203	110.6(2)
C205–C206	1.526(4)	C201–C202–C203	112.6(2)
F301–C304	1.361(4)	O201–C203–C204	108.9(3)
F302–C304	1.368(4)	O201–C203–C202	110.2(2)
F303–C305	1.352(4)	C204–C203–C202	109.3(2)
F304–C305	1.364(3)	F202–C204–F201	105.7(2)
O301–C303	1.413(4)	F202–C204–C205	109.0(2)
O302–C306	1.395(4)	F201–C204–C205	108.6(2)
O302–C307	1.444(4)	F202–C204–C203	110.5(2)
O303–C306	1.409(4)	F201–C204–C203	108.8(3)
O303–C302	1.446(3)	C205–C204–C203	114.0(2)
O304–C301	1.430(4)	F204–C205–F203	106.3(2)
C301–C302	1.514(4)	F204–C205–C204	109.7(2)
C302–C303	1.520(4)	F203–C205–C204	108.2(2)
C303–C304	1.522(4)	F204–C205–C206	111.1(2)
C304–C305	1.532(4)		
C305–C306	1.528(4)		
F203–C205–C206	108.6(2)	F301–C304–F302	106.3(2)
C204–C205–C206	112.7(2)	F301–C304–C303	111.1(3)
O202–C206–O203	114.1(2)	F302–C304–C303	108.7(2)
O202–C206–C205	107.4(2)	F301–C304–C305	109.1(3)
O203–C206–C205	108.2(2)	F302–C304–C305	108.2(3)
C306–O302–C307	112.9(3)	C303–C304–C305	113.2(3)
C306–O303–C302	112.7(2)	F303–C305–F304	106.6(2)
O304–C301–C302	110.3(3)	F303–C305–C306	108.3(2)
O303–C302–C301	107.4(2)	F304–C305–C306	111.1(2)
O303–C302–C303	108.4(2)	F303–C305–C304	108.0(2)
C301–C302–C303	112.5(3)	F304–C305–C304	109.0(3)
O301–C303–C304	110.0(2)	C306–C305–C304	113.5(3)
O301–C303–C302	109.4(2)	O302–C306–O303	113.2(2)
C304–C303–C302	108.9(3)	O302–C306–C305	106.8(2)
		O303–C306–C305	108.9(2)

Table 4. Anisotropic displacement parameters [$\text{\AA}^2 \times 10^3$]. The anisotropic displacement factor exponent takes the form: $-2\pi^2[h^2a^{*2}U^{11} + \dots + 2hk a^* b^* U^{12}]$.

Atom	U^{11}	U^{22}	U^{33}	U^{23}	U^{13}	U^{12}
F101	41(1)	25(1)	49(1)	-3(1)	8(1)	10(1)
F102	31(1)	41(1)	44(1)	17(1)	-11(1)	7(1)
F103	35(1)	37(1)	26(1)	1(1)	7(1)	3(1)
F104	22(1)	53(1)	65(2)	8(1)	12(1)	12(1)
O101	24(1)	15(1)	26(1)	0(1)	-6(1)	-1(1)
O102	29(1)	40(1)	35(2)	5(1)	-9(1)	-13(1)
O103	22(1)	20(1)	21(1)	4(1)	3(1)	-4(1)
O104	37(1)	32(1)	21(1)	-7(1)	8(1)	-13(1)
C101	37(2)	23(2)	21(2)	-5(1)	11(1)	-3(1)
C102	26(2)	21(2)	18(2)	3(1)	0(1)	-7(1)
C103	23(2)	20(2)	18(2)	3(1)	-2(1)	1(1)
C104	27(2)	26(2)	26(2)	2(1)	-6(1)	5(1)
C105	14(2)	38(2)	32(2)	5(2)	2(1)	7(1)
C106	22(2)	33(2)	24(2)	6(1)	0(1)	-3(1)
C107	49(3)	47(2)	38(2)	6(2)	-10(2)	-23(2)
F201	27(1)	21(1)	31(1)	10(1)	1(1)	-2(1)
F202	21(1)	18(1)	44(1)	-3(1)	1(1)	6(1)
F203	26(1)	23(1)	25(1)	0(1)	8(1)	1(1)
F204	23(1)	18(1)	30(1)	-6(1)	1(1)	-4(1)
O201	18(1)	20(1)	33(1)	2(1)	5(1)	1(1)
O202	18(1)	17(1)	24(1)	1(1)	6(1)	1(1)
O203	17(1)	16(1)	18(1)	1(1)	-1(1)	-1(1)
O204	24(1)	19(1)	30(1)	1(1)	7(1)	-2(1)
C201	22(2)	21(2)	23(2)	0(1)	2(1)	-2(1)
C202	18(2)	18(2)	17(2)	0(1)	-1(1)	1(1)
C203	18(2)	18(2)	26(2)	2(1)	1(1)	-1(1)
C204	21(2)	15(1)	25(2)	3(1)	5(1)	3(1)
C205	21(2)	17(1)	21(2)	-1(1)	5(1)	-4(1)
C206	16(2)	16(1)	21(2)	1(1)	1(1)	-2(1)
C207	20(2)	26(2)	34(2)	-2(1)	8(1)	4(1)
F301	40(1)	15(1)	34(1)	-7(1)	-4(1)	6(1)
F302	20(1)	33(1)	34(1)	-7(1)	5(1)	1(1)
F303	24(1)	22(1)	28(1)	1(1)	-2(1)	-6(1)
F304	35(1)	27(1)	19(1)	-7(1)	2(1)	1(1)
O301	26(1)	17(1)	26(1)	4(1)	1(1)	2(1)
O302	33(1)	20(1)	23(1)	4(1)	8(1)	0(1)
O303	16(1)	20(1)	16(1)	-2(1)	-1(1)	1(1)
O304	23(1)	16(1)	31(1)	-4(1)	-2(1)	0(1)
C301	28(2)	13(1)	22(2)	-1(1)	-1(1)	2(1)
C302	16(1)	18(1)	19(2)	-1(1)	-1(1)	-1(1)

C303	19(2)	17(2)	25(2)	−1(1)	−3(1)	1(1)
C304	19(2)	17(2)	27(2)	−6(1)	1(1)	2(1)
C305	23(2)	21(2)	15(2)	−5(1)	1(1)	−4(1)
C306	20(2)	20(2)	17(2)	1(1)	0(1)	1(1)
C307	42(2)	18(2)	38(2)	3(1)	7(2)	−1(2)

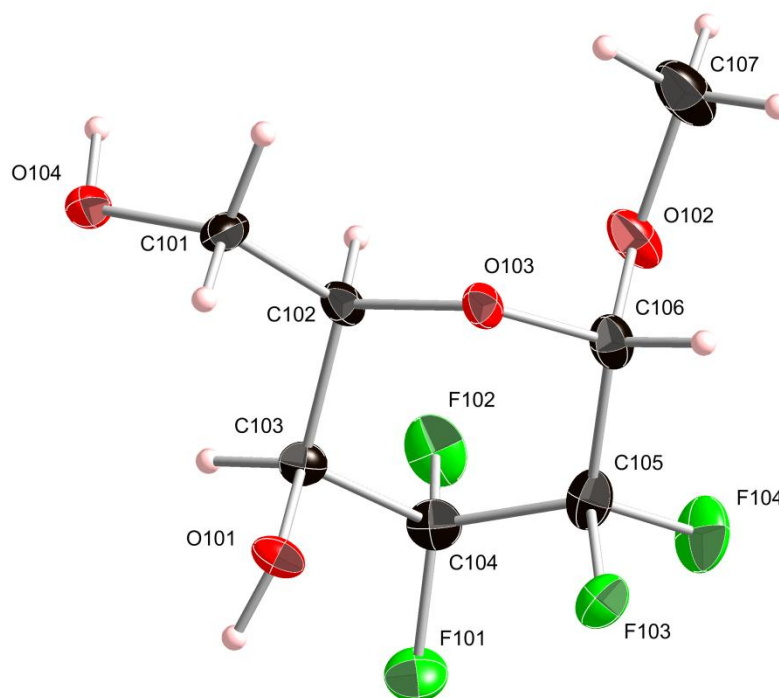
Table 5. Hydrogen coordinates [$\times 10^4$] and isotropic displacement parameters [$\text{\AA}^2 \times 10^3$].

Atom	<i>x</i>	<i>y</i>	<i>z</i>	<i>U_{eq}</i>	<i>S.o.f.</i>
H101	2931	6186	9182	34	1
H104	2929	3249	6279	45	1
H10A	3436	2790	8167	32	1
H10B	2749	1592	7420	32	1
H102	1287	3517	7233	26	1
H103	2211	5938	7711	25	1
H106	67	2105	9221	31	1
H10C	89	591	7411	68	1
H10D	−1162	987	7022	68	1
H10E	−852	433	8128	68	1
H201	9993	4550	4693	35	1
H204	9152	7361	4649	36	1
H20A	7751	8064	5927	26	1
H20B	8882	7177	6292	26	1
H202	7364	5328	5961	22	1
H203	9085	4120	5877	25	1
H206	5935	5009	3631	21	1
H20C	5129	6188	5243	39	1
H20D	4448	4655	5548	39	1
H20E	4379	5195	4430	39	1
H301	3689	3744	−252	35	1
H304	4387	−2254	−233	36	1
H30A	2804	−205	−778	26	1
H30B	4103	124	−687	26	1
H302	2875	−192	968	21	1
H303	2439	2324	195	25	1
H306	5249	354	2518	23	1
H30C	3839	−2431	1931	48	1
H30D	3385	−2596	2972	48	1
H30E	4666	−2274	2906	48	1

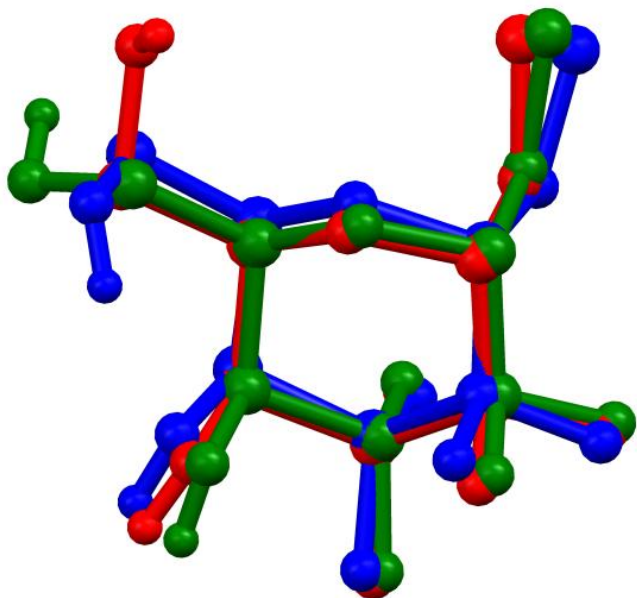
Table 6. Hydrogen bonds [\AA and $^\circ$].

$D-H\cdots A$	$d(D-H)$	$d(H\cdots A)$	$d(D\cdots A)$	$\angle(DHA)$
O101–H101 \cdots O304 ⁱ	0.84	1.84	2.652(3)	161.0
O104–H104 \cdots O203 ⁱⁱ	0.84	2.18	2.824(3)	133.3
O104–H104 \cdots O204 ⁱⁱ	0.84	2.61	3.377(3)	153.0
O201–H201 \cdots O204 ⁱⁱⁱ	0.84	1.91	2.732(3)	166.4
O204–H204 \cdots O201	0.84	1.95	2.663(3)	141.9
O301–H301 \cdots O101 ^{iv}	0.84	1.89	2.714(3)	166.8
O304–H304 \cdots O301 ^v	0.84	1.99	2.810(3)	164.5

Symmetry transformations used to generate equivalent atoms:
(i) $x, y+1, z+1$ (ii) $-x+1, y-1/2, -z+1$ (iii) $-x+2, y-1/2, -z+1$
(iv) $x, y, z-1$ (v) $-x+1, y-1/2, -z$

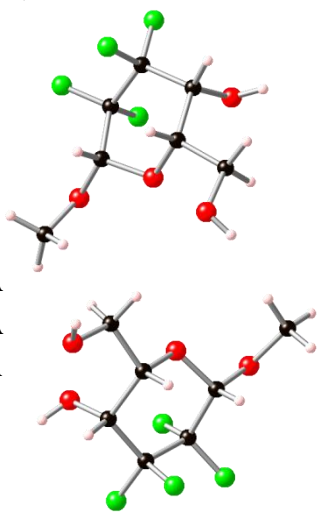


Molecular structure of one of the three independent molecules in the asymmetric unit. Thermal ellipsoids drawn at the 35% probability level.



Overlay of the 3 independent molecules in the asymmetric unit.

Table 1. Crystal data and structure refinement details.

Identification code	2010sot0051 (3.2)	
Empirical formula	C ₇ H ₁₀ F ₄ O ₄	
Formula weight	234.15	
Temperature	120(2) K	
Wavelength	0.71073 Å	
Crystal system	Tetragonal	
Space group	<i>P</i> 4 ₃ 2 ₁ 2	
Unit cell dimensions	<i>a</i> = 8.8756(6) Å <i>b</i> = 8.8756(6) Å <i>c</i> = 46.642(5) Å	
Volume	3674.3(5) Å ³	
<i>Z</i>	16 (<i>Z</i> ' = 2)	
Density (calculated)	1.693 Mg / m ³	
Absorption coefficient	0.184 mm ⁻¹	
<i>F</i> (000)	1920	
Crystal	Plate; Colourless	
Crystal size	0.40 × 0.30 × 0.02 mm ³	
θ range for data collection	3.17 – 26.37°	
Index ranges	–10 ≤ <i>h</i> ≤ 10, –6 ≤ <i>k</i> ≤ 11, –58 ≤ <i>l</i> ≤ 28	
Reflections collected	19674	
Independent reflections	2301 [<i>R</i> _{int} = 0.0902]	
Completeness to θ = 26.37°	99.7 %	
Absorption correction	Semi-empirical from equivalents	
Max. and min. transmission	0.9963 and 0.9300	
Refinement method	Full-matrix least-squares on <i>F</i> ²	
Data / restraints / parameters	2301 / 0 / 278	
Goodness-of-fit on <i>F</i> ²	1.058	
Final <i>R</i> indices [<i>F</i> ² > 2σ(<i>F</i> ²)]	<i>R</i> 1 = 0.0579, <i>wR</i> 2 = 0.1327	
<i>R</i> indices (all data)	<i>R</i> 1 = 0.1061, <i>wR</i> 2 = 0.1517	
Absolute structure parameter	Inferred from synthetic procedure	
Extinction coefficient	0.0075(11)	
Largest diff. peak and hole	0.375 and –0.425 e Å ⁻³	

Diffraction: Nonius KappaCCD area detector (ϕ scans and ω scans to fill *asymmetric unit*). **Cell determination:** DirAx (Duisenberg, A.J.M.(1992). *J. Appl. Cryst.* 25, 92–96.) **Data collection:** Collect (Collect: Data collection software, R. Hooft, Nonius B.V., 1998). **Data reduction and cell refinement:** Denzo (Z. Otwinowski & W. Minor, *Methods in Enzymology* (1997) Vol. 276: *Macromolecular Crystallography*, part A, pp. 307–326; C. W. Carter, Jr. & R. M. Sweet, Eds., Academic Press). **Absorption correction:** Sheldrick, G. M. SADABS - Bruker Nonius area detector scaling and absorption correction - V2.10 **Structure solution:** SHELXS97 (G. M. Sheldrick, *Acta Cryst.* (1990) A46 467–473). **Structure refinement:** SHELXL97 (G. M. Sheldrick (1997), University of Göttingen, Germany). **Graphics:** Cameron - A Molecular Graphics Package. (D. M. Watkin, L. Pearce and C. K. Prout, Chemical Crystallography Laboratory, University of Oxford, 1993).

Special details: All hydrogen atoms were placed in idealised positions and refined using a riding model - for methyl and hydroxyl groups the torsion was allowed to refine.

Relative Chirality: C102=R, C103=S, C202=R, C203=S

Table 2. Atomic coordinates [$\times 10^4$], equivalent isotropic displacement parameters [$\text{\AA}^2 \times 10^3$] and site occupancy factors. U_{eq} is defined as one third of the trace of the orthogonalized $U^{\bar{ij}}$ tensor.

Atom	x	y	z	U_{eq}	$S.o.f.$
F201	2008(4)	8817(4)	264(1)	43(1)	1
F202	359(4)	10301(3)	467(1)	44(1)	1
F203	-696(3)	8032(4)	785(1)	41(1)	1
F204	-504(4)	7358(4)	337(1)	45(1)	1
O201	5284(4)	6789(4)	1067(1)	36(1)	1
O202	1658(4)	9925(4)	991(1)	36(1)	1
O203	378(4)	5181(4)	742(1)	33(1)	1
O204	2203(4)	6796(4)	894(1)	31(1)	1
C201	4384(6)	8135(6)	1052(1)	33(1)	1
C202	3285(6)	7951(6)	811(1)	27(1)	1
C203	2437(6)	9410(6)	747(1)	28(1)	1
C204	1270(6)	9082(6)	514(1)	34(1)	1
C205	291(6)	7701(6)	574(1)	32(1)	1
C206	1286(7)	6353(6)	659(1)	36(1)	1
C207	1047(7)	3769(6)	680(1)	40(1)	1
F101	7716(4)	4068(4)	317(1)	42(1)	1
F102	5612(4)	5255(3)	399(1)	43(1)	1
F103	4055(3)	2684(3)	373(1)	37(1)	1
F104	5574(4)	2861(3)	9(1)	41(1)	1
O101	8250(4)	2795(4)	1265(1)	34(1)	1
O102	5241(4)	3884(4)	918(1)	33(1)	1
O103	5339(4)	17(4)	268(1)	33(1)	1
O104	6242(4)	1031(4)	681(1)	29(1)	1
C101	7405(6)	1657(6)	1119(1)	32(1)	1
C102	7232(6)	2110(6)	808(1)	31(1)	1
C103	6624(6)	3701(6)	765(1)	28(1)	1
C104	6361(6)	3946(6)	448(1)	31(1)	1
C105	5523(6)	2645(6)	298(1)	29(1)	1
C106	6222(6)	1149(6)	378(1)	28(1)	1
C107	6080(7)	-1401(6)	269(1)	39(1)	1

Table 3. Bond lengths [\AA] and angles [$^\circ$].

F201–C204	1.357(6)	F202–C204–C205	109.1(4)
F202–C204	1.368(6)	F201–C204–C203	108.4(4)
F203–C205	1.348(6)	F202–C204–C203	111.3(4)
F204–C205	1.347(5)	C205–C204–C203	113.9(4)
O201–C201	1.439(6)	F203–C205–F204	107.9(4)
O202–C203	1.409(5)	F203–C205–C204	109.2(4)
O203–C206	1.373(6)	F204–C205–C204	109.0(4)
O203–C207	1.417(7)	F203–C205–C206	110.9(4)
O204–C206	1.421(6)	F204–C205–C206	109.6(4)
O204–C202	1.457(6)	C204–C205–C206	110.2(4)
C201–C202	1.500(6)	O203–C206–O204	109.1(4)
C202–C203	1.528(7)	O203–C206–C205	109.0(4)
C203–C204	1.530(7)	O204–C206–C205	108.1(4)
C204–C205	1.529(8)	C106–O103–C107	112.4(4)
C205–C206	1.539(8)	C106–O104–C102	111.7(4)
F101–C104	1.354(6)	O101–C101–C102	108.8(4)
F102–C104	1.358(6)	O104–C102–C101	106.3(4)
F103–C105	1.350(6)	O104–C102–C103	110.5(4)
F104–C105	1.359(5)	C101–C102–C103	114.0(4)
O101–C101	1.430(6)	O102–C103–C104	109.8(4)
O102–C103	1.429(6)	O102–C103–C102	110.2(4)
O103–C106	1.373(6)	C104–C103–C102	108.4(4)
O103–C107	1.420(6)	F101–C104–F102	107.0(4)
O104–C106	1.422(5)	F101–C104–C103	108.5(4)
O104–C102	1.427(6)	F102–C104–C103	111.2(4)
C101–C102	1.514(7)	F101–C104–C105	106.5(4)
C102–C103	1.524(7)	F102–C104–C105	109.2(4)
C103–C104	1.515(6)	C103–C104–C105	114.2(4)
C104–C105	1.542(8)	F103–C105–F104	106.7(4)
C105–C106	1.512(7)	F103–C105–C106	110.7(4)
C206–O203–C207	111.4(4)	F104–C105–C106	110.7(4)
C206–O204–C202	111.5(4)	F103–C105–C104	109.1(4)
O201–C201–C202	107.8(4)	F104–C105–C104	109.1(4)
O204–C202–C201	107.8(4)	C106–C105–C104	110.4(4)
O204–C202–C203	108.9(4)	O103–C106–O104	109.0(4)
C201–C202–C203	112.0(4)	O103–C106–C105	108.4(4)
O202–C203–C202	111.1(4)	O104–C106–C105	108.3(4)
O202–C203–C204	107.7(4)		
C202–C203–C204	108.1(4)		
F201–C204–F202	106.6(4)		
F201–C204–C205	107.1(4)		

Table 4. Anisotropic displacement parameters [$\text{\AA}^2 \times 10^3$]. The anisotropic displacement factor exponent takes the form: $-2\pi^2[h^2a^{*2}U^{11} + \dots + 2hk a^* b^* U^{12}]$.

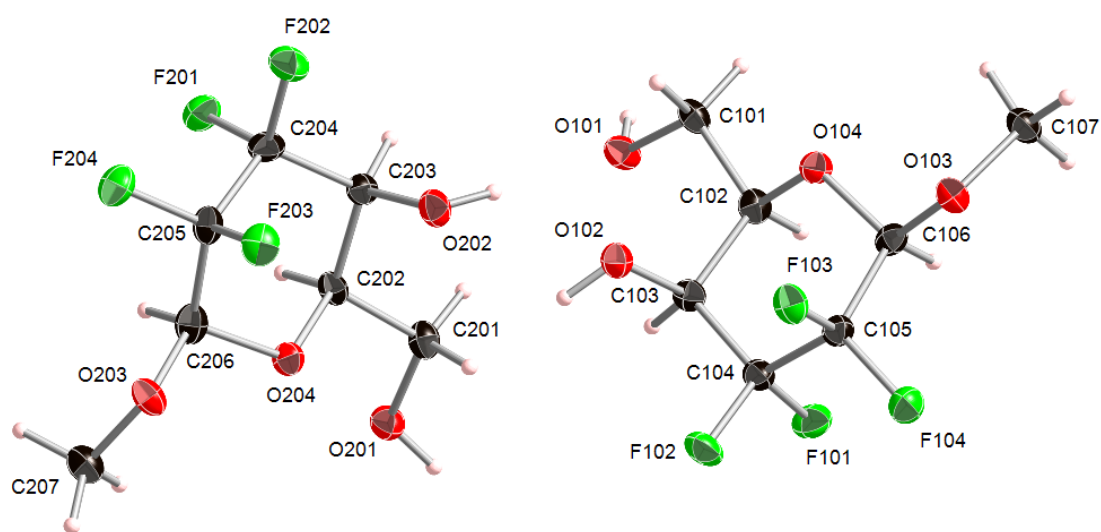
Atom	U^{11}	U^{22}	U^{33}	U^{23}	U^{13}	U^{12}
F201	56(2)	45(2)	29(2)	3(1)	3(2)	2(2)
F202	45(2)	34(2)	53(2)	3(2)	-6(2)	11(2)
F203	29(2)	49(2)	44(2)	-5(2)	2(1)	5(2)
F204	43(2)	52(2)	41(2)	-4(2)	-16(2)	3(2)
O201	36(2)	32(2)	39(2)	-1(2)	-5(2)	4(2)
O202	40(2)	33(2)	33(2)	-7(2)	7(2)	-3(2)
O203	27(2)	26(2)	46(2)	-5(2)	7(2)	-4(2)
O204	28(2)	32(2)	32(2)	1(2)	-4(2)	-6(2)
C201	27(3)	33(3)	38(3)	-8(3)	-1(2)	-1(3)
C202	24(3)	25(3)	32(3)	-2(2)	4(2)	-8(2)
C203	27(3)	27(3)	28(3)	-1(2)	2(2)	3(2)
C204	40(3)	31(3)	31(3)	4(2)	0(3)	13(3)
C205	31(3)	33(3)	31(3)	-9(2)	-1(3)	1(3)
C206	34(3)	39(4)	34(3)	-8(3)	2(3)	-5(3)
C207	40(4)	32(4)	48(3)	-2(3)	1(3)	-3(3)
F101	42(2)	44(2)	39(2)	6(1)	8(2)	-10(2)
F102	58(2)	24(2)	46(2)	4(1)	-7(2)	7(2)
F103	31(2)	37(2)	44(2)	-6(1)	-2(1)	6(2)
F104	50(2)	40(2)	31(2)	-1(2)	-3(2)	3(2)
O101	32(2)	32(2)	38(2)	1(2)	-10(2)	1(2)
O102	35(2)	30(2)	35(2)	-3(2)	6(2)	2(2)
O103	32(2)	27(2)	39(2)	-4(2)	-4(2)	0(2)
O104	31(2)	29(2)	28(2)	0(2)	-2(2)	-1(2)
C101	31(3)	23(3)	41(3)	-3(2)	0(2)	4(2)
C102	27(3)	31(3)	34(3)	-3(2)	-2(2)	-3(3)
C103	23(3)	28(3)	33(3)	2(2)	0(2)	3(2)
C104	32(3)	27(3)	34(3)	1(2)	8(2)	3(3)
C105	30(3)	31(3)	26(3)	2(2)	1(2)	4(2)
C106	24(3)	34(3)	27(3)	3(2)	4(2)	0(3)
C107	47(4)	26(3)	42(3)	-1(2)	-2(3)	6(3)

Table 5. Hydrogen coordinates [$\times 10^4$] and isotropic displacement parameters [$\text{\AA}^2 \times 10^3$].

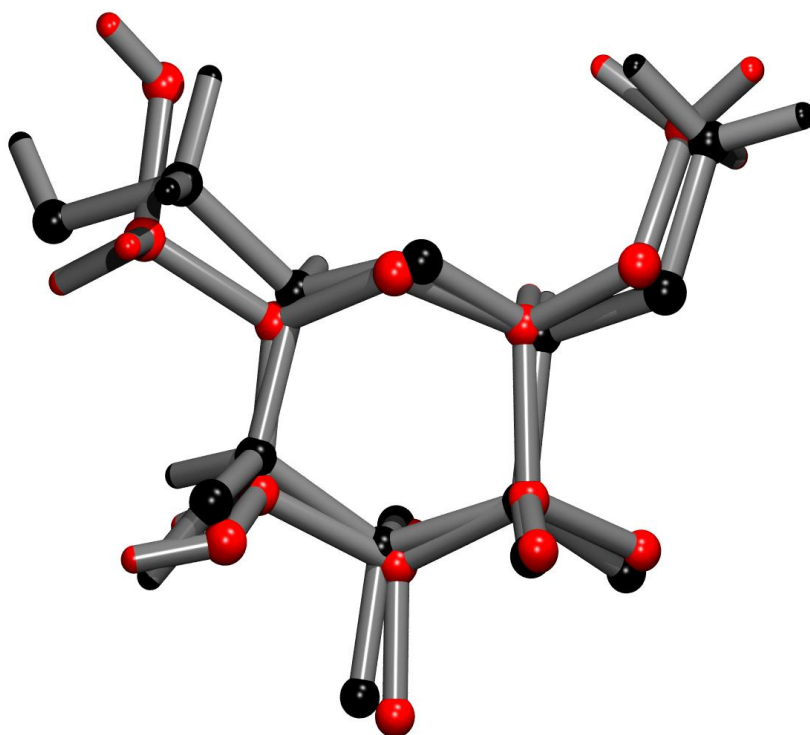
Atom	<i>x</i>	<i>y</i>	<i>z</i>	<i>U</i> _{eq}	<i>S.o.f.</i>
H201	5641	6697	1233	53	1
H202	2153	10619	1069	53	1
H20A	5035	9023	1018	40	1
H20B	3839	8287	1235	40	1
H20C	3835	7617	635	32	1
H203	3157	10200	679	33	1
H206	1930	6041	493	43	1
H20D	963	3563	475	61	1
H20E	530	2976	788	61	1
H20F	2113	3792	735	61	1
H101	8966	2392	1355	51	1
H102	5140	4791	966	50	1
H10A	6401	1547	1209	38	1
H10B	7935	678	1132	38	1
H10F	8237	2035	712	37	1
H103	7379	4448	837	34	1
H106	7269	1077	299	34	1
H10C	7011	−1334	157	58	1
H10D	5418	−2166	185	58	1
H10E	6324	−1683	467	58	1

Table 6. Hydrogen bonds [\AA and $^\circ$].

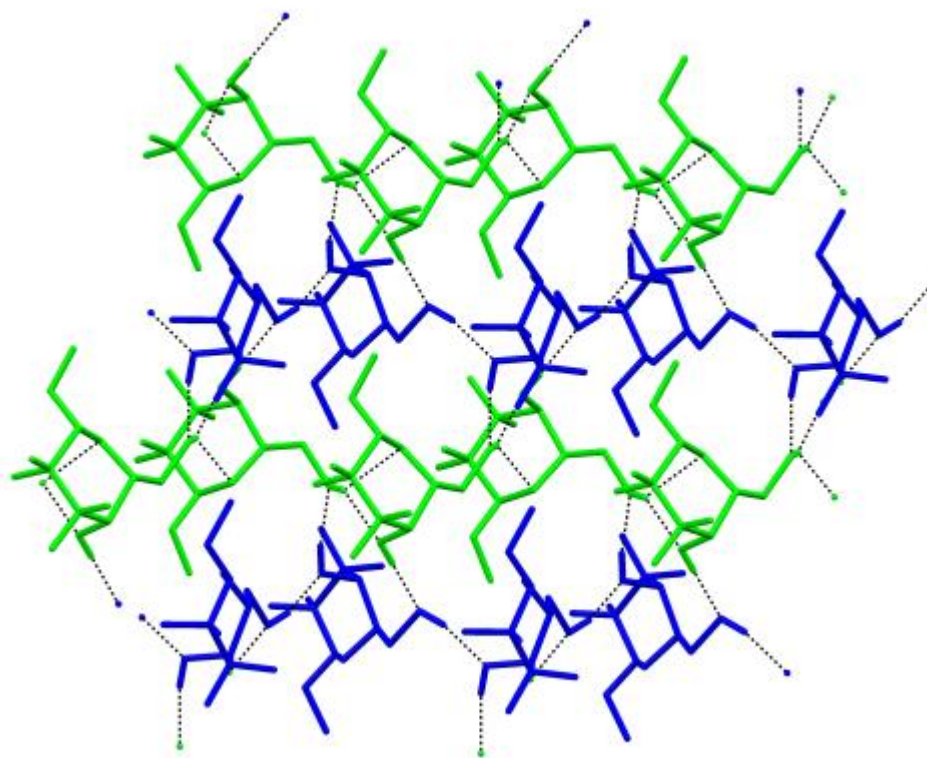
<i>D</i> –H... <i>A</i>	<i>d</i> (<i>D</i> –H)	<i>d</i> (H... <i>A</i>)	<i>d</i> (<i>D</i> ... <i>A</i>)	\angle (<i>DHA</i>)
O201–H201...O202 ⁱ	0.84	2.13	2.839(5)	141.5
O201–H201...F203 ⁱ	0.84	2.56	3.151(4)	128.8
O201–H201...O204 ⁱ	0.84	2.60	3.288(5)	140.2
O202–H202...O101 ⁱⁱ	0.84	1.88	2.718(5)	178.3
O101–H101...O102 ⁱⁱⁱ	0.84	1.92	2.744(5)	166.1
O102–H102...O201	0.84	1.84	2.670(5)	169.9
Symmetry transformations used to generate equivalent atoms:				
(i) $x+1/2, -y+3/2, -z+1/4$ (ii) $x-1/2, -y+3/2, -z+1/4$				
(iii) $x+1/2, -y+1/2, -z+1/4$				



Thermal ellipsoids drawn at the 35% probability level

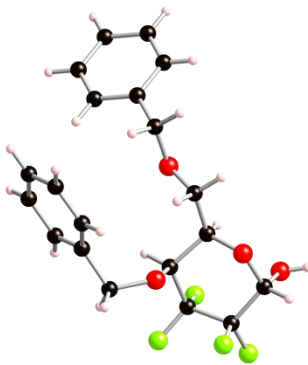


Overlay of molecules **1** and **2**



Part of the hydrogen bonded sheet viewed down the c axis. Colours depict the 2 independent molecules in the asymmetric unit.

Table 1. Crystal data and structure refinement details.

Identification code	2010sot1020 (α-1.57)	
Empirical formula	$C_{20}H_{20}F_4O_4$	
Formula weight	400.36	
Temperature	120(2) K	
Wavelength	0.71073 Å	
Crystal system	Orthorhombic	
Space group	$P2_12_12_1$	
Unit cell dimensions	$a = 6.09640(10)$ Å $b = 13.0735(3)$ Å $c = 22.9557(5)$ Å	
Volume	$1829.60(7)$ Å ³	
Z	4	
Density (calculated)	1.453 Mg / m ³	
Absorption coefficient	0.126 mm ⁻¹	
$F(000)$	832	
Crystal	Fragment; Colourless	
Crystal size	$0.22 \times 0.12 \times 0.05$ mm ³	
θ range for data collection	$3.08 - 27.47^\circ$	
Index ranges	$-7 \leq h \leq 7, -16 \leq k \leq 15, -25 \leq l \leq 29$	
Reflections collected	13476	
Independent reflections	2412 [$R_{int} = 0.0436$]	
Completeness to $\theta = 27.47^\circ$	99.8 %	
Absorption correction	Semi-empirical from equivalents	
Max. and min. transmission	0.9937 and 0.9727	
Refinement method	Full-matrix least-squares on F^2	
Data / restraints / parameters	2412 / 0 / 254	
Goodness-of-fit on F^2	1.145	
Final R indices [$F^2 > 2\sigma(F^2)$]	$R1 = 0.0354, wR2 = 0.0749$	
R indices (all data)	$R1 = 0.0394, wR2 = 0.0771$	
Absolute structure parameter	Not reliably determined	
Largest diff. peak and hole	0.266 and -0.206 e Å ⁻³	

Diffraction: Nonius KappaCCD area detector (ϕ scans and ω scans to fill *asymmetric unit*). **Cell determination:** DirAx (Duisenberg, A.J.M.(1992). J. Appl. Cryst. 25, 92-96.) **Data collection:** Collect (Collect: Data collection software, R. Hooft, Nonius B.V., 1998). **Data reduction and cell refinement:** Denzo (Z. Otwinowski & W. Minor, *Methods in Enzymology* (1997) Vol. 276: *Macromolecular Crystallography*, part A, pp. 307-326; C. W. Carter, Jr. & R. M. Sweet, Eds., Academic Press). **Absorption correction:** Sheldrick, G. M. SADABS - Bruker Nonius area detector scaling and absorption correction - V2.10 **Structure solution:** SHELXS97 (G. M. Sheldrick, Acta Cryst. (1990) A46 467-473). **Structure refinement:** SHELXL97 (G. M. Sheldrick (1997), University of Göttingen, Germany). **Graphics:** Cameron - A Molecular Graphics Package. (D. M. Watkin, L. Pearce and C. K. Prout, Chemical Crystallography Laboratory, University of Oxford, 1993).

Special details: All hydrogen atoms were placed in idealised positions and refined using a riding model.

Table 2. Atomic coordinates [$\times 10^4$], equivalent isotropic displacement parameters [$\text{\AA}^2 \times 10^3$] and site occupancy factors. U_{eq} is defined as one third of the trace of the orthogonalized $U^{\bar{ij}}$ tensor.

Atom	x	y	z	U_{eq}	$S.o.f.$
O1	194(3)	3880(1)	11556(1)	22(1)	1
O2	-1303(3)	3842(1)	9630(1)	22(1)	1
O3	-2499(2)	3522(1)	10579(1)	20(1)	1
O4	63(3)	1196(1)	11045(1)	21(1)	1
F1	2908(2)	3999(1)	10177(1)	23(1)	1
F2	3113(2)	5048(1)	10914(1)	27(1)	1
F3	507(2)	5619(1)	9968(1)	26(1)	1
F4	-1086(2)	5553(1)	10816(1)	26(1)	1
C1	539(4)	2490(2)	12668(1)	24(1)	1
C2	938(4)	1576(2)	12951(1)	28(1)	1
C3	2938(5)	1087(2)	12889(1)	32(1)	1
C4	4544(4)	1520(2)	12542(1)	33(1)	1
C5	4150(4)	2443(2)	12259(1)	28(1)	1
C6	2154(4)	2934(2)	12319(1)	21(1)	1
C7	1730(4)	3953(2)	12032(1)	27(1)	1
C8	1085(4)	3494(2)	11029(1)	19(1)	1
C9	1756(4)	4380(2)	10639(1)	20(1)	1
C10	-204(4)	4967(2)	10388(1)	20(1)	1
C11	-2009(4)	4270(2)	10150(1)	19(1)	1
C12	-662(4)	2875(2)	10708(1)	17(1)	1
C13	-1545(4)	1991(2)	11061(1)	20(1)	1
C14	-614(5)	314(2)	11368(1)	41(1)	1
C15	857(4)	-569(2)	11227(1)	25(1)	1
C16	238(4)	-1286(2)	10815(1)	32(1)	1
C17	1557(5)	-2106(2)	10684(1)	40(1)	1
C18	3561(5)	-2218(2)	10962(1)	37(1)	1
C19	4209(5)	-1506(2)	11369(1)	35(1)	1
C20	2869(4)	-682(2)	11499(1)	30(1)	1

Table 3. Bond lengths [Å] and angles [°].

O1–C8	1.418(2)	O1–C8–C9	109.56(17)
O1–C7	1.443(3)	O1–C8–C12	109.43(17)
O2–C11	1.387(2)	C9–C8–C12	107.83(16)
O3–C11	1.419(2)	F2–C9–F1	106.40(17)
O3–C12	1.435(2)	F2–C9–C8	112.24(16)
O4–C13	1.429(2)	F1–C9–C8	108.61(18)
O4–C14	1.431(3)	F2–C9–C10	109.10(17)
F1–C9	1.366(2)	F1–C9–C10	106.92(16)
F2–C9	1.359(2)	C8–C9–C10	113.21(18)
F3–C10	1.357(2)	F3–C10–F4	106.67(16)
F4–C10	1.358(2)	F3–C10–C11	110.54(17)
C1–C2	1.383(3)	F4–C10–C11	108.00(18)
C1–C6	1.396(3)	F3–C10–C9	109.46(18)
C2–C3	1.384(4)	F4–C10–C9	108.60(17)
C3–C4	1.384(4)	C11–C10–C9	113.32(17)
C4–C5	1.391(3)	O2–C11–O3	112.59(17)
C5–C6	1.383(3)	O2–C11–C10	108.91(18)
C6–C7	1.508(3)	O3–C11–C10	108.40(16)
C8–C9	1.521(3)	O3–C12–C13	106.50(17)
C8–C12	1.527(3)	O3–C12–C8	109.40(17)
C9–C10	1.533(3)	C13–C12–C8	113.27(17)
C10–C11	1.529(3)	O4–C13–C12	107.38(16)
C12–C13	1.510(3)	O4–C14–C15	109.64(19)
C14–C15	1.498(3)	C16–C15–C20	118.6(2)
C15–C16	1.382(3)	C16–C15–C14	120.5(2)
C15–C20	1.385(4)	C20–C15–C14	121.0(2)
C16–C17	1.374(4)	C17–C16–C15	121.3(2)
C17–C18	1.386(4)	C16–C17–C18	119.8(3)
C18–C19	1.376(4)	C19–C18–C17	119.6(2)
C19–C20	1.384(4)	C18–C19–C20	120.2(2)
C8–O1–C7	114.89(17)	C19–C20–C15	120.5(2)
C11–O3–C12	112.67(15)		
C13–O4–C14	112.02(17)		
C2–C1–C6	120.4(2)		
C1–C2–C3	120.4(2)		
C2–C3–C4	119.6(2)		
C3–C4–C5	120.1(2)		
C6–C5–C4	120.6(2)		
C5–C6–C1	119.0(2)		
C5–C6–C7	121.2(2)		
C1–C6–C7	119.8(2)		
O1–C7–C6	112.55(18)		

Table 4. Anisotropic displacement parameters [$\text{\AA}^2 \times 10^3$]. The anisotropic displacement factor exponent takes the form: $-2\pi^2[h^2a^{*2}U^{11} + \dots + 2hk a^* b^* U^{12}]$.

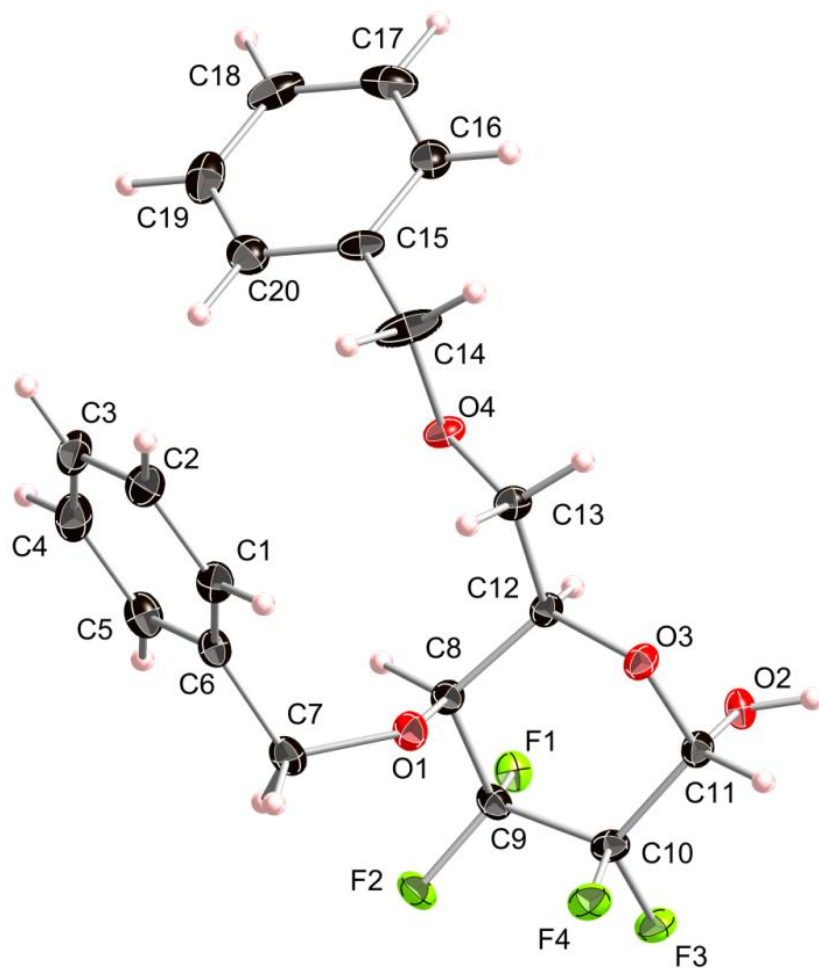
Atom	U^{11}	U^{22}	U^{33}	U^{23}	U^{13}	U^{12}
O1	26(1)	24(1)	16(1)	-3(1)	-1(1)	3(1)
O2	21(1)	26(1)	18(1)	-1(1)	-4(1)	1(1)
O3	16(1)	20(1)	23(1)	5(1)	1(1)	2(1)
O4	23(1)	17(1)	22(1)	4(1)	5(1)	2(1)
F1	17(1)	29(1)	23(1)	-1(1)	3(1)	1(1)
F2	28(1)	25(1)	28(1)	-1(1)	-6(1)	-10(1)
F3	31(1)	22(1)	25(1)	6(1)	1(1)	-4(1)
F4	35(1)	20(1)	25(1)	-5(1)	3(1)	5(1)
C1	24(1)	28(1)	21(1)	-3(1)	0(1)	3(1)
C2	32(1)	31(1)	22(1)	3(1)	0(1)	-2(1)
C3	42(2)	28(1)	26(1)	1(1)	-11(1)	6(1)
C4	28(1)	37(1)	33(1)	-7(1)	-6(1)	12(1)
C5	26(1)	37(1)	21(1)	-3(1)	1(1)	-2(1)
C6	27(1)	23(1)	14(1)	-2(1)	-4(1)	0(1)
C7	39(1)	25(1)	19(1)	-3(1)	-7(1)	-4(1)
C8	20(1)	18(1)	18(1)	0(1)	-1(1)	2(1)
C9	20(1)	22(1)	17(1)	-3(1)	-1(1)	-2(1)
C10	24(1)	17(1)	18(1)	2(1)	3(1)	-1(1)
C11	17(1)	21(1)	19(1)	4(1)	-1(1)	1(1)
C12	17(1)	17(1)	18(1)	-1(1)	0(1)	3(1)
C13	18(1)	19(1)	22(1)	-1(1)	3(1)	1(1)
C14	50(2)	25(1)	48(2)	17(1)	26(1)	7(1)
C15	29(1)	16(1)	28(1)	9(1)	7(1)	-1(1)
C16	32(1)	30(1)	33(1)	8(1)	-6(1)	-8(1)
C17	56(2)	23(1)	43(2)	-3(1)	5(1)	-10(1)
C18	43(2)	25(1)	45(2)	12(1)	14(1)	10(1)
C19	28(1)	45(2)	32(1)	20(1)	1(1)	4(1)
C20	35(1)	30(1)	24(1)	4(1)	0(1)	-9(1)

Table 5. Hydrogen coordinates [$\times 10^4$] and isotropic displacement parameters [$\text{\AA}^2 \times 10^3$].

Atom	<i>x</i>	<i>y</i>	<i>z</i>	<i>U</i> _{eq}	<i>S.o.f.</i>
H2	−2336	3849	9388	32	1
H1	−842	2818	12711	29	1
H2A	−167	1281	13190	34	1
H3	3206	458	13084	38	1
H4	5918	1187	12496	39	1
H5	5262	2739	12023	34	1
H7A	1149	4436	12326	33	1
H7B	3133	4232	11885	33	1
H8	2386	3053	11115	22	1
H11	−3352	4689	10075	23	1
H12	−30	2609	10336	20	1
H13A	−1814	2208	11468	24	1
H13B	−2945	1746	10893	24	1
H14A	−2149	140	11268	49	1
H14B	−546	463	11790	49	1
H16	−1126	−1210	10620	38	1
H17	1097	−2595	10403	48	1
H18	4482	−2782	10872	45	1
H19	5580	−1580	11561	42	1
H20	3333	−191	11778	35	1

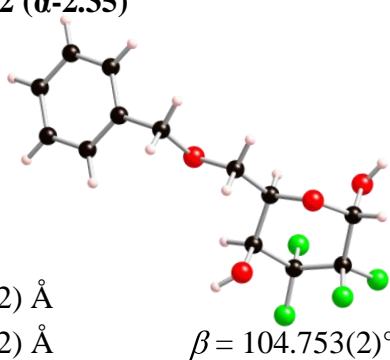
Table 6. Hydrogen bonds [\AA and $^\circ$].

<i>D</i> –H... <i>A</i>	<i>d</i> (<i>D</i> –H)	<i>d</i> (H... <i>A</i>)	<i>d</i> (<i>D</i> ... <i>A</i>)	\angle (<i>DHA</i>)
O2–H2...O4 ⁱ	0.84	1.87	2.704(2)	170.3
Symmetry transformations used to generate equivalent atoms:				
(i) $x-1/2, -y+1/2, -z+2$				



Thermal ellipsoids drawn at the 35% probability level

Table 1. Crystal data and structure refinement details.

Identification code	2010sot0412 (α-2.35)	
Empirical formula	$C_{13}H_{14}F_4O_4$	
Formula weight	310.24	
Temperature	120(2) K	
Wavelength	0.71073 Å	
Crystal system	Monoclinic	
Space group	$P2_1$	
Unit cell dimensions	$a = 8.4477(2)$ Å $b = 6.0345(2)$ Å $c = 13.8768(4)$ Å	$\beta = 104.753(2)^\circ$
Volume	$684.09(3)$ Å ³	
Z	2	
Density (calculated)	1.506 Mg / m ³	
Absorption coefficient	0.144 mm ⁻¹	
$F(000)$	320	
Crystal	Slab; Colourless	
Crystal size	$0.20 \times 0.20 \times 0.04$ mm ³	
θ range for data collection	3.04 – 27.48°	
Index ranges	$-10 \leq h \leq 10, -7 \leq k \leq 7, -18 \leq l \leq 18$	
Reflections collected	9328	
Independent reflections	1703 [$R_{int} = 0.0485$]	
Completeness to $\theta = 27.48^\circ$	99.7 %	
Absorption correction	Semi-empirical from equivalents	
Max. and min. transmission	0.9942 and 0.9717	
Refinement method	Full-matrix least-squares on F^2	
Data / restraints / parameters	1703 / 1 / 192	
Goodness-of-fit on F^2	1.081	
Final R indices [$F^2 > 2\sigma(F^2)$]	$R1 = 0.0387, wR2 = 0.0914$	
R indices (all data)	$R1 = 0.0442, wR2 = 0.0959$	
Absolute structure parameter	Not reliably determined	
Largest diff. peak and hole	0.171 and -0.259 e Å ⁻³	

Diffraction: Nonius KappaCCD area detector (ϕ scans and ω scans to fill *asymmetric unit*). **Cell determination:** DirAx (Duisenberg, A.J.M.(1992). J. Appl. Cryst. 25, 92-96.) **Data collection:** Collect (Collect: Data collection software, R. Hooft, Nonius B.V., 1998). **Data reduction and cell refinement:** Denzo (Z. Otwinowski & W. Minor, *Methods in Enzymology* (1997) Vol. 276: *Macromolecular Crystallography*, part A, pp. 307-326; C. W. Carter, Jr. & R. M. Sweet, Eds., Academic Press). **Absorption correction:** Sheldrick, G. M. SADABS - Bruker Nonius area detector scaling and absorption correction - V2.10 **Structure solution:** SHELXS97 (G. M. Sheldrick, Acta Cryst. (1990) A46 467-473). **Structure refinement:** SHELXL97 (G. M. Sheldrick (1997), University of Göttingen, Germany). **Graphics:** Cameron - A Molecular Graphics Package. (D. M. Watkin, L. Pearce and C. K. Prout, Chemical Crystallography Laboratory, University of Oxford, 1993).

Special details: All hydrogen atoms were placed in idealised positions and refined using a riding model.

Table 2. Atomic coordinates [$\times 10^4$], equivalent isotropic displacement parameters [$\text{\AA}^2 \times 10^3$] and site occupancy factors. U_{eq} is defined as one third of the trace of the orthogonalized $U^{\bar{ij}}$ tensor.

Atom	x	y	z	U_{eq}	$S.o.f.$
F1	8118(2)	7225(3)	8360(1)	23(1)	1
F2	5731(2)	7666(3)	8672(1)	22(1)	1
F3	5891(2)	10021(3)	7102(1)	30(1)	1
F4	8253(2)	11447(3)	7858(1)	29(1)	1
O1	7588(2)	10600(3)	11824(1)	20(1)	1
O2	6941(2)	13065(3)	9393(1)	19(1)	1
O3	9592(2)	10061(3)	9904(1)	24(1)	1
O4	4394(2)	11988(3)	8383(1)	23(1)	1
C1	8869(3)	7870(5)	13690(2)	29(1)	1
C2	8697(4)	6330(5)	14400(2)	36(1)	1
C3	7625(4)	6752(6)	14986(2)	43(1)	1
C4	6723(4)	8686(7)	14857(2)	45(1)	1
C5	6890(3)	10211(6)	14141(2)	34(1)	1
C6	7978(3)	9833(5)	13558(2)	24(1)	1
C7	8179(4)	11520(5)	12809(2)	28(1)	1
C8	7698(3)	12219(4)	11095(2)	19(1)	1
C9	6966(3)	11244(4)	10072(2)	16(1)	1
C10	7959(3)	9341(4)	9792(2)	18(1)	1
C11	7186(3)	8711(4)	8713(2)	19(1)	1
C12	6812(3)	10694(5)	8002(2)	21(1)	1
C13	5983(3)	12596(4)	8411(2)	20(1)	1

Table 3. Bond lengths [Å] and angles [°].

F1–C11	1.364(3)	F1–C11–C10	112.08(19)
F2–C11	1.370(3)	F2–C11–C10	108.12(18)
F3–C12	1.355(3)	F1–C11–C12	109.00(19)
F4–C12	1.361(3)	F2–C11–C12	107.28(19)
O1–C8	1.426(3)	C10–C11–C12	113.9(2)
O1–C7	1.441(3)	F3–C12–F4	106.85(18)
O2–C13	1.425(3)	F3–C12–C13	110.9(2)
O2–C9	1.444(3)	F4–C12–C13	108.4(2)
O3–C10	1.417(3)	F3–C12–C11	109.6(2)
O4–C13	1.383(3)	F4–C12–C11	108.06(19)
C1–C2	1.388(4)	C13–C12–C11	112.76(19)
C1–C6	1.391(4)	O4–C13–O2	112.93(19)
C2–C3	1.387(5)	O4–C13–C12	108.9(2)
C3–C4	1.380(6)	O2–C13–C12	107.58(19)
C4–C5	1.387(5)		
C5–C6	1.389(4)		
C6–C7	1.496(4)		
C8–C9	1.516(3)		
C9–C10	1.529(3)		
C10–C11	1.522(3)		
C11–C12	1.531(4)		
C12–C13	1.527(4)		
C8–O1–C7	109.81(19)		
C13–O2–C9	112.55(18)		
C2–C1–C6	120.8(3)		
C3–C2–C1	119.7(3)		
C4–C3–C2	120.1(3)		
C3–C4–C5	120.0(3)		
C4–C5–C6	120.7(3)		
C5–C6–C1	118.7(3)		
C5–C6–C7	120.2(3)		
C1–C6–C7	121.2(2)		
O1–C7–C6	108.9(2)		
O1–C8–C9	108.3(2)		
O2–C9–C8	104.51(19)		
O2–C9–C10	108.90(18)		
C8–C9–C10	114.22(19)		
O3–C10–C11	110.21(18)		
O3–C10–C9	108.9(2)		
C11–C10–C9	108.18(19)		
F1–C11–F2	106.04(19)		

Table 4. Anisotropic displacement parameters [$\text{\AA}^2 \times 10^3$]. The anisotropic displacement factor exponent takes the form: $-2\pi^2[h^2a^{*2}U^{11} + \dots + 2hk a^* b^* U^{12}]$.

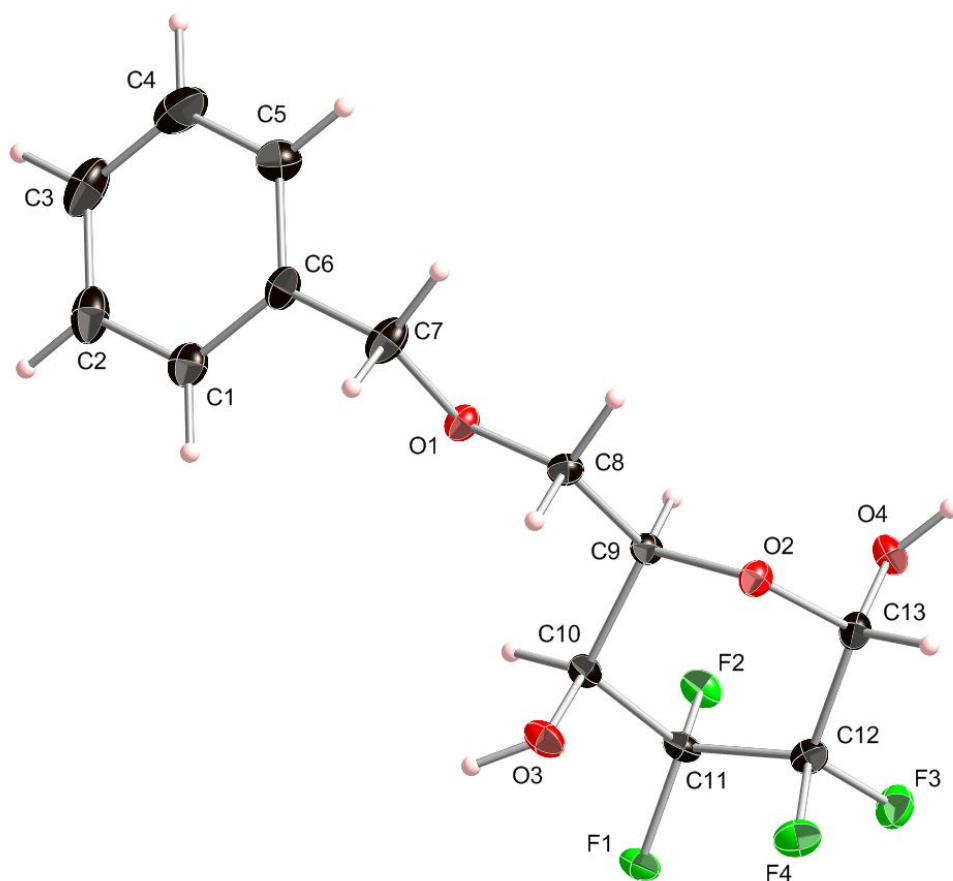
Atom	U^{11}	U^{22}	U^{33}	U^{23}	U^{13}	U^{12}
F1	21(1)	22(1)	28(1)	-6(1)	7(1)	4(1)
F2	17(1)	19(1)	32(1)	-2(1)	7(1)	-4(1)
F3	37(1)	29(1)	20(1)	-3(1)	1(1)	3(1)
F4	31(1)	30(1)	33(1)	2(1)	19(1)	-5(1)
O1	23(1)	18(1)	17(1)	-1(1)	4(1)	-3(1)
O2	22(1)	16(1)	18(1)	1(1)	5(1)	-2(1)
O3	14(1)	26(1)	31(1)	-5(1)	4(1)	2(1)
O4	20(1)	20(1)	28(1)	2(1)	3(1)	5(1)
C1	31(1)	30(1)	23(1)	-4(1)	1(1)	-1(1)
C2	48(2)	25(2)	26(1)	-1(1)	-7(1)	-1(1)
C3	59(2)	41(2)	26(1)	8(1)	6(1)	-14(2)
C4	49(2)	58(2)	33(2)	3(2)	19(1)	-6(2)
C5	35(1)	37(2)	31(2)	-3(1)	10(1)	3(2)
C6	27(1)	26(1)	16(1)	-2(1)	-2(1)	-6(1)
C7	39(2)	26(1)	18(1)	-5(1)	3(1)	-10(1)
C8	20(1)	18(1)	20(1)	-1(1)	8(1)	-1(1)
C9	17(1)	14(1)	19(1)	1(1)	6(1)	-1(1)
C10	17(1)	16(1)	21(1)	0(1)	5(1)	1(1)
C11	16(1)	16(1)	27(1)	-2(1)	9(1)	1(1)
C12	21(1)	22(1)	19(1)	-2(1)	6(1)	-3(1)
C13	24(1)	18(1)	17(1)	1(1)	2(1)	0(1)

Table 5. Hydrogen coordinates [$\times 10^4$] and isotropic displacement parameters [$\text{\AA}^2 \times 10^3$].

Atom	<i>x</i>	<i>y</i>	<i>z</i>	<i>U</i> _{eq}	<i>S.o.f.</i>
H903	10241	9078	10200	36	1
H904	3790	13115	8280	35	1
H1	9606	7579	13290	34	1
H2	9311	4993	14483	44	1
H3	7511	5709	15476	52	1
H4A	5987	8972	15258	54	1
H5	6253	11528	14049	41	1
H7A	7554	12875	12874	34	1
H7B	9349	11926	12925	34	1
H8A	8857	12624	11163	23	1
H8B	7092	13573	11189	23	1
H9	5822	10737	10025	20	1
H10	7942	8039	10236	22	1
H13	5962	13935	7983	24	1

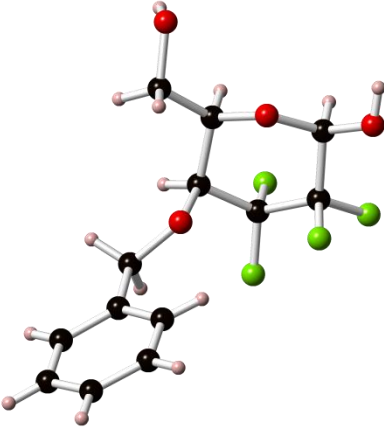
Table 6. Hydrogen bonds [\AA and $^\circ$].

<i>D</i> –H... <i>A</i>	<i>d</i> (<i>D</i> –H)	<i>d</i> (H... <i>A</i>)	<i>d</i> (<i>D</i> ... <i>A</i>)	\angle (<i>DHA</i>)
O3–H903...O2 ⁱ	0.84	2.38	3.086(2)	141.8
O3–H903...O3 ⁱ	0.84	2.44	3.091(3)	135.6
O4–H904...O1 ⁱⁱ	0.84	1.88	2.719(2)	174.4
Symmetry transformations used to generate equivalent atoms:				
(i) $-x+2, y-1/2, -z+2$ (ii) $-x+1, y+1/2, -z+2$				



Thermal ellipsoids drawn at the 35% probability level

Table 1. Crystal data and structure refinement details.

Identification code	2012sot0018 (β-3.5)	
Empirical formula	$C_{13}H_{14}F_4O_4$	
Formula weight	310.24	
Temperature	100(2) K	
Wavelength	0.71075 Å	
Crystal system	Orthorhombic	
Space group	$P2_12_12_1$	
Unit cell dimensions	$a = 6.409(3)$ Å $b = 13.252(6)$ Å $c = 15.665(7)$ Å	
Volume	$1330.5(10)$ Å ³	
Z	4	
Density (calculated)	1.549 Mg / m ³	
Absorption coefficient	0.149 mm ⁻¹	
$F(000)$	640	
Crystal	Fragment; Colourless	
Crystal size	$0.21 \times 0.13 \times 0.10$ mm ³	
θ range for data collection	$3.02 - 27.48^\circ$	
Index ranges	$-8 \leq h \leq 7, -17 \leq k \leq 9, -19 \leq l \leq 20$	
Reflections collected	4576	
Independent reflections	1766 [$R_{int} = 0.0363$]	
Completeness to $\theta = 27.48^\circ$	99.3 %	
Absorption correction	Semi-empirical from equivalents	
Max. and min. transmission	0.9853 and 0.9695	
Refinement method	Full-matrix least-squares on F^2	
Data / restraints / parameters	1766 / 0 / 198	
Goodness-of-fit on F^2	1.164	
Final R indices [$F^2 > 2\sigma(F^2)$]	$R1 = 0.0439, wR2 = 0.0708$	
R indices (all data)	$R1 = 0.0482, wR2 = 0.0724$	
Largest diff. peak and hole	0.272 and -0.251 e Å ⁻³	

Diffraction: Rigaku AFC12 goniometer equipped with an enhanced sensitivity (HG) Saturn724+ detector mounted at the window of an FR-E+ SuperBright molybdenum rotating anode generator with HF Varimax optics (100µm focus). **Cell determination, Data collection, Data reduction and cell refinement & Absorption correction:** CrystalClear-SM Expert 2.0 r7 (Rigaku, 2011), **Structure solution:** SHELXS97 (G. M. Sheldrick, Acta Cryst. (1990) A46 467–473). **Structure refinement:** SHELXL97 (G. M. Sheldrick (1997), University of Göttingen, Germany). **Graphics:** CrystalMaker: a crystal and molecular structures program for Mac and Windows. CrystalMaker Software Ltd, Oxford, England (www.crystallmaker.com)

Special details: All hydrogen atoms were placed in idealised positions and refined using a riding model, except those of the OH which were freely refined.

Table 2. Atomic coordinates [$\times 10^4$], equivalent isotropic displacement parameters [$\text{\AA}^2 \times 10^3$] and site occupancy factors. U_{eq} is defined as one third of the trace of the orthogonalized $U^{\bar{ij}}$ tensor.

Atom	x	y	z	U_{eq}	$S.o.f.$
F2A	3523(2)	8387(1)	2688(1)	23(1)	1
F2E	3065(3)	9949(1)	3090(1)	26(1)	1
F3A	-841(2)	9972(1)	2596(1)	19(1)	1
F3E	1136(2)	9348(1)	1584(1)	19(1)	1
O1	3019(3)	8440(1)	4388(1)	19(1)	1
O4	-211(3)	7410(1)	1909(1)	17(1)	1
O5	142(3)	7771(1)	3748(1)	14(1)	1
O6	-3955(3)	6881(1)	4129(1)	19(1)	1
C1	1308(4)	8672(2)	3879(1)	16(1)	1
C2	2098(4)	9040(2)	3012(2)	17(1)	1
C3	292(4)	9142(2)	2366(1)	15(1)	1
C4	-1169(4)	8236(2)	2334(1)	13(1)	1
C5	-1724(4)	7939(2)	3254(1)	13(1)	1
C6	-2989(4)	6981(2)	3309(1)	16(1)	1
C7	-918(4)	7304(2)	1045(1)	19(1)	1
C8	345(4)	6512(2)	589(1)	14(1)	1
C9	-455(4)	6107(2)	-169(1)	18(1)	1
C10	642(4)	5375(2)	-619(1)	18(1)	1
C11	2543(4)	5038(2)	-313(1)	19(1)	1
C12	3371(4)	5445(2)	426(1)	19(1)	1
C13	2285(4)	6187(2)	876(1)	17(1)	1

Table 3. Bond lengths [Å] and angles [°].

F2A–C2	1.357(3)	C1–C2–C3	111.2(2)
F2E–C2	1.361(3)	F3A–C3–F3E	106.57(18)
F3A–C3	1.367(3)	F3A–C3–C4	108.46(19)
F3E–C3	1.367(2)	F3E–C3–C4	111.83(18)
O1–C1	1.390(3)	F3A–C3–C2	107.23(18)
O4–C4	1.421(3)	F3E–C3–C2	107.9(2)
O4–C7	1.435(3)	C4–C3–C2	114.43(19)
O5–C1	1.423(3)	O4–C4–C3	110.9(2)
O5–C5	1.442(3)	O4–C4–C5	110.04(19)
O6–C6	1.432(3)	C3–C4–C5	108.30(18)
C1–C2	1.530(3)	O5–C5–C6	106.61(19)
C2–C3	1.543(3)	O5–C5–C4	110.54(19)
C3–C4	1.523(3)	C6–C5–C4	113.23(18)
C4–C5	1.534(3)	O6–C6–C5	111.24(19)
C5–C6	1.508(3)	O4–C7–C8	110.2(2)
C7–C8	1.506(3)	C13–C8–C9	118.9(2)
C8–C13	1.391(3)	C13–C8–C7	122.9(2)
C8–C9	1.400(3)	C9–C8–C7	118.2(2)
C9–C10	1.390(3)	C10–C9–C8	120.8(3)
C10–C11	1.384(4)	C11–C10–C9	119.6(2)
C11–C12	1.383(3)	C12–C11–C10	120.2(2)
C12–C13	1.395(3)	C11–C12–C13	120.4(2)
C4–O4–C7	112.38(18)	C8–C13–C12	120.0(2)
C1–O5–C5	112.61(18)		
O1–C1–O5	108.14(19)		
O1–C1–C2	108.6(2)		
O5–C1–C2	108.16(18)		
F2A–C2–F2E	107.0(2)		
F2A–C2–C1	110.6(2)		
F2E–C2–C1	110.60(19)		
F2A–C2–C3	108.42(18)		
F2E–C2–C3	108.90(19)		

Table 4. Anisotropic displacement parameters [$\text{\AA}^2 \times 10^3$]. The anisotropic displacement factor exponent takes the form: $-2\pi^2[h^2a^{*2}U^{11} + \dots + 2hk a^* b^* U^{12}]$.

Atom	U^{11}	U^{22}	U^{33}	U^{23}	U^{13}	U^{12}
F2A	16(1)	36(1)	18(1)	3(1)	3(1)	6(1)
F2E	27(1)	29(1)	22(1)	5(1)	-7(1)	-14(1)
F3A	21(1)	15(1)	21(1)	-2(1)	1(1)	4(1)
F3E	20(1)	26(1)	11(1)	3(1)	3(1)	-1(1)
O1	16(1)	29(1)	13(1)	3(1)	-3(1)	-2(1)
O4	22(1)	17(1)	11(1)	-4(1)	-3(1)	6(1)
O5	13(1)	16(1)	14(1)	2(1)	-2(1)	-1(1)
O6	20(1)	21(1)	17(1)	4(1)	3(1)	-2(1)
C1	16(1)	17(1)	15(1)	-1(1)	-1(1)	-3(1)
C2	15(1)	16(1)	18(1)	-1(1)	-1(1)	-1(1)
C3	18(1)	18(1)	10(1)	1(1)	3(1)	3(1)
C4	13(1)	14(1)	12(1)	-2(1)	-2(1)	4(1)
C5	12(1)	15(1)	12(1)	0(1)	-2(1)	0(1)
C6	18(1)	20(1)	11(1)	-2(1)	-1(1)	1(1)
C7	22(1)	22(1)	11(1)	-3(1)	-5(1)	2(2)
C8	16(1)	14(1)	13(1)	2(1)	0(1)	-2(1)
C9	18(1)	18(1)	18(1)	1(1)	-3(1)	1(1)
C10	23(2)	17(1)	15(1)	-2(1)	1(1)	-7(1)
C11	23(2)	18(1)	18(1)	2(1)	8(1)	2(1)
C12	17(1)	21(1)	19(1)	6(1)	4(1)	4(1)
C13	19(1)	19(1)	13(1)	3(1)	-2(1)	-2(1)

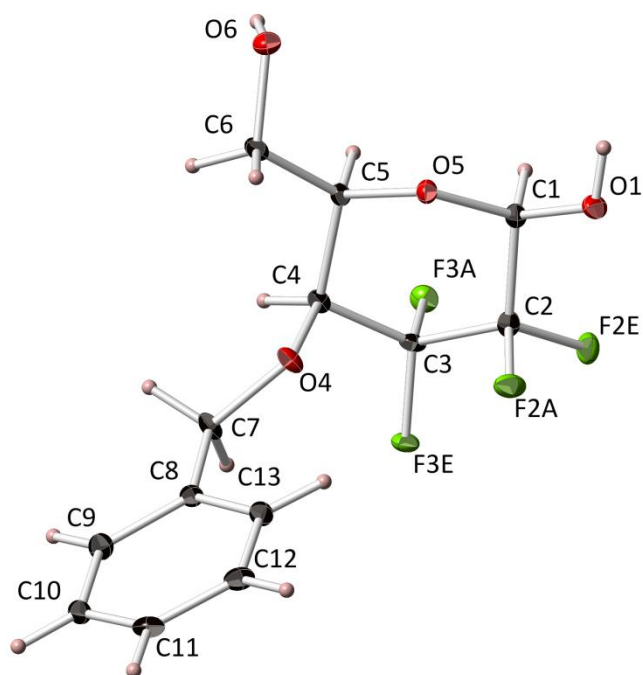
Table 5. Hydrogen coordinates [$\times 10^4$] and isotropic displacement parameters [$\text{\AA}^2 \times 10^3$].

Atom	<i>x</i>	<i>y</i>	<i>z</i>	<i>U</i> _{eq}	<i>S.o.f.</i>
H1	424	9200	4158	19	1
H4	−2473	8428	2023	16	1
H5	−2537	8500	3520	16	1
H6A	−4079	6987	2861	20	1
H6B	−2070	6394	3205	20	1
H7A	−779	7958	744	22	1
H7B	−2410	7111	1041	22	1
H9	−1764	6335	−378	21	1
H10	89	5107	−1134	22	1
H11	3281	4526	−611	23	1
H12	4687	5218	629	23	1
H13	2872	6471	1378	20	1
H1A	2590(60)	8340(20)	4871(19)	54(11)	1
H6	−4880(50)	7350(20)	4155(18)	40(10)	1

Table 6. Hydrogen bonds [\AA and $^\circ$].

<i>D</i> –H... <i>A</i>	<i>d</i> (<i>D</i> –H)	<i>d</i> (H... <i>A</i>)	<i>d</i> (<i>D</i> ... <i>A</i>)	\angle (<i>DHA</i>)
O1–H1A...O6 ⁱ	0.82(3)	1.88(3)	2.679(3)	168(3)
O6–H6...O1 ⁱⁱ	0.86(3)	2.01(3)	2.862(3)	172(3)

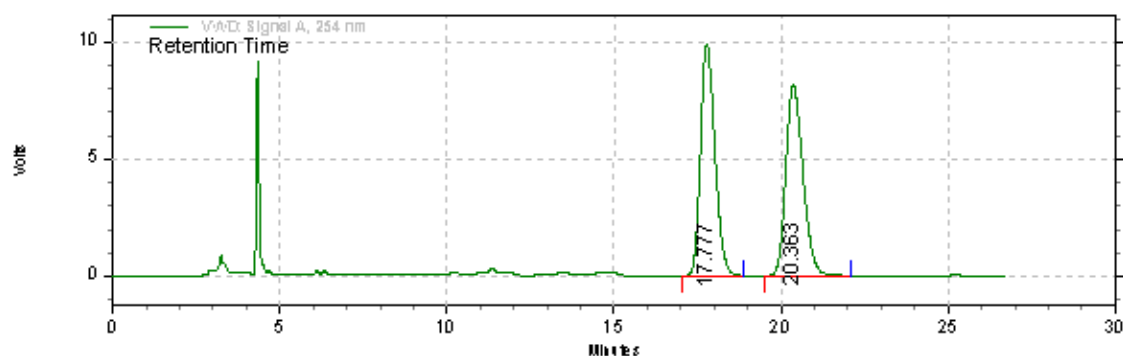
Symmetry transformations used to generate equivalent atoms:
(i) $x+1/2, -y+3/2, -z+1$ (ii) $x-1, y, z$



Thermal ellipsoids drawn at the 35% probability level.

10.2 Appendix B: Analytical Chiral HPLC Data

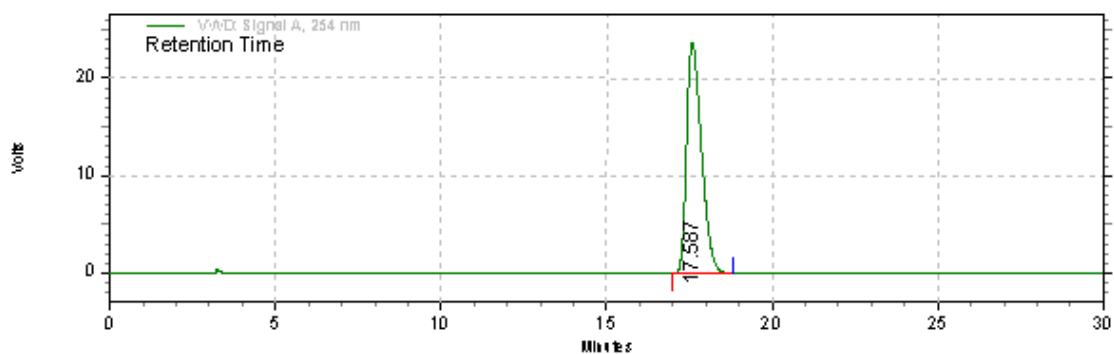
rac-1.49



VWD: Signal A, 254 nm Results

Retention Time	Area	Area %	Height	Height %
17.777	5017492	50.31	166226	54.83
20.363	4955034	49.69	136918	45.17

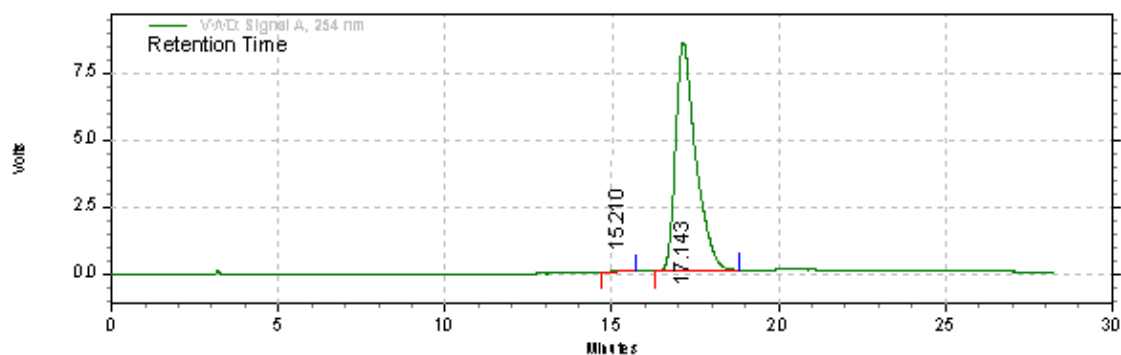
1.49



VWD: Signal A, 254 nm Results

Retention Time	Area	Area %	Height	Height %
17.587	12366555	100.00	396868	100.00

ent-1.49



**VWD: Signal A,
254 nm Results**

Retention Time	Area	Area %	Height	Height %
15.210	23069	0.38	819	0.57
17.143	6008004	99.62	143080	99.43